NASA TECHNICAL MEMORANDUM NASA TM-77687

ELECTRICAL CONDUCTIVITY OF ROCKS AT HIGH PRESSURES AND TEMPERATURES

E. I. Parkhomenko, A. T. Bondarenko

Translation of: "Elektroprovodnost' gornykh porod pri vysokikh davleniyakh i temperaturakh," Nauka Press, Moscow, 1972, 278 pages.

(NASA-TM-77687) ELECTRICAL CONDUCTIVITY OF ROCKS AT HIGH PRESSURES AND TEMPERATURES (National Aeronautics and Space Administration) 299 p HC A13/MF A01 CSCL 08G G3/46

N86-24060

Unclas 06007

NATIONAL AERONAUTICS AND SPACE ADMINISTRATION
WASHINGTON, D. C. 20546 JANUARY 1986

STANDARD TITLE PAGE

1. Report No. NASA TM-77687	2. Government Accession No.	3. Recipient's Catalog No.
4. Title and Subtitle ELECTRICAL CONDUCTIVITY OF ROCKS AT HIGH PRESSURES AND TEMPERATURES		5. Report Date January 1986 6. Performing Organization Code
7. Author(s) E.I. Parkhomenko and A.T. Bondarenko		8. Performing Organization Report No. 10. Work Unit No.
9. Performing Organization Name and Address Leo Kanner Associates Redwood City CA 94063		11. Contract or Grant No. NASW-4005 13. Type of Report and Period Covered Translation
12. Sponsoring Agency Name and Address National Aeronautics and Space Administration, Washington, D.C. 20546		14. Sponsoring Agency Code

15. Supplementary Notes

Translation of "Elektroprovodnost' gornykh porod pri vysokikh davleniyakh i temperaturakh," Nauka Press, Moscow, 1972, pp. 1-212. (UDC 552.1:537.311)

16. Abstract The book describes the results of studies of the electrical conductivity in the most widely distributed types of igneous rocks, at temperatures of up to 1200°C, at atmospheric pressure, and also at temperatures of up to 700°C and at pressures of up to 20,000 kg/cm^2. The figures of electrical conductivity, of activation energy and of the preexponential coefficient are presented and the dependence of these parameters on the petrochemical parameters of the rocks are reviewed. The possible electrical conductivities for the depository, "granite" and "basalt" layers of the Earth's crust and of the upper mantle are presented, as well as the electrical conductivity distribution to the depth of 200-240 km for different geological structures.

17. Key Words (Selected by Author(s))	18. Distribution Statement Unclassified - Unlimited		
19. Security Classif. (of this report) Unclassified	20. Security Classif. (of this page) Unclassified	21. No. of Pages 292	22.

Electrical Conductivity of Rocks at High Pressures and Temperatures

E. I. Parkhomenko and A. T. Bondarenko

Nauka Press, Moscow, 1972

Editor-in-Chief: Professor M. P. Volarovich

CONTENTS

Electrical Conductivity of Rocks at High Pressures and Temperatures
E. I. Parkhomenko, A. T. Bondarenko, Nauka Press, Moscow, 1972
211 pages

This book describes the results of studies of the electrical conductivity in the most widely distributed types of igneous rocks, at temperatures of up to 1200°C, at atmospheric pressure, and also at temperatures of up to 700°C, and at pressures of up to 20,000 kg/cm^2. The figures of electrical conductivity, of activation energy and of the preexponential coefficient are presented and the dependence of these parameters on the petrochemical parameters of the rocks are reviewed. The possible electrical conductivities for the depository, "granite" and "basalt" layers of the Earth's crust and of the upper mantle are presented, as well as the electrical conductivity distribution to the depth of 200-240 km for different geological structures.

The book is aimed at researchers and engineers-geophysicists, geologists, mine-workers, teachers and students of appropriate departments and higher schools of education.

The book contains 36 tables and appendices, 97 figures and 211 references.

E. I. Parkhomenko and A. T. Bondarenko have written jointly the introduction, Chapter III, 4,4; Chapter IV, 3,4; Chapter V, 1-3, 6,7; Chapter VI, 2; E. I. Parkhomenko wrote Chapter I, 1,2; Chapter V, 4,8 and conclusions; Chapter VI, 1; Conclusion; A. T. Bondarenko wrote Chapter III, 5,9; Chapter V, 5, 6, 9; Chapter VI, 3.

In the sections written by E. I. Parkhomenko, the experimental results obtained by A. T. Bondarenko are marked in the text and captions by a star.

Editor-in-Chief
Professor M. P. Volarovich

ELECTRICAL CONDUCTIVITY OF ROCKS AT HIGH PRESSURES AND TEMPERATURES

E. I. Parkhomenko, A. T. Bondarenko

Order of Lenin Institute of Earth Physics, named after O. Yu. Schmidt, Academy of Sciences of the USSR

Introduction

/5*

The electrical conductivity studies of the magmatic rocks and minerals as a function of the pressure and temperature is just one part of the general study of physical properties of the matter within the Earth's interior, located at great depths [1, 2]. In the course of development of geophysics, the major sources of information regarding the structure and composition of the interior of the Earth were the field data and observations of seismological, gravimetric and magnetometric nature. In the last decade, the study of natural electromagnetic fields has broadened extensively.

A promising method of electromagnetic probing of the interior of the Earth has been developed and theoretically substantiated in the Soviet Union, under the leadership of the Academician A. N. Tikhonov and with the participation of numerous scientists (M. N. Berdichevskiy, L. L. Van'yan, N. P. Vladimirov, V. I. Dmitriyev, N. V. Lipskaya, I. I. Rokityanskiy, N. M. Rotanov and M. M. Shakhsuvarov) [3-9].

At the present time, the intensive development of the field work of the magnetotellurium probing made it possible to accumulate an extensive material on the electrical parameters of the interior rocks. It was also discovered that some layers in the Earth's crust and of the mantle have electrical conductivity which is higher approximately by 2-3 orders of magnitude than the rocks above these layers and below them. It is necessary to point out that within the Earth's crust, at the depth with the anomalous electrical conductivity, one detects decreased seismic velocities (I. L. Nersesov, N. N. Matveyev, S. Muller). However, it is not always possible to correlate the data describing the layers with anomalous conductivity, with the result of seismic, magnetic, thermal and gravitational data.

Because the electrical conductivity of the rocks is quite sensitive to changes of temperature, pressure, humidity and melting process, the method of magnetotellurium probing opens up new avenues

*Numbers in the margin indicate pagination in the foreign text.

for handling a number of important questions in geophysics, such as: better definition of the composition and structure of the Earth's crust and of the upper mantle, the temperature distribution as a function of depth and also the amount of moisture found in the rocks. Even now, it has become possible, by using the electromagnetic probing, to determine the depth of the magma formation zone and of other conducting zones, to evaluate its extent and to outline its area. However, all these questions can be answered /6 only by comparing the observations in the field with the laboratory data and with the theoretical studies. In spite of the importance of a comprehensive investigation of the electrical properties of different rock-forming minerals, and of the rocks at high temperatures and pressures, the scope of these studies is insufficient. There is only fragmented information in regard to the electrical conductivity of some rocks and of chemical compounds under such conditions. Quite recently, Academician M. A. Sadovskiy [10], in pointing out the pertinence of the whole problem of physical and physical-chemical studies at high pressures and temperatures, has emphasized that in particular, it is of great importance to investigate the electrical and other properties of the rocks in different thermodynamic conditions.

This book presents in a comprehensive form the results of experiments, on the electrical conductivity of minerals and rocks of different composition and origin, which were carried out by the authors during a number of years at the Order of Lenin Institute of the Earth Physics, Academy of Sciences of the USSR.

In our opinion, the information presented in this study will make it possible to develop a general concept regarding the electrical parameters of the rocks which are a part of the Earth's crust and the upper layers of the upper mantle, to the depth on the order of 80-100 km and more.

This is important, since within the depth range indicated, one observes in the mantle the physical, physical-chemical and tectonic processes which are reflected in some other physical phenomena in the Earth's crust. Therefore, the obtained experimental data which defines the electrical conductivity of the rocks and minerals as a function of the pressure and temperature, and the construction of geoelectrical cross sections of different tectonic regions, extended to that depth, may be effectively used, already at this time. In addition, the rapidly expanding method of geothermic studies of the interior of the Earth, in parallel with the investigation of the seismic velocities and making use of the electrical conductivity data as a function of depth, will help to define more accurately the geothermic gradient in the upper mantle [11].

It is possible to determine experimentally the activation energies and the preexponential coefficient which are being used for the

theoretical calculations of the temperature and the electrical conductivity at great depth (V. N. Zharkov and V. A. Magnitskiy [12-13]). The activation energy (the width of the forbidden zone) is one of the basic energy parameters of the crystalline state of matter, and it is being used to compute the zonal structure of semiconducting crystals. The specific figures of activation energy correlate well with the isobaric thermodynamic potential of reactions and crystalline formation. The study of this parameter, and ellucidation of the temperature parameters, needed for conglomeration and crystallization, may also produce valuable information.

CHAPTER ONE. BRIEF INFORMATION FROM THE PHYSICS OF SEMICONDUCTORS, DIELECTRICS AND THE METHOD OF MEASURING THE ELECTRICAL CONDUCTIVITY

The rock formations are essentially the multiphase systems, /7
consisting in a general case of the solid (predominantly crystalline, less often - amorphous), liquid and gaseous phases. The major component of the rocks are the minerals which may have properties of metals, semiconductors and of dielectrics. The rock pore moisture, in spite of its small content, may affect significantly the electrical properties of the rocks. The electric conductance of the dry rocks is defined by the mineral content and by the structure of the rocks. However, in the presence of pore moisture, of great significance is not only the amount of such moisture, but also the specific surface area of the solid phase. In conjunction with this, it becomes clear why the electrical conductance of the rocks varies within a considerably wider range than any other physical parameters, such as for example, the density. Let us first consider the mechanism of electrical conductance in different solid materials, and also let us investigate the electrical conductivity in such materials as a function of temperature.

1. Some Information About the Electrical Conductivity in Different Materials at High Temperatures

It is known that the solid materials, depending on the electrical conductivity, are divided into three groups: conductors, semiconductors and dielectrics (solid electrolytes). Of these, the best conductors are the metals and metal alloys. The specific electrical conductivity of the latter changes between 10^3 and 10^6 $ohm^{-1} \cdot cm^{-1}$.

In contrast to these, the solid electrolytes are the materials which conduct current poorly, and their specific electrical conductivity is ordinarily less than 10^{-9} $ohm^{-1} \cdot cm^{-1}$. In terms of electrical conductance, the semiconductors occupy and intermediate position, in the range between 10^4 to 10^{-9} $ohm^{-9} \cdot cm^{-1}$.

Electrical Conductivity of Metals.

The minerals which feature the conductivity of metals are encountered only as nature-made metals, comprising the least frequently encountered group of minerals. Therefore, the electrical conductivity of metals will be only briefly described.

The metal model is a sum of positive ions, located at the points of the crystalline lattice, between which a large number of free electrons is located. These electrons, just like the ions, are randomly oscillating. The geometric sum of speeds of the

free electrons within a sufficiently large volume of the metal is equal to zero. If however, one is to apply the voltage to the metal, the electrons will acquire additional velocity along the field, thus the electric current is generated. In the case of the metals, just like in the case of some other conductors, the electrical conductivity σ may be expressed by the following, well-known formula

$$\sigma = nqu = \frac{q^2 n\lambda}{2mv},$$

where n is the number of electrons in 1 cm^3, q is the electron charge, u is the electron mobility, m is the electron mass and v is the average speed of the thermal motion of the electron, inside of the metallic conductor and λ is the mean free path of the electron. In terms of the electron concentration and the speed of the thermal motion, the conductors differ only slightly. The difference in electrical conductance in the metals is associated with their structure, which is associated with different lengths of the free path of the electrons. As the temperature in the metallic conductor increases, the thermal motion of the electrons changes only slightly and the concentration of electrons remains constant. As the temperature increases, the ion oscillation within the crystalline lattice is enhanced, creating obstacles in the directional motion of the electrons, and this results in the decreased mean free path, and reduced mobility of the electrons. Therefore, the specific electrical conductivity of metals will decrease with the temperature increase. Figure 1 shows a typical curve of the specific resistivity change ρ with the temperature increase. Within a narrow temperature range, the $\rho=f(t)$ relationship may be approximated by a straight line dependence, and at the end of the temperature interval under consideration, the specific resistivity may be calculated by using the following formula /9

$$\rho_t = \rho_0(1 + \alpha\Delta t),$$

where ρ_0 is the specific resistivity at the beginning of the interval, α is the temperature coefficient of resistivity and Δt is the temperature increment. As the material, from its solid state, goes into a liquid phase, one observes in the case of many metals an increase of specific resistivity in a leap-frog fashion, and in the case of some metals - a decrease during melting [14,15].

Electrical Conductivity of Semiconductors.

The majority of mineral ores, the oxides, sulfides, tellurides and selenides are semiconductors. In addition to the chemical compounds, the semiconducting properties are also possessed by a group of elements which occupy an intermediate position between the metals and insulators. The electrical conductance of metals

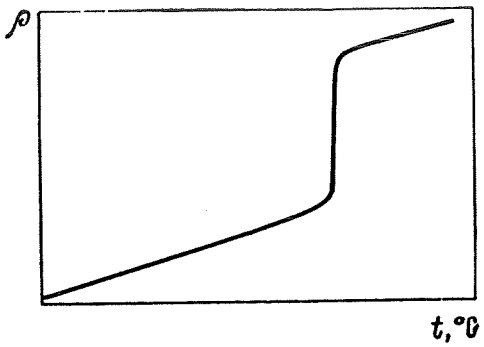

Figure 1. Specific electrical resistivity of copper as a function of temperature. The jump in the curve corresponds to the melting temperature of copper (1083°).

and semiconductors is due to the same current carriers, namely the electrons. The basic difference between the metals and semiconductors is associated with the energy-related state of the electrons. The activation energy of electrons in metal is equal to zero, and in semiconductors - it varies from several decimal fractions of eV to several eV. A small number of valence-defining electrons which take part in the current transfer are the reason for a considerably smaller electrical conductivity in the semiconductors, as compared to the metals. The mobility, however, of the current-carriers in the semiconductors may be greater or smaller than in the metals.

It has been established that in the semiconductors, the constant of the Hall effect, R, is not only different but it also has a different sign. Consequently, the charge of the current carrier may be both positive and negative. The above-mentioned phenomenon is well explained by the zone theory of the solid body. According to this theory the semiconductors, in parallel with the valence zones which are completely filled with electrons, also have a vacant zone. In the presence of some stimulating factors, the electrons pass from the valence zone into the vacant conductivity zone, thus beginning to participate in the electrical conductance. The external electric field induces the electrons to acquire higher levels and the result is the sequential displacement in the opposite direction of the "electron holes." Therefore, the displacement of these "holes" is equivalent to the movement of the positive charge to somewhat lower levels. As we can see, the electrical conductivity of conductors may be brought about by either the electrons or by the "holes" which are equivalent to the positive current carriers.

Depending on the predominance in the above-mentioned current carriers, one differentiates between the semiconductors of p type, with the hole, and of n type, with the electron conductivity mechanisms. One should also not here that in parallel with the excitation of the electrons, one is also faced with the reverse process, the electron recombination and the return of the electrons from the conductance zone to the valence zone. As a result of these

two processes, regardless of the temperature, an equilibrium state /10
is being established between the number of "holes" and the electrons (n)

$$n = 2\frac{(2\pi\sqrt{m_n \cdot m_p}kT)^{3/2}}{h^3} e^{-\frac{\Delta E}{2kT}},$$

where ΔE is the width of the forbidden zone, k is the Boltzmann constant, h is the Planck constant, m is the effective mass of the current carrier (m_n - the electrons and m_p - the "holes").

Let us consider in somewhat greater detail the laws governing the change in the electrical conductivity mechanism in the semiconductors, depending on their "purity," since in natural conditions, the mineral compounds which feature the semiconducting properties are characterized by the inhomogeneous structure and variable chemical composition. The electrical conductivity in semiconductors is rather sensitive, even to the smallest changes in the chemical composition of the mineral. On the other hand, the impurities in semiconductors, just like in the dielectrics, are the sources of the current carrier. By impurities one should understand not only the inclusion of atoms of some heterogeneous material, but also the excess or shortage of one of the atoms, forming the chemical compound, and also the different defects in the crystalline lattice. As a rule, the atoms of impurities are isolated from each other and therefore, the energy-related levels of these atoms are not split into the zones and the valence electrons here are located at the narrow energy levels which may be found in the forbidden zone. If the levels of impurities are in proximity to the conductivity zone, less energy will be required to transfer the electrons from these levels into the vacant conductivity zone than to excite the electrons and bring about the conductivity by electron movements within the basic material.

The "holes" which are being formed at the levels of impurities, because of their localized state, cannot move or participate in the development of current. Therefore, the electron conductivity is being formed. The impurties or doping material in this case are called the donors, and the impurity levels are called the donor levels [15]. There is another case possible, when the unfilled impurity levels, while being in the proximity of the valence zone, could create the so-called "hole" character of conductivity. This is due to the fact that the width of the forbidden zone between the levels is considerably narrower than the width of the forbidden zone between the valence and conductivity zones. Therefore, what we see is the electron transfer from the valence zone, not into the conductivity zone, but to the impurity level which is not completely filled. The electrons from the impurities levels cannot take part in the generation of current, and this results in a purely "hole" conductivity.

The impurities which produce partially unfilled levels which can be occupied by the electrons from the valence zones are being called the acceptors, and the energy level of these impurities is being called the acceptor level.

If the semiconductor has two types of impurities, then the sign of conductivity is defined by the component which is in excess. /11

The physical reason that the electrons from the atoms of the doping material are easily separated is the ease of medium polarization in which the atom is located. The polarization process weakens the bonds between the electrons and the nucleus, resulting in the decrease of energy which would be required to remove the electron from the atom. The available experimental data indicates that with the increase of dielectric penetrability ε, the width of the forbidden zone in the semiconductor E_0 will decrease. For a number of semiconductors, the $E_0\varepsilon^2 = \text{const}$ relationship is valid.

The electrical conductivity of a semiconductor changes with the temperature increase because of the change in the concentration of the current carriers and of their mobility. Let us consider separately the effect of temperature on these parameters.

Figure 2 shows the most typical cases of the concentration change in the current carriers, for the semiconductors with different percentage content of impurities. In the case of the first and second semiconductor, as one increases the temperature, we observe the exponential increase of the current carrier concentration, because of the impurities (the $a - \delta$, $a' - \delta'$ segments). At the temperatures T and T', the impurity sources are exhausted and one observes on the $\delta - b$, $\delta' - b'$, a constant concentration of the current carriers. At the temperatures above T', the intrinsic conductivity begins to prevail. It is easy to see in this figure that the straight line inclination within the $a - \delta$ interval, and the transition temperature from the impurity conductivity to the intrinsic one depends on the amount of impurities. The more impurities are present, the higher will be the temperature of such transition, and the lower will be the straight line slope which is characterized by the activation energy E_0. In the case of the third semiconductor with rather high impurity content (the curve a and b, the concentration of the current carriers does not change within a broad temperature range. This is due to the fact /12 that the impurity levels, by splitting, form a zone which overlaps the conductivity zone. As a result of this, the semiconductor acquires the properties which are characteristic for a metal. Such semiconductors form a particular group of compounds which are being called the semimetals.

The current carrier mobility u, in the semiconductors, depends only slightly on the temperature, and is of different character

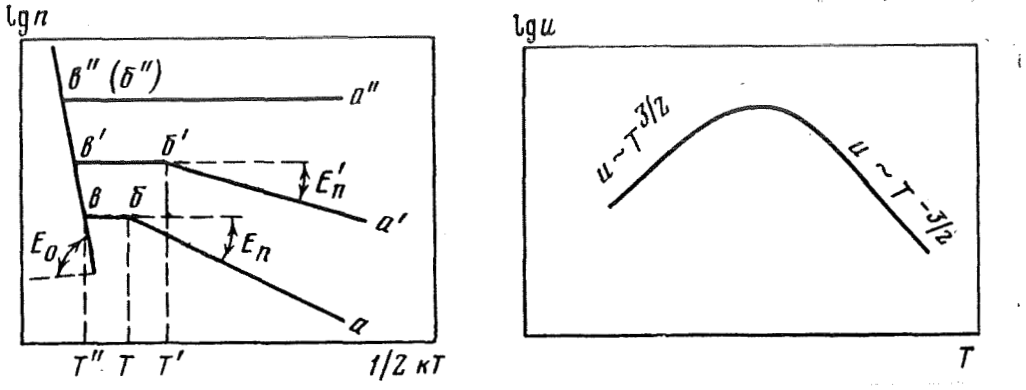

Figure 2. Concentration of the current carriers as the function of temperature.
a - δ is the extrinsic conductivity; b - b" is the intrinsic conductivity.

Figure 3. Mobility of the current carriers as a function of temperature.

for the atomic and ionic semiconductors. Within the atomic lattices, in conjunction with the mechanism of the current carrier scattering (the thermal oscillations of the lattice and the ionization impurity scattering), the mobility as a function of temperature is defined by the following formula

$$u = aT^{+3/2} + bT^{-3/2},$$

where a and b are the coefficients of proportionality.

At low temperature, the first term within the sum plays the predominant role, and at high temperature, the second term (Figure 3). The position of the maximum depends on the amount of impurities. With the increase of this amount, the maximum is shifted toward higher temperatures.

In the ionic crystals, mobility is smaller than in the atomic. This is due to a stronger interaction between the current carriers and the ions than the interaction with the neutral atoms.

As one can see, the electrical conductivity as a function of temperature is defined predominantly by the character of the relationship between the current carrier concentration and the temperature, since it changes exponentially, while the mobility changes according to the power law. The current carrier mobility somewhat affects the σ value as a function of temperature only when the impurities are exhausted. In this case the electrical

conductivity as a function of temperature, because of the decrease or increase of mobility, may acquire different forms. The general character of the electrical conductivity in semiconductors as a function of temperature, in the presence of different amounts of impurities, is shown in Figure 4.

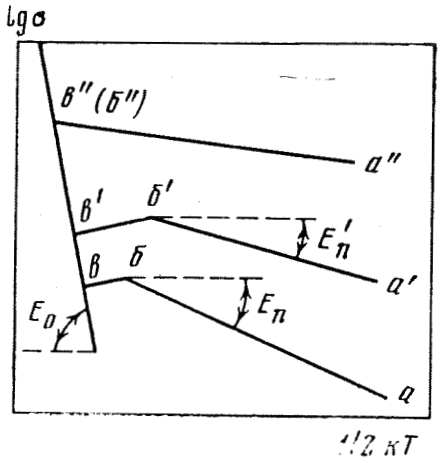

Figure 4. Electrical conductivity in semiconductors as a function of temperature, in the presence of different amounts of impurities. a - δ is the conductivity with impurities; b - b" is the intrinsic conductivity.

In many cases, the crystalline structure of the material defines its electrical properties, since the width of the forbidden zone depends on the position of atoms within the crystalline lattice. However, as the lattice is being destroyed, as for example during the process of melting, the electrical conductivity for some compounds will change only slightly. Consequently, the major factor which influences the σ quantity is not the organized position of the atoms at great distances, but the position of neighboring atoms, their number and mutual position. /13

In recent times, a new hypothesis acquires greater and greater importance as to the decisive nature of chemical bonds which affect the electrical conductivity. In particular, the homeopolar bonds facilitate the development of semiconducting properties.

Among the major factors which define the increased electrical conductivity in the polycrystalline materials, as compared to the monocrystals, are [14-17]:

a) concentration at the grain boundaries of a considerable amount of impurities which play the role of conducting channels;

b) the difference of energy states in the atoms which are near the grain boundaries, and those which are at a distance from such boundaries;

c) shorter lifespan of the current carriers in the polycrystalline materials than in the monocrystals.

Electrical Conductivity in Dielectrics.

The majority of minerals are ionic, crystalline dielectrics. The current conductivity in such dielectrics is brought about first of all by the ions of the least size (for the same charge) or by the ions with the least charge and similar in size. In conjunction with this, it is important to know the ionic radii.

Table 1 shows the ionic radii for the ions which are encountered most frequently in minerals. The same table shows their polarizability which is also an important physical parameter of the material.

TABLE 1. RADII AND POLARIZABILITY OF DIFFERENT IONS

Ion	Radii $r \cdot 10^8$, cm	Polarizability $\alpha \cdot 10^{24}$, cm^3	α/r^3	Ion	Radii $r \cdot 10^8$, cm	Polarizability $\alpha \cdot 10^{24}$, cm^3	α/r^3
Na^{1+}	0,98	0,197	0,210	Pb^{2+}	1,32	4,32	1,89
K^{1+}	1,33	0,879	0,382	Fe^{2+}	0,83	—	—
Ag^{1+}	1,13	1,85	1,28	Fe^{3+}	0,67	—	—
O^{2+}	1,32	2,74	1,2	Cr^{3+}	0,57	0,067	0,36
Mg^{2+}	0,78	0,114	0,24	Al^{3+}	0,57	0,067	0,36
S^{2+}	1,74	5,9	1,12	Si^{4+}	0,39	0,039	0,657
Ca^{2+}	1,06	0,531	0,44	Ti^{4+}	0,64	0,272	1,04
Hg^{2+}	1,12	1,99	1,41				

[Note. Commas in tabulated material are equivalent to decimal points.]

In the dielectrics, just like in the semiconductors, the electrical conductivity is divided into two types - the impurity-related and intrinsic, depending on the ions which are involved in the development of current. The first conductivity is observed at relatively low temperatures, and the second one - at high temperatures.

The mechanism of electrical conductivity in the ionic crystals is associated with the presence of defects in them. There are the defects according to Frenkel, and defects according to Schottky.

According to Ya. I. Frenkel, in the specific points of the lattice, the atom (ion) may be absent which moves from the corresponding point of the lattice into the interpoint region. As a result, there are two defects present, the interpoint atom (ion) and the vacancy (the place from which the atom moves into the interpoint region) which are ordinarily called the defects, according to Frenkel. Schottky believes that the ions which leave the points of the lattice because of thermal fluctuations form the new layers of the normal crystalline lattice. The vacancies (holes) which are formed in this process are moving into the crystal and a "pair" of vacancies (anionic and cationic) represent a defect, according to Schottky.

It should be noted that the crystals with porous structure, in which the ions are not packed very tightly and differ quite significantly in terms of their size, are the most favorable for ionic movement within the interpoint space of the crystalline lattice. The comparison of calculated and experimental data shows that the electrical conductivity of the alkaline-haloid crystals and the haloid-silver compounds is associated with the presence of defects, in accordance with Schottky and Frenkel. For the conductivities under consideration, the electrical conductivity as a function of temperature obeys the same law

$$\sigma = \sigma_0 e^{-E_a/kT}.$$

As we can see, the current in dielectrics is brought about by the movement of the defects, which, being acted upon by the external electrical field, becomes well-ordered.

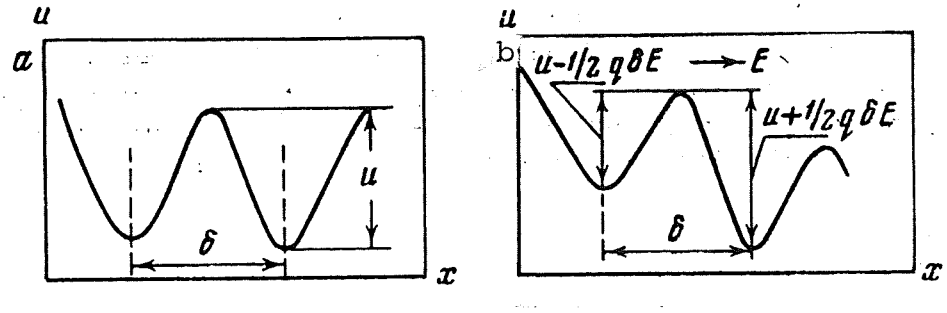

Figure 5. Systematic depiction of the potential energy of the interpoint space ion; a - in the presence of thermodynamic equilibrium; b - with the application of the electrical field.

In the absence of such field, the weakly bound ion may occupy two positions, equally probable (Figure 5a) and the frequency of its transfer, in the presence of thermodynamic equilibrium, is described by the following formula /15

$$W = \nu e^{-u/kT},$$

where ν is the frequency of ionic oscillations, k is the Boltzmann constant, T is the absolute temperature and u is the free activation energy, according to Gibbs, or the height of the potential barrier.

As the electrical field is being applied, the magnitude of the potential energy of the ion, which has the q charge, will change by $qE\delta/2$ at the $\delta/2$ distance. As a result, the number of transfers along the field will begin to exceed the number of transfers against the field. It is clear that the total number of ions intersecting a unit of surface area per unit of time is equal to the difference in the number of transfers in the direction of the field W', and in the opposite direction W", in other words

$$W' - W'' = \nu\left[e^{-\frac{u-\frac{q\delta E}{2}}{kT}} - e^{\frac{-u+\frac{q\delta E}{2}}{kT}}\right] = \nu e^{-\frac{u}{kT}}\left[e^{-\frac{q\delta E}{2kT}} - e^{\frac{q\delta E}{2kT}}\right].$$

By expanding into a series the $e^{q\delta E/kT}$ expression and limiting ourselves to the first term of expansion, we will obtain from the last expression the following

$$W' - W'' = W \cdot \frac{q\delta E}{kT}.$$

The speed of ion movement in this case will be expressed as follows

$$v = (W' - W'')\,\delta = W\frac{q\delta^2 E}{kT} = \frac{qE\delta^2\nu}{kT}e^{-\frac{u}{kT}}.$$

The concentration of defects n_t which corresponds to the number of the current carriers at a given temperature, is determined from the following relationship

$$n_t = n_0 e^{-\frac{u_q}{kT}},$$

where n_0 is the total number of ions per 1 cm^3, u_q is the dissociation energy, which is also being called the free thermodynamic energy of the defect formation, according to Frenkel or Schottky. By substituting the values of υ into the expressions for electrical conductivity $\sigma=j/E$, we will obtain

$$\sigma_t = \frac{nqv}{E} = \frac{n_0 q^2 \delta^2 v}{kT} e^{-\frac{u_q+u}{kT}} = \sigma_0 e^{-\frac{E_0}{kT}},$$

where E_0 is the activation energy of the current carriers, and it is equal to the sum of two energies, one which is being expended for the defect formation u_q and the second one, u, for the defect movement. In the low temperature range, E_0 is small and is considerably smaller than at high temperatures, since in the first case, it is equal to the energy, necessary only to induce the migration of already existing current carriers (the impurity ions), while at the high temperatures, the intrinsic defects are the result of the increased temperature and therefore, some additional energy will be required. /16

In a number of cases, the activation energy of the current carriers coincides, in terms of magnitude, with the activation energy defined by the diffusion methods, which indicate a similar mechanism of the ion movement during the diffusion and the current movement in the material. The following relationship exists between the coefficient of diffusion $D=D_0 e^{-\frac{E_0}{kT}}$ (D_0 is the pre-exponential multiplier, E_0 is the diffusion activation energy) and the electrical conductivity

$$\sigma = D\frac{nq^2}{kT},$$

where n is the number of pairs per unit volume. The disagreement between activation energy or mobility, generated by different methods is explained by the fact that not all diffusion processes result in the development of current.

2. Equipment and Methods to Measure the Electrical Conductivity in Rocks at High Temperatures

The temperature range in which the rocks of which the Earth's crust and upper part of the mantle are composed is between 20 and 1400°C. In the presence of atmospheric pressure, the majority of rocks would either partially or completely melt at such temperatures, and therefore the measurements were carried out primarily while heating the samples up to 1100°C. In the experiments with the rocks of high melting point, the temperature was increased to 1200°C. For heating purposes, the electric oven, specially designed in the laboratory, was used. The heating element of the oven was made of nichrome wire, with R=10-12 ohms, which was wound in a bifilar fashion on a quartz tube of 40 mm diameter and 180 mm high. Asbestos, 50 mm thick, was employed for thermal

insulation. The oven was connected to a 127 V main by means of a transformer RNO-250-2. The maximum current at t=1100°C was 6A.

In measuring the electrical conductivity of the rocks, the common requirement is the minimum transition resistivity between the electrode and the sample. A reliable contact between the electrode and the sample is the major obstacle in the experiments, while measuring the electrical conductivity at high temperatures. At the temperatures above 300-350°C, the graphite electrodes cannot be used because of graphite burn-out and the silver electrodes cannot be used because of the diffusion of silver, into the sample. For the temperatures above 400°C, gold or platinum electrodes are /17 recommended, which are made by sputtering in vacuum [18] and quite good results may be obtained by using the celite electrodes. In our experiments, we have utilized platinum foil for the electrodes, the foil was 0.05 mm thick and was pressed toward the sample surface, the force being 15-20 kg.

The diagram of our assembly is shown in Figure 6. The rock sample with the electrodes was mounted horizontally between two ceramic discs, which were used simultaneously as insulators and which helped to improve the contact between the electrodes and the sample. The sample, platinum electrodes and insulators were mounted between the ceramic holders which were of cylindrical shape, 150 mm long and 25 mm in diameter. The ceramic holders were placed into a bracketed holder, the upper part of which features a spring-loaded cup, creating a uniform and constant load during the whole experiment, exerted on the sample with the electrode.

For the measurement of temperature, we have used the platinum platinum-rhodium thermocouple, the junction of which was placed at the opening of the ceramic disk. This made it possible to measure with a sufficient degree of accuracy (±5°C), the temperature of the sample, by using the instrument of MPP-254M type. The platinum terminals from the electrodes and from the thermocouple were placed into the ceramic tubes for the purpose of insulation. The rock sample may be in the shape of a cube, a parallelepiped, a cylinder or a disk. The major requirement is to have the parallel faces and well-polished face surfaces. In addition, the rock sample must be several times larger than grain size, since in the opposite case it would not be representative, because of the predominant role of the separate minerals in the sample, their random combination or the lack of structural homogeneity. The reproducibility of measured results, by using two samples, cut out of the same piece of rock, depends on the homegeneity of the rock and a significant scatter of the electrical conductivity values is due to the non-uniform distribution of the ores and the minerals which conduct the current quite well.

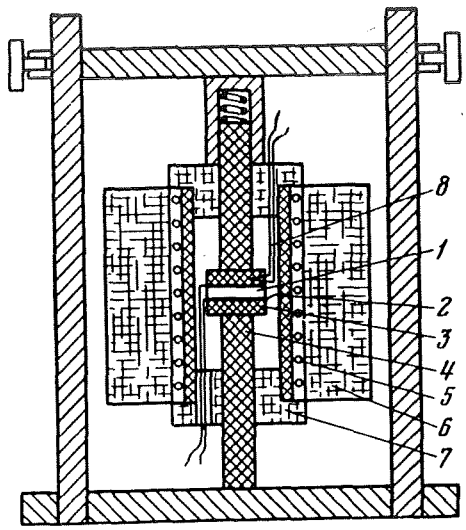

Figure 6. Schematic diagram of the assembly to measure the electrical conductivity in the rocks at high temperatures.
1 - sample; 2 - electrodes; 3 - ceramic disk; 4 - ceramic cylinder; 5 - quartz tube; 6 - oven; 7 - ceramic sleave; 8 - thermocouple.

The studies were conducted by using the samples cut out from the centers of the rocks. The samples were in the shape of disks of 20-30 mm diameter and 3-5 mm thick. /18 The sample working surfaces were polished and the parallelism face deviation was ±0.01 mm.

The methods and instruments used to determine the electrical conductivity in the semiconductors and dielectrics, in the laboratory conditions, are also applicable for measuring the electrical conductivity of the rocks. The first methods make use of the d.c. current and the second method - a.c. current. Because of the frequency dispersion in the electrical conductivity of the rocks, particularly noticeable at $\rho > 10^6$ ohm^1·cm^1 and at the frequencies above 10^3 Hz, one should utilize the current of not more than 10^3 Hz frequency. This helps to exclude the high voltage polarization effect.

The study [19] presents the most widely used methods and approaches and also describes the instruments which are used to measure the electrical conductivity of the rocks. In our experiments, we used as the measuring devices, depending on the magnitude of the electrical resistivity of the rock, the teraometer E6-3 ($\rho > 10^5$ ohm) or the bridge of R-333 type ($\rho < 10^5$ ohm) and also, the tester TT-3.

For the sake of homogeneous temperature distribution, the sample was kept at constant temperature between 5 and 15 minutes, depending on the sample size, and prior to the beginning of measurements, in order to remove completely the moisture, the sample was kept at t=200°C for several hours.

The electrical conductivity of the rocks at high temperatures was determined on the basis of its average values, measured by passing the current in two mutually opposing directions.

The control measurements, by using the samples, cleaned first with alcohol and well dried, produced similar results either by employing the protective ring or omitting it. Therefore, the measurement of electrical conductivity of the rocks at high temperatures was carried out without the protective ring.

The reproducibility of electrical conductivity in the course of several cyclic heatings and also by heating and cooling the sample, depends on the petrochemical nature of the rock, and on its thermochemical stability. If the rocks contained relatively high percent of iron oxide, or if one detected a region of the anomalous electrical conductivity which is due to the irreversible changes in the rocks, the shapes of the curves, describing the electrical conductivity as the function of temperature, while heating and cooling the sample, do not quite coincide.

CHAPTER TWO. ELECTRICAL CONDUCTIVITY IN THE MINERALS AT HIGH TEMPERATURES

The rock samples differ from each other in terms of the elastic and electrical properties [20, 21]. To elucidate the reasons for such a large range of electrical conductivity in the rocks, one must first of all obtain the data as to the electrical conductivity in the components of the rock. Quantitatively speaking, in all rocks, the solid phase formed by different minerals will predominate. The physical properties of the rocks depend, in a rather complex fashion, on the physical properties of the rock-forming minerals and sometimes, also on the secondary, in terms of importance, minerals. In conjuction with this, let us first consider the electrical properties of the major minerals which are of greatest importance in the elucidation of the mechanism of electrical conductance in such multiphase materials as rocks, at high temperatures. /19

1. Oxides

The predominant oxygen-containing compounds in the Earth's crust are in the form of oxides and various salts. Almost all of them have crystalline structure, with ionic bonding of structural units.

The corundum, Al_2O_3 is found in there polymorphous modifications - two hexagonal (α and β) and one cubic (γ) symmetries. The first of these is the most stable in nature and it is being formed at the temperature of 500-1500°. The conversion to α and β modification at 1500-1800° is the results of rather slow cooling The γ Al_2O_3 is of crystalline structure of spinel type. In the corundum α and β modifications, the oxygen ions feature the tightest hexagonal packing, forming layers superimposed on each other, perpendicular to the triple axis. The aluminum cations are located hexagonally, in the spaces between the layers. The electrical conductivity of corundum has been investigated by using the samples made of ceramics of different purity and by using the monocrystal samples. The results of measurements which will be presented below indicate that the electrical conductivity of the monocrystalline corundum is lower than its caked difference [22]. The presence in corundum ceramics of even a small quantity of impurities increases significantly its electrical conductivity (see page 20). /20

It should be noted that the electrical conductivity of aluminum oxide at high temperatures depends on the medium in which the measurements are being taken and on the type of electrodes [23].

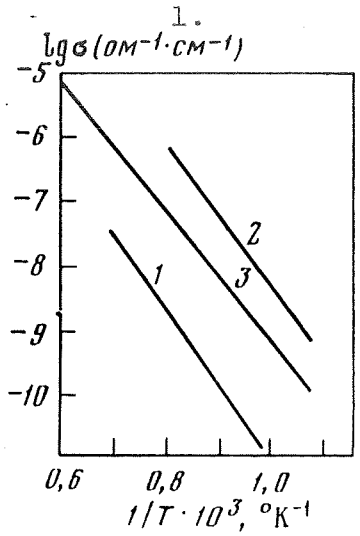

Figure 7. Electrical conductivity of MgO as a function of temperature.

At E_0, eV: 1 - 2.2 [24]; 2 - 2.3 [26]; 3 - 2.0 [25].

Key: 1. $ohm^{-1} \cdot cm^{-1}$

In the hydrogen environment the electrical conductivity of corundum is lower than in the air. In addition, it will be the lowest in the case of platinum electrodes which is related to the difference of the emission components of electrical conductivity. The activation energy of corundum at the temperature below 900°, is 2.2 eV, and in the range of 900-1050°C, it is equal to 0.8 eV [23]. The change in the activation energy is related to the absorption by corundum of some oxygen [23].

The magnesium oxide MgO is present only in one modification, which is the periclase mineral of cubic symmetry. The mineral frequently contains the isomorphous admixtures of FeO, MnO, ZnO (up to 10%) and is associated with the limestones which are found near active volcanoes. The electrical conductivity of periclase at low temperatures depends significantly on these impurities. The admixtures, even in the amounts of 1%, may increase the electrical conductivity by two orders of magnitude. At temperatures above 800°C the effect of impurities is insignificant. However, the difference in the electrical conductivity ($ohm^{-1} \cdot cm^{-1}$) of spectrally pure and technically pure magnesium oxide is also retained at high temperature (see page 20).

For the temperatures below 800°C, very pure periclase is characterized by σ which at 300°C is 10^{-14}-10^{-15} and at 700°C - $4.3 10^{-10}$ $ohm^{-1} \cdot cm^{-1}$. Figure 7 shows the electrical conductivity of magnesium oxide as a function of temperature, under different experimental conditions. In spite of some disagreement in the electrical conductivities, the activation energy is close to 2.0 eV. The dissimilar σ for the same temperatures is explained by the differences in experimental techniques and the methods of sample preparation. In the studies [22-26] one can find more information as to the electrical conductivity of MgO.

In terms of the electrical conductivity, magnesium oxide should be included into the dielectric group, but in recent years, many researchers have shown its semiconducting properties [24-27].

The calcium oxide CaO in its pure form in nature is hardly ever encountered. But calcium compounds, in particular the bicarbonate salts, are frequently encountered as marble, limestones and chalk.

Electrical conductivity of corundum materials /21

Temperature, °C	14	100	200	300	600	800	900	1000	1100
Electrical conductivity $ohm^{-1} \cdot cm^{-1}$									
Corundum ceramics	10^{-16}	$5{,}0 \cdot 10^{-16}$	$2{,}5 \cdot 10^{-15}$	$3{,}3 \cdot 10^{-14}$	—	$2{,}9 \cdot 10^{-9}$	—	—	—
Corundum material with 1% impurities	$3{,}0 \cdot 10^{-15}$	$3{,}3 \cdot 10^{-15}$	—	$8{,}0 \cdot 10^{-12}$	10^{-8}	—	—	—	—
Caked corundum	—	—	—	—	—	—	$1{,}0 \cdot 10^{-6}$	$2{,}5 \div 5{,}0 \cdot 10^{-6}$	$1{,}1 \div 1{,}4 \cdot 10^{-5}$
Monocrystal	—	—	—	—	—	—	$1{,}1 \div 1{,}0 \cdot 10^{-10}$	$10^{-8} \div 2{,}0 \cdot 10^{-9}$	$10^{-7} \div 2{,}5 \cdot 10^{-8}$

Electrical conductivity of magnesium oxide

Temperature, °C	800	950	1000	1100	1200	1300
Magnesium oxide						
Technically pure	—	$8{,}3 \cdot 10^{-6}$	$1{,}0 \cdot 10^{-5}$	$1{,}6 \cdot 10^{-5}$	$3{,}3 \cdot 10^{-5}$	$3{,}3 \cdot 10^{-4}$
Spectrometrically pure	$2{,}5 \cdot 10^{-12}$	$8{,}3 \cdot 10^{-11}$	$1{,}4 \cdot 10^{-9}$	$1{,}6 \cdot 10^{-8}$	$1{,}3 \cdot 10^{-7}$	$1{,}0 \cdot 10^{-6}$

[Commas in tabulated material are equivalent to decimal points.]

Calcium oxide has the cubic symmetry. The electrical conductivity of caked powders of CaO at high temperatures has been investigated by Miake [22], Hauffe and Tränckler [28] and Norton [22]. /22

These investigators have pointed out the decrease of electrical conductivity from 10^{-2} to 10^{-7} $ohm^{-1} \cdot cm^{-1}$ at the elevated oxygen pressure from 10^{-6} to 10^{-2} mm of mercury. Any further increase of oxygen pressure from 10^{-2} to 10^{2} mm of mercury result in the uniform increase of electrical conductivity. The minimum σ is explained by the change of the mechanism of electrical conductivity from n type to p type.

According to the data by Norton [22], the electrical conductivity of calcium oxide at high temperatures is as follows

Temperature, °C	763	930	1235	1370	1460
Specific electrical conductivity, $ohm^{-1} \cdot cm^{-1}$	$1,4 \cdot 10^{-8}$	$2,4 \cdot 10^{-7}$	10^{-5}	$5,0 \cdot 10^{-4}$	$1,1 \cdot 10^{-3}$

[Commas in tabulated material above are equivalent to decimal points.]

The activation energy fluctuates between 1.6 and 2.9 eV and depends on the manner in which the sample has been prepared and on the heating rate [22].

Spinel group. The compounds having a general formula MeR_2O_4, where Me and R are the two and trivalent cations, are being called the spinels. They are characterized by the crystallin lattice of cubic system. Many spinels are encountered in nature as minerals. The minerals of this group are formed predominantly at high temperatures and pressures. All natural spinels have a complex composition and contain different two and trivalent cations. For example, the spinel of (Mg, Fe) Al_2O_4 type will be green in color because of replacement of Mg ions by Fe ions. Pure spinels are obtained only synthetically and they may be subdivided into three groups [29]: the aluminates, chromates and ferrites which are characterized by specific parameters of the lattice and by specific electrical conductivity (Table 2).

TABLE 2. SOME PROPERTIES OF SPINELS [29]

Chemical formula	Lattice parameter, Å	Specific weight, g/cm^3	Electrical conductivity at 900°C, $ohm^{-1} \cdot cm^{-1}$	Type of conductivity
$MgAl_2O_4$	8,09	3,55	$1,3 \cdot 10^{-6}$	Electron
$NiAl_2O_4$	8,03	4,52	$2,9 \cdot 10^{-6}$	Hole
$ZnAl_2O_4$	8,06	4,64	$5,3 \cdot 10^{-6}$	Electron
$CoAl_2O_4$	8,08	4,44	$8,5 \cdot 10^{-6}$	Hole
$ZnCr_2O_4$	8,3	5,41	$1,1 \cdot 10^{-3}$	»
$MgCr_2O_4$	8,31	5,41	$1,1 \cdot 10^{-4}$	»
$CoCr_2O_4$	8,31	5,24	$2,5 \cdot 10^{-3}$	»
$FeCr_2O_4$	8,34	5,11	$1,8 \cdot 10^{-3}$	»
$MgFe_2O_4$	8,37	4,51	$4,0 \cdot 10^{-2}$	Electron
$NiFe_2O_4$	8,31	5,41	$1,9 \cdot 10^{-2}$	»
$ZnFe_2O_4$	8,42	5,35	$1,25 \cdot 10^{-2}$	»

[Note: Commas in tabulated material are equivalent to decimal points.]

It follows from the data shown in Table 2 that with the increase of the lattice parameter, the electrical conductivity of spinels increases. Of defining nature, in regard to the electrical conductivity for this group of compounds, is not the type of cation metal, but the type of R_2O_4. /23

The magnetites $FeFe_2O_4$ contains FeO - 31% and Fe_2O_4 - 69%. It is characterized by the ionic bonding and has the crystalline structure which is analogous to the structure of spinel. The magnetite belongs to the class of ferrites. The mechanism of electrical conductivity in ferrites differs from the mechanism of conductivity in the semiconductor of germanium and silicon type, having a longer free path of the current carriers. In the magnetites the Fe^{2+} and Fe^{3+} ions at $t>120^{\circ}K$ are located within the octahedrons. As a result of thermal motion, the electrons move from one iron ion to the neighboring one which has a different valence. With the temperature increase, the probability of such transfer increases. Figure 8 shows the $\lg \sigma = f(1/T)$ relationship for three types of ferrites. They are characterized by a sharp bending point at temperatures of Curie point. This specificity can be followed through by comparing the data presented below:

Ferrite	Temperature at the bending point, °C	Curie temperature, °C
Copper	480	480
Nickel	595	590
Manganese	335	315

In some cases, in the temperature range between 390 and 500°C, because of the oxygen absorption by the ferrite, one observes not the increase, but decrease of electrical conductivity [30]. At higher temperatures, one observes the reduction of iron which is due to the loss of oxygen. This process results in a sharp increase of electrical conductivity. Some data as to the character of electrical conductivity as a function of temperature for different ferrites is presented in the studies [30-33]. /24

The electrical conductivity of magnetite may vary appreciably, depending on the nature of impurities. For example, the electrical conductivity of magnetite with the increase in it of spinel $MgCr_2O_4$, thus forming a solid solution, will increase, something which can be seen in Figure 9. The decrease of electrical conductivity in the Fe_3O_4 - $MgCr_2O_4$ system in this case is due to the fact that the introduced ions of magnesium and chromium do not take part in the recharging of Fe^{2+} and Fe^{3+}.

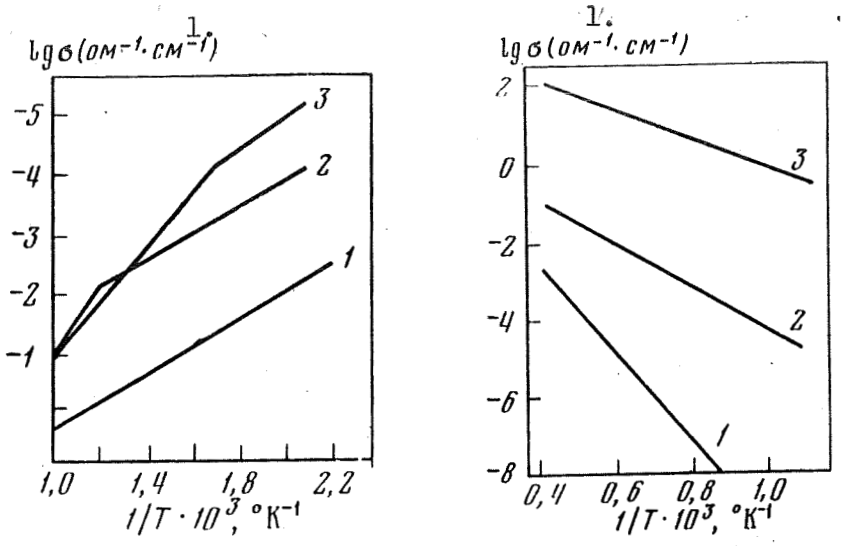

Figure 8. Electrical conductivity as a function of temperature for different ferrites.
1 - copper; 2 - nickel; 3 - manganese. Key: 1. $ohm^{-1} \cdot cm^{-1}$

Figure 9. Electrical conductivity of Fe_3O_4 as a function of temperature.
Amount of $MgCr_2O_4$, %: 1 - 49.4; 2 - 39.4; 3 - 1

Key: 1. $ohm^{-1} \cdot cm^{-1}$

Hematite α-Fe_2O_3. There are two known polymorphous modifications of the iron oxide found in nature, the stable trigonal α-Fe_2O_3 and the unstable cubic β-Fe_2O_3. Sometimes one finds in it the isomorphous impurities of titanium (titanium magnetite) and of magnetite. Let us consider only some results of the studies of electrical conductivity in hematite of different purity at high temperatures [34, 35]. It has been established that the α-Fe_2O_3 samples containing a high percentage of impurities have much lower electrical conductivity than the samples in which these impurities are only in trace amounts. For the hematite with impurities, for a broad temperature range (20-1350°C) one observes the linear relationship between lg σ and 1/T (Figure 10).

The following values of E_0 and σ_0 parameters have been obtained:

No. of sample	$\sigma_0 \cdot 10^3 \cdot ohm^{-1} \cdot cm^{-1}$	E_0, eV
1	40.8	1.18
2	21.1	1.17
3	12.6	1.17
4	0.74	1.03

As one can see, the activation energy E_0 is comparatively stable.

The electrical conductivity of high purity hematite as one increases the temperature has no linear relationship. On the $\lg \sigma = f(1/T)$ curve, one can separate three regions with different values of E_0 parameter (see Figure 10).

A region: $E_0 \simeq 0.7$ eV, $t < 450^\circ$C.

B region: $E_0 \simeq 0.1$ eV, $450^\circ C > t < 800^\circ$C.

C region: $E_0 \simeq 1.0$ eV, $t > 800^\circ$C.

The appearance of A region is associated with the oxidations which take place at the grain boundary, the B region is associated with the change in mobility of the current carriers, and finally, the C region is associated with the change in concentration of the current carriers. The latter is substantiated by the fact that the electrical conductivity of monocrystalline and polycrystalline samples, containing a considerable amount of impurities and having practically zero impurities, are all falling on a straight line.

The iron oxide may be a semiconductor of either n or p type, depending on the cation valence. /25

It should be pointed out that the electrical conductivity in $Ti_xFe_{2-x}O_3$ is affected particularly strongly by the amount of titanium. As one can see in Figure 11, iron oxide (an insulator having $\sigma = 10^{-10}$ ohm^{-1}cm^{-1}), after adding some titanium to it, becomes a good electrical conductor [36].

Quartz group. The minerals of this group represent a series of polymorphous modifications of SiO_2. In terms of the crystalline structure, they occupy a special position among the oxides, since their structure has a direct relationship to the silicates. The crystalline structure of quartz, just like its other polymorphous modifications, is characterized by the fact that the Si^+ is always found in the quaternary surrounding of oxygen ions, located at the tetrahedron apexes. Each apex of such tetrahedron is also the apex of the adjoining tetrahedron.

The electrical conductivity of quartz, as a function of temperature, was investigated by a number of researchers [37], as well as by us, by using the artificially grown and natural crystals. The measurements refer to two crystallographic directions, along the optical and along the electrical axes. In addition, in the case of natural quartz, the electrical conductivity was determined along the mechanical axis, in other words in the

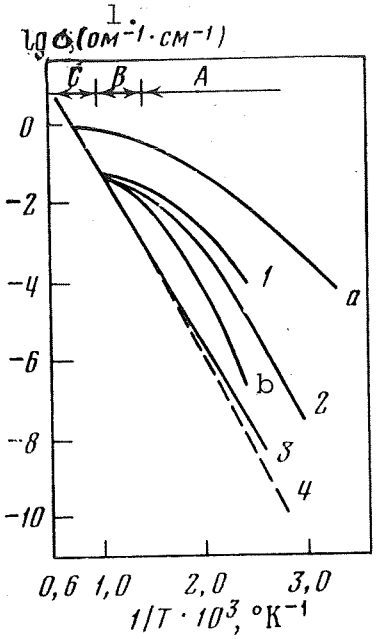

Figure 10. Electrical conductivity of Fe_2O_3 as a function of temperature.
1, 2 are the samples containing the traces of impurities. 3 and 4 have a considerable amount of impurities; a - 0.05% Mg; b - 0.0288% Mn.
Key: 1. $ohm^{-1} \cdot cm^{-1}$

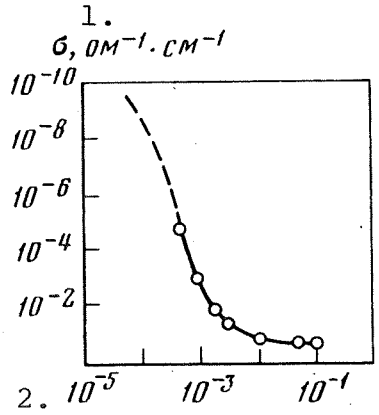

Figure 11. Electrical conductivity of $Ti_xFe_{2-x}O_3$ at 23°C as a function of the amount of Ti.
Key: 1. $ohm^{-1} \cdot cm^{-1}$; 2. Amount of x in $Ti_xFe_{2-x}O_3$

y direction. It is known that α quartz at t=573°C (modified) becomes high temperature β quartz, which is crystallized as a hexagonal syngenesis. It appeared that in connection with the displacement of the centers of the silicon-oxygen tetrahedrons, which takes place at 573°C, one would be able to observe a sharp bend in lg σ=f(1/T) curve. However, we have not observed any clearly defined changes in the electrical conductivity as the temperature was changed. For the man-made quartz, as one can see in Figure 12, the lg σ= =f(1/T) relationship is defined by a straight line in the two crystallographic directions, with a low activation energy, equal to 0.86-0.89 eV. In the case of natural quartz, one observes the anomalous breaks in the curve in the temperature range 600-700°C and in the high temperature range it was possible to observe high activation energies, as compared to the former (Table 3). At 870°, the β quartz becomes β tridomite. This transition occurs slowly and is accompanied by a considerable change in the volume and in the specific weight (the specific weight of βquartz is 2.51 g/cm^3 and that of β tridomite - 2.26 g/cm^3) and it appears that during a slow change of electrical conductivity this phenomenon will manifest itself at the appropriate temperature change. /26

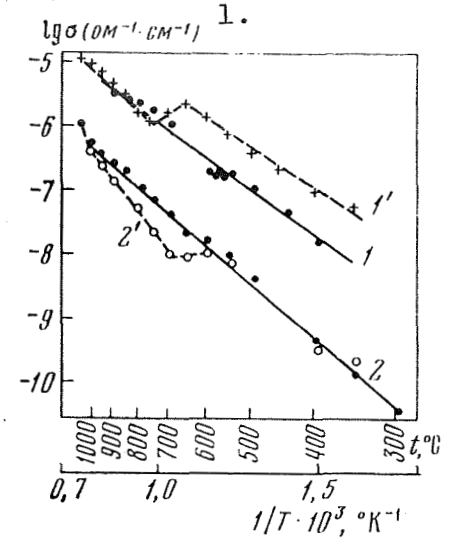

Figure 12. Electrical conductivity of natural (1',2') and artificially grown (1,2) quartz.

1, 1' - along the optical axis; 2, 2' - along the electrical axis.

Key: 1. $ohm^{-1}.cm^{-1}$

One should note a rather strong anisotropy of the electrical conductivity which was observed in measuring σ along the optical axis C (z) and the electrical axis x. The analogous anisotropy manifests itself in the case of the elastic wave rates, although in such case, it is not as sharply defined. It is interesting that the maximum electrical conductivity along the optical axis of quartz correlates well with the intensive increase of the dielectric penetrability, as one increases the temperature to 200°C and the greatest velocity of the longitudinal waves. The anisotropy of physical and mechanical properties of quartz is explained by its structure. The crystalline structure of quartz consists of a number of tetrahedrons, tightly connected to each other and packed more densely along the optical axis than along the electrical one. It appears that such tighter packing of ions along the optical axis also brings about higher rates of longitudinal wave V_p, facilitatiing the increase of polarizability and the latter defines the increased electrical conductivity. On the whole, the oxygen packing of ions in quartz is not too tight. The tetrahedral structures feature some vacancies. In the low temperature modifications, they are of small size and in the high temperature modifications, which are not as dense, they are of larger size. The bonding in all modifications is the same - through the tetrahedron apexes, but the orientation and general symmetry of tetrahedron location is different.

TABLE 3. ELECTRICAL CONDUCTIVITY (in $ohm^{-1} \cdot cm^{-1}$) OF QUARTZ

Monocrystal	axis	Temperature, °C									Temperature range t, °C	E_a, eV	$\lg \sigma_0$, $ohm^{-1} \times cm^{-1}$
		200	300	400	500	600	700	800	900	1000			
Man-made	x	10^{-12}	$3,7 \cdot 10^{-11}$	$4,8 \cdot 10^{-10}$	$4,4 \cdot 10^{-9}$	$2,1 \cdot 10^{-8}$	$6,5 \cdot 10^{-8}$	$9,0 \cdot 10^{-8}$	$4,5 \cdot 10^{-7}$	$3,1 \cdot 10^{-7}$	200—900	0,86	—3,0
	z	—	$3,6 \cdot 10^{-10}$	$1,7 \cdot 10^{-8}$	$1,0 \cdot 10^{-7}$	$2,5 \cdot 10^{-7}$	$9,8 \cdot 10^{-6}$	$4,4 \cdot 10^{-5}$	$3,5 \cdot 10^{-5}$	—	200—1000	0,89	—3,75
Natural	x	10^{-12}	$8,6 \cdot 10^{-11}$	$2,3 \cdot 10^{-10}$	$6,0 \cdot 10^{-10}$	$8,6 \cdot 10^{-9}$	10^{-8}	$4,6 \cdot 10^{-8}$	$1,2 \cdot 10^{-7}$	$3,7 \cdot 10^{-7}$	600—1050	1,4	—2,9
	x^*	—	—	$7,1 \cdot 10^{-11}$	—	—	$6,2 \cdot 10^{-8}$	—	—	$5 \cdot 10^{-6}$	200—1200	1,36	—1,9
	y	10^{-9}	$1,3 \cdot 10^{-9}$	10^{-9}	$3,4 \cdot 10^{-9}$	$3,7 \cdot 10^{-8}$	$5,1 \cdot 10^{-8}$	$5,9 \cdot 10^{-8}$	10^{-8}	$1,9 \cdot 10^{-7}$	800—1050	0,88	—2,4
	y	$4,5 \cdot 10^{-10}$	10^{-9}	$7,4 \cdot 10^{-8}$	$3,2 \cdot 10^{-7}$	$1,25 \cdot 10^{-6}$	$1,2 \cdot 5^{-6}$	$1,6 \cdot 10^{-6}$	$3,7 \cdot 10^{-6}$	10^{-6}	750—1050	1,0	—1,25

*The sample was cut out of a monocrystal of different origin.

[Note. Commas in tabulated material are equivalent to decimal points.]

Below we shall present the above-mentioned parameters for the quartz monocrystal: /28

Parameter	Temperature, °C	Along the optical axis z	Along the electrical axis x
Electrical conductivity, $ohm^{-1} \cdot cm^{-1}$	20	$1.0 \cdot 10^{-14}$	$5.0 \cdot 10^{-17}$
	300	$1.4 \cdot 10^{-8}$-$3.6 \cdot 10^{-10}$	$3.7 \cdot 10^{-11}$
Dielectric penetrability, ε	20	4,55	4.49
	300	20.0*	4.5
Velocity of longitudinal waves, km/s	20	6.3-6.7	5.1-5.4

*Frequency f=40 kHz

By generalizing all the experimental data, the following conclusions can be made.

1. The major factors which define the electrical properties of minerals - the oxides in a broad temperature range, are the: a) metal type, which plays the role of the cation; b) the structural specific features of the oxide; c) the number and specifics of the impurities; d) the energy-related parameters (the ionization energy of the cations and the lattice energy); e) the "history" of the mineral, by which we mean the preliminary thermal treatment of the sample; f) the composition of gaseous environment in which the sample was placed at high temperatures.

2. The high insulation properties of corundum, of the periclase and of calcium oxide are related to the presence in these oxides of ionic bonds and the small ionic radii of the cations, which display only slight polarizability. One observes for this group of minerals a specific relationship between the electrical conductivity and the cation radius, the polarizability and also the energy of the crystalline lattice, which can be seen from the data presented below:

Cation	σ_{1000°, $ohm^{-1} \cdot cm^{-1}$	Cation radius $\cdot 10^{8}$, cm	Polarizability $\alpha \cdot 10^{24}$, cm^3	Lattice energy, eV per ion pair
Al^{3+}	10^{-9}	0.57	0.037	157.0
Mg^{2+}	$1.4 \cdot 10^{-9}$	0.78	0.114	41.36
Ca^{3+}	10^{-7}	1.06	0.531	37.53

The increase of electrical conductivity as a function of the cation radius increase is explained in the following manner. In its first approximation, one may assume that the ionization energy W is related to the ion radius r in the following way, $W=q^2/r$, where q is the ion charge. Consequently, the radius increase results in the decrease of the ionization energy, which facilitates the increase of the electrical conductivity.

The increase of electrical conductivity in oxides, which is /29
the function of polarizability increase, is due to the fact that the polarizability decreases to a considerable degree the energy which is needed to bring about the transition from the normal state of the ion to the interpoint position, or to the movement into the unoccupied lattice point, and as one can see, the electrical conductivity is also directly related to the energy of the lattice, which correlates well with the theory.

With the decrease of the lattice energy, one observes a consistent decrease of the activation energy in the particles, the decrease of specific weight and of hardness in the case of Al_2O_3, MgO and CaO oxides (Table 4). The relatively low temperature of melting of corundum drops from the consideration of these relationships, if we are to assume the direct relationship between the melting temperature and the lattice energy, and it should be higher than in the case of periclase.

3. In terms of the electrical conductivity at $t=900^\circ C$, the spinels are divided into three groups: the aluminates which have a very low electrical conductivity (10^{-6} $ohm^{-1} \cdot cm^{-1}$), chromites - intermediate conductivity ($10^{-3} ohm^{-1} \cdot cm^{-1}$) and ferrites which have high conductivity ($10^{-2} ohm^{-1} \cdot cm^{-1}$). The magnitude of electrical conductivity depends on the chemical nature of the compounds and bonding.

In the case of the spinel group, one can trace out a direct relationship between the electrical conductivity and the lattice parameter, which gives us reason to assume that as this parameter

TABLE 4. COMPREHENSIVE TABLE OF PHYSICAL PROPERTIES OF MINERALS - OXIDES

Mineral	Chemical formula	Symmetry type	Lattice constant	Specific weight, g/cm^3	Impact hardness	t_m, °C	σ, ohm$^{-1}\cdot$cm^{-1} 300°C	σ, ohm$^{-1}\cdot$cm^{-1} 900°C	E_0 in region of intrinsic conductivity	σ_0, ohm$^{-1}\times$cm^{-1}	Remarks
Corundum	α-Al_2O_3	Trigonal	5.12 (distance between lattice layers (2,16)	3,95—4,01	9	2040	$3,3\cdot10^{-14}$	$1,0\cdot10^{-6}$	2,2	—	Ceramic
								$1,1\cdot10^{-10}$	—	$2,0\cdot10^{4}$	Monocrystal
Periclase	MgO	Cubic	4,2	3,56—3,65	5,5—6,0	2800	—	$8,3\cdot10^{-6}$	2,0÷2,3	—	Technically pure
						±13		$8,3\cdot10^{-11}$	—	—	Spectrometrically pure
Calcium oxide	CaO	"	4,799	3,35	4,5	2570 ±10	—	$2,3\cdot10^{-7}$	1,6÷2,9	—	
Spinel	$MgAl_2O_4$	"	8,09	3,5—3,7	8	2150	—	$1,3\cdot10^{-6}$	—	—	Electron conductivity
	$MgCr_2O_4$	"	8,31	5,41	—	—	—	$1,1\cdot10^{-4}$	—	—	Hole conductivity
	$MgFe_2O_4$	"	8,37	4,51	—	1750	—	$4,0\cdot10^{-2}$	—	—	Electron conductivity
Magnetite	$FeFe_2O_4$	"	8,374	4,9—5,2	5,5—6,0	1597	—	—	—	—	
Hematite	α-Fe_2O_3	Trigonal	5,029	5,0—5,2	—	—	—	—	1,0	$2,0\cdot10^{4}$	
Quartz	SiO_2	"	4,904	2,5—2,8	7,0	1713	$3,6\cdot10^{-10}$÷ ÷$3,7\cdot10^{-11}$	$3,5\cdot10^{-5}$÷ ÷$4,5\cdot10^{-7}$	0,89	10^{-3}	

[Note. Commas in tabulated material are equivalent to decimal points.]

is increased, the lattice energy will decrease. This is substantiated in some degree by the corresponding change in the specific weight of spinels, the exception from this rule is only the spinel $MgFe_2O_4$ (see Table 4). As one can see, the replacement of Cr^{2+} ion by Fe in $MeCr_2O_4$ results in a sharp increase of electrical conductivity, althouth the lattice parameter in this case changes only slightly.

4. The hematite and magnetite are the oxides of transition metals which do not have many properties characteristic for the semiconductors of silicon and germanium type. In the case of the former, one does not observe the Hall effect and photo conductivity. Therefore, the study of the charge transfer is based primarily on the measurement of the t.-e.m.f. and of the electrical conductivity. In the oxides of transition metals, the electrical conductivity is brought about by the electron transfer from the ion which has one valence to the other ion of different valences. For example, the presence in magnetites, simultaneously, of Fe^{3+} and Fe^{2+} facilitates and easy electron exchange. If however, one is to replace either all Fe^{2+} ions or part of them by the ions of some other bi-valent metals, the electrical conductivity of ferrites will decrease. This phenomenon may be explained qualitatively in that for the electron transfer from the ion of some other bi-valent metal, a greater energy would be required. The mobility of current carriers in this case is rather low and will exponentially increase with the temperature increase.

5. The quartz manifests a rather strong anisotropy of electrical conductivity in two crystallographic directions, which is due to the structural features of quartz.

2. Haloid Compounds /31

The majority of minerals in this group are primarily the light metal halogenoids, referring to the compounds with purely ionic bondings (heteropolar). Among the minerals of this class we shall consider the three most widely found compounds in nature: the halite, sylvite and fluorite. These minerals have cations with relatively large ionic radii and small charge and therefore, they have a low specific weight, they are easily soluble and have low melting temperature.

The halite NaCl and sylvite KCl are characterized by similar electrical parameters (Table 5), which is explained by similar structure and similar properties of the respective cations. The study of different purities of these minerals indicates that the impurities affect very significantly the $\lg \sigma = f(1/T)$. For example, by introducing into sylvite 0.02% $CaCl_2$, the electrical resistance in the crystal will decrease by a factor of almost 100 in the temperature range between 200 and 600°C [38].

The mechanism of electrical conductivity in the NaCl and KCl minerals corresponds to the "hole" mechanism of electrical conductivity, according to Schottky [16] since the calculated data indicates that the difference between the energy of filling the lattice and that of the lattice with the "holes", is less than the difference between the energy of the lattice filling and the lattice with ions located at the interpoint space. Therefore the ion transfer from one point into a free point of the crystalline lattice is the most probable description of the ionic motion in the crystals of NaCl and KCl.

Fluorite CaF_2. In this mineral (Ca - 51.2%, F - 48.8%), one encounters most frequently the admixture of Fe_2O_3 and sometimes of uranium and gallium. The fluorite crystals which we have studied in the temperature range of 200-1000° are characterized by the linear dependence of lg σ as a function of 1/T, with the activation energy of 1.4 eV. The absence of a break in the curve, and a sufficiently high activation energy of the particles which take part in the charge transfer indicate that the electrical conductivity is brought about by the major ions or by the impurities, which are contained in a considerable amount. According to the data presented in the study [39] fluorite is characterized by some other activation energies: E_0=0.54 eV up to t=300° and E_0=0.87 eV above 300° and has somewhat lower electrical conductivity. Such difference may be due to the presence of impurities of different chemical composition. The analysis of the data presented in Table 5 and also available in the bibliography [16, 39] for some other halogens makes it possible to draw the following conclusion.

1. For the group of haloid compounds, the activation energy of the charge carriers depends on the lattice energy, in the region of the intrinsic conductivity and the impurity-related conductivity. In both cases, and for the same cation, the activation energy will decrease with the increase of the anion (Figure 13). This relationship is explained by the effect of polarizability which increases with the increase of the anion radius, facilitating the cation mobility.

2. The electrical conductivity of haloid crystals, just like /32 the activation energy, is characterized by the dependence on the lattice energy. With the increase of lattice energy and having the same cation, the electrical conductivity will decrease. In addition, one is able to observe the relationship between the electrical conductivity and the cation radius. With the increase of the latter, in the case of the compounds with the constant anion, the electrical conductivity will decrease, which, as it appears, is due to the change in the cation mobility.

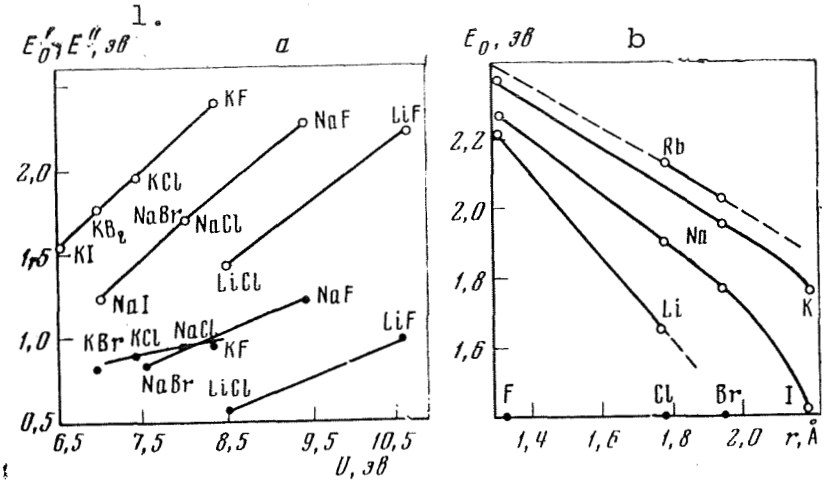

Figure 13. Activation energy as a function of the lattice energy E (a) and of the anion radius r in the alkaline haloid compounds (b) [39].
Key: 1. eV

3. In the case of the halogens formed by the same anion and cations of the same valence, one observes the decrease of the specific weight, of the hardness and of the melting temperature, as one decreases the lattice energy. As one can see from Table 5, the lattice energy in KCl is somewhat smaller than in the case of NaCl, which is due to the lower specific weight, hardness and melting temperature.

4. The comparison of electrical properties of the three minerals from this group of halogens under investigation indicates that the fluorite has the highest electrical conductivity and smallest activation energy. At the same time, the crystalline lattice energy in fluorite exceeds considerably the energy of the crystalline lattice in halite and sylvite, which, in accordance with the general applicable rules, is reflected in its specific weight, its impact hardness and its melting temperature. A somewhat low activation energy and relatively high electrical conductivity contradict somewhat this data. Such contradiction in these two parameters, as compared to the other parameters, may be explained if we take into account the effect of polarizability on E_0 and σ. The high dielectric penetrability in CaF_2 as compared to NaCl and KCl indicates the possible effect of polarizability on the electrical conductance and on the electrical state of the current carriers, in other words, on their activation energy. If /33
the anion takes part in the electrical conductivity, one should not exclude from considerations this effect on the σ quantity. The ionic radius in F^{1-} anion is sufficiently different from the ionic radius in Cl^{1-} anion (in the case of the first one it is

1.33 Å, and in the case of the second one - 1.88 Å). It is possible that because of smaller ionic radius, the mobility of F^{1-} is significantly greater than in Cl^{1-}, which may explain somewhat higher conductivity in fluorite, compared to NaCl.

3. Silicates

Approximately about one third of all minerals known in nature belong to the class of silicates, and in terms of weight, they comprise about 75% of the Earth's crust. Many silicates are the most important rock-forming minerals in all magmagtic rocks. Therefore the $\sigma=f(t)$ study of this group of minerals is of great theoretical and practical importance.

The most important elements which are incorporated in the silicates in the form of salts, having different silicon-oxygen radicals, are: Na, K, Li, Ca, Mg, Fe^{2++}, Mn, Be, Si, Zn, Ti, Al, Fe^{3+}, B, O, F, H (in the form of H^{1+}, $[OH]^{-1}$). The basic structural unit of all silicates is the tetrahedron $[SiO_4]^{4-}$, at the apexes of which, the O^{2-} ions are located, which surround the Si^{4+} ion.

In the crystalline silicate structures, the tetrahedrons may be in the form of structural SiO_4, which are isolated one from another, or more frequently, in the form of complex anion radicals. The differences in spatial forms of the anion complex radicals and their physical properties - the specific weight, the refraction index, the double refraction, should be associated with the specific features of the silicon-oxygen tetrahedrons.

Depending on the SiO_4 bonding, all of them, according to Betekhtin [40], are devided into five subclasses. We shall describe below the electrical properties of some of the most widespread representatives of the minerals, in terms of each of five silicate subclasses.

4. Silicates with Separate Tetrahedrons Within the Crystalline Structures

The olivine group includes forsterite, fialite and the olivine itself. It is known that olivine is the major component of Earth's mantle and of meteorites. Therefore, the study of the electrical and other physical parameters of the minerals within the olivine group is of great interest.

The forsterite Mg_2SiO_4 is a pure magnesium member within the forsterite-fialite series. It has the least specific weight and rather low electrical conductivity, which at 700-1500°C is as follows [41]: /35

t, °C	700	900	1100	1300	1500
σ, $ohm^{-1} \cdot cm^{-1}$	$3.3 \cdot 10^{-7}$	$1.6 \cdot 10^{-6}$	$2.0 \cdot 10^{-5}$	$3.3 \cdot 10^{-4}$	10^{-2}

The activation energy, computed by us on the basis of this data, is 0.8-1.0 eV, up to 1050°, and at higher temperatures - 2.6-3.0 eV. The authors of the same study [41] cite the activation energy of E_0=2.4 eV.

Fialite Fe_2SiO_4. The chemical composition of fialite is characterized by a clear predominance of FeO. In this predominantly ferrous mineral, its content reaches 76%. The amount of MgO does not exceed several percent. One frequently finds in this mineral, in addition to FeO, some Fe_2O_3. The presence of large quantities of iron oxide result in a rather high electrical conductivity in this mineral. We have encountered the levels of σ($ohm^{-1} \cdot cm^{-1}$) which were obtained at high pressures, with a part of these figures which were obtained at 23 kbar and are presenting the electrical conductance properties of fialite below [42, 43]:

t, °C	200	300	500
σ, $ohm^{-1} \cdot cm^{-1}$	10^{-2}	$6 \cdot 10^{-2}$	-
	$1.5 \cdot 10^{-4}$	$2.0 \cdot 10^{-3}$	$6.5 \cdot 10^{-2}$

The predominant iron oxides in fialite determine the low activation energy (8.18-0.3 eV) and high electrical conductivity. In the presence of oxides FeO and Fe_2O_3, the iron atoms are in the form of Fe^{2+} and Fe^{3+} ions. The current in this case, as has already been noted earlier, is established by electron transfer from Fe^{2+} ion to the neighboring Fe^{3+} ion, with insignificant activation energy. Therefore, the higher is the concentration of Fe^{2+} and Fe^{3+} ions, the higher will be the electrical conductivity of fialite.

Olivine $(Mg, Fe)_2SiO_4$ is the iron-containing variant of forsterite, which is in the form of a solid solution Fe_2SiO_4 and Mg_2SiO_4. The chemical composition ordinarily varies in the following range: MgO - 45-50%, FeO - 8-12%, less often, up to 20%, SiO_2 is the remainder.

Figure 14 shows lg σ as a function of 1/T, obtained by Noritomi [44] for two olivine crystals of different origin. According to the X-ray analysis, these crystals are typical olivines. The significant difference in electrical properties of these two olivines is explained by dissimilar amounts of impurities. According to X-ray analysis, the olivine 2 is

characterized by a higher amount of impurities than olivine 1. The anisotropy of electrical conductivity, the activation energy and lg σ_0 for crystallographic directions of the parallel and perpendicular optical axis, is rather small (Table 6).

TABLE 5. PHYSICAL PROPERTIES OF HALOGENS

Mineral	Cation parameter: radius r, Å	Cation parameter: Polarization α·10²⁴, cm³	lattice constant, Å	lattice energy, eV	E_0, eV	ε	σ, ohm⁻¹·cm⁻¹: 300° C	σ, ohm⁻¹·cm⁻¹: 900° C	specific weight, g/cm³	Impact hardness	t_m, °C
Halite	0,98	0,197	5,6287	7,93	1,72	5,6—6,4	10^{-11}	melting	2,1—2,2	2,0	800
Sylvite	1,33	0,879	6,278	7,23	1,9—2,04	4,7—4,8	$5\cdot10^{12}$	»	1,97—1,99	1,5—2,0	768
Fluorite	1,06	0,51	5,45	27,15	1,4	6,2—8,5	$2,4\cdot10^{-9}$	$3,4\cdot10^{-3}$	3,18	4,0	1240

[Commas in tabulated material are equivalent to decimal points.]

TABLE 6. ACTIVATION ENERGIES E_0 AND lg σ OF OLIVINES [4]

Olivine	Temperature range, t, °C	E_0, eV	lg σ, ohm⁻¹×cm⁻¹	Olivine	Temperature range, t, °C	E_0, eV	lg σ, ohm⁻¹×cm⁻¹	Olivine	Temperature range, t, °C	E_0, eV	lg σ, ohm⁻¹×cm⁻¹
				2' parallel to C axis				2 ⊥ to C axis			
1	До 470	0,66	—3,8		До 480	0,64	—2,0		До 490	0,64	—1,8
	470—620	1,0	—1,4		480—630	0,8	—0,9		490—650	0,83	—0,7
	620—1050	1,64	2,3		630—1050	1,2	1,3		650—1020	1,3	1,5
	1050—1170	4,6	13,4		1050—1170	5,2	14,5		1020—1120	3,2	9,4
	1170—1300	0,7	—0,2		1170—1300	0,8	0,7		1120—1300	0,8	0,7

(Commas in tabulated material are equivalent to decimal points.)

It is likely that the extremum activation energies within the /36
temperature range of 1050-1150°C are associated with the structural changes or phase transitions, which occur at high temperatures. One can draw the following conclusion in regard to the electrical properties of the minerals of the olivine group, on the basis of the data presented above.

The electrical conductivity of the forsterite, fialite and olivine minerals is totally defined by the type of metal (Me) in the formula $Me[SiO_4]_2$. This is due to the fact that in the the silicon-oxygen tetrahedron, $[SiO_4]_2$ is a common structural unit and the oxygen ions are bonded to silicon much more strongly than to the cations of other metals. The comparison of curves shown in Figure 14 indicates that forsterite has the least electrical conductivity, in spite of the fact that the measurements were conducted on the ceramic structure, rather than a stoichiometrically organized monocrystal. The highest electrical conductivity was found in fialite and the intermediate electrical conductivity was found in olivine.

The magnesium oxide and the Mg^{2+} ion are characterized by the high crystalline lattice energy and ionization potential, respectively, and therefore one observes here somewhat low electrical conductivity in MgO and a sufficiently high activation range. The forsterite, /37 if compared to magnesium oxide, has higher electrical conductivity. It appears that the dissimilar character of the structural bonding of Mg^{2++} in the forsterite and in the magnesium oxide result in a difference in energy states in the case of these two compounds, which results in the higher electrical conductivity of forsterite.

The replacement in forsterite of Mg^{2+} ion by the iron ion, which is the source of the current carriers with low activation energies results in a sharp increase of electrical conductivity in olivine in a braod temperature range. The defining role of the iron ions in terms of electrical conductivity in this group of minerals can be traced out quite well by using monomineral rocks, the olivinate, the measured σ of which is presented below. But even the comparison of the data presented above for these three minerals is convincing enough, indicating that iron ions play an important role. The amounts of fialite in olivines at the level of 10-15% will result in a significant increase of the electrical conductivity in the latter.

Danburite $CaB_2(SiO_4)_2$ is a colorless mineral rarely encountered in nature. It belongs to a rhombic system. The electrical conductivity measurements at high temperatures were conducted in three crystallographic directions.

This mineral shows a considerable anisotropy of electrical conductivity. In this case the major feature of the temperature dependence of electrical conductivity in danburite is the considerable activation energy of the current carriers, in the presence of relatively low temperatures (300-500°C), which fluctuates between 0.1 and 1.2 eV, and a low activation energy (0.60-0.70 eV) at temperatures above 600°C. The temperature

range from 500 to 600°C, is characterized by the disruption of the linear relationship in lg σ=f(1/T), in all three directions. It is interesting that while the three samples have a considerable difference in terms of electrical conductivity, the activation energies are somewhat similar at high and low temperatures. It appears that, depending on the crystalline direction, the concentration changes quite appreciably and possibly, also the current carrier mobility.

The garnet group. The theoretical composition of the major mineral types of the garnet group, having a general formula $A_3B_2[SiO_4]_3$, where A is Mg, Fe^{2+}, Mn, Ca and B is Al, Fe^{3+}, Cr, is shown in Table 7.

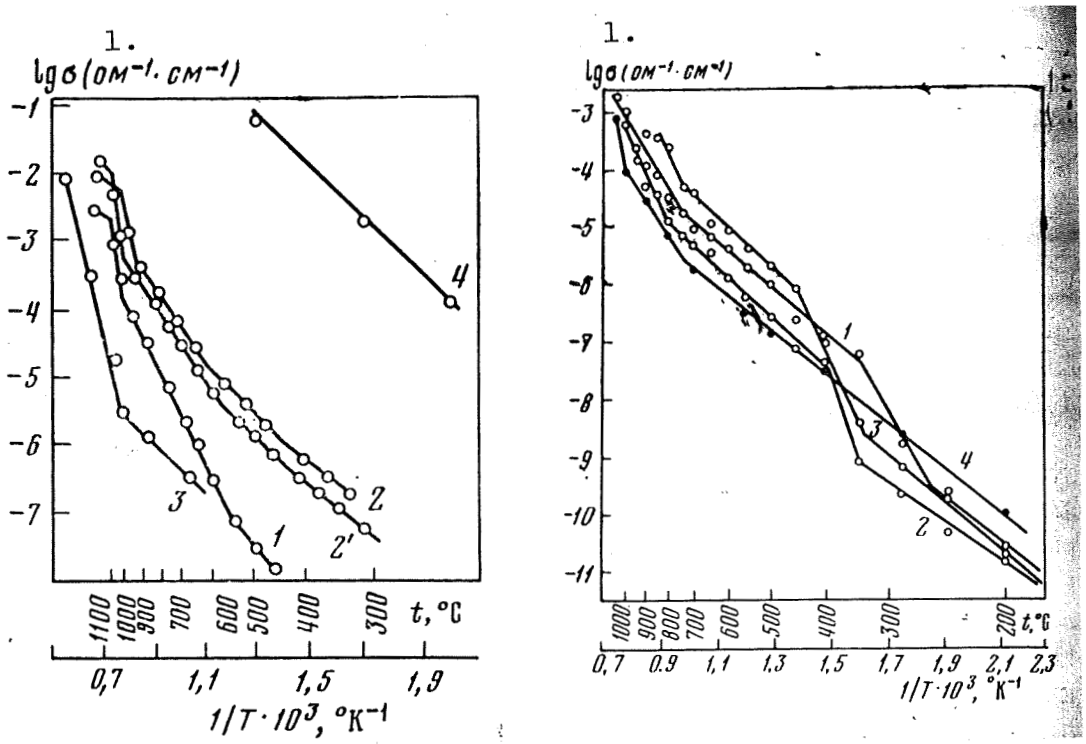

Figure 14. Electrical conductivity as a function of temperature. 1 - olivine; 2 - olivine $\perp$ C; 2' - olivine $\parallel$ C; 3 - forsterite [41]; 4 - fialite [43].

Figure 15. Electrical conductivity as a function of temperature, in the three mutually perpendicular directions for garnet (1-3) and for sphene* (4).

Key: 1. $ohm^{-1} \cdot cm^{-1}$

The chrome containing garnets are seldom encountered in nature. The Mg^{2+} and Fe^{2+}, and also Fe^{2+} and Mn^{2+} ions within this group of minerals may be interchanged at will. The chemical formula and composition (see Table 7) of the garnets indicates that their electrical properties are defined by the presence of two cations. Keeping in mind the electrical conductivity of the oxides which are present in garnets, the parameters (the radius and polarizability) of the cations Mg^{2+}, Al^{3+}, Mn^{2+}, Ca^{2+}, Fe^{2+}, and Fe^{3+} and also their quantitative relationship, it may be assumed that the pyrope and spessartite have the lowest electrical conductivity. In addition, the electrical conductivity of spessartite must be higher, since the Mn^{2+} ion radius is greater than in the case of Mg^{2+}. The intermediate position in terms of the electrical conductivity within the garnets is occupied by grossularite and uvarovite and the highest electrical conductivity will be featured by almandite and andradite, because of the presence of Fe^{2+} ions. Garnet was studied in three mutually perpendicular directions. The relationship between lg σ and 1/T for garnet is shown in Figure 15.

TABLE 7. CHEMICAL COMPOSITION OF GARNETS (WEITHT-%)

Mineral	MgO	FeO	MnO	CaO	Al_2O_3	Fe_2O_3	Cr_2O_3	SiO_2	Specific weight, g/cm³
Almandite series $(Mg,Fe,Mn)_3Al_2[SiO_4]_2$									
Pyrope	29,8	—	—	—	25,4	—	—	44,8	3,51
Almandite	—	43,3	—	—	20,5	—	—	36,2	4,25
Spessartite	—	—	43,0	—	20,6	—	—	36,4	4,18
Andradite series $Ca_3(Al, Fe, Cr)_2(SiO_4)_2$									
Grossularite	Андрадитовый ряд $Ca_3(Al, Fe, Cr)_2(SiO_4)_2$								
Andradite	—	—	—	37,3	22,7	—	—	40,0	3,53
Uvarovite	—	—	—	33,0	—	31,5	—	36,5	3,75
	—	—	—	33,5	—	—	30,6	35,9	3,75

(Note: commas in tabulated material are equivalent to decimal points.)

Let us note first of all the dissimilar character of this relationship for all three directions, something which should be expected on the basis of the cubic symmetry of the mineral. However, some difference in electrical conductivity does take place and may be detected even in two adjoining samples, cut out in the same direction. This may be due to the inhomogeneous distribution of impurities within the samples. One of the specific features of the garnet which we have investigated is its high activation energy at the low temperature range ($t<350^{o}$), which is at the level of 1.0 eV, and a sharp increase of electrical

conductivity in the course of change of the electrical conductivity mechanism. As a result of this, a narrow temperature range is obtained with the high E_0 and low σ_0 which unquestionably are fictitious and do not characterize the conductivity process. The formation of transition zones, as it appears, is related to a sharp increase in the number of new current carriers, which have a high activation energy, similar to the activation energy of the former (0.8-1.0 eV).

In the region of intrinsic conductivity for two directions 2 and 3 (see Figure 15) one observes similar activation energies E_0=1.7-2.0 eV, and only in the 1 direction - one observes lower E_0=1.42 eV. The reason for such deviation in E_0, from the figures obtained for the other two samples, may be the presence of local concentration of defects in the samples, a fact which is indicated by somewhat higher electrical conductivity, as compared to the samples which were cut out in the 2 direction (see Figure 15). The high activation energy in all three temperature ranges, it appears, is connected with the specifics of the garnet structure, in other words with the increased coordination number (n)Mg^{2+} and Fe^{2+}, as compared to the other silicates. In all silicates, Mg^{2+} and Fe^{2+} have the coordination number n=6, while in the garnets, n=8. The increased coordination makes the iron-magnesium garnets somewhat denser. /39

The sphene* $CaTi[SiO_4]O$ is a mineral, frequently encountered in the basic intrusive igneous rocks, and is a characteristic mineral for metamorphic rocks. The following oxides are present in its chemical composition (in %): CaO - 28.6; TiO_2- 40.8; SiO_2 - 30.6. The impurities present are FeO - up to 6%, sometimes MnO - up to 3%, Mg, Fe_2O_3, Al_2O_3 $(Y, Ce)_2O_3$ -up to 12%, and sometimes $Cr_2O_3Zr_2$ - up to 0.18%. In terms of electrical conductivity, sphene differs only slightly from the garnet-almandite group which we have investigated for a broad temperature range (see Figure 15) although its chemical composition is represented by other oxides. The high degree of hardness and high specific weight of this mineral indicates high crystalline lattice energy. It appears that the latter causes high activation energy, which, in the region of intrinsic conductivity, reaches 3.5 eV.

5. Silicates with Separate Tetrahedron Groups within the Crystalline Structures

We have investigated two minerals within this subclass of silicates, the beryl and eudialyte.

Beryl $Be_3Al_2[Si_6O_{18}]$ belongs to the silicates with the ring anion radicals. The chemical composition is as follows (in %): BeO - 14.1; Al_2O_3 - 19.0; SiO_2 - 66.9. The following oxides are found here as impurities (up to 7%): Na_2O, K_2O, LiO_2. Sometimes one also finds helium and water. More often than not, this mineral is encountered in pegmatite veins. The beryl was investigated in two directions, and for it the $\lg \sigma = f(1/T)$ relationship remains linear for a broad temperature range. However, in one direction, this relationship is characterized by one straight line and in the other direction, for the two samples under investigation, one observes the sharp curve break at $t=830^{\circ}$. Beryl is a clear example of a strong manifestation of not only the anisotropy in electrical conductivity, but also in the E_0 and σ_0 paremeters. It appears that the Be ions are the current carriers in beryl, since they are in the quaternary oxygen surrounding and the Al ions are surrounded by six oxygens. This however, should not exclude the possibility of a significant effect on the electrical conductivity of the Na, K and Li ions. Ordinarily, these ions are located at the vacancies formed by the radical rings and probably, are not as tightly bound to the other ions as Be^{2+} and Al^{3+}.

Eudialyte* $(Na, Ca)_6 ZrSi_6O_{18}[OH, Cl]$ is widely distributed in the magmatic basic rocks, and is frequently a basic rock-forming mineral. It has the following chemical composition (in %): /40
Na_2O - 11.6-17.3; CaO - 8.9-11.3; ZrO_2 - 12.0-14.5; $(Ce, La, Y)_2O_3$ - 0.3-2.9; FeO - 3.1-7.1; MnO - 0.3-3.1; SiO_2 - 47-51.2; H_2O - 0.3-2.9; Cl - 0.7-1/6.

Eudialyte is characterized by a relatively high electrical conductivity (Appendix 1) which is associated with the high amount of sodium oxide in it, which may be used as a source of the current carrier with a low activation energy, in the structurally sensitive region, as well as in the high temperature region.

6. Silicates with Continuous Tetrahedron Chains within the Crystalline Structures

The major representatives of the silicates of this subclass are the pyroxenes and amphibioles, which are the typical metasilicates. They differ from the olivine group (orthosilicates) by a higher amount of SiO_2, by a significant role which Ca is playing, in addition to Mg and Fe, and by lower purity (it frequently contains Al_2O_3, Na_2O and sometimes Fe_2O_3 and other impurities). The major structural features of these minerals are the strong bonding between Si-O-Si as compared to the metallic cations Ca^{2+} and Mg^{2+} which are located between the chains, a less dense packing but tighter bonding than in the case of the orthosilicates.

The pyroxene group, which is subdivided into monclinic and rhombic, belongs to the silicates with ordinary anion chains. The most important minerals within this group are:

Monoclinic pyroxenes	Rhombic pyroxenes
Diopside Ca Mg $[Si_2O_6]$	Enstatite Mg_2 $[Si_2O_6]$
Gegenbergite CaFe $[Si_2O_6]$	Hyperstene $(Mg, Fe)_2[Si_2O_6]$
Augite Ca (Mg, Fe, Al) $[Si, Al)_2O_6]$	
Jadeite Na Al $[Si_2O_6]$	
Eugirite Na Fe $[Si_2O_6]$	
Spodumene Li Al $[Si_2O_6]$	

The electrical parameters at high temperatures were measured in the case of three minerals: diopside, eugirite and jadeite, which were in the polycrystalline form.

Diopside is a typical binder compound, as is an external member of an important isomorphous series $CaMg[Si_2O_6]$ - $CaFe[Si_2O_6]$. Diopside is widely found as a rock-forming mineral in the igneous rocks. It has the following chemical composition (in %): CaO - 25.9; MgO - 18.5 and SiO_2 - 55.6.

The electrical conductivity of diopside was investigated in two crystallographic directions. Figure 16 shows the lg σ=f(1/T) relationship. One can see from this graph that the lg σ=f(1/T) /41 relationship is disrupted with the anomalous change of electrical conductivity in the 700-900°C range. The activation energies of the charge carriers, before and after this range, are quite similar and are in the range between 0.93 and 1.1 eV, in other words, they are within the range of measuring error. The cause of the anomalous electrical conductivity within a specific range is not clear, since the diopside has no water of crystallization and contains only small quantities of iron oxides Fe_2O_3, which stimulate such phenomena. In investigating the second crystal of diopside, the analogous anomaly was not observed. In this case the lg σ=f(1/T) relationship corresponds to a straight line and the activation energy is 0.68-0.80 eV, in other words, it differs only slightly from the activation energy of the first mineral. The most probable current carrier in the diopside is the Ca^{2+} cation which has the lower ionization potential as compared to the Mg^{2+} ion. It should be noted that in addition to the above-mentioned oxides, the diopsides may contain iron oxides and chromium oxides. It is known that the diopside minerals - salite, ferrosalite and gegenbergite form a complete series of solid solutions. The total amounts of iron oxide in diopside does not exceed 8%, and in salite and gegenbergite it may reach 25%. Therefore, the electrical conductivity in the series diopside-gegenbergite will change within a broad range, because of the difference in the amount of iron oxide.

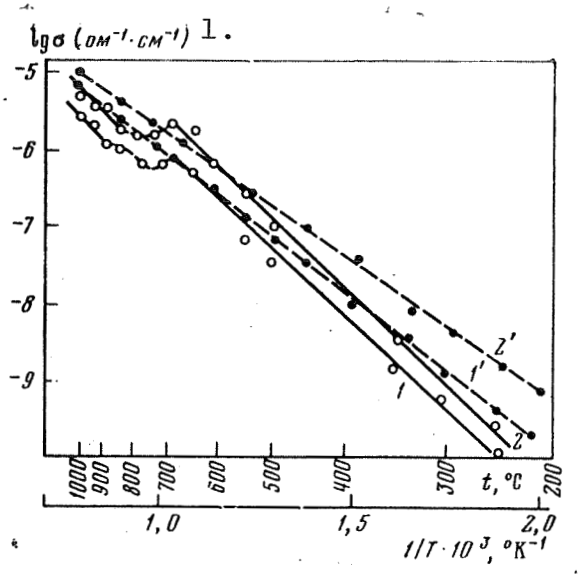

Figure 16. Electrical conducivity for two monocrystals of diopside as a function of temperature.

1 and 1' - along the optical axis; 2 and 2' - perpendicular to the optical axis (1'*, 2'*).

Key: 1. $ohm^{-1} \cdot cm^{-1}$

Eugirite* $NaFe[Si_2O_6]$ is an important rock-forming mineral of numerous basic rocks. The chemical composition (in %) is: Na_2O - 13.4; Ve_2O_3 - 34.6; SiO_2 - 52. One frequently encounters impurities here, which are K_2O, CaO, FeO, MgO, Al_2O_3 and others. Of all mineral types within the pyroxene group eugirite has the highest electrical conductivity because of the presence in it of Na^{1+} and Fe^{3+} cations. The amounts of sodium and iron ions cause increased electrical conductivity, as compared to the other pyroxenes and eudialyte at high temperatures. The electrical conductivity of eugirite was measured in an arbitrary direction. The electrical conductivity data for it is presented in Appendix 1. The temperature dependence of σ in eugirite is characterized by three regions: /42 775 and 900° temperatures the break point corresponds to the (see Figure 17a). There is some doubt as to the high values of E_0 and σ_0 parameters which are equivalent to 3.1 eV and $9.0 \cdot 10^8 ohm^{-1} \cdot cm^{-1}$, respectively, in the region of the intrinsic conductivity. It is not excluded that this is due to the structural rearrangement which produces an analogous effect in olivines. By comparing the electrical conductivity of eugirite and eudialyte, one can see that at high temperatures the former is characterized by high σ, which is associated with the presence in it of Na^{1+} and Fe^{3+} ions.

Jadeite $NaAl[Si_2O_6]$. The chemical composition of many jadeites (SiO_2 - 58-59%, Al_2O_3 - 23-25, Na_2) - 12.3-14.4%) differs only slightly from the ideal composition $NaAlSiO_2O_6$, which is an intermediate between nephelite and albite.

The measured electrical conductivity of the polycrystalline jadeite at high temperatures is shown in Figure 17a. The jadeite, in terms of its electrical properties, occupies an intermediate position between diopside and eugirite. This is associated with

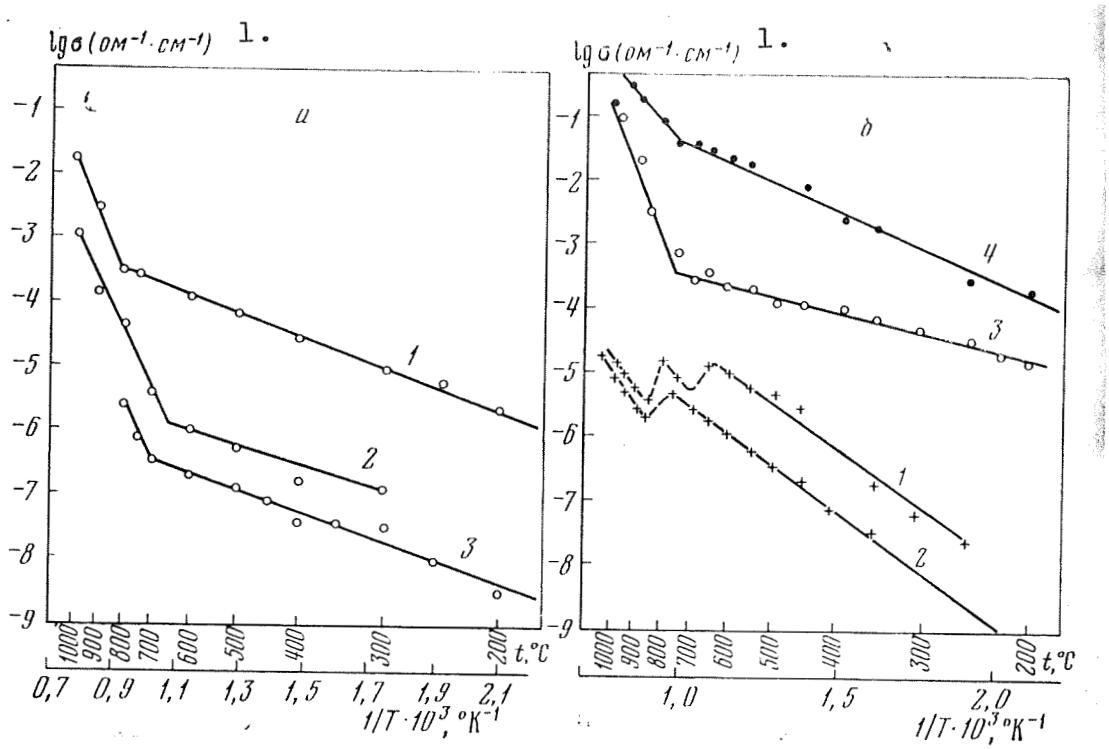

Figure 17. Electrical conductivity as a function of temperature. a - for eugirite* (1) and jadeite (2,3); b - for hornblender (1, 2) and rubecite (3,4).
Key: 1. $ohm^{-1} \cdot cm^{-1}$

the fact that in jadeite, instead of Ca^{2+} cations, which as it appears, are the major current carriers in the diopside, one finds Na^{1+} cations which are more mobile as compared to Ca^{2+} and therefore, the electrical conductance of jadeite will be higher than the electrical conductance of diopside. On the other hand, jadeite lacks Fe_2O_3 oxides which are found in eugirite in the quantities of 34%. As a rule, the latter in the presence of FeO is even more effective in the current transfer than Na^{+}. Because of high polarizability of jadeite, one cannot accurately measure the electrical conductivty at temperatures above 700°C, and consequently, to determine the activation energy. The approximate estimate indicates that the possible activation energies of the current carriers in this temperature range are between 2.0 and 2.8 eV. /43

The following conclusions may be made as to the elctrical conductivity of the pyroxene group. Within this mineral series, the least electrical conductivity will be in the case of enstatite $MgSi_2O_6$ (Mg - 60%; SiO_2 - 40%) on the assumption that FeO impurity is present in small amounts (up to 5%). The enstatite with high

amounts of FeO (between 10 and 14%) will have higher electrical conductivity. In the diopside, a part of the magnesium ions is replaced by Ca^{2+} ions which facilitates its increased electrical conductivity. The highest electrical conductivity will be in the case of eugirite, because of the presence in it of Na^{1+} and Fe^{3+} cations.

As we can see, by using the example of the distribution of minerals within the pyroxene group, in terms of electrical conductivity, the presence of specific types of the cation metals is of defining nature.

Amphibole group. The amphibole structure, when compared to pyroxene, is more complex, although from the point of view of composition, there is substantial similarity. The characteristic feature of the ampibioles is the fact that the binary change of the silicon-oxygen tetrahedrons $(Si_4O_{11})^{6-}$ is found in its crystalline structures and that the remaining oxygen ion is incorporated as an independent univalent anion $[OH]^{1-}$. Therefore, the general negative charge of the anion complex is equal to 7. The replacement of two oxygen ions which are not bound by two univalent ions $[OH]^{1-}$, results in the decrease in the number of cations, for example, in the case of Mg ions in antophyllite, there will be not 8, but 7 cations. In the amphibiole group, the most important ones are the following:

Monoclinic amphiboles

Tremolite $Ca_2Mg_5[Si_4O_{11}]_2[OH]_2$

Actinolite $Ca(Mg,Fe)_5[Si_4O_{11}]_2[OH]_2$

Hornblende $Ca_2Na[Mg,Fe^{2+}]_4(Al,Fe^{3+})[(Si,Al)_4O_{11}]_2[OH]_3$

Rubecite $Na_2Fe_3Fe_2[Si_4O_{11}]_2[O, OH]_2$

Glaucophene $Na_2(Mg,F2)_2Al_2[Si_4O_{11}]_2[OH, F]_2$

Arphvedsonite $Na_3(Mg,Fe)_4(Fe,Al)[Si_4O_{11}]_2[OH,F]_2$

Rhombic amphiboles

Antophyllite $(Mg,Fe)_7[Si_4O_{11}]_2[OH]_2$

The presence in amphiboles of hydroxyl, fluorine and sometimes chlorine indicates that their formation in igneous and metamorphic rocks is associated with the participation of mineralizers which cause the crystallization at relatively lower temperatures. /44

The minerals tremolite and actinolite which are within the hornblende group, are stable at low temperatures and are to be found in many igneous rocks, predominantly basic ones, which were subject to hydrothermal metamorphism. The electrical conductivity was studied only by using polycrystalline samples of the hornblende, and the monocrystals of actinolite and rubecite.

The hornblende is characterized by the changes within a broad range of the ratio between Mg and Fe^{2+} and Al and Fe^{3+}. Potassium is sometimes found in greater quantities than sodium, and one almost always finds TiO_2 in the quantities of 0.1-1.25%. The hornblende is widely found in the amphibiole shales and gneiss. The amphiboles consisting of hornblende and plagioclase have been formed in many cases during the metamorphism of the basic rocks, in particular of gabbro. The temperature dependence and electrical conductivity of two samples of hornblende, cut out in the two mutually-perpendicular directions, is characterized by a considerable anisotropy up to 600-700°C. Within the temperature range 600-850° (curve 1) and 750-850° (curve 2) one observes the disruption of the linear dependence of $\lg \sigma = f(1/T)$ (see Figure 17b), which is associated with the evolution of water. The assumption was made by L. N. Ovchinnikov et al. [45], by undertaking the thermal, chemical and X-ray studies of 14 samples of hornblende, that about one half of the water of crystallization evolves within the temperature range of 400-800°C and the remaining water - within the 900-1100°C range. The temperature range which corresponds to the σ anomaly occupies an intermediate position and quite likely this is associated with the specifics of the structure of this particular sample.

Actinolite* $Ca_2(Mg,Fe^{2+})_5[Si_4O_{11}]_2[OH]_2$. In terms of its chemical composition, it is an iron-containing variant of tremolite and contains FeO - 13% and also some Al_2O_3 plus some Na_2O impurities. The actinolite electrical conductivity as a function of temperature is characterized by an anomalous change of σ at 630-830°, which is due to dehydration and low activation energies at t>830°C (Appendix 1).

Rubecite $Na_2Fe_3Fe_2[Si_4O_{11}]_2[O,OH]_2$, which has the following composition (in %): SiO_2 - 51.01; Fe_2O_3 -16.4; FeO - 17.62; Na_2O - 7.98; K_2O - 1.8; H_2O - 0.91; F - 1.7; Al_2O_3 -0.8, and is a component of the acidic igneous rocks. Within the minerals of glaucophene-rubecite series, the main substitutions are $Mg^{2+} \rightleftarrows Fe^{2+}$ and $Al^{3+} \rightleftarrows Fe^{3+}$.

Rubecite was studied in two mutually perpendicular directions. As one can see in Figure 17b, it is characterized by a considerable electrical conductivity which basically (curve 4) is higher than the electrical conductivity of eugirite, although the total amounts

of Fe_2O_3, FeO and Na_2O oxides in eugirite is higher than in the /45
rubecite by about 4%. The high electrical conductivity of rubecite is due to the presence of the two and trivalent iron ions, in approximately equal quantities, with the appearance of the electron mechanism of electrical conductivity, in the presence of a high concentration of electrons. In eugirite, however, the iron cations are primarily in the Fe^{3-} form and the change in the iron valence which affects the level of electrical conductivity is due only to the presence of FeO, with the ordinary amount not exceeding several percentage points.

7. Silicates with Continuous Tetrahedron Layers within the Crystalline Structures

The talcum-pyrophillite group is represented by the minerals which are quite specific in terms of their physical properties. The difference between them is only in the fact that in the talcum structures, the Mg^{2+} cations occupy all hexacoordination places between the two hexagonal network layers $[Si_4O_{12}]$, while in the pyrophillite structure, the Al^{3+} cations occupy only two thirds of these places.

Talcum $Mg_2[Si_4O_{10}][OH]_2$ has the following composition (in %): MgO - 31.7; SiO_2 - 63.5; H_2O - 4.8. Sometimes one encounters the minerals in which a part of the MgO is replaced by FeO (up to 2-5%), and also some in which small quantities of NiO are found.

The electrical conductivity of talcum was measured in one arbitrary direction. The talcum in a broad interval range (200-900°C) does not change its electrical conductivity. At these temperatures, it has low σ and the activation energy of it is equal to 1.0 eV [46].

Pyrophillite $Al_2[Si_4O_{10}][OH]_2$ primarily consists of oxides (in %): Al_2O_3 - 28.3; SiO_2 - 66.7 and H_2O - 5.0. One finds MgO up to 9%, FeO up to 5%, Fe_2O_3, CaO in trace quantities, alkalis and titanium oxide as impurities. The crystals which can be used for measurements are not encountered, and therefore, the experiments were carried out by using samples cut out in an arbitrary direction. In terms of its electrical conductivity and the character of $\lg \sigma = f(1/T)$ relationship, pyrophillite is analogous to talcum. The activation energy for talcum and for pyrophillite within the temperature range of 300-900°C is about 1.0 eV. It is interesting that in this temperature range, as it appears, no water evolution takes place, since one does not observe any anomalous electrical conductivity as a function of temperature. It is possible that the water is evolved at somewhat higher temperatures.

It appears that the charge transferring agents within the temperature range which is characterized by the activation energy of 1.0 eV are the impurities. In this case, the major role is being played by the iron and nickel oxides.

Since the isomorphous replacement of Mg^{2+} by Fe^{2+} and Ni^{2+} /46
and also of Al^{3+} by Fe^{3+} within the talcum-pyrophillite series, takes place in a narrow range, the electrical conductivity of talcum and pyrophillite minerals of different origins should not change within a broad range. Because of the small quantity of these oxides in pyrophillite and talcum, one observes a sufficiently high activation energy for the region where the impurities facilitate conductivity. In the case of talcum, at 950°C, the substitution of the currend carriers takes place, which is probably due to the participation of Mg ions, since the activation energy here is 2.5 eV.

These two minerals not only have similar electrical parameters, but also similar hardness and specific weight because of almost similar crystalline structure.

The high electrical resistance and elastic properties of pyrophillite and of talcum lead to their use as a medium which transmits pressure.

Mica group. The micas belong to a broad range of minerals found in nature which are primarily encountered in acidic intrusive rocks, and in the crystalline mica shales. The total amount reaches 3.8%. The chemical composition of micas is not constant. The widely fluctuating isomorphous mixtures were found in micas in which one finds, as usual, the replacement of Mg^{2+} by Fe^{2+} and Al^{3+} $Al^{3+} \rightarrow Fe^{3+}$ and on the other hand - one encounters the heterovalent isomorphous substitutions. In accordance with the specifics of the chemical composition of mica, the following subgroups are established: biotite (magnesium-iron mica), muscovite (aluminum mica) and lepidolite (lithium mica). We have investigated only three types of micas, namely: phlogopite, biotite and muscovite, the chemical composition of which is presented below (Table 8).

TABLE 8. CHEMICAL COMPOSITION OF MICAS

Mica	K_2O	MgO	Al_2O_3	SiO_2	H_2O	FeO	Impurities
Phlogopite $KMg_3[Si_3AlO_{10}][OH, F]_2$	7,0—10,3	21,4—29,4	10,8—17,0	38,7—45,0	0,3—5,4	До 9%	Fe_2O_3, Na_2O, BaO
Biotite $K(Mg, Fe)_3[Si_3AlO_{10}] \cdot [OH, F]_2$	6,18—11,43	0,28—28,34	9,43—31,69	32,83—44,94	0,89—4,64	2,74—27,6	Fe_2O_3 0,13—20,65
Muscovite $KAl_2[AlSi_3O_{10}][OH]_2$	11,8	—	3,85	45,2	4,5	—	Cr_2O_3

(Commas in tabulated meterial are equivalent to decimal points.)

The electrical conductivity of micas was measured up to 950°C in vacuum (10^{-3} mm mercury)[1], in the direction perpendicular to the mica layers. The results of measurements for phlogopite and biotite and of two samples of muscovite are shown in Figure 18a, and in the Appendix. As compared to numerous other minerals within the silicate class, all micas are characterized by the lowest electrical conductivity in the region where the impurities facilitate the conductance, up to temperatures of 500°C. The least electrical conductivity up to 350°C was found in the case of biotite and muscovite. The high insulation properties of muscovite, as it appears, are due to its major structural feature, namely the replacement of 3 $(Mg, Fe)^{2+}$ by 2 Al^{3+}, and the major role here is the depletion of Fe^{2+} ions. /47

The different degree of anomalous change in electrical conductivity as a function of the temperature increase from 450 to 700°C was displayed by two different samples of muscovite, and this was due to the evolution of the water of crystallization. The intensive increase of electrical conductivity at the initial moment of water evolution, as it appears, is related to a sharp disruption of the energy state of the crystalline lattice, which results in the increase in the number of current carriers. After the additionally generated current carriers are depleted, as the temperature is increased, one observes the decrease of σ, the process which takes place before the new mechanism of electrical conductivity is activated. In biotite, the anomalous region is primarily featured as a sharp increase of the electrical conductivity in a narrow temperature range (500-570°) with the subsequent slight decrease of conductivity, as we go up to 650°C. It should be noted that the water evolution in phlogopite does not result in the phenomena which are observed in biotite and muscovite. Within a narrow temperature range (300-350°), one merely observes a sharp jump of σ. At high temperatures, the electrical conductivity of muscovite and phlogopite is similar, with a slight decrease in the case of one of the muscovite samples. In terms of the activation energy and of lg σ_0, these micas also do not differ at all, which is related to the similar type of crystalline structure. The micas investigated have a sufficiently high activation energy (2.0 and 2.4 eV) at the temperatures above 750°C. Therefore, the data in termso of the electrical conductivity of muscovite and phlogopite indicates that the replacement of the Mg ion by the Al ion is of no significant importance in the area of intrinsic conductivity. However, the high conductivity of biotite indicates that in the case of a different type of Mg^{2+} replacement, namely, by the Fe^{2+} ions, a significant change of conductivity takes place in the region of high temperatures. Since the major charge carriers for

[1]Measurements were conducted at the Tomsk Polytechnical Institute, as requested by us.

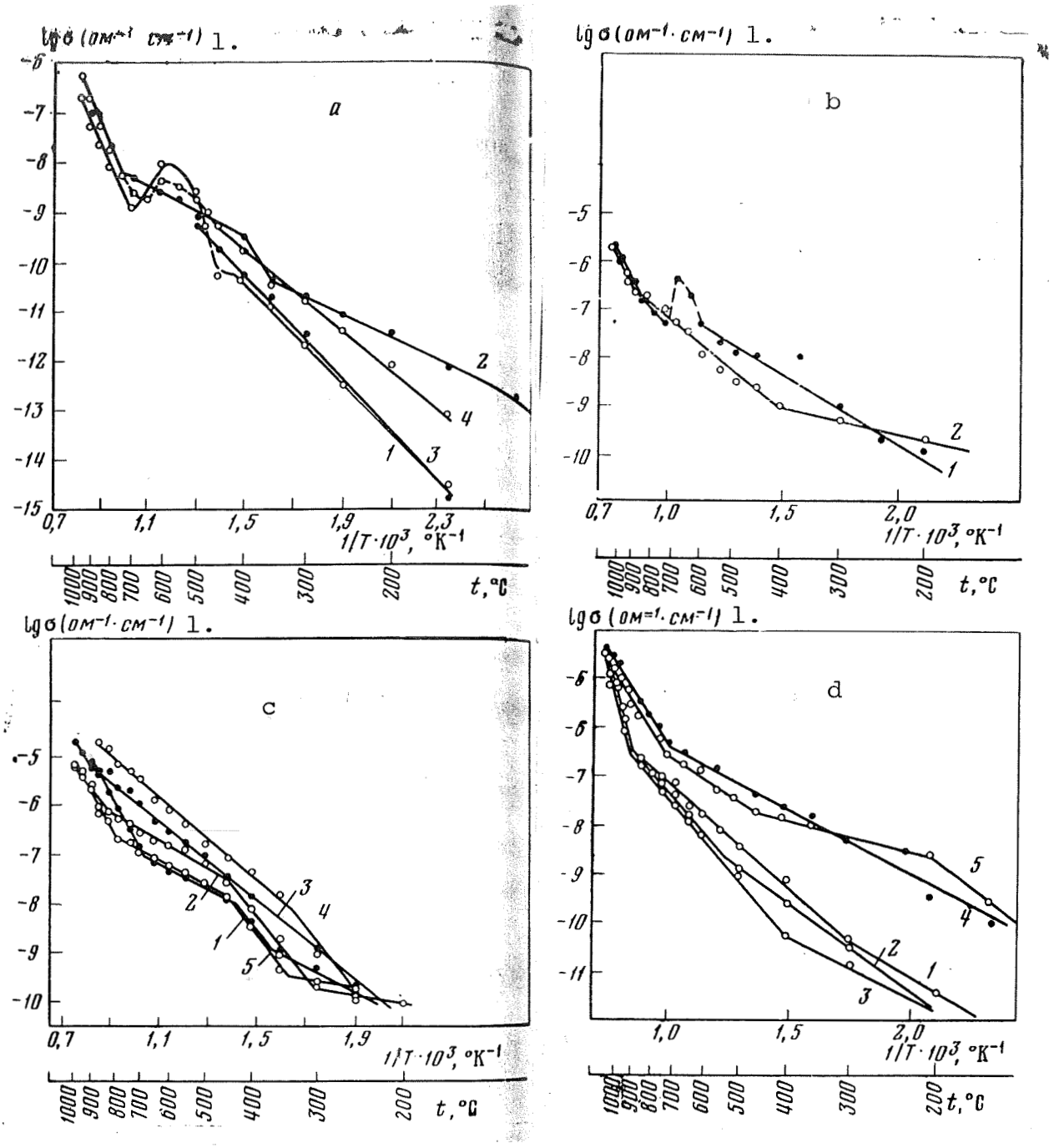

Figure 18. Electrical conductivity as a function of temperature.

a - muscovite (1, 4), for phlogopite (2), for biotite (3); b - for two monomineral serpentines (1,2); c - for albite (1,2,4) and for oligoclase (3,5); d - for orthoclase (1), microcline (2,3) and for nephelite in two mutually perpendicular directions (4,5).

Key: 1. $ohm^{-1} \cdot cm^{-1}$

the electrical conductivity are K^{1+}, Na^{1+}, Fe^{2+} and Fe^{3+} which are located primarily between the packets which have the following formula $Mg_3[Si_3AlO_{10}][F, OH]_2$, it is possible that the role of the chemical composition, particularly of the impurities, will be significantly greater if the measurements are taken along the layers. In phlogopite, inside of the multilayerd packets, between the two aluminum and silicon-oxygen layers, at all sides of hexagonal coordination, the Mg^{2+} ions are located. Because of this, in the absence of impurities, its electrical conductivity anisotropy will not be too great.

Serpentine $Mg_6[Si_4O_{10}][OH]_8$, just like talcum, pyrophillite /48
and the mica group, belongs to the silicates with continuous layers of tetrahedrons SiO_4 within the crystalline structures. The component relationship (in %) is MgO - 43.0; SiO_2 - 44.1 and H_2O - 12.9 which varies somewhat, particularly in the water-rich samples. The always present impurities are FeO, Fe_2O_3 and NiO. The electrical properties of serpentines were investigated by using the two monomineral samples. There is some difference observed in electrical conductivity at the beginning of the temperature treatment of these serpentines, but the difference practically disappears at the temperatures above 900°C. /49

As a result, the activation energy and σ_0, in the region of intrinsic conductivity for two samples which were investigated, agree quite well. It is interesting that in only one sample, at the temperature between 600 and 700°C, one was able to observe the anomalous change of electrical conductivity which manifests itself, as one can see in Figure 18b, first in a sharp increase in electrical conductivity, and then in its decrease, down to the initial level. This anomaly of σ is associated with the expulsion of $(OH)^{1-}$ group in the form of water. It is possible that the same anomaly occurs also in the second sample, but in a more narrow temperature range, and therefore it was not detected by us. The investigated serpentines have a low electrical conductivity. However, because of lack of constancy in such impurities as FeO, Fe_2O_3 and NiO, which strongly affect the electrical conductivity, a considerable fluctuation of conductivity is possible even within the range of intrinsic conductivity, if the amounts of these impurities exceeds 10%.

8. Silicates with Continuous Tridimensional Building Blocks, Made of Tetrahedrons $(Si, Al)O_4$, within the Crystalline Structures

Feldspar group. Of all silicates, the feldspars are most frequently encountered within the Earth's crust, comprising on the whole about 50% of its weight. Approximately 60% of feldspar is found in the igneous rocks, and about 30% are in the metamorphous rocks.

Plagioclase subgroup. Plagioclase is a binary series of isomorphous mixtures and the extreme members of these series are albite and anorthite. The classification of this isomorphous series is presented below: /50

	Amounts of anorthite molecules (%)	No. of plagioclase
Albite $Na[AlSi_3O_8]$	0-10	10
Oligoclase	10-30	25
Andesine	30-50	50
Labrador	50-70	70
Bytownite	70-90	75
Anorthite $Ca[AlSi_3O_8]$	90-100	100

According to the chemical composition presented below:

Composition, %	No. of plagioclase				
	10	25	50	75	100
Na_2O	10.76	8.84	5.89	2.92	-
CaO	-	5.03	10.05	15.08	20.10
Al_2O_3	19.40	23.70	28.01	32.33	36.62
SiO_2	68.81	62.43	56.05	46.67	43.28

the amount of SiO_2 in plagioclase decreases as we go from albite to anorthite, and of Al_2O_3 - increases, while the total sum of these oxides decreases from 88.21 to 79.9%. In addition, as the number of plagioclase increases, the substitution of univalent ion Na^{1+} by the bivalent ion Ca^{2+} is on the increase.

Orthoclase subgroup (potassium-sodium feldspar) depending on the temperature, may be crystallized in different modifications.

Series	Syngenesis
Monocline, high temperature	
Sanidine $K[AlSi_3O_8]$	Monocline
Natrosanidine $(K, Na)[AlSi_3O_8]$	"
Monocline, low temperature	
Orthoclase $K[AlSi_3O_8]$	"
Natronoclase $(K, Na)[AlSi_3O_8]$	"
Tricline	
Microcline $K[AlSi_3O_8]$	Tricline
Anorthoclase $(K,Na)[AlSi_3O_8]$	"

Albite and oligoclase are the two neighboring minerals within the series of isomorphous plagioclase mixtures. If we assume that the current carrier sources are the oxides of Na_2O and CaO, then the albite, across the whole temperature range, must have higher electrical conductivity than the oligocase since the Na^{1+} cations are more mobile current carriers than Ca^{2+}. We have investigated these minerals in three mutually perpendicular directions, using one sample for each direction, with the exception of oligoclase (two samples). The albite and oligoclase cannot be clearly differentiated in terms of the magnitude of electrical conductivity (Figure 18c and Appendix 1). However, in the case of oligoclase, the tendency of having higher electrical conductivity, as compared to albite, is evident, which is due to the local defects. In the case of albite, one observes the anisotropy of electrical conductivity in two directions, and in the case of oligocase - even in three. This causes some doubts, since structurally they are identical. It is not excluded that the difference in electrical conductivity in oligoclase in different directions is the result of nonuniform distribution of impurities or the local structural defects. The differentiation between albite and oligoclase, in terms of the other two parameters, E_0 and σ_0, is much more strongly pronounced than the electrical conductivity. In this case, the albite is characterized by smaller E_0 and σ_0 than oligoclase, and the anisotropy of these parameters is manifesting itself only in two directions. /51

Orthoclase and microcline have the same chemical composition (in %): H_2O - 16.9; Al_2O_3 -18.0; SiO_2 - 64.7 and the impurities are BaO, FeO, Fe_2O_3 and others, but they do differ from each other in terms of syngenesis.

The electrical parameters of microcline were studied in two directions, parallel and perpendicular to the layers and in the case of orthoclase, the sample had arbitrary orientation. At 900°C, one could clearly see the change in mechanism of the electrical conductivity, shown as a sharp break in line, in the case of microcline and orthoclase (Figure 18d). In the temperature range of 200-900°, these minerals have similar electrical conductivity, but differ from albite and oligoclase by having lower electrical conductivity. This is due to the fact that the K^{1+} ions which are the basic current carriers are more tightly bound at the points of the crystalline lattice, than Na^{1+} ions, and therefore a greater energy would be required to move them from the lattice point to the vacancy or to the interpoint space. The potassium feldspar at 900°C undergoes high temperature modification. It is not excluded that the straight line $\lg \sigma = f(1/T)$ for the temperature range of 900-1100°C and the values of E_0 and σ_0 which were calculated on the basis of this, characterize not the mechanism of

the intrinsic electric conductivity, but rather reflect the restructuring process. In terms of their structural features, the minerals within this subclass are closer to the minerals composed of SiO_2 than the other silicates. The anion complexes of these compounds, consisting of SiO_4 and AlO_4 tetrahedrons are joined together into tridimensional building blocks. The cations which occupy the vacancies within these building blocks are the ions which have large ionic radii, Na^{1+}, Ca^{2+}, K^{1+} and Ba^{2+}. It appears also that in quartz, they are the major charge carriers. In addition, because of the presence of vacancies in the direction of the optical axes, the movement is facilitated. As a result, just like in the case of quartz, one observes a considerable electrical conductivity, and the presence of anisotropy in two directions.

Nepheline. The chemical composition of natural nephiline does /52 not correspond precisely to the formula $Na[AlSiO_4]$ since SiO_2 is always in some excess (up to 3-10%) which is associated with the substitution of some sodium and aluminum ions by the silicon ions, according to the following reaction

$$(Na^{1+}, Al^{3+}) \rightarrow Si^{4+}.$$

The electrical conductivity of nepheline was measured in two mutually perpendicular directions: along the optical axis (4) and perpendicular to it (5). The anisotropy of the electrical conductivity, as well as that of the E_0 and σ_0 parameters, is only slightly displayed and in the case of both samples, one observes the transition from the impurity-related electrical conductivity to the intrinsic conductivity, with the activation energy of the current carriers of 1.66 eV (see Figure 18d). The same activation energy was obtained in the case of albite, in which the major cation which participates in the current transfer, is also Na^{1+}.

The intrinsic electrical conductivity of nepheline at the temperature below 450°C is higher than in the case of albite. Within the intermediate temperature range, one observes similar σ, E_0 and σ_0. The pure nepheline exists in four modifications, depending on the temperature. The hexagonal nepheline at 680°C is converted into a triclinic metastable form, which exists up to the temperautre of 1248°C and at t>1248°C, the cubic α shape is formed. A. A. Golovin [47] has conducted measurements of the coefficient of linear expansion of nepheline as a function of temperature, and has found three points of temperatures (335, 445 and 575°C, at which, one observes a sharp jump. The breaks in the nepheline curves, describing the electrical conductivity, correspond approximately to these temperatures. Some data as to the electrical conductivity of these and other minerals may be found also in the bibliography [48, 49].

TABLE 9. ELECTRICAL CONDUCTIVITY OF HIGH RESISTANCE MINERALS

Mineral	+++ ΣAl_2O_3, MgO, SiO_2, CaO +++	++ ΣFeO, Fe_2O_3, Na_2O, K_2O ++	σ, $ohm^{-1} \cdot cm^{-1}$ 300° C	σ, $ohm^{-1} \cdot cm^{-1}$ 1000° C	E_a, eV	Mean atomic weight, $\bar{M} \equiv M/n$, g	Mean atomic volume $\bar{V} = M/\rho n$, cm^3	V_k, (Å)³	b, 100 (Å)³	d	X
				Group 1							
Corundum α-Al_2O_3	100,0	—	$3,3 \cdot 10^{-14}$	$1,1 \cdot 10^{-10}$	2,2	20,6	5,1	10,4	4,7	135,0	1,0
Periclase MgO	100,0	—	10^{-14}	10^{-10}	2,0—2,3	20,0	5,65	13,8	5,3	78,0	0,75
Calcium oxide CaO	100,0	—	10^{-14}	$2,0 \cdot 10^{-7}$	1,6—2,9	28,0	8,35	20,4	3,6	35,2	0,51
Forsterite Mg_2SiO_4	93,0	7,0	—	$2,0 \cdot 10^{-6}$	2,2—2,4	20,1	6,24	13,4	4,1	79,0	0,78
Talcum $Mg_3[Si_4O_{10}][OH]_2$	95,0	5,0	$2,8 \cdot 10^{-11}$	$2,2 \cdot 10^{-6}$	2,5	17,8	6,4	13,5	3,1	75,5	—
Pyrophillite $Al_2[Si_4O_{10}][OH]_2$	95,0	5,0	$6,2 \cdot 10^{-11}$	10^{-3}	1,1	18,0	6,45	12,6	2,8	80,0	—
Phlogopite $KMg_3[Si_3AlO_{10}][OH]_2$	92,0	8,0	$2,0 \cdot 10^{-11}$	$4,0 \cdot 10^{-7}$	2,4	18,2	6,8	14,9	3,2	59,0	—
Biotite $K(Mg, Fe)_3(Si_3AlO_{10})(OH)_2$	90,0	10,0	$3,3 \cdot 10^{-12}$	—	2,0	23,3	8,0	—	—	—	—
Muscovite $KAl_2(AlSi_3O_{10})(OH)_2$	84,0	16,0	10^{-12}	$6,1 \cdot 10^{-7}$	2,25	18,9	6,5	13,99	3,0	67,5	—

(Note: Commas in tabulated material are equivalent to decimal points.)

(Table 9 is continued on the following page)

TABLE 9. ELECTRICAL CONDUCTIVITY OF HIGH RESISTANCE MINERALS (continued)

Mineral	ΣAl_2O_3, MgO, SiO_2, CaO (+++)	ΣFeO, Fe_2O_3, Na_2O, K_2O (++, +++)	σ, $ohm^{-1}.cm^{-1}$ 300° C	σ, $ohm^{-1}.cm^{-1}$ 1000° C	E_a, eV	Mean atomic weight, $\bar{M} = M/n$, g	Mean atomic volume $\bar{V} = M/\rho n$, cm^3	V_k, (Å)	b, 100 (Å)	d	X
Serpentine $Mg_6[Si_4O_{10}][OH]_8$	87,0	13,0	$9,5\cdot10^{-10}$	$1,3\cdot10^{-6}$	1,8—2,0	16,0	6,0	—	—	—	—
Diopside $CaMg[Si_2O_6]$	100,0	—	10^{-10} $6,3\cdot10^{-10}$	$4,7\cdot10^{-6}$ $2,4\cdot10^{-6}$	1,0	21,6	6,6	13,5	3,6	80	0,77
Quartz	100,0	—	$3,0\cdot10^{-10}$	$2,0\cdot10^{-7}$	—	20,0	7,55	13,9	2,65	76,0	0,75
Anorthrite	79,9	10,0	—	—	—	21,4	7,72	15,5	3,0	62,0	0,68
Albite $Na[AlSi_3O_8]$	86,1	13,9	$5,0\cdot10^{-10}$	$4,0\cdot10^{-6}$	1,6	20,2	7,72	15,5	3,0	62,0	0,68
Oligoclase	83,1	16,9	$1,2\cdot10^{-9}$ $2,7\cdot10^{-10}$	$1,3\cdot10^{-5}$ $7,6\cdot10^{-6}$	1,2 2,0	20,2	7,72	15,5	3,0	62,0	0,68
Microcline	83,1	16,9	$3,2\cdot10^{-11}$	$6,2\cdot10^{-6}$	3,7	21,4	8,4	16,7	2,7	53,0	0,63
Orthoclase	83,1	16,9	$4,2\cdot10^{-11}$	$7,1\cdot10^{-6}$	3,7	21,4	8,4	16,7	2,7	53,0	0,63
Group II											
Olivine $(Mg, Fe)_2SiO_4$	88,0	8—12,0	$3,1\cdot10^{-10}$	$2,0\cdot10^{-3}$	1,2—1,6	—	6,2—6,6	13,0—14,0	4,1	79,0	0,78
Nepheline $Na[AlSiO_4]$	80,0	20,0	$4,0\cdot10^{-9}$	$2,7\cdot10^{-5}$	1,6	20,0	7,9	16,55	3,4	55,5	—

(Note: Commas in tabulated material are equivalent to decimal points.)

Table 9 is continued on the following page.

TABLE 9. ELECTRICAL CONDUCTIVITY OF HIGH RESISTANCE MINERALS (continued)

Mineral	ΣAl_2O_3, MgO, SiO_2, CaO (+++)	ΣFeO, Fe_2O_3, Na_2O, K_2O (++)	σ, ohm^{-1}·cm^{-1} 300° C	σ, ohm^{-1}·cm^{-1} 1000° C	E_0, eV	Mean atomic weight $\bar{M} = M/n$, g	Mean atomic volume $\bar{V} = M/\rho n$, cm^3	V_k (Å)^3	b, 100 (Å)	d	X
Danburite $CaB_2[SiO_4]_2$	—	—	$1{,}3\cdot10^{-10}$	Melting	1,3	—	—	—	—	—	—
Hornblende $Ca_2Na(Mg, Fe^{2+})_4(Al, Fe^{3+})[(Si,Al)_4O_{11}]_2[OH]_2$	—	—	$6{,}4\cdot10^{-8}$ $2{,}3\cdot10^{-9}$	$1{,}8\cdot10^{-6}$ $8{,}2\cdot10^{-6}$	1,2—1,46	20,0	6,8	—	9,5	—	0,78
Garnet-almandite $Fe_3Al_2[SiO_4]_3$	56,0	44,0	$2{,}4\cdot10^{-10}$ $2{,}4\cdot10^{-9}$	$6{,}0\cdot10^{-4}$	1,4—2,0	20,1—24,0	5,6—5,7	11,5 11,8	4,2	107,0	0,88
Beryl $Be_3Al_2[Si_6O_{18}]$	85,9	14,0	$3{,}0\cdot10^{-10}$ $1{,}3\cdot10^{-9}$	$2{,}0\cdot10^{-6}$ $6{,}3\cdot10^{-6}$	(2,6)?	26,8	10,1	—	—	—	—
Sphene $CaTi[SiO_4]O$	60,0	40,0	$1{,}8\cdot10^{-9}$	$9{,}8\cdot10^{-5}$	—	24,5	6,95	13,6	—	77,0	076
Group III											
Fialite Fe_2SiO_4	24,0	76	$6{,}0\cdot10^{-2}$ $2{,}0\cdot10^{-3}$	10^{-1}	0,2—0,1	29,1	6,57	14,2	3,9	72,0	0,73
Jadeite $NaAl[Si_2O_6]$	79,0	21,0	$3{,}4\cdot10^{-8}$ $1{,}3\cdot10^{-7}$	$1{,}2\cdot10^{-3}$	(2,0)?	20,2	6,1	12,5	4,0	96,0	0,83
Eudialyte $(Na,Ca)ZrSi_6O_{18}[OH, Cl]$	47—51,2	50,0	$1{,}0\cdot10^{-7}$	$8{,}2\cdot10^{-3}$	2,76	25,1	8,9	—	—	—	—
Eugirite $NaFe^{3+}[Si_2O_6]$	52,0	48,0	$1{,}3\cdot10^{-5}$	$1{,}0\cdot10^{-2}$	—	23,09	6,4	—	—	—	—
Rubecite $Na_2Fe_3Fe_2[Si_4O_{11}]_2[O,OH]_2$	47—51	53,0	$4{,}2\cdot10^{-4}$	$3{,}8\cdot10^{-1}$	0,9	21,6	7,1	—	—	—	—

(Note: Commas in tabulated material are equivalent to decimal points.)

9. The Connection Between Electrical Conductivity, Chemical Composition and Structure of the Minerals

It is known that the major factors which define the physical and mechanical properties of crystals are the chemical composition and the crystalline structure. The electrical properties of minerals as a function of specific ionic structures and atomic structures have not been considered. Therefore, an attempt was made to analyze the experimental data obtained, describing the electrical conductivity of minerals from the point of view of various properties of components and particles involved. Among the most important parameters of the atom or of the ion, are their radii, polarizability and the coordination number. The physical properties of the material also depends very much on the crystalline lattice energy.

In terms of the electrical conductivity, for the sake of convenience, all minerals under investigation were separated into three groups: those with low conductivity, the average one and high. This seperation is arbitrary, since some of the minerals, /56 in terms of the electrical conductivity, are occupying the intermediate position, and could be placed into the next, neighboring group.

Among the minerals with low electrical conductivity are the oxides, a part of the silicates and the halogens. The electrical /56 conductivity in the region of impurity-related conductivity at $t=300^{\circ}C$, is less than $10^{-10}ohm^{-1}\cdot cm^{-1}$, and in the region of intrinsic conductivity ($t=1000^{\circ}C$, - not more than $10^{-6}ohm^{-1}.cm^{-1}$. As one can see from Table 9, in the case of all above-mentioned minerals, the relatively high activation energies of the major current carriers are quite characteristic (1.6-2.5 eV). In the case of the majority of these, the activation energies are 2.0-2.2 eV.

The physical nature of good insulating properties of these minerals is as follows. Within the group of minerals, the cations are the univalent Na^{1+} and K^{1+}, bivalent Ca^{2+} and Mg^{2+} and trivalent Al^{3+} ions.

Table 10 gives the basic information regarding these cations and also the anions which form this group of minerals.

TABLE 10. PARAMETERS OF IONS IN THE MINERALS OF GROUP I

Cation	Cation radius $r \cdot 10^8$, cm	Polarizability $\alpha \cdot 10^{24}$, cm	Chemical compound	Lattice energy, eV per ion pair	Constant of the lattice, Å
Al^{3+}	0,57	0,067	Al_2O_3	—	2,16—5,12
Mg^{2+}	0,76	0,114	MgO	41,36	4,2
Ca^{2+}	1,06	0,531	CaO	37,53	4,799
Na^{1+}	0,98	0,197	NaCl	7,93	5,62
K^{1+}	1,33	0,879	KCl	7,23	6,27
Cl^{1-}	1,81	3,43	—	—	—
O^{2-}	1,32	2,76	—	—	—
SiO_2^{2-}	0,39	0,039	—	—	—

[Commas in tabulated material are equivalent to decimal points.]

According to Table 10, the Al and Mg cations have the smallest radii, the largest charge and the minimal polarizability. Therefore, in accordance with the physical description of dielectrics (see Chapter I) and also keeping in mind the formulas for the crystalline lattice energy

$$U = 256 \sqrt[3]{\frac{4\pi}{3}} \frac{z \cdot \eta_a \eta_c}{\sqrt[3]{v}},$$

(where z is the number of ions per structural unit, $\eta_{a,c}$ is the valence of the anion and cation, and v is the volume of the molecule) the electrical conductivity of the minerals, formed by such type of cations, must be rather small.

By comparing the electrical conductivity of the oxides and halogen minerals in which Na^{1+} and K^{1+} are the cations we observe a difference in the electrical conductivity of three orders of magnitude. The higher conducting properties of halogens are explained by the fact that they are being formed by K^{1+} and Na^{1+} cations which, when compared to Al^{3+} and Mg^{2+} ions, are characterized by greater polarizability but smaller charge. This combination decreases considerably the energy associated with the point placement of these cations within the crystalline lattice. Because of smaller size, the Na^{1+} cation is more mobile than the K^{1+} cation, and consequently, the presence of sodium should facilitate the increase in electrical conductivity to a greater degree than the presence of potassium. /57

The silicate minerals, in addition to the Mg^{2+} or Al^{3+} cations, contain another cation, either K^{1+}, Na^{1+} or Ca^{2+} which increases their electrical conductivity. Naturally, the more of Na_2O and K_2O one has, the greater would be their electrical conductivity. Among the minerals under consideration, one is to isolate a subgroup in which the high resistance oxides are in the amounts of 90-95% and another subgroup in which these oxides comprise 80-90%. The difference in total amounts of high resistance oxides in these two subgroups does not exceed 15%, and the electrical conductivity sometimes differs by one order of magnitude (see Table 9).

One should also consider the effect of the anion on the electrical conductivity in a mineral and the electrical conductivity as a function of temperature. According to the experimental data, in the case of the alkaline haloid compounds, the electrical properties of the material depends on the anion parameters [37, 39]. With the increase of the anion radius, the electrical conductivity will increase, but the activation energy in the region of intrinsic conductivity will drop. By comparing the electrical conductivity of periclase and forsterite, we can see that the replacement of O^{2-} anion by the complex anion $(SiO_2)^{2-}$ results in the electrical conductivity increase. The increased electrical conductivity in this case is not related to the direct participation of the $(SiO_2)^{2-}$ anion in the conductivity, since bonding of silicon and oxygen is quite strong and the anion itself is not very mobile, because of its considerable size and charge. The increased electrical conductivity in forsterite, as it appears, is due to the decrease in the crystalline lattice energy.

It is necessary also to point out a particular effect of the complex anion $(OH)^{1-}$ on the conducting properties of minerals. This hydroxyl group is not as tightly embedded within the crystalline lattice as $(SiO_2)^{2-}$, and in addition, it increases the effective radius of the complex anion, which facilitates the decrease in the crystalline lattice energy, and consequently, the increase of electrical conductivity. The removal of the hydroxyl group in the form of water, as one increases the temperature, disrupts the linear dependence in $\lg \sigma = f(1/T)$ within the corresponding temperature range.

The second group incorporates the minerals, the electrical conductivity of which is: at $t=300^{\circ}C$ in the range 10^{-10}-10^{-9}ohm$^{-1}\times$ $\times$cm^{-1} and at $1000^{\circ}C$ - more than 10^{-6}ohm$^{-1}\cdot$cm^{-1}. As one can see from Table 9, this group of minerals is characterized by lower activation energies than the first one. The activation energy for these materials is within the range of 1.2-1.6 eV. /58

In addition to the cations which are characteristic for the first group, one finds here in some minerals also the iron cations. The amount of high resistance oxides in the minerals of this group is rather large - 80-85%. In conjuction with the small difference in the amounts of these oxides, one does not observe any sharp difference between the electrical conductivity in the first and in the second group of minerals. However, even the insignificant increase in the amount of Na^{1+} cations, in the presence of the iron ions, will already result in the somewhat increased electrical conductivity, particularly in the structurally-sensitive region. The electrical conductivity of garnet and olivine will be considered below.

The third group of minerals differs considerably from the first two in terms of the electrical conductivity, which in this case is higher. The high electrical conductivities of minerals are quite characteristic for the impurity-related region, as well as in the case of intrinsic electrical conductivity. The second feature of such minerals is a large range of activation energies which, for the majority of minerals, is 2.0-2.7 eV.

The sharp difference between minerals, in terms of the electrical parameters, is associated primarily with the presence in them of the Fe^{2+}, Fe^{3+} and Na^{1+} cations, which are found in greater quantities here than in the first two groups of minerals.

According to Table 9, the greatest electrical conductivity is displayed by the fialite in which the amount of FeO may reach 76%. In terms of the electrical conductivity, rubecite is not far behind, containing in equal quantities the oxides of FeO and Fe_2O_3 (about 30%), coupled to high levels of alkali oxides. The stimulating effect of Fe^{2+} and Fe^{3+} ions on the electrical conductivity of minerals has already been mentioned. One might only point out that the greatest effect of the iron ions manifests itself when the Fe^{2+} and Fe^{3+} ions are found in equal quantities.

The analysis of the experimental data, related to the electrical conductivity of minerals, and the comparison of σ with the type of cations involved, show the defining quality of the cations in development of the electrical conductivity in minerals. Figure 19 shows the curves which depict the impurity-related and intrinsic electrical conductivities for two temperatures (300 and 1000°C) as a function of the total amounts of oxides Na_2O, K_2O, FeO and Fe_2O_3. One can clearly see that the range of σ in the area of intrinsic electrical conductivity is much narrower than at low temperatures. The electrical conductivity at t=20-500°C is quite sensitive, not only to the changes in the composition and amounts of impurities, /59 but also to some structural disruptions. The data available on chemical composition of minerals indicates that all minerals may be characterized by a considerable variation, in terms of composition and quantities of impurities. In addition, the degree of structural disruption depends on the conditions under which the mineral was formed and its subsequent history.

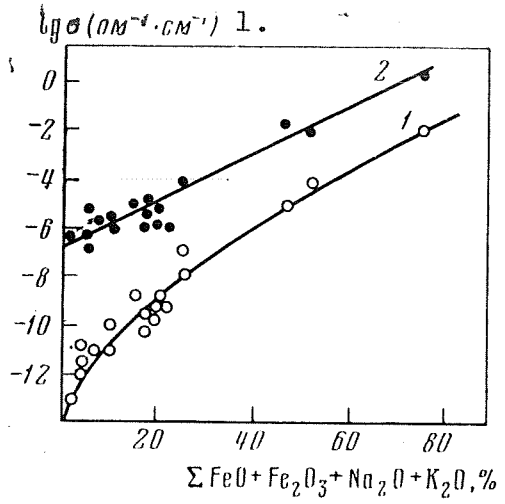

Figure 19. Electrical conductivity of minerals as a function of total amount of conducting oxides.

at t, °C:
1 - 300, 2 - 1000.

Key: 1. $ohm^{-1}.cm^{-1}$

Relationship between the electrical conductivity of minerals and their structure. To understand the mechanism of electrical conductivity in minerals, it is necessary, in parallel with the chemical properties of the material, to define the relationship between the electrical conductivity and the structure of the mineral.

The position of particles, of which the crystalline lattice is made, the lattice parameters, packing density and the coordination numbers of ions must be reflected in a specific way in the physical parameters of crystals. By accounting for the effect of the structural factor on the electrical conductivity, it becomes possible to understand better not only the processes associated with the passage of the current through the crystals, but also to change the electrical parameters in the artificially grown minerals, in the necessary direction. The relationship between the critical structure of minerals and the physical properties, until the present time, have not been well studied and there is practically no data which describes the electrical conductivity as a function of the ion packing and the lattice parameters, even for the most widely distributed minerals, as for example the oxide group. Keeping in mind that the Earth's crust and mantle consist of oxides and silicates, let us consider first the effect of the oxygen packing density on the electrical parameters of each group of minerals, separately. The coefficient of packing density X, proposed by V. S. Sobolev [50] is equal to the ratio of volumes per each oxygen ion, in the mineral with the densest packing (for example, in corundum) and the corresponding volume for a given mineral. In comparing the electrical conductivity as a function of the oxygen packing density, it was of interest also to determine the presence of a relationship /60 between the electrical parameters and the mean atomic weight $\bar{M}$, and also the mean atomic volume $\bar{V}$. In addition, Table 9 presents a true volume per each oxygen ion V_o, taking into account the volume of vacancies (between the spheres) in which the cations are located. The V_0 parameter is calculated on the basis of the following expression [51]:

$$V_o = \frac{V_c \cdot 0.74}{Z \cdot n_o},$$

where V_o is the volume $\mathring{A}^3$ per each oxygen ion, V_c is the volume of the elementary cell of the mineral $\mathring{A}^3$, Z is the number of formula units per cell and n_o is the number of oxygen ions in a given chemical formula of the mineral. According to the study [51] 74% of the volume within the mineral structure is occupied by the spherical oxygen ions which touch each other, and which have different effective radius R.

Since in addition to the packing density, everything else being equal, the important effects are the cation radius, its valence and also, as it appears, the number of bonds per unit of volume, just like in the case of considering the elastic properties, we have utilized the b and d parameters [51, 52]. The b parameter (dimensionless) indicates the number of cations per unit volume of a given compound (in 100 $\mathring{A}^3$), in other words, the cation distribution density within the material, and this can be calculated in the following manner:

$$b = \frac{n_c Z}{V_c} \cdot 100,$$

where n_c is the number of cations in the chemical formula of the minerals, Z is the number of formula units per elementary cell, V_c is the volume of an elementary cell, $\mathring{A}^3$. The d parameter is determined by using the following formula

$$d = bW_{av}\ell(\mathring{A})^{-3},$$

where W_{av} is the average valence of the cations in a given compound and $\ell = \frac{1}{V_o}$ is the oxygen ion packing density. For the simple oxides which contain one cation, the average valence is equal to the valence of this cation and in the case of more complex compounds, the V_{av} is computed as a ratio of the number of valence charges to the number of cations. For example, in the case of spinel and forsterite W_{av}=8:3, for garnet W_{av}=24:8 [51].

As we look at the data shown in Table 9, we can see on one hand a definite trend toward the increase of electrical conductivity with the increase of the average atomic volume and on the other hand, one observes the inverse relationship between the electrical conductivity and b, d and X parameters. The exception here would be the calcium oxide. One should note that of all the above-mentioned

parameters, the electrical conductivity is most sensitive to b, d, X and to the average atomic volume. In the minerals series of the first group (oxides-silicates) the b value changes from 5.3 to 2.7; d changes from 135 to 53; X changes from 1 to 0.63 and the average atomic volume - from 5.1 to 8.4. As we can see, with the increase of the average atomic volume, one observes lower packing density, lower number of cations per unit volume, and consequently, lower number of bonds. It is possible that with the decrease of packing density, and also of the number of bonds, a greater freedom of ionic motion becomes available, which facilitates increased electrical conductivity. /61

It is difficult to find any relationship in the case of the second group of minerals, since in terms of electrical conductivity, they differ only slightly. Of greatest interest is to compare the parameters of garnet and olivine, in which the structural factor manifests itself particularly clearly. The garnet-almandine, in spite of a high percentage of iron oxide (44%) has the electrical conductivity which, in terms of its magnitude, is comparable to σ in olivines, in which the amounts of FeO is ordinarily only 8-12%. The decreased electrical conductivity in garnet is explained by greater ionic packing density (X=0.88), a high d parameter and a large coordination number 8:6:4. In the case of olivine, all the above-mentioned parameters are smaller. Therefore, with the increase of the ionic packing density, the stimulating role of cations (Na, K, and Fe) in the whole process of electrical conductivity will decrease. This indicates that in the high pressure area, when the change in electrical conductivity is due not to the macro, but to the microstructural alterations, one should observe a decrease of σ, with the increase of pressure. This relationship between σ and V, b, d, X parameters indicates the need to consider this question in depth, by using a large number of minerals.

The minerals which were investigated, in the course of measurements in different directions, display the anisotropy to a different degree. This becomes particularly clear from investigating quartz, hornblende, rubecite, danburite, beryl and to a lesser degree, the feldspar. In studying the mechanical properties of silicates, it was established that the anisotropy of the elastic parameters increases with the increase if the anisotropy in the crystalline structure, in other words, as we proceed from orthosilicates to the chain, band, layered and tridimensional silicates [53]. In addition, in the case of the whole silicate group, one observes approximately equivalent velocities of the elastic waves along the directions which coincide with the direction of continuous structural blocks, and the relationships in the other directions are the function of the presence of specific cations [53]. On the other hand, the electrical conductivity, regardless of the crystallographic direction, is defined to a considerable degree by the type of cation. However the anisotropy of electrical conductivity indicates that the effect of the cation depends on the structural components. Any further studies must be directed toward the elucidation of the relationship between the effect of the cation on σ and the specifics of crystalline structure.

CHAPTER THREE. ELECTRICAL CONDUCTIVITY OF ROCKS AT HIGH TEMPERATURES

In considering the data which characterizes the governing laws /62
of electrical conductivity change in rocks at high temperatures as a function of their mineral and chemical composition, and also some other properties, the reasonable approach would be to subdivide all rocks under investigation, in terms of the following groups: acidic and intermediate, basic (effusive and intrusive), ultrabasic, alkaline and metamorphous.

The electrical parameters of dry rocks are defined primarily by their mineral composition. Therefore the petrographic description will be presented in this book at an appropriate time and place.

1. Acidic and Intermediate Rocks

The most extensively found representative of igneous acidic rocks are the granites, granodiorites and porphyrites. Let us remind the reader that the total surface area occupied by acidic rocks on the territory of the USSR comprises 50% of the whole area of all magmatic rocks. The granites (in percentages) consist of: quartz - 25-30, feldspar - 50-60, and the non-ferrous minerals - 10-15. In terms of the character of feldspar, the granites subdivided into: 1) alkaline-limestone or normal; 2) alkaline-potassium.

In the normal granites the feldspar is most often represented by orthoclase and microcline, and less frequently - by anorthoclase. If, in normal granite, instead of potassium one finds sodium, such rocks are called plageogranites. In the alkaline granites, feldspar is mostly of potassium-sodium origin (microcline, anorthoclase) and less frequently - a pure sodium (albite). The dark non-ferrous components of the alkaline granites are the alkaline hornblende (rubecite, arphvedsonite), alkaline pyroxenes (eugirite-augite, eugirite). Ordinarily, in terms of the character of the non-ferrous mineral, one can differentiate the following types of alkaline granites: 1) biotite and mica, 2) rubecite and arphvedsonite, 3) eugirite, 4) alkaline alaskite. The rock which is similar in composition /63
is the granodiorite, which is also an essentially quartz rock, enriched to a greater degree by feldspar, predominantly of limestone-sodium type. In the granodiorites, the non-ferrous mineral is represented by hornblende and by biotite. Pyroxene is encountered more often in the granodiorites than in granite. Let us consider the specifics of electrical properties of granites selected in different areas of origin in the Soviet Union.

The granites from the western part of Central Kazakhstan are represented by the samples taken from different areas of the top granite intrusions [46, 54, 55]. The major rock-forming minerals in these granites are: quartz - 28-35%, feldspar - most frequently, potassium feldspar - 35-55% and mica, in the form of muscovite and biotite - up to 15%. Appendix 2 shows the experimental data of electrical conductivity, of the activation energy and of the logarithm in the pre-exponential coefficient, for the impurity-related region and the intrinsic electric conductivity. One should note first of all that the change of electrical conductivity in granites as a function of the temperature, going from 200 to 1200°C, is quite large and is between 7 and 10 orders of magnitude. The different values of electrical conductivity in different granites at the same temperature do not exceed one order of magnitude. In terms of the electrical conductivity of intrinsic type, for example, at 1000°C, the granites under consideration may be subdivided into two groups. In the case of one, at t=1000°C, σ is between 10^{-5}-$1.3\cdot10^{-5}$ ohm$^{-1}\cdot$cm^{-1}, and in the case of the other one, the electrical conductivity is less and changes between $9.0\cdot10^{-6}$ and $2.6\cdot10^{-6}$ ohm$^{-1}\cdot$cm^{-1}. In the impurity-related region, the conductivity of granites of the first group is not always characterized by the greater electrical conductivity.

The lg σ=f(1/T) relationship for granites is shown in Figure 20. As we can see, in the case of all granites, we observe a sharp inflection point on the curves, which describe the logarithm of electrical conductivity as a function of temperature. For the sake of apparency, Figure 21 also shows the activation energies which correspond to the specific temperature intervals. The first sharp inflection on the curve of lg σ=f(1/T) occurs most often within a more narrow temperature range, from 400 to 700°C. In the case of some granites, the first segment of the curve is characterized by quite low activation energy (0.2-0.5 eV, Appendix 2).

At the second segment on the curve (300-900°C, it is considerably higher and is in the range between 0.8-1.1 eV, and only in the case of granite in which the amount of micropertite is 40-45%, it reaches 1.22 eV. The temperature range which corresponds to the upper limit of the activation energies is between 650 and 900°C. The greatest activation energy of the current carriers is observed at temperatures above 800-850°C, and is 3.4 eV. It should be pointed out that of ten Kazakhstan granites which were studied, only two have such high activation energy, and in the case of other granites, it comprises 2.0-2.6 eV. In the case of granites from the Caucasus /64 which were investigated, quite typical is the low electrical conductivity across the whole temperature range, and this range is characteristic for the second group of Kazakhstan granites. For

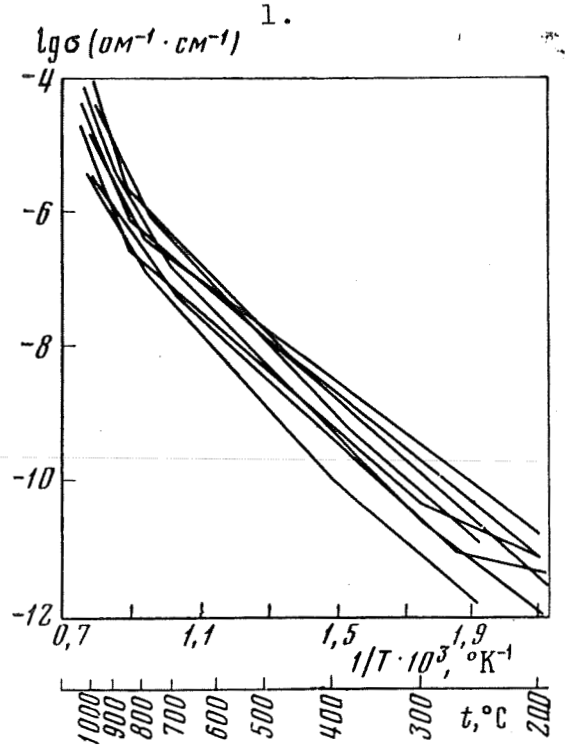

Figure 20. Electrical conductivity of granite as a function of temperature.

Key: 1. $ohm^{-1} \cdot cm^{-1}$

the three samples of granites, one observes on the lg σ=f(1/T) curve just one sharp inflection point and only in the case of one granite which had the highest electrical resistance, one observes two sharp inflection points. The differences of this kind in lg σ= =f(1/T) may be explained qualitatively in the following manner. It appears that the electrical conductivity within the intermediate temperature range (400-900°C), is brought about not by one type of current carriers, but by either two or more types. As a result, what we are observing is the summary effect, the magnitudes of which may fluctuate, depending on the degree of participation of one specefic cation. In addition, when the difference between the activation energies of two current carriers is small, the first inflection point will not be seen, and in the opposite case, it will be well defined at the temperature which depends on the activation energy of the ions which are not as strongly bonded and on the concentration of these ions. The absence of the inflection point on the lg σ= =f(1/T) curve in the presence of two types of current carriers is an experimentally established fact. For example, in NaCl at high temperature, the electrical conductivity is brought about by both Na^{1+} and Cl^{1-}, but there is no inflection point on the curve. It should be noted also that in the case of granites, the activation energy of which does not exceed 0.9 eV, up to t=900°C, we have two regions of /65 electrical conductivity in which the activation energy is 0.9 eV and more, and there is another area in the 200-600°C temperature range, where the activation energy is about 0.6 eV.

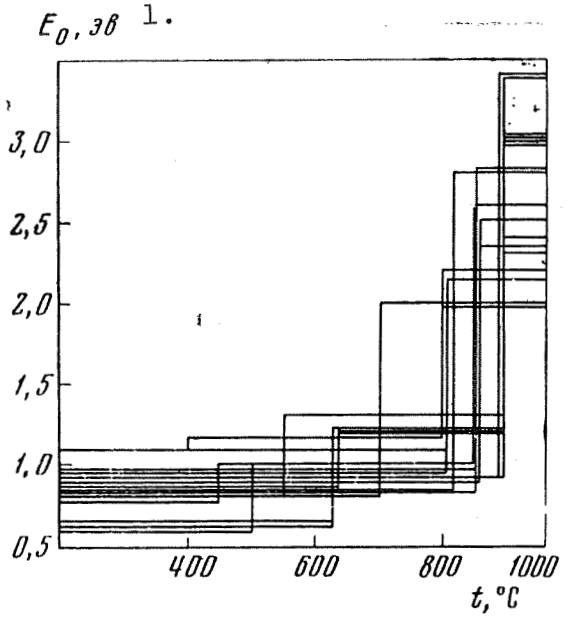

Figure 21. Activation energy of granites in the impurity-related region and the intrinsic conductivity.

Key: 1. eV

Diorite group. In terms of availability, the diorite andesine group is below the gabbro-basalt group. The andesites and their analogues comprise 25% of the total mass in magmatic rocks. The diorites, which are the intermediate-size rocks consisting primarily of plagioclase (andecite - 65-70%), of the hornblende (3.5%) and sometimes of pyroxene or biotite. If the quartz content is up to 6% - this is an ordinary diorite, and if it is 6-10% - it is called the quartz-containing diorite and above 10% - quartz diorite.

The rocks with high amount of alkaline feldspar belong to the granodiorite group. The most widely found non-ferrous mineral in diorite is the hornblende, and the least frequently encountered - biotite. The geological relationship between the granites, granodiorites and diorites is so close that it is difficult to differentiate them within a rock.

In terms of electrical properties, the closest among the diorite group to the granites are the quartz diorites. The electrical conductivity of the latter at the low temperature range is in the same range as the electrical conductivity of granites (see Appendix 2) and at t=1000°, it is in the range between $1.3 \cdot 10^{-5}$-$4.8 \cdot 10^{-5}$ $ohm^{-1} \cdot cm^{-1}$ which corresponds to the lower limits of σ, typical for granites. The electrical conductivity of Kazakhstan quartz diorites at the temperatures of 200-600°C is somewhat lower than in the same rocks of Vorenezh anteclase. In addition, the latter display, within a narrow temperature range, the anomalous electrical conductivity. It is possible that in diorite 2619, this may be explained by the presence of a considerable amount of biotite and of hornblende, and in the diorite 2600 - by the secondary minerals - sericite and chlorite. The low temperature and high temperature ranges are characterized by the parameters which, in terms of magnitude, are within the limits typical for acidic rocks.

The granodiorites, as has been mentioned earlier, are also similar in terms of mineral composition to the granites. However, the presence in these rocks, in somewhat greater quantities than in granites, of basic feldspar and of the non-ferrous minerals in the form of amphibole or hornblende, which have higher electrical conductivity as compared to quartz, result in the increase of electrical conductivity in the granodiorites, particularly in the region of impurity-related conductivity. The Kazakhstan granodiorites, in which there is more quartz, in terms of σ, are closer to granites than the Ural granodiorites. Nonetheless, the above-mentioned difference in mineral composition of granodiorites and granites is reflected in a certain way also, in the character of $\lg \sigma = f(1/T)$, in the activation energies and in the pre-exponential term. In all granodiorites which we have investigated, the electrical conductivity as a function of the temperature relationship shows just one bending point near 900°C, with the exception of one sample of granodiorite in which this inflection point is observed at 720°C. The average /66 activation energy in the region of impurity-related conductivity and in the region of intrinisic conductivity is less than in the case of granites and does not exceed 0.8 and 2.34 eV, respectively.

The diorites at the temperatures below 600-700°C, are characterized by the greatest electrical conductivity, as compared to the quartz diorites and granites, and in addition, in the case of diorites, it is higher than in the above-mentioned rocks, by one and sometimes two orders of magnitude. As the temperature is raised, the difference in electrical conductivity between the granites and the diorite group decreases, but in the case of granodiorites, nonetheless it is higher than in the case of granite. For example, at t=1000°C, σ in diorites will be about 10^{-5}ohm^{-1}.cm^{-1}, and in the granites - 10^{-6}ohm^{-1}.cm^{-1}.

Analogous to granodiorite, the diorites display also two temperature regions. The diorite samples which were studied are characterized by approximately the same values of $\lg \sigma_0$ and E_0 parameters. The comparison of temperature relationship, as it affects the electrical conductivity in the diorites with montdiorites (the Gor'kiy complex) indicates that these rocks, in terms of electrical properties, differ quite significantly. The montdiorites display a considerably greater electrical conductivity, and in addition, at the temperature range of 800-1050°C, in the case of one rock, and of 500-720°C in the case of another rock, one observes the disruption of exponential relationship of the electrical conductivity as a function of temperature. This, as it appears, is related to the secondary changes in the plagioclase, which are manifested in its albitization and also partial pelletization. It is possible that in addition to these causes, there are some others which result in the observed deviations of σ, also causing an irregular change of the rock at high temperatures.

In conclusion, the following points must be noted.

1. One observes a definite relationship of electrical conductivity as a function of mineral composition for the rocks of granite-diorite group. With the decrease of quartz content in these rocks, one observes a definite increase of electrical conductivity. Figure 22 shows the electrical conductivity in the rocks as a function of the amount of quartz within the impurity-related region (at t=200°C) and the intrinsic conductivity (at t=1000°). One can see that the decrease of the amount of quartz from 35 to 5% in the impurity-related conductivity region is accompanied by a rapid increase of electrical conductivity (from $\sigma=10^{-12}$ to $5\cdot10^{-8}$ ohm^{-1}.cm^{-1}).

The increase of electrical conductivity with the decrease within the rock of high resistance mineral quartz is accentuated by the increased quantities within the rock of the hornblende, which, as has been shown earlier in the preceding chapter, has higher electrical conductivity than quartz.

Naturally, the replacement of quartz by hornblende or by hypersthene must facilitate the increase of electrical conductivity. At the same time, the biotite and augite diorites have low electrical conductivity. The variable mineral composition of diorites result in a broader range of electrical conductivities as compared to the granites. The intensive increase of electrical conductivity because of change in the mineral composition within the granite-diorite rock series is being observed up to 600-700°C and at higher temperatures, this difference practically disappears. This is related to the fact that the rock-forming minerals, in terms of their electrical conductivity, differ from each other primarily in the impurity-related region of conductivity (see Appendix 1) and have the σ values which are similar to those found within the intrinsic conductivity region. /67

2. In parallel with the analysis of the effect of mineral composition on the level of electrical conductivity, the comparison of electrical conductivity of the rocks, as a function of their chemical composition, was also carried out (Table 11). It was discovered first of all that there is a strong dependence of the electrical conductivity on the amounts of silicon oxide SiO_2. In a series of rocks, containing SiO_2, with the decrease of the latter, the electrical conductivity will increase correspondingly. The analogous relationship between the electrical conductivity and the amount of some other high resistance oxide (Al_2O_3 and MgO) is not being observed. One might point out only the increase of it in the diorites, as compared to granites, which must be due to the decreased electrical conductivity in the former.

The oxides, because of which one might observe the increase of electrical conductivity, are Fe_2O_3, FeO, Na_2O, K_2O, and also, CaO in such case when one observes the replacement of MgO and Al_2O_3 by CaO.

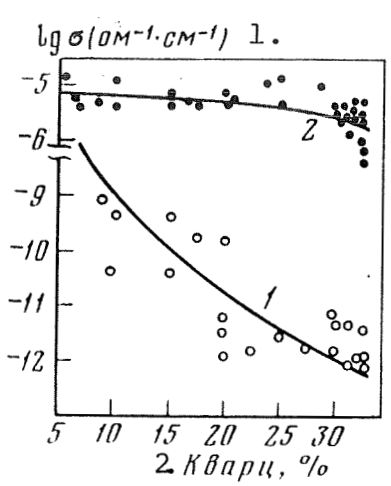

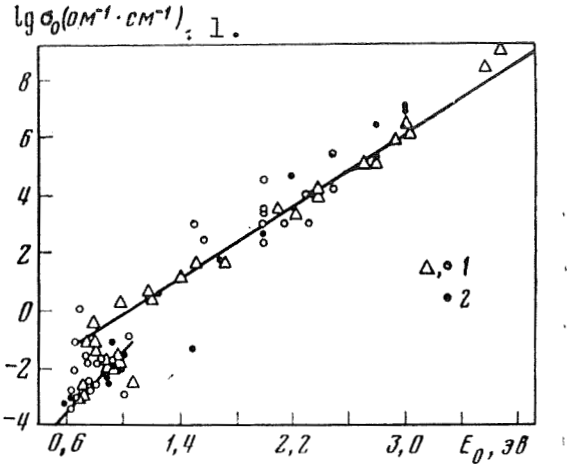

Figure 22. Electrical conductivity of the acidic and intermediate rocks as a function of the quartz content.

At t, °C: 1 - 200°; 2 - 1000°.

Key: 1. $ohm^{-1} \cdot cm^{-1}$; 2. Quartz

Figure 23. Pre-exponential coefficient as a function of the activation energy for the granite-diorite rock group, on the basis of the author's data.

1 - Granite; 2 - Diorite.

Key: 1. $ohm^{-1} \cdot cm^{-1}$

One can see from Table 11 that the total sum of iron oxide increases approximately from 4 to 7% and that of the alkaline oxides Na_2O and K_2O, on the contrary, decreases from 7.5 to 5.2%, and finally, that the amount of CaO increases from 2 to 6.7%. With the decrease of /68 rock acidity, the amounts of TiO_2 increases rather rapidly. In the diorites, these amounts are greater than in the granites by a factor of from 2 to 4. Therefore, the increase of electrical conductivity within the granite-diorite group is primarily observed because of the SiO_2 replacement by the iron oxides, and also possibly, as a result of the increase in the amounts of CaO. Such replacement within the rocks, as one can see from the presented data, is reflected primarily in the level of electrical conductivity within the impurity-related conductivity region (extrinsic conductivity).

TABLE 11. CHEMICAL COMPOSITION OF THE ROCKS WITHIN THE GRANITE-DIORITE GROUP

Rock	SiO_2	TiO_2	Al_2O_3	Fe_2O_3	FeO	MgO	CaO	Na_2O	K_2O	N_2O	P_2O_5
Granite(Saltykovskiy)	68,67	0,34	15,07	0,72	2,90	2,22	1,14	4,31	3,6	0,33	—
Granite(Pavlovskiy)	69,6	0,21	14,04	1,77	2,18	0,47	1,76	4,2	7,62	0,2	—
Granite [56]	69,3	0,23	16,81	0,28	0,26	1,08	3,34	6,0	1,39	0,5	—
Granites, basic [56]	69,21	0,41	14,41	1,98	1,67	1,15	2,19	3,48	4,23	0,85	0,3
Granodiorites [56]	65,01	0,57	15,94	1,74	2,65	1,91	4,42	3,7	2,75	1,04	0,2
Quartz diorites	61,59	0,66	16,21	2,54	3,77	2,80	5,38	3,37	2,1	1,22	0,25
Diorites [56]	56,77	0,84	16,67	3,16	4,40	4,17	6,74	3,39	2,12	1,36	0,25

[Commas in tabulated material are equivalent to decimal points.]

3. The change of mineral and chemical composition within the group of granite-diorite rocks causes not only the dispersion of electrical conductivity but also affects somewhat the activation energy and the pre-exponential coefficients. In this case, while because of the two above-mentioned factors, the differentiation of these rocks, in terms of the electrical conductivity, is being observed only within the range of intrinsic conductivity, the values of E_0 and $\lg \sigma_0$ parameters change in the intrinsic, as well as in the impurity-related conductivity regions. According to Appendix 2, the majority of granites within the temperature range of 600-900°C are characterized by the activation energy E_0=1.0-1.2 eV, and above 900°C - 2.3-3.0 eV, and only in two granites, the activation energy reached 3.4 eV. In the diorites, the activation energies for the temperature ranges as indicated, fluctuate between 0.6-0.8 and 2.0-2.5 eV. The decrease of activation energy in the current carriers within the granite-diorite series is associated with the fact that the E_0 of hornblende and of other non-ferrous minerals is lower than that for the minerals of the feldspar and quartz group.

4. Within the impurity-related region and within the intrinsic electrical conductivity region for the granite-diorite group of rocks,

one finds a linear proportional relationship between lg σ_0 and E_0 /69 (Figure 23). The analogous relationship is known for the impurity-related ionic conductivity in silicates [57] and is also established for some mountain rocks [58]. In the first case [57] it is related to the change in the concentration ratio of two or more types of impurities. For the system $xK_2O(1-x)Na_2O \cdot 2SiO_2$, as x goes from 0 to 0.5, E_0 and σ_0 also increase, reaching a maximum. With any further increase of "x" from 0.5 to 1.0, the E_0 and σ_0 parameters decrease. This observable rule is explained by the differen radii of K^+ and Na^+ ions and different effect of these ions on the silicate structure. The Na^+ ions are not as tightly bound and therefore their replacement by K^+ ions strengthens the structural bonds. In such case, the activation energy also increases. Such substitution will occur until all Na^+ ions which are not as tightly bound, will be displaced. If the concentration of K^+ ions will continue to increase, these ions, not being able to displace potassium, are being placed at the other vacant lattice points, where the bonds are weaker. In such case, the structure becomes less dense, and E_0 correspondingly will decrease.

To elucidate the physical nature of such bonding, let us consider what are the factors on which the lg σ_0 and E_0 depend. The pre-exponential coefficient σ_0 in the formula $\sigma_t = \sigma_0 e^{-\frac{E}{kT}}$ is defined by the following expression:

$$\sigma_0 = \frac{n_0 q^2 \delta^2 \nu}{\sigma k T},$$

where n_0 is the number of ions per 1 cm^3, which participate in the current transfer, δ is the distance between the lattice point and the vacancy or between the interpoint space and ν is the ionic vibration frequency.

It follows from this expression that σ_0 may increase because of the increase of n_0, δ and ν. Of all these quantities, n_0 may be varied the most, in other words, the defect concentration may be the most varied, and the variation of δ and ν are less pronounced. It is known that even in the simplest ionic crystals, the ions feature a complex distribution in terms of energy [59]. For example, the K^+ ion may have the activation energy from 0.6 to 1.4 eV, depending on its position within the structural network. In the complex silicates, as it appears, this range will be even broader,

and it will depend on the crystalline lattice and on the rock history. If we assume in the first approximation that the $\lg \sigma_0 = f(E_0)$ relationship is defined only by the increase of n_0, as the activation energy increases, this enables us to have a general idea as to the particle distribution, with respect to the activation energies, for a given group of rocks. It appears that this fact should not be completely excluded from considerations. In addition, we believe that the activation energy must be a direct function of δ. This parameter is found in the nominator, as a squared function, in the expression for σ_0. As we can see, even with the slow increase of δ, one must observe the intensive increase of σ_0. It appears that the activation energy also is directly related to ν. According to /70
G. Stewells [57] the change of ionic vibration frequency is possible as the activation energy increases. This analysis enables us to explain only qualitatively the experimentally established relationship of $\lg \sigma_0 = f(E_0)$. For a greater understanding in depth, some additional experimental data and theoretical calculations will be necessary.

The andesites with basalts represent the most frequently encountered group of rocks. According to the calculations, the andesites represent 24% of the rocks found in North America and basalts - 21% of the total mass of igneous rocks.

The values of electrical conductivity of andesites from Kamchatka, the Soviet Far East and Sakhalin at high temperatures are presented in Appendix 3. It is known that andesites are the analogues of diorites in terms of chemical composition and are similar to a considerable degree in terms of mineral composition. By comparing the σ values of andesites and diorites in the low temperature range, in other words, within the so-called structurally-sensitive region, we can see that there is a considerable discrepancy and this difference is also extended to the high temperature range. Therefore, the andesites have a significantly greater electrical conductivity than the diorites group for the whole temperature range between 200 and 1100°C. At 1000°C, the electrical conductivity of andesite in a number of cases is greater by approximately a factor of 100 than in the diorites. The exceptions are only two montdiorites, which in terms of the electrical parameters, are quite similar to andesites. The activation energy of andesites within the structurally-sensitive region is in the range of 0.54-0.74 eV. However, while in the case of some diorites, one observes even higher E_0 than 0.74 eV, in the case of the andesites, this is the maximum value. On the other hand, at high temperatures, the activation energy of the intrinsic charge carriers in andesites is considerably lower than in diorites and does not exceed 1.4 eV (Figure 24), while in the case of diorites, the typical value would be 2.0 eV. It should also be noted that all andesites which were investigated are characterized only by two temperature regions which differ in terms of the mechanism of electrical conductivity (see Appendix 3).

As we can see, in spite of the similar chemical composition of diorites and andesites and an insignificant difference in mineral composition, one observes a clear delineation between these rocks in terms of the electrical conductivity and of the activation energy in the high temperature range. The main reason for such differentiation of the rocks which we have evaluated, in terms of their electrical properties at high temperatures, is the structural factor. The andesites are effusive analogues of diorites which incorporate frequently the remainder of the crystallized part of the rock. The question of the effect of the amorphous phase on the electrical parameters of mountain rocks is described in greater detail below in conjunction with the electrical conductivity of basalts.

In addition, the effusive rocks, and in particular the andesites, feature small crystalline structure which increases to a considerable degree the surface conductivity across the boundaries of the grains. This in turn will result in the total increase of electrical conductivity. According to the obtained data, the fraction of the amorphous phase in the rock, and the thin crystalline structure of the rock not only increase the electrical conductivity but also decrease the activation energy of the current carriers within the region of intrinsic conductivity. /71

The representative andesites investigated by us do not embrace by any means the whole comprehensive class of these rocks which have a great variety and content of non-ferrous minerals. The data presented above for the minerals of pyroxene, of the hornblende and mica group, indicate considerable differences in σ. Therefore, one may assume that in the course of further study of andesites, the limiting values of σ, E_0 and $\lg \sigma_0$, obtained by us, may be considerably expanded.

2. Effect of the Age and Cataclasis on the Electrical Conductivity of a Series of Acidic Rocks

A. A. Vorob'yev and F. S. Zakirova [60, 61] have established on the basis of an extensive experimental material, related to the study of electrical conductivity in different potassium-containing minerals and rocks that the magnitude of electrical conductivity at the bending point in the region of high temperatures (800-1000°C) depends on their age. With the increase of potassium-containing mineral age, the electrical conductivity at the second bending point decreases. The authors [60, 61] believe that this observable rule is due to the radioactive conversion of K^{40} into Ca^{40} with the corresponding, internal β particle emission.

We have investigated the effect of age by using a number of acidic rocks with the crystalline base (Voronezh anteclase) which belong to the archeozoic and proterozoic eras.

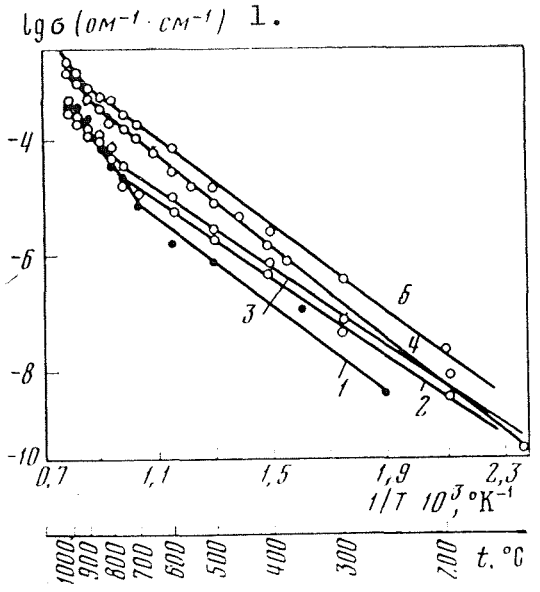

Figure 24. Electrical conductivity of andesites as a function of temperature.

1 - 1010; 2 - 1373; 3 - 1011; 4 - 1380; 5 - 1374.

Key: 1. $ohm^{-1}.cm^{-1}$

The experimental results /72 pertaining to electrical properties of the above-mentioned rocks are presented and are being discussed in accordance with the vertical positioning of the geologic complexes of magmatic and metasomatic rocks, from the archeozoic era to the proterozoic era.

The oldest rocks (the late archeozoic era) are represented by gneiss of the Oboiansk formation. Their main feature is the presence of anomalous change in σ within the temperature range of 750-850°C. The electrical conductivity of these rocks at the point of inflection in the straight line $\lg \sigma = f(1/T)$ is in the range of 10^{-7}-$6.0 \cdot 10^{-6}$ $ohm^{-1} \cdot cm^{-1}$. The electrical conductivity of gneiss is being considered in greater detail, while analyzing the electrical parameters of the metamorphized rocks.

The investigated cataclase microcline granite and plageogranite belong to the plageogranite-magmatite Saltykov tract, which was the result of the anteclinor elevations of the extensively metamorphized rocks of the archeozoic era, of the amphibollite-gneiss formation. The age of these rocks is approximately 2750 million years. According to the petrographic analysis, these rocks display some traces of intensive cataclasis, which is apparent by observing the fractured grains of quartz and their gradual disappearance. In addition, in the granite 2585, the plageoclase is strongly cericitized, particularly within the cataclasis zones.

The above-mentioned features of the rocks have exerted the appropriate influence on the electrical conductivity, by increasing it in the low temperature range, as compared to the electrical conductivity of granites from other areas. In addition, one observes its anomalous decrease with the temperature increase. The irregular behavior of σ within the range of 300-600°C has been established while measuring three adjoining samples of the granite 2862 (Figure 25a).

The Oskoletsk formation of granitoids has been evolved within the proterozoic synclinore zone, and in terms of its age, belongs to the late proterozoic era (2185-2000 million years). It is represented predominantly by the migmatites which underwent different exposures. The areas of Oskoletsk granitoids coincide with the fracture zones.

The migmatites are characterized by a variety of morphological types, among which one could name the laminated, bröggerite-like and schistose. The fluctuation of mineral composition is due on one hand to the degree of age exposure of plagiogranites, and on the other hand, by the intensity of microclinization.

The electrical conductivity of migmatites was investigated by using three biotite-plageoclase migmatites and one schistose. The plageoclase migmatite is encountered in the form of thinly paired, cericitized and frequently, crushed. All migmatites which were investigated (2797, 2572, 2192 and 2198) display the linear relationship in terms of lg σ and 1/T without any anomalies which are being observed in the gneiss and granite of Oboiansk and Saltykov tracts. The temperature relationship between the electrical conductivity of the three first migmatites is characterized by three regions and for the microcline migmatite 2198 - by two regions (Figure 25b). In the migmatites 2572 and 2797, /73 which feature the greatest electrical conductivity as compared to the other two, in the I region of low temperatures, approximately down to 350°C, the current is generated by the particles with a rather low activation energy (E_0=0.23-0.3 eV). The small lg σ_0 in this region indicates insignificant concentration of the current carriers, and also their low mobility. In the case of migmatite 2192, the low temperature region is extended to t=600°C, and is characterized by higher E_0 and σ_0 parameters. All this point to other types of current carriers, and to their higher mobility and concentration. In the second region (600-900°C), the particles with the activation energy of 0.72-1.0 eV are taking part in the charge transfer. As it appears, the source of these particles is primarily the feldspar, since in the microcline and orthoclase within this temperature range, the current carriers are characterized by similar electrical parameters. For the granite sample 2198, because of the small quantity of impurities, the first region at t<300°C has not been observed.

The intrinsic electrical conductivity of all migmatites commences at the temperatures close to 900°C. In this case, σ at the inflection point fluctuates between $6.0 \cdot 10^{-7}$ to $2.0 \cdot 10^{-6}$ $ohm^{-1} \cdot cm^{-1}$. The migmatites 2198 and 2192 have the smallest intrinsic electrical conductivity because of relatively high amounts of quartz.

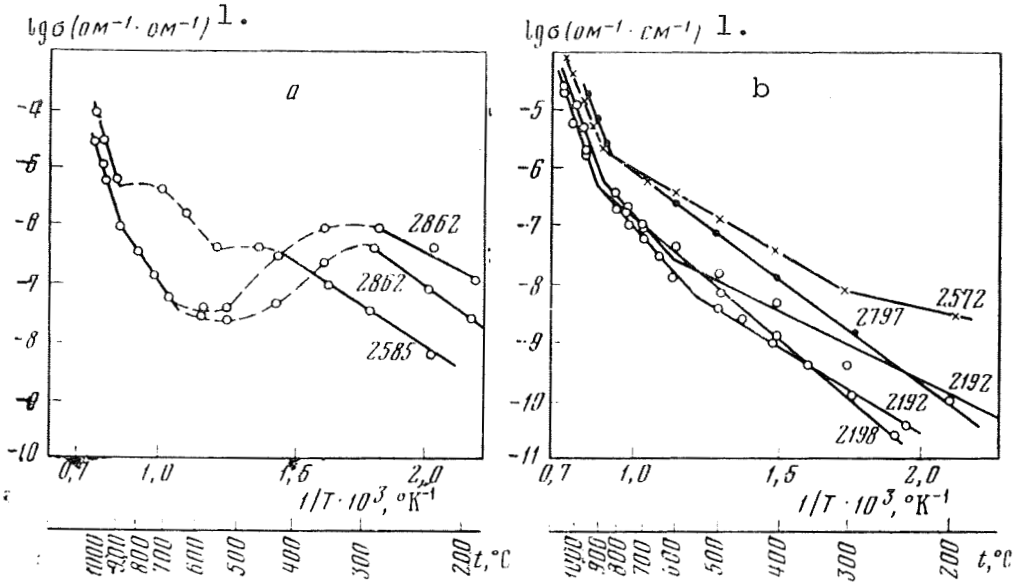

Figure 25. Electrical conductivity of granites and migmatites as a function of temperature.

a - cataclasticgranites of the Saltykov tract (archeozoic era);
b - migmatites of Oskoletsk formation (late proterozoic erea).
1. $ohm^{-1} \cdot cm^{-1}$

The Pavlovsk-Voronezh rock formation tract is the youngest one (1750 million years) of all formations which have been investigated. The rocks from this formation (plageomigmatite 2193, /74
metasomatic granite 2573, polymigmatite 2187 and granite 2574) differ at high and low temperatures by a considerably greater scattering in E_0 and σ_0 values than in the case of the rocks from other formations. This correlates well with the substantial change in the mineral composition of the rocks, the structural differences in terms of the depth of formations, the intensive display of metasomatic processes, in particular the alkaline metasomatosis.

The plageomigmatite 2193, when compared to the other rocks within this formation, displays the greatest electrical conductivity within this group of rocks, up to the temperature of 700°C. The high electrical conductivity of plageomigmatite in the low temperature range (200-780°C) is due to the presence of ionic impurities with low activation energy (E_0=0.48 eV). Because of the presence of the latter, one cannot determine the intermediate region (within the range of 600-900°C) with the intermediate values of E_0 and σ_0 parameters. In addition, as it appears, the impurity ions with the above-mentioned activation energy, affect to some degree the energy state of the basic current carriers in the high

temperature range, since the E_0 and σ_0 for this rock are lower than in the case of granite 2573 and migmatite 2187, at the temperature above 900°C. The most probable current carriers within this range are the potassium cations since the amount of K_2O in them is greater than in the rocks of other complexes. The range of electrical conductivity in the Pavlovsk granites at the temperatures of about 900°C is somewhat higher than the analogous range of σ for older rocks, comprising $2.0 \cdot 10^{-6}$-$9.0 \cdot 10^{-6}$ ohm^{-1}.cm^{-1}.

One therefore notes, for the investigated rocks of Voronezh anteclase, an insignificant decrease of electrical conductivity in the high temperature point of the straight line inflection $\lg \sigma = f(1/T)$ with the increase of the rock age. In a number of cases, this relationship is not being obeyed because of the secondary processes. In addition, the relatively young rocks (the proterozoic era) are as a rule characterized by a clearly defined linear σ as a function of $1/T$, while in rocks of the archeozoic era, this relationship is frequently not obeyed.

The granites which were subject to intensive tectonic activities display higher electrical conductivity at the low temperature region (down to 500°C) as compared to the younger rocks, which were not affected by these processes. It is known that at low temperatures, the current carriers are the ions which have the lowest activation energy. It appears that the cataclasis and the secondary changes facilitate the increase in the number of such ions, without any significant disruption of the general energy state, since the levels of activation energy for all granites differ only slightly.

In the cataclastic rocks, of the late and intermediate archeozoic era, one detects the region of anomalous change in electrical conductivity as a function of temperature. It is known that of /75
all rock-forming minerals in granites and migmatites, a clearly expressed anomaly in σ is displayed by mica, because of the evolution of the water of crystallization. This gives us grounds to believe that the reason for such temperature anomaly, associated with electrical conductivity, is due to mica. However, in the absence of cataclasis and even in the presence of higher quantities of mica in the rocks, the analogous phenomenon was not observed. Consequently, the primary cause is the changes which are associated with the cataclasis in mica. The other possible cause of the anomaly in σ may be the secondary minerals which contain the $(OH)^{1-}$. It should be pointed out that these processes have no significant effect on the electrical parameters in the high temperature range. The electrical conductance, E_0 and $\lg \sigma_0$ are within the range which is typical for this class of rocks.

3. Basic Intrusive Rocks

Among the major intrusive and effusive rocks, of greatest importance is the gabbro-basalt group. In terms of its availability within the Earth's crust it is comparable to granites.

Gabbro belongs to deep-lying decrystallized rocks, with evenly distributed grainy structure. The major rock-forming minerals in gabbro are basic plageoclase from the labradorite—bytownite-anorthite series (50-60%) and the non-ferrous minerals (35-50%). The non-ferrous mineral is the monocline or rhombic pyroxene or hornblende. The secondary components of gabbro are frequently olivine, followed by biotite, sometimes quartz and orthoclase. The auxiliary minerals in gabbro are apatite, ilmenite, magnetite, sometimes pyrrhotine and chromite. In conjunction with small quantities of silica (45-52%) the rocks of the gabbro-basalt group are of basic type. They contain large quantities of calcium (CaO - 10.5-11.5%), of iron (Fe_2O_3+FeO - 10.5-12.0%), of magnesium (MgO - 6.5-8.5%), of sodium (Na_2O - up to 2.5%) and an insignificant amount of potassium (K_2O - 1%).

The investigation of electrical properties of gabbro at high temperatures were conducted by using the rocks from Voronezh anteclase, from the Gor'kiy region, from the Cola peninsula and from the South Ural mountains. In all, about 50 samples of gabbro were investigated. It should be noted that the electrical conductivity in the rocks of gabbro type fluctuates in a broader range than in the case of granites and diorites, because of greater variety in mineral composition. All samples which were investigated were divided into two groups: those which were undergoing cataclasis and those which were not. In addition, some of these were combined in terms of their petrographic qualities.

Let us first consider the electrical properties of gabbros which had not undergone cataclasis.

Gabbro of the Mamonov complex in Voronezh anteclase, in /76
contrast to older basites and ultrabasites, either did not undergo any regional metamorphosis or underwent only slight metamorphosis. The gabbro-norites contain hypersthene which has higher iron content and plageoclase in the form of andesite. The ore minerals are in the form of magnetite, ilmenite and pyrite.

The gabbro-norites 2622 and 2609 display the highest electrical conductivity across the whole temperature range. The somewhat high electrical conductivity of gabbro 2622 (see Appendix 4) is due to the secondary changes in the basic rock-forming minerals since the sample of this rock was cut out from the rocks at the boundary with a weathered crust. The secondary change in the minerals is also the basic reason for the appearance of the zone within which the anomalous change of electrical conductivity, as a function of

temperature, takes place. It is not excluded that the secondary mineral changes also affect the activation energy at t>900°C, which was only 1.76 eV.

The origin of higher electrical conductivity in the second type of gabbro rocks - gabbro 2609, is associated with the considerable quantities of magnetite (about 10%) which is found in the rock in the form of separate grains, and in the form of deposits along the grain boundaries. In this case, the uneven distribution of magnetites in the rock causes some scattering in the electrical conductivity readings in the case of two samples, which were sequentially cut out from the same piece of rock. The second mineral which facilitates increased electrical conductivity in gabbro 2609 is the hypersthene with increased amounts of iron, which was found to be at the level of 25%. This mineral also displays lowered activation energy, at the level of 1.6 eV, in the high temperature range. As we can see, the gabbro 2622 and 2609 have similar E_0 and lg σ_0 which are quite typical for gabbro in the low temperature range and at high temperatures correspond to the lowest limits of E_0. In terms of the electrical conductivity, the c l o s e s t to gabbro 2609, is the gabbro-norite 2621.

The major distinctive feature of gabbro is the anomalous change of σ (at temperatures above 720°C) which manifests itself first in the slight, and then in a sharp increase of electrical conductivity. The beginning of such anomalous change as a function of temperature is most likely associated with the high temperature melting of separate grains within the rocks.

The gabbro-norite 2616, just like the two previous rocks, contains a considerable quantity of hypersthene. However, because of the absence of magnetite and because of a sufficient quantity of plageoclase (about 60%) its electrical conductivity is lower than in the case of gabbro 2609 and 2621.

The gabbro amphiboles 2620, 2608, 2618 and 2863 are characterized by similar electrical conductivity within a broad temperature range which is likely because of the high content of minerals from the amphibole group. In the case of all the above-mentioned samples, one observes at high temperatures the disruption of linear relationship between lg σ and 1/T (Figure 26a). The analogous disruption within the high temperature range is quite typical for almost all rocks which incorporate the amphiboles in a considerable quantity. /77

The electrical parameters E_0 and lg σ_0 in these rocks are within the range which is quite characteristic for this class of rocks. The major distinguishing feature of gabbro-diabase 2863 are the low E_0 and lg σ_0 which may be due to high amounts of hornblende, just like in the case of gabbro-diabase 2618. It is not

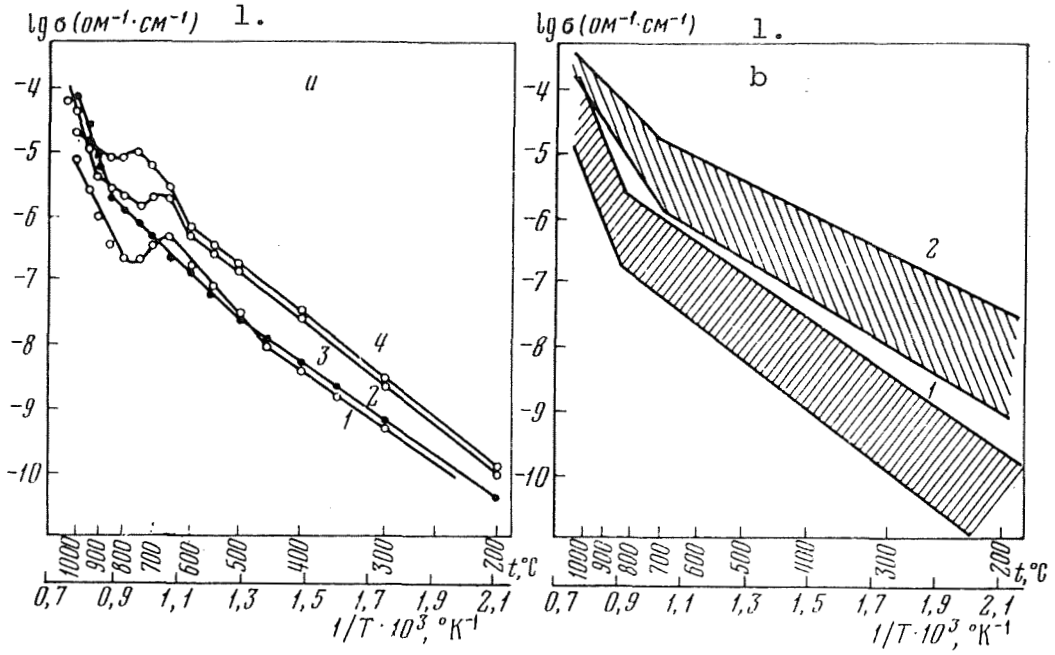

Figure 26. Electrical conductivity of gabbro as a function of temperature.
a - amphibole gabbro (1-2620, 2-2608, 4-2618); 3 - gabbro 2615; b - level of σ values in the unaltered gabbro of different composition (1), and of the cataclasticgabbro (2).
Key: 1. $ohm^{-1} \cdot cm^{-1}$

excluded that the quantities of titanite and the diabase structures also lower these parameters. The gabbro-diabase 2617, in terms of its mineral composition, is similar to plageoclase-pyroxene gabbro 2622, but differs from the latter by lower electrical conductivity across the whole temperature range which was investigated and also by higher activation energy E_0 at elevated temperatures. These differences once again substantiate the significant effect of the secondary changes on the electrical parameters, to which the gabbro 2622 was subjected.

It follows on the basis of the experimental data that all gabbros, in terms of their mineral composition and the electrical parameters, should be split into three basic groups: the first one /78
is the plageoclase - pyroxene, the second one - plageoclase-hypersthene, and the third one - plageoclase-amphibole. The gabbro 2622, 2617 and 2615 belong to the first group. Among these rocks, only gabbro 2622 displays high electrical conductivity because of the secondary changes, while the remaining gabbro, which were not subject to the weathering processes, have lower conductivity. The

hypersthene gabbro (2609, 2616, 2621), because of the increased amounts of iron oxide, display higher electrical conductivity than the gabbro in which the pyroxene, in the form of diopside, is prevailing, and also the amphibole gabbros. The amphibole gabbros (2618, 2608, 2863 and 2620) are characterized by the lowest electrical conductivity, particularly in the case when quartz is present. In the above-mentioned gabbros, with the exception of gabbro 2863, at the temperatures between 600 and 900°C, one observes the anomalous behavior of electrical conductivity which is due to the presence of amphibole. The comparison among these three groups of gabbro, in terms of the activation energy, indicates that at the low temperature range, the lowest activation energy is displayed by the pyroxene-diopside gabbro (E_0=6.63-0.7 eV) and in the case of the other two groups, the E_0 quantity is between 0.73-0.88 eV. In the region of intrinsic conductivity, these groups of rocks, in terms of the increasing activation energy, may be organized as follows: amphibole (1.0-1.6 eV), if we are to disregard the gabbro 2620 which has higher activation energy, hypersthene (1.6-1.9 eV) and diopside (1.76-2.5 eV).

The gabbro of the South Ural mountains has been investigated by using six samples which differed primarily in terms of the amounts and types of non-ferrous minerals. The highest electrical conductivity in the low temperature range was displayed by the amphibole gabbro and the lowest - gabbro 272. The remaining samples occupy the intermediate position and are quite similar. At high temperatures, the electrical conductivity fluctuates within a sufficiently narrow range and is quite typical for this type of rocks. The specificity of the South Ural mountain gabbro is the relatively high activation energy of the charge carriers at high temperatures, which comprised 2.6-3.3 eV, and only in two gabbros, the activation energy was considerably lower. These were the gabbro 143 with high amounts of hornblende and the gabbro 272, the mineral composition of which is not known. The Cola peninsula gabbro in which pyroxene is represented by augite, and contains amphibole, is characterized by σ which coincides with σ in amphibole gabbros of the Mamonov tract. However, at high temperatures, the former display higher conductivity, possible because of the augite. The gabbro-norite 466 and metagabbro 1450* practically are similar to the South Ural gabbro and to some Mamonov tract gabbros. In terms of the activation energies, this gabbro is closest to the South Ural mountain gabbro, since E_0 is in the range between 2.0 and 3.1 eV. Figure 26b shows the region in which the values of σ are determined for the gabbros which were investigated, and Appendix 3 gives the values of σ, E_0 and lg σ_0. /79

Cataclastic gabbros were investigated by using the rocks from the Gor'kiy formation. These rocks, while forming, underwent intensive cataclasis, which affected significantly their electrical properties.

Gabbro 2795 displayed exceptionally high electrical conductivity, with the increase by 3-4 orders of magnitude, up to the t=300°C, of the average σ for this type of rock. In addition, in the temperature range of 300-850°C, one observes an irregular change of σ which fluctuates between $3.4 \cdot 10^{-5}$-$8.0 \cdot 10^{-5}$ ohm^{-1}.cm^{-1} and only at the temperatures above 850°C, the lg σ as a function of 1/T relationship becomes linear. The E_0 and lg σ_0 values in the case of gabbro 2795 are considerably lower (Appendix 4) than has been determined for gabbro in the Momanov formation. The specific properties of gabbro 2795 may be explained by the high degree of fissures across the grain of the rock-forming minerals and by the secondary changes in the plageoclase which underwent intensive cataclasis, has been albetized and in some areas - pelletized (pelletization is the kaolin - like darkening and the change in the feldspar).

According to our measurements, the albite displays higher electrical conductivity than the potassium feldspar, by a factor of 10-100. In conjunction with this, the albitization, in parallel with some other changes which were due to the cataclasis, facilitate the considerable increase in the electrical conductivity of gabbro, and the decrease of activation energy. The gabbroids 2861, 2794 and 2791 display similar electrical conductivity and approximately the same change in them, as a function of temperature, with insignificant fluctuations in E_0 and lg σ_0 quantities across the whole temperature range. In contrast to many other rocks, including the gabbro of the Mamonov formation, the three above-mentioned gabbros display only two temperature regions, which differ in the mechanism of electrical conductivity. The change in the mechanism of electrical conductivity takes place within the temperature range between 620 and 860°C. The low temperature range is characterized by low activation energies, which are within the narrow range of 0.5-0.58 eV. This indicates that the degree of the effect of the secondary processes, causing the weakening of bonds in the impurity-related current carriers, is approximtely the same. In addition, the main source of the current carrier with low activation energy, as it appears, is plageoclase, which is intensively cataclized and biotized, and in gabbro 2861 - magnetized. In the high temperature range, the activation energy of these rocks changes within a somewhat broader temperature range, namely, from 1.11 to 1.66 eV. This relationship may be explained in that at high temperatures, all rock-forming minerals are participating in the electrical conductivity and therefore, depending on their percentile relationship or different degree of cataclasis, one observes the total effects which are different. /80

In terms of their electrical properties, among the rock group under consideration, we should cite gabbro 2864 in which the plageoclase is albetized and cataclized to a considerable degree. The difference between them is only in terms of the

temperature at which the current carriers type will change. In the case of gabbro 2864, it is higher, corresponding to 860°C. The gabbro 2790 and 2865 comprise the second group of rocks with somewhat lower electrical conductivity, but with approximately the same low activation energies (0.26-0.52 eV) for both the low temperature and high temperature (1.2-1.4 eV) ranges.

The presence of the region with low activation energies (up to 300°C) in gabbro 2790 is probably due to the presence of magnetite. The comparison of electrical properties of the Mamonov formation gabbro and Gor'kiy formation gabbro indicates that the metasomatosis and cataclasis affect appreciably the temperature relationship, which in turn is reflected in the electrical parameters of the rocks within this class. However, the degree of changes is different at low and high temperatures. As a result of the secondary factors, the electrical conductivity will increase particularly strongly in the low temperature range (up to 500-600°C) and at higher temperature range it will be approximately the same as in the case of some other rocks. However, the activation energy of the current carrier will decrease quite considerably in both the impurity-related region and in the region of intrinsic conductivity. On the basis of these results, in investigating the electrical properties of gabbro, the following should be noted.

1. In the case of gabbro, not only the mineral composition but also the rock history affects significantly the electrical properties. The weathering and cataclasis processes significantly affect the electrical parameters of gabbros.

2. The gabbro which underwent cataclasis differs from the young gabbro in featuring high electrical conductivity in the low temperature range and lower activation energies in both, the region with the impurity-related conductivity and in the region of intrinsic conductivity. The sharp difference of electrical parameters in the gabbro which underwent cataclasis is due first of all to the secondary mineral changes. These changes, in the case of the three gabbros (2861, 2791, 2790) are reflected in the replacement of the nonferrous mineral by magnetite, the amounts of which in the rocks reaches 11%. Such quantities of magnetite affect the electrical conductivity in the rock. In some other rocks, the cataclasis process, in combination with albitization of plageoclase and some other mineral changes, reflect the change in σ quantity. No particularly high quantities of magnetite were discovered in these rocks.

In addition to macroscopic changes in the rocks which underwent cataclasis, as it appears, there are some disruptions within the crystalline lattice, causing the lowering of ionic bonding energy associated with the charge transfer. /81

3. The South Ural mountain gabbro differs from the Voronezh anteclase and Gor'kiy region gabbro by having high activation

energy in the region of intrinsic conductivity (about E_0=3.0 eV). The exception is gabbro 143, in which E_0=1.0 eV. This rock has large quantities of hornblende which, as has been noted earlier, causes lowered activation energy.

4. The unaltered gabbro is characterized by electrical conductivities which, in the majority of cases, are overlapping with the electrical conductivities of diorites. However, some of these gabbros have lower electrical conductivity than some of the diorites. This is due to the fact that the electrical conductivity of hornblende, which is one of the main components of diorites, is higher than that of some monocline pyroxenes, as for example, diopside, enstatite and augite.

The diabases are essentially the fully crystalline, ordinarily intermediate or small grain rocks, consisting of augite and plageoclase. The plageoclase in diabases is represented more often than not by labradorite, but the andecite is also encountered. The conversion of augite into the fibrous material is a frequently encountered event. The augite is also frequently replaced by chlorite.

The electrical properties of diabases have been investigated by using three rocks, selected in the Ural mountains. In terms of the electrical conductivity, and also in terms of E_0 and σ_0 values, these diabases are similar to basalts. This, as it appears, is due to the small grain structure and to the chemical composition which is analogous to basalt. In the case of two diabases, one observes the anomalous σ within the temperature range of 700-900°C, which is due to the secondary changes and the higher electrical conductivity, as compared to the unaltered diabases, is also associated with such changes.

4. Basic Effusive Rocks

The basalts belong to a large group of gabbro-basalt rocks which are widely distributed in nature in the form of effusive rocks on the continents, in the form of plato-basalts, and geosyncline (ophiolite) magmatites, in the oceans (the basalts of central oceanic ridges, the rift zones and island arcs) and also in the transition zones between the continents and oceans [62-66]. The basalts are of interestin solving a number of important problems in geology: the drift of continents, the problem of rifts and eclogites, the nature of the conducting layer within the upper mantle. Of the basalts, 50% is made of plageoclase (labradorite) and of iron-magnesium minerals, chiefly augite, with the possible admixture of some ore minerals. Olivine is a frequent, but not necessary, component of basalt. The major effusive rocks which were studied were selected in different regions of the Soviet Union (Siberia, the USSR Far East, Caucasus, Kareliya, etc). Also, some basalts from rifts and from the islands in the Indian Ocean, as well as from the rift of Baikal region, were used. /82

The investigated dolerites 29, 60, 60-r, 61b, 83, 108 are essentially the young, small crystalline rocks, with the ophite and poyciloophite structure, having the average grain size 0.1-0.2 mm, in the case of the small grain formations, and 0.4-0.6 mm in the case of the large grain layers. In all samples of dolerite, with the exception of samples 83 and 108, one finds the admixture of small quantities of volcanic glass (up to 4-5%). In the small grain dolerite sample 61, the amounts of volcanic glass was higher (on the order of 15-20%) which is due to the rock intercertal structure. The volcanic glass is mostly decomposed. In a number of dolerites (the 60, 60-r, 61 samples), one observes the evolution of calcite. One observes in polished microsections considerable quantities of the ore mineral (2-5%) which is primarily the titanium-magnetite. To some extent one also finds ilmenite and pyrrhotine (Appendix 5, sample 29). The evolved shapes of the ore mineral found are rectangles, squares, plates and irregular spongy materials. The average size of the grains fluctuates between 0.1-0.2 and 0.5-0.7 mm, and in general this correlates quite well with the average grain size of the basic rocks. On the whole, in terms of its composition and structure, these samples may be assumed to be typical representatives of the Siberian plate traps [62, 66]. As one can see from data in Appendix 5, the dolerites which are similar in their mineral composition, are characterized by approximately the same electrical conductivities. However, large quantities of volcanic glass within the dolerite 61 and primarily, of the thinly dispersed ore minerals within the areas where the volcanic glass has been forming, will increase its σ. These common features make the dolerites similar to the basalts of the rift zone in the Indian Ocean (see Appendix 5, samples 54a, 161, 313). In contrast to the sample 61, the dolerites 83 and 108 contain no volcanic glass and the ore mineral is in the form of a large formation, and therefore, they display the lowest σ among all the dolerites which were investigated. In terms of the ore mineral distribution and in terms of $\lg \sigma = 5(1/T)$ values, the dolerites 60 and 60-r are similar to dolerite 61.

N. E. Galdin, working with a number of rocks, has briefly described the translucent and polished microsections, made of the samples which were previously heated to 1000-1200°C. This data is of interest in explaining the character of change in the electrical conductivity of the rocks as a function of temperature, enabling one to evaluate the degree of the change in the rock as a function of heating (oxidation, melting), and the effect of these /83 processes on the mechanism and on the absolute conductivity. It turned out that the rocks underwent, in this case, significant changes: oxidation, pore formation and partial melting. The samples after such heating acquired a reddish tinge, and the number of pores and cracks has increased. In the rocks which contain considerable quantities of volcanic glass, one observes partial melting with glass-like evolved formations, which emerge from the cracks of the sample. The fully crystalline rocks (see Appendix 5, samples 83 and 108) undergo less significant changes.

Microscopically, the rocks after such heating display a large number of rather large pores of either irregular or circular form and a number of cracks. The evolution of titanium-magnetite is retained but one observes a clearly defined decay of the solid solution of magnetite-ilmenite, with the formation of different decay structures. It appears, a partial martitization of magnetite also takes place. The sulfide impurities completely disappear. So far, it has not been possible to establish the nature of the pinkish coloring after such heating process. As it appears, it is due to the evolution of small, finely dispersed particles of iron hydro-oxide which is the result of decomposition of volcanic glass and of secondary minerals of chlorite type. In some samples, by using a translucent microsection, it was possible to detect, after the experiments, a dense and thin layer of ore mineral which was not detected on the microsections prior to the experiment. The ilmenite evolution in the rocks, as it appears, does not change significantly.

The above-mentioned changes in the rocks are reflected in the increased electrical conductivity as a function of temperature and consequently, it also affects the energy (E_0=3.2-3.5 eV). The latter in this case reflects now not the mechanism of the electrical conductivity, but the specific petrochemical changes which occur in the rock, while it is being heated at t>900-1000°C. In addition, according to the study [67], at such temperatures, in the case of some minerals, the constitution water is removed from the lattice.

As we can see from Appendix 5, the electrical parameters of dolerites from the Caucasus are within the range which is typical for dolerites of other regions. However, in terms of σ and E_0 quantities, they are clearly differentiated from the basalts of the Caucasus (Figure 27).

Dolerite basalts (1295, 1312, 1319) from the Caucasus, in terms of σ quantity, resemble the dolerites because of the following specifics of mineral composition. In the dolerite basalts, the plageoclase, in terms of the the composition, resembles bytovite, in which there is more anorthite than in the case of basalts, containing labradorite. Their increased electrical conductivity is primarily associated with the large quantities of ore mineral, and the presence of uralite, which has a relatively high electrical conductivity because of the presence in it of the trivalent iron, of sodium cations and of water of crystallization. The Caucasus /84
basalts, compared to the dolerites, in the majority of cases have lower electrical conductivity. The numerous data, in terms of electrical conductivity in dolerites, and the Caucasus basalts of different origins, make it possible to find the regions in which the lg σ=f(1/T) curve would fit. Figure 28a shows that the region of dolerites is a narrow zone which is shifted upward with respect to the region of basalts.

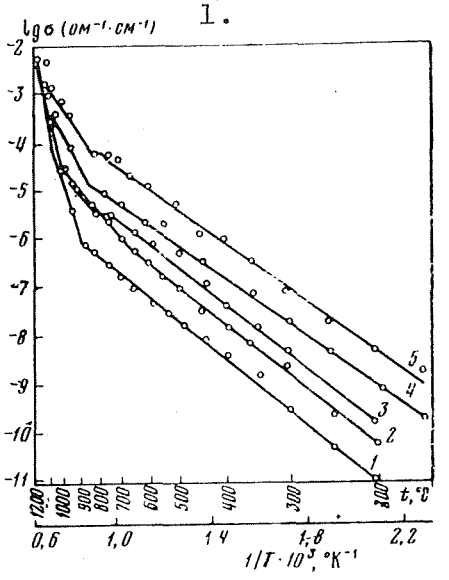

Figure 27. Electrical conductivity as a function of temperature.

1 - 3 - for basalts, 4, 5 - for dolerites.

Key: 1. $ohm^{-1} \cdot cm^{-1}$

The highly porous and low-pore basalts (see Appendix 5, samples 602, 5/22, 4) differ from dolerites by having a large quantity of volcanic glass. In terms of chemical composition, these rocks, except for sample 4, as it appears, belong to the toleite basalts. The translucent microsections show the unchanging composition of the basic mineral mass. One observes only small inclusions of plageoclase, of pyroxene and of olivine, and one also observes the finely dispersed ore mineral, evenly distributed across the whole rock. On the whole, the rocks of this group may be assumed to by typical representatives of the effusive toleite basalts.

The samples of Sikhote-Alinsk basalts 602 and 5/22 which differ somewhat in porosity (they are more porous in sample 5/22), in terms of composition and structure of the basic material (the sample 5/22 has less volcanic glass and somewhat more of ore mineral), display significant differences in σ and E_0 at high temperatures and, as will be shown later, at high pressures. The electrical conductivity of basalt 602, across the whole temperature range which was investigated, is higher (see Appendix 5) than in the case of 21 and 4. The similar σ in these rocks is observed only at 950°C. In terms of the conductivity parameters, the alkaline basalts, just like the other basalts of similar composition, are similar to the basalts of the Indian Ocean rifts and of the Baikal region. At the present time, the problem of rifts is of great significance in investigating the structure of the Earth's crust and of the upper mantle, of the physical and geological processes which take place at great depth.

In conjunction with this, we shall consider separately the electrical properties of basalts within the Indian Ocean rift zone and in the Baikal region.

The island basalts are represented by two samples 3-3 and 3-11 from Mae Island and by two samples 19-3 and 19-5 from Tromlen Island. Both basalts are represented as well crystallized rocks

with small grain structure, but differing in terms of the ore mineral grain size. In the basalt 19-3 and 19-5 the ore mineral is in the form of large grains, of the size of about 0.1 mm, and in the basalt 3-3 and 3-11, the average size of the ore mineral is 27 μm. The above-mentioned basalts have similar electrical conductivity across the whole temperature range, but differ in terms of the activation energy and of lg σ_0. In the area of intrinsic conductivity, the activation energy of basalts 19-3 and 19-5 is considerably higher (E_0=2.44-2.5 eV) than in the case of basalts 3-3 and 3-11 (E_0=1.87 eV). It is possible that the presence of powdery ore material makes the crystalline lattice of the minerals in basalts 3-3 and 3-11 somewhat more loose, thus creating the favorable conditions for the participation of ore mineral in the electrical conductivity. As a result of this, one observes the lowered activation energies in the current carriers in the area of intrinsic conductivity. The relatively high conductivity of the island basalts, while the latter are completely decrystallized, is apparently also associated with the increased content of the iron ions Fe^{2+} and Fe^{3+}, or is due to the early history of the rocks. The basalts 7-1 from Godwana (olivine basalt) and 173-11 and 173-5 differ from the island basalts in having the lower electrical conductivity at high temperatures (at t=1000°C, the electrical conductivity is approximately lower by one order of magnitude than the island samples) and also displaying a low activation energy (E_0=0.8-0.9 eV). /86

The basalts of the Indian Ocean rift zone which were investigated by us were taken from the tip of the ridge (54 and 54a) and from the central part of the rift zone (161). The basalt 54, in terms of its electrical parameters $\sigma_{300°}$ and $\sigma_{1000°}$, E_0' and E" and also in terms of lg σ_0' and lg σ_0'' differ only slightly from the Godwana basalts. However the basalt 161 (dolerite) has higher electrical conductivity in the area of impurity-related conductivity than the basalts from Godwana and from the islands. This is partially due to the changes in the ore material and is possibly also the result of the tectonic stresses to which these rocks were probably exposed at the fracture zone. The common feature of the basalts 54 and 54a is low activation energy (E_0=0.6-0.92 eV).

The basalts 54 and 54a are weakly decrystallized rocks and are characterized by a thin powdery ore mineral in the quantities of 4-6% (the average size of the grains is 1.7 μm). The basalt 161 is the polycrystalline, small grain rock, with the average size of the ore inclusions of 20 μm. The factor which decreases significantly the activation energy is a weak decrystallization. Table 12, for the purposes of comparison, shows the activation energies in the area of intrinsic and impurity-related conductivity and the data as to the grain size of the rocks.

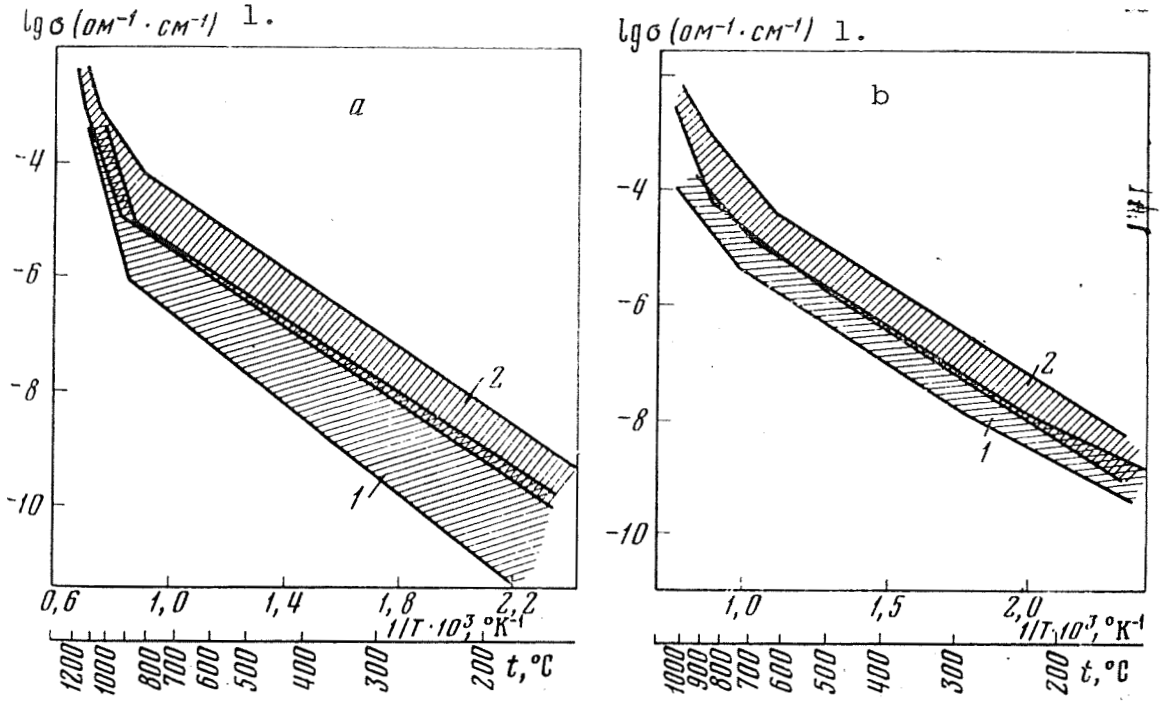

Figure 28. Different values of electrical conductivity in the effusive rocks of different origins.

a - are the basalts (1) and dolerite from the Caucasus (2)
b - are the basalts of the rift zone in the Indian Ocean, from different areas (1, 2).

Key: 1. $ohm^{-1} \cdot cm^{-1}$

TABLE 12. ACTIVATION ENERGIES OF BASALTS

Rock	Structure	Area of impurity-related conductivity E_0', eV	Area of intrinsic conductivity E_0'', eV
Basalt	Weakly decrystallized		
54		0,5	0,6—0,92
54a	Ibidem	0,4	0,62
161	Fully crystalline, low grain	0,2—0,8	0,8
3—3	Decrystallized	0,45	1,87
3—11	Average grain	0,6	1,87
19—3	Large grains of ore mineral	0,45	2,5

[Commas in tabulated material are equivalent to decimal points.]

C-2

As one can see, there is a clearly defined relationship between the activation energy and the decrystallization for a number of basalts in the area of intrinsic conductivity. At low temperatures it is veiled by the effect of some other factors (the amounts of impurities, the surface conductivity, and others).

We have investigated another group of basalts which belong to the rift zone of the Indian Ocean, but which were taken from another area. All these basalts have similar electrical conductivity across the whole temperature range and are characterized by three temperature regions, which differ in terms of different electrical conductivity mechanisms (Figure 28b). By comparing the two above-mentioned groups of basalts, we can see that the second group is less conducting at both low and high temperatures. In addition, the basalts 2-2, 2-1 and 4-1 are characterized by the sufficiently high activation energy (E_0=1.6-1.8 eV) in the area of intrinsic conductivity. /87

The Baikal region basalts. A considerable part of the Baikal region basalts, taken from different areas feature high electrical conductivity at t=200-300°C. Among these are the basalts 5_3 and 517 (at t=200°C, $\sigma=2.1\text{-}2.7\cdot10^{-7}$ ohm$^{-1}\cdot$cm^{-1}) and then the basalts 5_2, 518, 5d and 506, which at the same temperature, have somewhat lower electrical conductivity (see Appendix 5). The other group of basalts - 528, 531, 520 and 523 is characterized by the electrical conductivity which is lower by 1-2 orders of magnitude. At higher temperatures, the differentiation in terms of the electrical conductivity is not as clearly defined. For the majority of Baikal region basalts, σ at t=1000°C fluctuates between $1.1\cdot10^{-3}$ and $3.1\cdot10^{-3}$ ohm$^{-1}\cdot$cm^{-1}, the exclusions being the samples 506, 520 and 522, in which the electrical conductivity was equal to $7\cdot10^{-4}$, $1.1\cdot10^{-4}$ and $5.5\cdot10^{-4}$ ohm$^{-1}\cdot$cm^{-1}, respectively.

In parallel with the investigation of the electrical properties of basalts from the north-eastern part of the Baikal region, we have investigated the electrical properties of basalts from the south-western region of Baikal.

Two of these belong to the group which has the highest conductivity at the low and high temperatures, and the two others - belong to the high resistivity basalts. The observed difference in electrical conductivity of the Baikal region basalt may be explained on the basis of the petrographic analysis in the following manner. The high electrical conductivity of the basalts 5_3 and 517 is due to a considerable quantity of the ore mineral, which in the basalt 5_3 is located at the grain boundaries and in 517 is observed as separate grains. However, one should not exclude the possibility that in the latter case, the microscopic deposits of the ore mineral

are also located at the grain boundaries which will increase the basalt conductivity. The basalt 5g contains less ore material than the basalts 5_3 and 517, which naturally is reflected in σ values, which is lower by one order of magnitude in the area of impurity-related conductivity. The basalt 518 has a small grain structure with sufficiently large quantities of the ore material, the grains of which are evenly distributed across the whole microsection of the sample. Such structural distribution of the ore material causes even lower electrical conductivity of this rock. In terms of its mineral composition, the basalt 5d is similar to basalt 5g, but it is decrystallized to a greater degree which results in a somewhat lowered electrical conductivity. In terms of the mineral composition, the basalt 506 differs only slightly from the basalt 518 which also displays the similar electrical parameters, with the exception of σ at 1000°C, which is lower in the case of basalt 506 than in the case of basalt 518. /88

The basalts 531, 523, 520 and 522 are characterized by lower electrical conductivity in the structurally sensitive region which is associated primarily with the small quantities of the amorphous phase found in it, and also with the likely presence in these basalts of the olivine spinel.

In addition to the island basalts and the basalt of the rift zones, we have investigated the continental basalts from the Sakhalin Islands, from Kamchatka and from Mongolia in order to elucidate the role of the amorphous phase. The electrical conductivity of basalt 1380 and basalts 1696, 1690 (Sakhalin Islands) is on the same order in terms of the impurity-related conductivity and does not exceed $7.1 \cdot 10^{-1}$ ohm^{-1}.cm^{-1} at 200°C. However, at the temperature range between 600 and 1050°C, one observes some differentiation in terms of the σ and E_0 quantities, which is related primarily to the different amounts of glass, something which is apparent by comparing the following data at t=1000°C:

No. of the basalt sample	Amount of glass, %	$\sigma_{t=1000^\circ}$, ohm$^{-1}\cdot$cm^{-1}	E_0, eV
520	10	$1{,}1 \cdot 10^{-4}$	2.18
1696	25	$1{,}3 \cdot 10^{-4}$	2.0
1690	35	$1{,}5 \cdot 10^{-3}$	1.32
1380	40	$1{,}7 \cdot 10^{-3}$	1.2
M-1	80	Melting	0.85*

*At t=900°C.

The basalt M-1 consisting almost completely of glass has the electrical conductivity which is approximately the same in terms of its level as in the case of the basalts 1690 and 1380, and has a low activation energy up to 900°C. However, at about 1000°C, the basalt M-1 has melted.

In conclusion, let us note the following. The functional relationship between the electrical conductivity of the rocks and the mineral, chemical composition, as well as of the structural features of each specific basalt rock, complicates the matter because of considerable quantities of the amorphous phase. As a result, the electrical conductivity, E_0 and $\lg \sigma_0$ in these basalts is significantly affected by the amorphous phase, and by the rock composition. With the increase of the amorphous phase from 10 to 40%, the activation energy decreases from 2.2 to 1.2 eV.

It is known that the electrical conductivity of the alkaline glass and also of the glass which has zero alkali, if the latter have higher electrical conductivity, will decrease considerably during crystallization, which is associated with the increase of activation energy in the ions which take part in the charge transfer [68]. The data presented below for some glasses substantiates this relationship:

Formula of the compound	$\lg \sigma_{300}$°, $ohm^{-1} \cdot cm^{-1}$	E_0, eV	$\lg \sigma_0$, $ohm^{-1} \cdot cm^{-1}$
Na_2OSiO	-3.25/8.00*	0.48/1.04	1.61/1.42
$Na_2O \cdot 3CaO \cdot 6SiO_2$	-9.78/-10.46	1.15/1.37	1.82/2.14
$2Na_2O \cdot CaO \cdot 3SiO_2$	-4.30/-9.90	0.77/1.25	2.64/2.71

/89

*Glass is in the numerator and the crystal - in the demoninator.

As one can see, the electrical conductivity in crystals, as compared to the amorphous material at t=300°C may be lower by a factor of 10 to 10^5 and the activation energy is significantly greater. The analogous relationship in terms of the electrical parameters is observed by comparing the basalts and fully crystallized analogues of these basalts - the gabbro. The increase of activation energy as the material is transformed from its amorphous state into the crystalline state is due to the proper positioning of the particles, which in turn causes the increased bonding energy. Among the basalts, one also observes a certain relationship between the electrical conductivity, the activation energy and the amounts of amorphous phase. With the increase of the latter, the electrical conductivity is increasing and the activation energy decreases. However, one should point out that this relationship does not manifest itself sufficiently clearly in a number of cases because of

the dissimilar composition of the amorphous phase and because of different character of the ore mineral evolution as well as of the evolution of the secondary minerals. With respect to the effect of the chemical composition on the electrical conductivity in the alkaline and nonalkaline glass, the following information is available. The electrical conductivity of the alkaline glass depends quite strongly on the amounts of alkali oxides at low concentration and of iron oxide Fe_2O_3. As the amounts of these oxides increases, the number of charge carriers will increase in the glass and this will result in the increase of $\lg \sigma_0$ and decrease of the activation energy. The introduction of bivalent oxides, as for example, CaO and MgO result in the opposite effect, in other words in the decrease of electrical conductivity.

As we can see, in having the same quantity of glass in the basalts but with a dissimilar amount of the above-mentioned oxides, one can observe a considerable difference in the electrical parameters. This difference will be particularly large when the amorphous phase is found among the grains of the minerals, in other words, when this phase plays the role of the filling medium. However when the amorphous phase plays the role of inclusions, its effect on the electrical properties of the rock will decrease.

Because of the absence of data in terms of chemical composition in all of the above-mentioned basalts, one may only note the qualitative relationship between the electrical conductivity and the chemical composition of the basalts. Table 13 shows the electrical parameters and chemical composition of the basalts which were investigated. In addition, we present separately the total amounts of oxides, facilitating both the increase of electrical conductivity (Fe_2O_3, FeO, K_2O, Na_2O), and its decrease (SiO_2, Al_2O_3 and MgO), and the amounts of CaO is presented separately.

In looking at the samples, those which differ most in terms /91
of their electrical properties, namely 520a 3/2, 531 and 161, the following relationship has been observed - the electrical conductivity increase with the decrease of the quantities of high resistivity oxides. The effect of the conducting oxides is also manifested but interestingly, the variation in the quantities of these oxides in the range of 14.54 and 18.09% affects only the electrical conductivity in the intrinsic area. In the other cases, as it appears, it parallel with the chemical composition, of significant importance is the character of the ore mineral distribution and the degree of decrystallization. The increased effect of the ore mineral, which is evolved as a thinly dispersed dust across the whole rock, has been substantiated in a number of basalts from the Indian Ocean, from

TABLE 13. CHEMICAL COMPOSITION OF BASALTS AND DOLERITES AND THEIR PARAMETERS OF ELECTRICAL CONDUCTIVITY

No. of the sample	$\sigma_{200°}$, $ohm^{-1} \cdot cm^{-1}$	$\sigma_{1000°}$, $ohm^{-1} \cdot cm^{-1}$	E'_0, eV	E''_0, eV	SiO_2	Al_2O_3	MgO	Σ*	CaO	TiO_2	Fe_2O_3	FeO	K_2O	Na_2O	Σ**
520a	$5,2 \cdot 10^{-10}$	$1,1 \cdot 10^{-4}$	0,60	2,18	50,22	15,51	7,52	73,25	9,27	1,92	2,28	9,18	1,06	2,92	17,36
523	$5,2 \cdot 10^{-10}$	$1,1 \cdot 10^{-3}$	0,82	1,54	50,17	15,35	7,31	72,83	9,32	1,92	2,26	9,37	1,10	2,90	17,55
525	$1,8 \cdot 10^{-8}$	melting	0,64	—	50,07	15,24	7,04	72,35	8,76	2,08	3,07	9,15	1,20	2,74	18,24
528	$3,5 \cdot 10^{-9}$	$1,2 \cdot 10^{-3}$	0,60	1,6—2,2	48,16	15,20	8,58	71,94	8,04	1,30	4,37	7,20	1,83	3,01	17,71
526a	10^{-3}	$1,0 \cdot 10^{-2}$	—	—	50,21	15,61	7,77	73,59	9,12	1,30	3,38	7,96	1,46	3,17	17,27
532	$1,2 \cdot 10^{-9}$	$1,0 \cdot 10^{-4}$	—	—	48,44	14,59	8,06	71,09	9,10	2,00	5,70	6,94	1,69	3,14	18,77
530	—	—	—	—	48,92	15,26	9,76	73,94	8,84	1,60	2,88	8,34	1,53	2,80	17,05
531	$5,0 \cdot 10^{-9}$	$1,2 \cdot 10^{-3}$	0,76	2,7	49,20	14,73	9,06	72,99	8,56	1,70	3,70	7,95	1,65	3,09	18,09
3/2	$2,1 \cdot 10^{-9}$	$2,0 \cdot 10^{-4}$	0,60	1,2—1,8	49,40	14,83	7,80	72,09	10,16	1,50	4,71	6,82	1,47	3,15	16,65
2/1	$2,8 \cdot 10^{-9}$	$1,3 \cdot 10^{-4}$	0,40	1,6	48,92	15,76	7,70	72,38	11,48	1,60	1,24	8,44	0,28	2,98	14,54
161	$1,4 \cdot 10^{-7}$	$1,2 \cdot 10^{-3}$	0,20	0,8	47,52	14,09	8,13	69,74	9,55	1,27	4,41	7,46	3,00	0,31	16,46
Dolerites and basalts from the Caucasus															
511	$2,9 \cdot 10^{-9}$	$6,0 \cdot 10^{-4}$	0,74	1,5	49,47	17,35	7,16	73,98	8,41	1,28	4,68	6,01	0,94	3,62	16,53
527	$1,9 \cdot 10^{-9}$	$4,9 \cdot 10^{-5}$	0,74	3,5	49,56	17,35	6,85	73,76	8,41	1,20	6,14	4,49	1,17	3,62	16,62
482	$1,5 \cdot 10^{-9}$	$3,2 \cdot 10^{-4}$	0,66	1,8	47,57	17,99	6,34	71,90	8,69	1,32	6,23	4,58	1,00	3,91	17,94
490	$6,0 \cdot 10^{-10}$	$1,7 \cdot 10^{-4}$	0,70	2,0	48,42	17,24	7,67	73,33	9,39	1,25	3,14	7,36	0,83	3,70	16,28
1109	$5,6 \cdot 10^{-11}$	$4,6 \cdot 10^{-5}$	0,82	—	50,42	17,56	5,83	73,81	8,97	1,20	5,94	2,96	1,66	4,26	16,02
1131	$7,1 \cdot 10^{-10}$	$1,4 \cdot 10^{-4}$	0,60	4,0	50,13	17,23	6,24	73,60	9,11	1,35	5,38	3,95	1,33	4,33	17,34

* Σ $SiO_2 + Al_2O_3 + MgO$.

** Σ $FeO + Fe_2O_3 + K_2O + Na_2O$.

[Note: commas in tabulated material are equivalent to decimal points.]

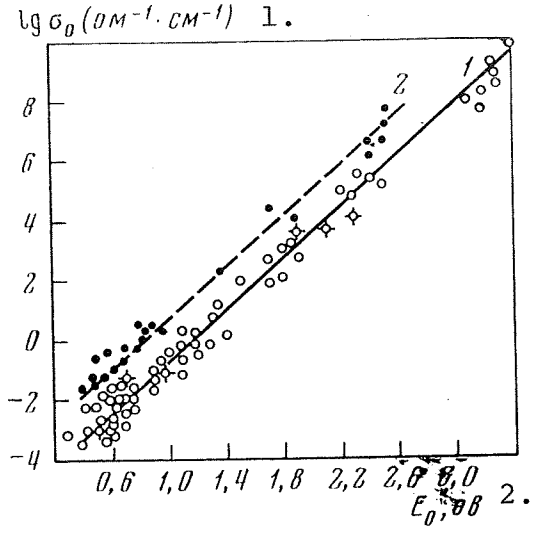

Figure 29. Correlational relationship between the pre-exponential coefficient and the activation energy.

1 - continental basalts
2 - rift zone basalts

Key: 1. ohm^{-1}·cm^{-1}; 2. E_0, eV

Sichote-Alinsk and from the Baikal region. In addition, one should not exclude the role of the rock history. For example, the basalt 531 and the basalt of dolerite 161 type differ significantly in the area of impurity-related conductivity and the conductivity here is in an inverse relationship to the total amounts of the conducting oxides, displaying the same values at t=1000°C. The extensive experimental data on basalts made it possible to construct the correlational relationship between the σ_0 and E_0 parameters. /92

As one can see in Figure 22, this relationship is of linear character. For the basalt of the Indian Ocean rift zone, the straight line $\sigma_0 = f(E_0)$ is shifted toward increased σ_0 which is the result of the higher electrical conductivity.

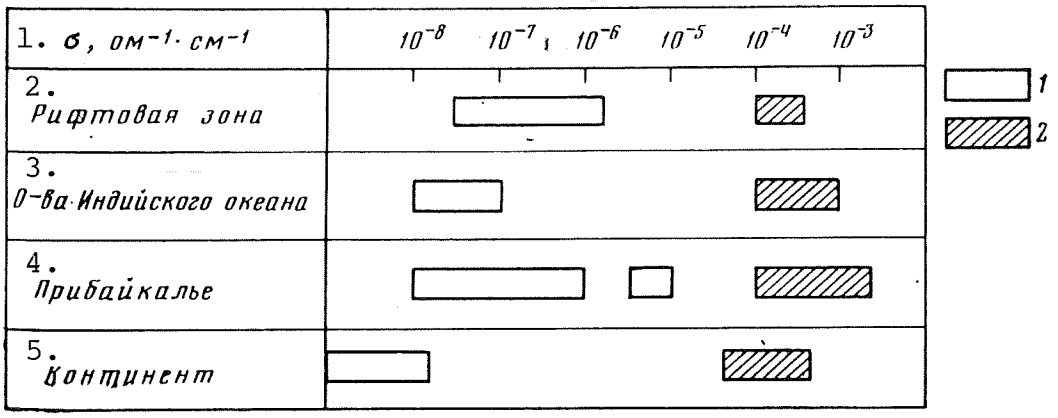

Figure 30. Range of electrical conductivities in the basalts of different origin.

At t, °C:
1 - 300, 2 - 1000.

Key: 1. ohm^{-1}·cm^{-1}; 2. Rift zone; 3. Islands of the Indian Ocean; 4. Baikal region; 5. Continental region.

In concluding the consideration of basalts of different geological structures, it should be noted that the highest electrical conductivity in the structurally sensitive region is displayed by the basalts of the Baikal region and Indian Ocean rift zones (Figure 30). Similar values of σ are displayed by the alkaline basalts and the continental basalts of the Caucasus and the dolerites display the greatest differences. In the region of high temperatures, the range of electrical conductivities of the basalts which were considered are predominantly overlapping. The lowest σ, as one can see, are in the case of basalts from the Caucasus.

5. Electrical Conductivity of Xenoliths in the Ultrabasic Rocks, the Mantle Eclogites and Kimberlite Flows of Yakutiya

The geological and petrochemical studies have shown that the xenoliths of eclogites and of the ultrabasic rocks in kimberlite flow "Obnazhennaya" and in some others, are representatives of different pyrope-containing rocks, which by effusive action of the kimberlite magma, were brought from the upper mantle [69-86]. The xenoliths of eclogites and of some other deep rocks of which the samples were made, were of circular-oval shape, which indicates the origin at great depth. The electrical conductivity of these rather interesting rocks was hardly ever studied [87-88]. There is only some data on electrical conductivity in the case of the ordinary crystalline rocks of this type which were obtained on the surface and from the drilled holes in the other areas [89-92]. Therefore, the information as to the electrical conductivity as a function of temperature and also the computed E_0 and σ_0 of these rocks are of unquestionable interest for the geophysicist involved in the study of the composition of the upper mantle [72, 77, 87, 88]. Of no lesser interest in this area are the ultrabasic inclusions in the basalts [94].

We are presenting below the data on the electrical parameters for the specific ultrabasic rocks. The particular conditions of formation and the unique composition of these rocks are reflected in the values of the electrical parameters. Figure 31a shows the $\lg \sigma = f(1/T)$ curves for the eclogites in the flow "Obnazhennaya." These mantle eclogites, containing up to 50% magnesium garnet (pyrope) and also the monocline pyroxene with chromium, in terms of the temperature relationship σ and in terms of the E_0 magnitude, differ from the ultrabasic rocks. For example, in the case of the mantle eclogites, one almost always observes only one inflection point on the $\lg \sigma = f(1/T)$ curve at 850°C, while in the case of the ordinary ultrabasic rocks, one observes the bending point at 450 and 750°C (see Figure 31a). The E_0 in this case is 1.8-2.5 eV, and in the case of pyrope eclogites E_0 is 2.8-3.0 eV. In the case of eclogites, at 1200°C, the electrical conductivity is lower by one order of magnitude than in the case of ordinary peridotites /93

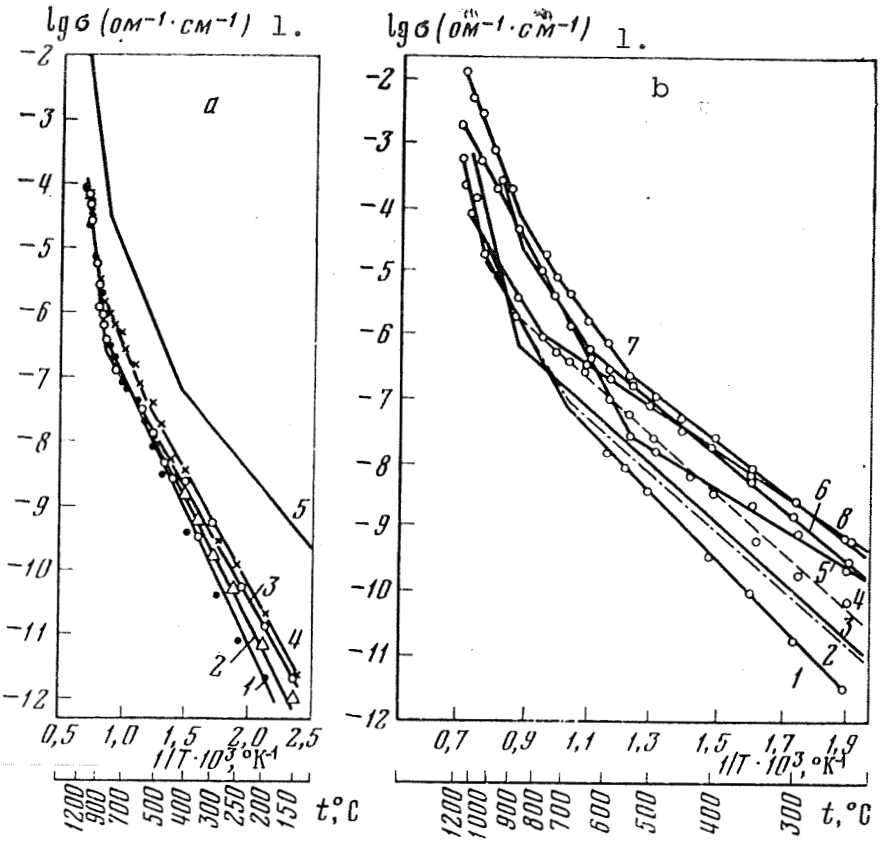

Figure 31. Electrical conductivity as a function of temperature. a - for eclogites: 1-4 - pyrope eclogites from kimberlites; 5 - almandine eclogites; b - xenoliths in kimberlites: 1 - olivine-forsterite from the rock 2162; 2 - pyrope peridotite 2161; 3 - dunite AO-151; 4 - pyrope peridotite A-66-016; 5 - spinel dunite 2162; in the basaltoids: 6 - olivinite 625/4K; 7 - olivinite from the island Reunion; 8 - Olivinite nodule 780/1B from Baikal region.

Key: 1. $ohm^{-1} \cdot cm^{-1}$

and is $2 \cdot 10^{-4}$ $ohm^{-1} \cdot cm^{-1}$ (Appendix 6). Such difference in electrical properties of these two types of rocks may be explained by the fact that both the pyrope eclogites and the pyrope periodotites, according to the data in [80] were crystallized while being exposed to the magmatic source at higher temperatures and pressures. In addition, they are magnesium-rich rocks (Table 14) and also contain chromium which neutralizes the ionic charges during the conductivity processes [73, 95].

The high activation energy, the inflection point on lg σ=f(1/T) curve at higher temperatures, and the decreased electrical conductivity at 1200°C, enable us to consider this particular type of rock as a product of the first stage of crystallization, at the primary magmatic source. Ordinarily, however, the ultrabasic rocks of the Monchegorsk pluton peridotites, in terms of their electrical parameters, differ from the xenoliths from kimberlite flows and, as it appears, are the recrystallization product of ultrabasic magma. This is also substantiated by the curve inflection point related to the impurity-associated conductivity, observed in the case of the ordinary ultrabasic rocks, and occurring at lower temperatures. This relationship is associated with the fact that during the recrystallization, the material is freed from the extraneous impurities and therefore the effect of these impurities on the electrical conductivity is limited to the region of lower temperatures. Figure 31a (curve 5) shows the mean electrical conductivity for the almandine eclogite 1320. This sample contained 47% of garnet-almandine, in other words, of the iron-containing garnet which is not typical for eclogites in general. Its composition contains 52% of monocline pyroxene and the secondary minerals - 2% of hornblende and isolated grains of apatite. As one can see from these curves, the garnet-containing rocks, depending on the composition of the garnet, may be characterized at high temperatures by either high or low electrical conductivities. The electrical conductivity of the almandine eclogites within the temperature range of 200-1200°C is higher approximately by two orders of magnitude than that of the pyrope eclogite (Figure 31, Appendix 6). /95

In Appendix 6, and in Figure 31b, we show the data on the conductivity for the mantle pyrope peridotite-xenolith in the kimberlite flow "Obnazhennaya" in Yakutiya, which is composed of high magnesium olivine, chrome diopside, enstatite and pyrope garnet. The same figure shows the curve of σ=f(1/T) for the olivine xenoliths from the basalts of Baikal region, from the Avanchinsk volcano in Kamchatka and from the Seychelles Islands of the Indian Ocean.

On the basis of this data one can draw the conclusion that all xenolith kimberlites are characterized by the lowest electrical conductivity and by a sufficiently high activation energy in the areas of low and high temperatures. For these rocks, the straight lines of lg σ=f(1/T) are close to each other, with the exception of the pyrope peridotite A66-016. The electrical conductivity curves of the olivine xenoliths of basalts are in the region of somewhat higher σ. At higher temperatures, the electrical conductivity of the xenoliths increases quite appreciably, which is due to the anomalously high E_0 and σ_0.

According to the experimental data the spinel-containing xenoliths are always displaying higher electrical conductivity than the dunites which do not contain it. The investigated xenolith of dunite AO-151 consists of (in %) 95 - olivine (see Table 14), 1-2 - pyrope, 1-2 - chromium spinel, 1-2 - chromium diopside, 1-2 -

TABLE 14. AVERAGE CHEMICAL COMPOSITION OF THE KIMBERLITES AND GARNET-PYROPES FROM KIMBERLITES AND FROM OTHER ULTRABASIC ROCKS (IN %)

Compound	Rocks*														
	1	2	3	4	5	6	7	8	9	10	11	12	13	14	15
SiO_2	27,81	41,54	41,78	41,47	38,12	32,84	40,82	50,78	42,28	50,74	40,40	43,96	49,16	43,31	40,14
TiO_2	1,63	0,36	0,74	0,18	0,40	0,52	0,74	0,24	0,40	0,55	0,20	0,16	0,09	0,06	0,04
Al_2O_3	3,40	20,25	20,70	21,10	1,35	2,90	0,10	4,20	20,79	4,73	0,03	2,40	4,27	2,03	2,80
Cr_2O_3	0,13	3,70	0,92	0,08	—	—	0,003	0,76	2,56	17,5	—	0,25	—	—	—
Fe_2O_3	5,40	2,03	2,57	2,01	0,21	1,48		2,09	1,72	0,58	0,16	1,74	Trace	2,66	3,82
FeO	2,82	6,36	8,25	14,11	11,46	8,01	8,20	3,6	5,82	2,33	7,10	7,00	9,84	8,33	8,12
MnO	0,12	0,31	0,27(25)	0,35	0,14	0,14	0,12	0,12	0,26	0,03	0,12	0,12	0,4	0,13	0,14
NiO	0,14	—	—	—	—	—	—	—	—	—	—	—	—	—	—
MgO	25,53	19,61	19,27	13,07	41,39	33,83	50,70	33,26	19,30	17,91	49,55	41,13	30,94	40,30	42,12
CaO	12,21	5,54	5,28	7,56	1,57	5,78	0,20	2,30	4,64	16,47	0,09	1,65	3,61	1,62	1,44
Na_2O	0,33	0,12(2)	0,12(10)	0,07(3)	0,05	0,13	—	0,10	—	2,16	—	0,25	0,34	0,21	0,21
K_2O	0,66	0,18(2)	0,13(10)	0,16(3)	0,06	0,53	—	0,7	—	0,38	—	0,18	0,18	0,12	0,12
P_2O_5	0,50	0,02(2)	0,03(7)	0,02(2)	—	—	—	—	—	—	—	—	—	—	—
$H_2O^{+105°}$	—	0,34(5)	0,16(19)	0,02(6)	3,63	0,63	—	2,00	—	—	0,52	0,12	0,11	0,08	0,03
П.п.п.	19,42	0,50(8)	0,37(16)	0,04(8)	1,27	5,22	—	—	—	—	0,4	—	1,36	1,40	1,01
Total		100,86	100,59	100,24	99,65	92,00	100,38	99,52	97,77	96,59	98,31	98,98	99,93	100,17	99,96

*1 - kimberlites from Yakutiya, 339 analysis; 2 - first generation pyrope (violet-lilac-red); 3 - second generation pyrope (orange-red); 4 - garnet of pyrope almandine series from the inclusions of eclogites of metamorphic origin [76]: 5 -dunite AO-151; 6 - peridotite AO-5A; 7 - olivine from AO-15; 8 - enstatite from AO-15; 9 - pyrope from AO-5A; 10 - chrome diopside from AO-5A; 11 - olivine from AO-5A; 12 - red nodule 652/4 from basalts of Baikal region; 13 - peridotite 608 from Cola Peninsula; 14 - peridotite 588 from Cola Peninsula; 15 - peridotite 609 from Cola Peninsula.

[Note: commas in tabulated material are equivalent to decimal points.]

enstatite, 1 - black binder of basaltoid composition. The olivine /96 displays isometric translucent grains of green color, of 2-8 mm size, and contains 92% forsterite and 8% fialite. The specific weight of it is 3.82 g/cm^3. One can only rarely observe in the microsections of the sample, within small cracks in it, traces of serpentinization, with the evolution of ore mineral. The garnet contains up to 73-75% pyrope component which is faintly violet in color, is translucent and has no traces of secondary changes. Figure 31b shows that within the investigated temperature range, this dunite AO-151 has σ which is lower by 1.5 order of magnitude than in the case of the same xenolith of dunite 2162, which contains a considerable quantity of spinel. Let us note that the increase of σ as a function of temperature in the spinel rocks is considerably smaller. As a result of this, within the region of intrinsic electrical conductivity E_0 does not exceed 2.3-2.6 eV. The dielectric properties of dunite AO-151 are explained by the forsterite presence and the exremely small quantities of Fe_2O_3 and of the alkalis.

Among the investigated xenoliths from basalts, the olivinite 1484 which is the inclusion in the oceanite from the Seychelles Islands, has a high electrical conductivity, which at the temperature >900°C cannot be explained by oxidation or by polymorphic changes, since the activation energy in this temperature range is only 2.6 eV and the E_0, in the case of the above-mentioned processes, is on the order of 3.4-4.0 eV. As it appears, the high electrical conductivity of this xenolith is due to the intergrain inclusions of basaltoid material which is of higher conductivity and which cements this rock. In terms of the electrical conductivity, the sample of olivine (red) xenolith 625/4, from the basalt rift zone from the Baikal region, displays the same similarities. The microscopic study, and the quantitative minerological analysis show that it, just like the light colored xenoliths, is the websterite, consisting of the monocline pyroxene (omphacite) - 45%, of the rhombic pyroxene (enstatite) - 35-40, of the olivine (forsterite) - 10-15% and of the auxiliary green spinel. The red colored xenoliths differ from the green variants by the presence of iron oxides along the cracks and at the edges of the pyroxene and olivine grains. The activation energy of red xenolith 625/4 in the impurity-related region (150-600°C) is 0.78 eV, and in the intrinsic region (600-900°C) - 1.48 eV. The part of the curve at 900-1200°C which shows a sharp increase of σ and activation energy which is equal to 3.8 eV, cannot be explained by the intrinsic conductivity of the xenolith, containing websterite. The E_0 quantity, as it appears, characterizes the conversion of rhombic pyroxene into the monocline variety. There is some data which indicates that enstatite, at the temperature of 985°C, is converted into the high temperature rhombic form - the protoenstatite [96-98]. As we can see, the above-mentioned conversions in pyroxenes at temperatures above 900°C, which are defined on the curve as a

sharp jump in the electrical conductivity, are associated with higher activation energies. /97

Let us consider below the conductivity parameters in the kimberlite rocks of Yakutiya. Figure 32 shows by shaded area the region in which the electrical conductivity fits the olivine kimberlite. At the center of this region, one can observe the broken line, based on the arithmetic mean σ. It should be noted that in terms of the electrical conductivity, the kimberlites at 1200°C are similar to the ultrabasic rocks. The activation energy in kimberlites is higher than in the case of the ultrabasic rock (see Table 15). In addition, the high temperature break in the curve, which indicates the activation of intrinsic conductivity, is in the case of the kimberlites, within the region of higher temperatures. This is explained on one hand by the fact that the kimberlite magma has been formed under particular conditions and has been enriched by the magnesium oxides, by the chromium-containing spinels and by the diopside [76] and on the other hand, by the fact that it is the product of primary crystallization.

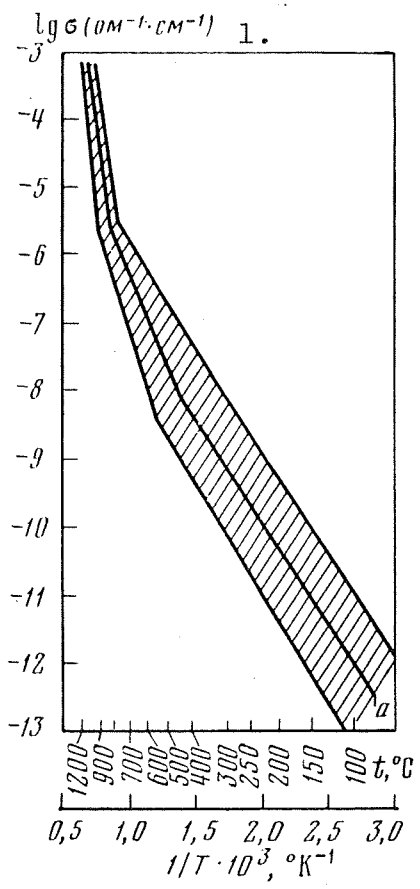

Figure 32. Electrical conductivity of kimberlites from Yakutiya (a - averaged-out curve).

Key: 1. $ohm^{-1} \cdot cm^{-1}$

By considering Table 15, we can see that in terms of the electrical parameters, the kimberlites of "Obnazhennaya" flow differ quite considerably from the other tunneled kimberlites. The experimental data indicates that the "Obnazhennaya" kimberlites, in terms of the electrical properties, are analogous to the pyrope peridotite. This is not an accidental occurrence. It has been established by the geologists and geophysicists that the kimberlite from this tunneled flow, in terms of some other mineral and chemical analysis, corresponds to the hyperbasite inclusions series, formed under specific tectonic conditions. On the basis of such data, it follows that the electrical parameters have a close relationship to the chemical and mineral composition and to the specific geological conditions of crystallization. All this data may be used to develop the general concept of evolution and of the thermodynamic conditions of the media in which these rocks were formed [80]. For greater certainty of these

concepts, it is necessary to carry out a systematic study of the electrical parameters of the kimberlite rocks, as they undergo transition from the typical pyrope peridotites (hyperbasites) to the kimberlites, containing the products of the hyperbasites and resembling the alkali basaltoids of the porphyrous alkali-ultrabasic rocks, and ending up with the alkali basaltoids [81].

As we can see, the experimental data indicates that the /98
pyrope-containing xenoliths from kimberlite have the electrical conductivity which is 1-2 orders of magnitude lower than the olivine and pyroxene xenoliths from basalts. In the case of the first, one observes the anomalously high σ and E_0 at 900-1200°C and therefore, the obtained values of σ and E_0 in the high temperature range for these rocks is associated with the intrinsic /99
electrical conductivity.

In terms of the electrical conductivities, the olivinite from drilled holes and from the surface areas, with 10-15% of fialites in them, in terms of the intrinsic conductivity, are similar to the olivines and olivinite pyroxenes-xenoliths from basalts. However, in the case of the first of these, one observes higher σ and E_0 in the region of intrinsic conductivity. It should be noted that in olivinites, just like in the case of dunites, containing 5-10% of serpentine, one does not observe at high temperatures any sharp change in σ and $E_0 < 2.6$ (see Appendix 6).

The samples of olivinite and olivines after testing were subjected to petrographic analysis. The comparison of microsections before and after the experiments indicates that the major changes are related to the intensive oxidation. This defines the color of the rock after the experiments. The oxidation brings about the appearance of secondary hematite, which has a characteristic metallic luster at the fracture point. The hematite is being formed along the grain boundaries, along the cracks and coarse faces, embracing the adjoining sections of the crystalline grains. The hematization occurs in the majority of cases selectively, primarily in olivines, not affecting the pyroxene, and proceeds more intensively at the boundaries between the grains of olivine and pyroxene. The boundaries of grains and small cracks are changed particularly strongly in the samples in which the secondary serpentine has been extensively developed. One also observes the zones of crushing. The changed segments of the sample may occupy the sample volume from several percentile points up to 40-50%. In the case of the olivine samples, made of xenolith from the lava of Avachinsk volcano, a chemical analysis was carried out to determine the amounts of iron before and after the experiment:

TABLE 15. ELECTRICAL PARAMETERS OF KIMBERLITES

Rocks, origin	Temperature range t, °C	σ at the point of inflection ohm^{-1}·cm^{-1}	E_0, eV	σ_0, ohm^{-1}·cm^{-1}
Kimberlites, olivine 1409, tunneled flow "Obanazhennaya"	100—450	$5\cdot10^{-13}$	0,7	$6\cdot10^{-3}$
	450—850	$2,6\cdot10^{-8}$	1,1	$3\cdot10^{-1}$
	850—1200	$4\cdot10^{-6}$	3,4	$2\cdot10^{8}$
		$1\cdot10^{-3}$		
Kimberlite, olivine 1409_2 tunneled flow "Obanazhennaya	50—450	$1\cdot10^{-12}$	0,5	$2\cdot10^{-4}$
	450—850	$2,6\cdot10^{-8}$	1,0	$3\cdot10^{-5}$
	850—1200	$4\cdot10^{-6}$	3,4	$2\cdot10^{8}$
		$1\cdot10^{-3}$		
Kimberlite 1404, tunneled flow "Bezymyannaya"	50—700	$1\cdot10^{-10}$	0,4	$2\cdot10^{-4}$
	700—950	$2,6\cdot10^{-6}$	1,54	$4,5\cdot10^{-1}$
	950—1200	$4\cdot10^{-5}$	2,6	$5\cdot10^{5}$
		$1\cdot10^{-3}$		
Kimberlite, olivine 1411, tunneled flow "Obanazhennaya"	100—500	$1\cdot10^{-13}$	0,6	$8\cdot10^{-5}$
	500—950	$4\cdot10^{-9}$	1,2	$9\cdot10^{-2}$
	950—1200	$1\cdot10^{-5}$	3,5	$1\cdot10^{7}$
		$4\cdot10^{-4}$		
Kimberlite 1319, tunneled flow "Udachnaya"	100—400	$4\cdot10^{-12}$	0,64	$5\cdot10^{-4}$
	400—470	$4\cdot10^{-9}$	Anomalous section	
	470—700	10^{-9}	1,0	$9\cdot10^{-2}$
	700—1200	$4\cdot10^{-8}$	2,8	10^{9}
		10^{-3}		
Kimberlinte 1319_2, tunneled flow "Udachnaya"	150—400	$4\cdot10^{-10}$	0,3	$5\cdot10^{-5}$
	400—470	$4\cdot10^{-9}$	—	—
	470—700	10^{-9}	1,0	$9\cdot10^{-2}$
	700—1200	$4\cdot10^{-8}$	2,8	10^{9}
		10^{-3}		
Kimberlite 1404 (two samples, tunneled flow "Bezymyannaya"	50—450	$5\cdot10^{-13}$	0,7	10^{-2}
	450—600	$4\cdot10^{-7}$	Anomalous section	
	600—950	$2\cdot10^{-7}$	1,5	$2\cdot10^{1}$
	950—1200	$1,6\cdot10^{-6}$	2,74	$7\cdot10^{5}$
		$8,5\cdot10^{-4}$		

[Commas in tabulated material are equivalent to decimal points.]

Oxides	Before experiment	After experiment at t=1200°C
FeO	4.47	2.23
Fe_2O_3	2.45	4.70
Total	6.92	6.93

One can see from this data that more than one half of FeO found in the rock at t=1200°C is being oxidized. If one is to take into account that the bulk of the iron is in the form of fialite, the scale of oxidation becomes clear for the whole restructuring of the crystals and the development of secondary minerals. The changes observed in the samples may significantly affect their electrical conductivity, even more so because the secondary minerals are being developed within the weakly-bonded regions, in all directions within the sample. It is possible that such changes in the rocks at great depth do not occur because of the absence of free oxygen. By observing the electrical conductivity rate increase in the temperature range of 850-950°C, one should mention the study [99], in which G. V. Belinskiy and G. V. Pinus, indicate that the heating of up to 900°C of the ordinary olivines, /100 which are not bound very tightly, will result in the structural changes. In addition, at that temperature, the olivines will have the highest coefficient of linear expansion. The authors believe that the high pressures result in the appearance of some cleavage within the low temperature range. In the quartz during such processes, the reconstruction of the crystalline lattice in the olivines may take place, by the introduction of calcium which isomorphously will replace, within the structures, a certain number of magnesium ions. The greater ionic radius of calcium will result in the increase of the elementary cell, and the decrease associated with it of the bondings between ions. All these processes in this temperature range may be accompanied by a rapid growth of electrical conductivity. One may assume that in the course of plastic deformations, and taking into account that the olivines which are not completely deformed do not display cleavages, one could expect great changes in electrical conductivity. The studies of such type are of great interest, since within the seismically important and active zones, one may observe plastic deformations within the rocks at a certain depth.

The electrical conductivity and E_0 and σ_0 quantities were also measured in the case of pyrope-spinel dunite 2162 (Figure 33) and of the olivine derived from it, and also of the compressed olivine powder. One can see in these curves that there are significant differences between the samples in terms of the electrical conductivities and of the E_0 and σ_0 parameters (Table 16).

One observes similar electrical conductivities all the way up to 850°C in the case of the sample of the olivine grain and the sample which was made from the olivine powder. At higher temperatures, the electrical conductivity in the former sharply increases

TABLE 16. ELECTRICAL PARAMETERS OF OLIVINES AND PERIDOTITES AT HIGH TEMPERATURES

/101

Rock	Temperature range t, °C	E_0, eV	σ_0, ohm^{-1}·cm^{-1}	Bibliography
Fosterite (at p = 23 kbar)	300—700	1,9	$2 \cdot 10^6$	[42]
Fosterite	1060—1420	2,2	$2 \cdot 10^8$	[22]
Olivine (10% fialite at p = 23 kbar	600—700	2,3	$2 \cdot 10^8$	[42]
Olivinite	1060—1170	4,6	$4 \cdot 10^3$	[44]
Peridotite	1063—1210	2,7	$4 \cdot 10^5$	[102]
	1063—1210	2,5	$4{,}6 \cdot 10^3$	[100]
	1100	2,5	$1 \cdot 10^5$	[101]
Plageoclase peridotite	620—1000	2,66	$7 \cdot 10^9$	[90]
Olivinites and peridotites (average values)	550—1200	2,3	$6 \cdot 10^4$	[89]
Dunites (serpentinites)	700—1200	2,0	$5 \cdot 10^2$	[88]
Pyrope-spinel dunite	850—1200	2,78	$7 \cdot 10^6$	[87]
Pyrope peridotite with entatite	850—1200	3,6	$2 \cdot 10^9$	[87]
Olivinite 1479 (Habozero, 3 samples)	150—575	0,8	$2 \cdot 10^{-2}$	
	575—750	1,22	0,4	
	750—1200	2,3	$5 \cdot 10^4$	[88]
Olivinite 1423 (Monchegorsk)	150—500	0,73	10^{-3}	
	500—900	1,35	0,9	
	900—1200	3,1	$8 \cdot 10^7$	[88]
Olivinite 1439 (Kurginsk tract)	100—450	0,6	$7 \cdot 10^{-5}$	
	450—850	1,5	10^2	Authors
	850—1200	3,3	$4 \cdot 10^8$	
Olivinite 1482 (Avachinsk sinolite)	150—435	0,88	$9{,}5 \cdot 10^{-4}$	
	435—925	1,33	0,3	
	925—1200	3,3	$8 \cdot 10^7$	[88]
Olivinite 1484 (from the inclusions in Oceanite, Seychelles Islands)	150—575	0,65	$4 \cdot 10^{-3}$	
	575—850	1,21	0,8	
	850—1200	3,26	$4 \cdot 10^8$	[88]
Olivine (forsterite) 2162	200—700	1,0	$9 \cdot 10^{-3}$	
	700—1050	1,76	$7 \cdot 10^1$	Aurthors
	1050—1200	3,8	10^{10}	
Olivine pyroxenite	500—860	1,4	1,2	
	>860	3,5	$7{,}0 \cdot 10^9$	[19]

[Commas in tabulated material are equivalent to decimal points.]

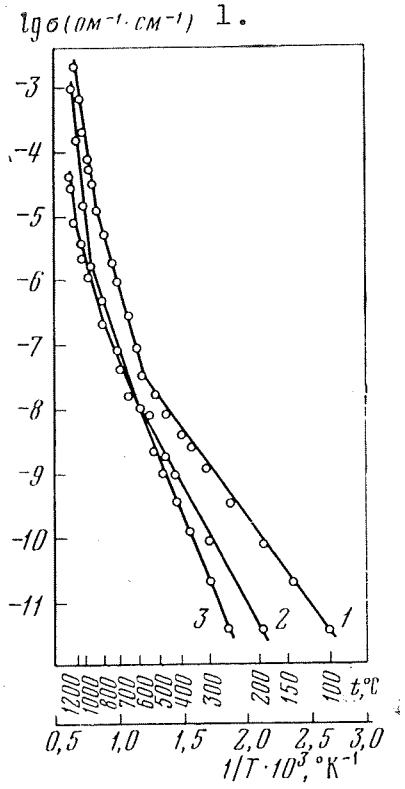

Figure 33. Electrical conductivity of olivine and pyrope-spinel dunite as a function of temperature.

1 - pyrope-spinel dunite 2162 (tunneled flow "Obnazhennaya"), 2 - olivine crystal from rock 2162, 3 - sample made of olivine powder, obtained from the rock 2162.

Key: 1. $ohm^{-1} \cdot cm^{-1}$

and at 1200°C, it becomes higher by 1.5 order of magnitude than in the case of the second sample. It is possible that the higher electrical conductivities in the olivine and in the pyrope-spinel dunite are due to the additional thermoelastic stresses which occur in the minerals at high temperatures. However, in the case of the olivine samples made of the powder, these stresses are relieved by the crystal crushing. The analogous, anomalously high /102 E_0 and σ_0 are also cited by the other authors.

It is not excluded that these figures are due to the oxidative and polymorphous transitions at higher temperatures. Therefore, the true values of the intrinsic conductivities in the olivine rocks under atmospheric conditions were obtained by us, together with I. S. Fel'dman, on the basis of experimental data, by marking off the points of inflection in the electrical conductivity curve (Figure 34). The method of the inflection points for the ionic and semiconducting electrical conductivities is based on the fact that with the temperature increase, the point of inflection which reflects the conversion of impurity-related electrical conductivity to the intrinsic conductivity will superimpose on a straight line of the corresponding temperature relationship, describing the intrinsic /103 conductivity of an ideally pure crystal [16].

This is due to the fact that the samples having similar composition and similar crystalline structure have the same intrinsic conductivity but differ in terms of concentrations and, possible, in terms of different types of impurities. In the natural silicates,

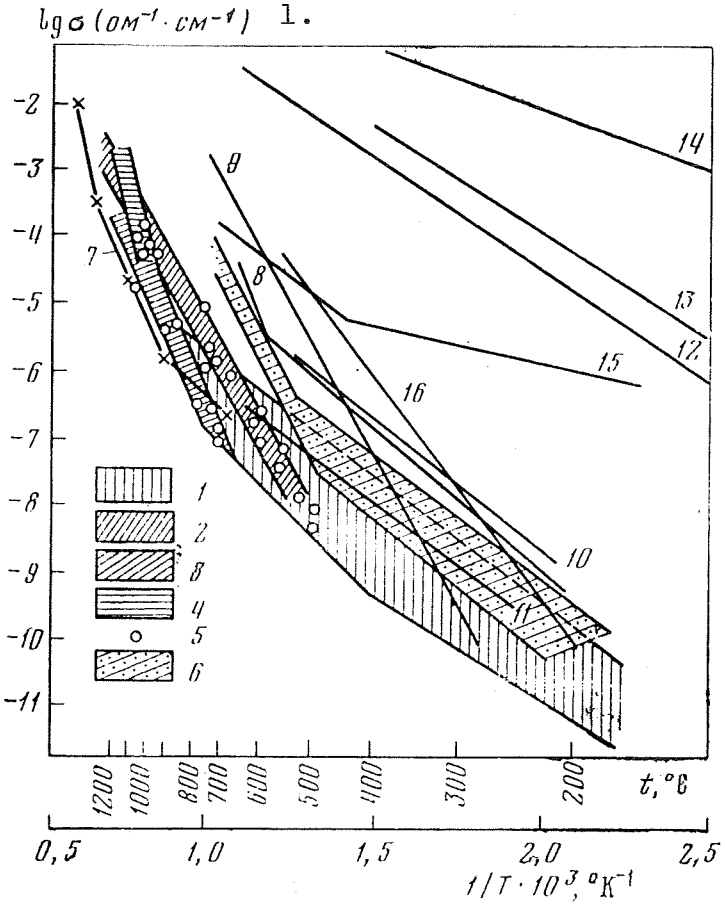

Figure 34. Comprehensive curves describing the electrical conductivity of olivines and olivine-containing rocks as a function of temperature.
1 - the zone of impurity-related conductivity for I-II group of curves (see Table 17); 2,3 are the IV and V groups, the zones of intrinsic conductivity; 4 - VI group; 5 - temperature points of inflection; 6 - region of electrical conductivity of olivinites and peridotites at 20,000 kg/cm^2; 7 - forsterite, 100% [41]; 8 - olivine, 10% fialite [43]; 9 - forsterite, 100%, 23 kbar [43]; 10 - olivine, 10% fialite [103]; 11 - olivine, 17.5% fialite [103]; 12 - olivine, 50% fialite [43]; 13 - fialite, 100%, 23 kbar [43]; 14 - fialite, 100%, spinel phase [42]; 15 - garnet-almandine at 20,000 kg/cm^2; 16 - garnet-pyrope from the tunneled flow "Obanazhennaya" at 20,000 kg/cm^2[58].
Key: 1. $ohm^{-1} \cdot cm^{-1}$

such as olivinites, the bulk of the sample is represented by the olivine in which the crystalline structure is defined by forsterite, with the smaller quantities of fialite as the isomorphous component. In different samples, the amount and composition of the secondary minerals and also the quantities of impurities will change. The ratio of fialite and forsterite will also change within a narrow range. These changes will be reflected in the electrical conductivity parameters within the zone of impurity-related conductivity but they cannot significantly change the temperature relationship within the zone of intrinsic conductivity. Therefore, the inflection points define the straight line or the region within the straight lines, the parameters of which characterize the temperature relationship within the zone of intrinsic conductivity (see Figure 34). It is important that we are generating the data at such temperatures that in the course of experimental work in the atmosphere, there are still no significant changes in relationships.

In processing the experimental data and utilizing the method of inflection points, it turned out that all obtained curves of $\lg \sigma = f(1/T)$ are to be found within the zones (regions) shown in Figure 34 by different shading. It should be pointed out that these zones also incorporate the data, describing the $\lg \sigma = f(1/T)$ for fresh peridotite and pyrope peridotites from xenoliths of the tunneled flow "Obnazhennaya" and olivine inclusions in the basalts. To obtain the comprehensive parameters of conductivity, we have analyzed curves for each sample separately. The analysis of the electrical conductivity curves were carried out as follows. One selected for each curve the straight line segments in which, we have believed, one specific charge carrier was predominant. Ordinarily, these rectilinear segments were combined within a specific region. Then within these regions, the E_0 and σ_0 parameters were calculated for each type of carrier and for each temperature, in the beginning and at the end of the rectilinear segment. The position of the zones in which the curves of electrical conductivity would fit are shown in Figure 34 [58]. This figure gives us the general idea as to the E_0 and σ_0 quantities, as well as of the temperatures at the point of inflection. The point of inflection in the curves in Figure 34 are shown by circles. This figure shows a clearly defined grouping of E_0 and σ_0 parameters within a specific range for each temperature range. This is even more apparent in the histograms of distributions for several temperature ranges (Figure 35, a, b). Within the zone of impurity-related conductivity, one observes clearly, up to the temperature of 800°C, three groups of curves (I-III), which produce three separate maxima, for both E_0 and σ_0. In Figure 34, these groups of curves have similar shading. This /104 fact indicates that it is possible to have three different types of current carrier within the low temperature range.

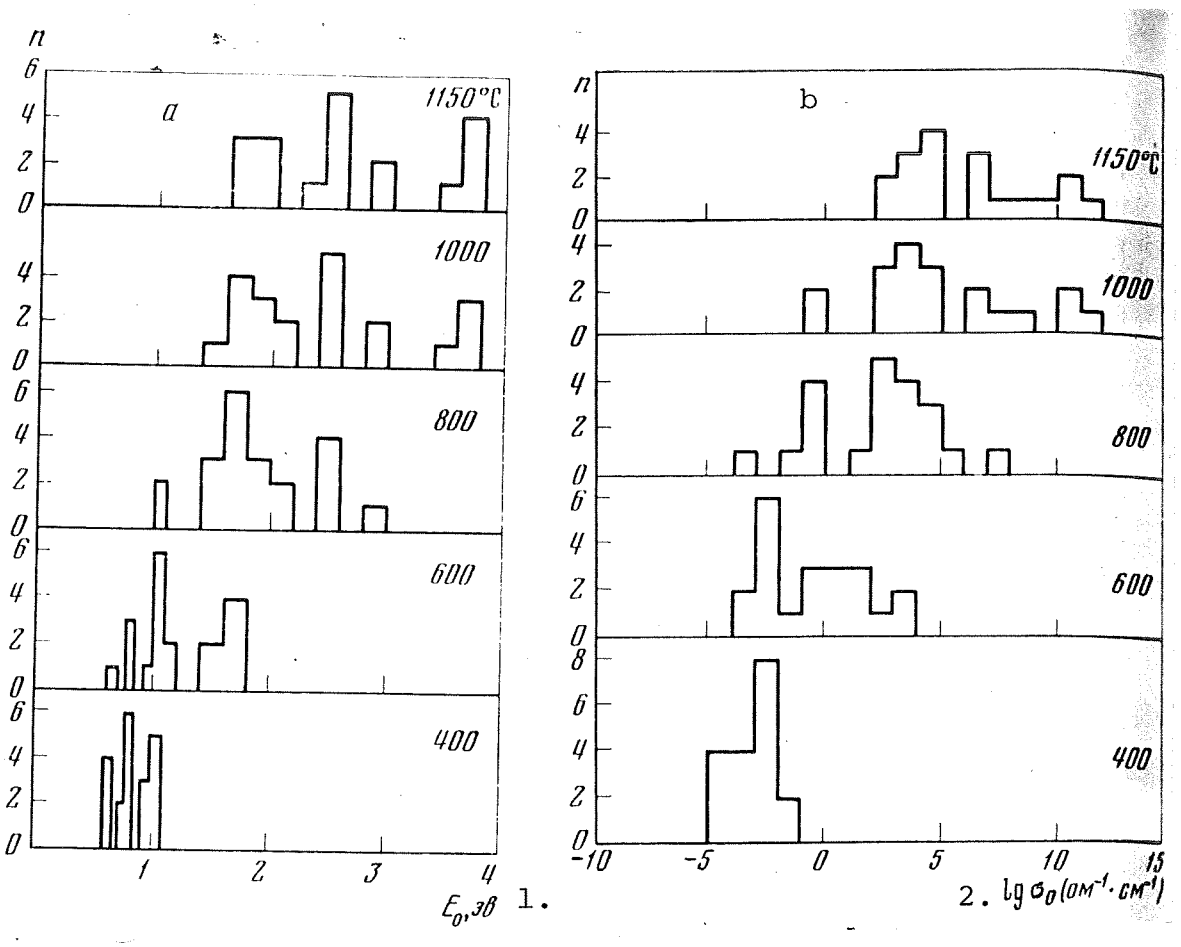

Figure 35. Histograms of the activation energy distribution (a) and the pre-exponential coefficient (b) in the olivines and in the olivine-containing rocks, at different temperatures (n is the number of samples).

Key: 1. E_0, eV; 2. ohm^{-1}·cm^{-1}

Within the high temperature range, from 500 to 1200°C, one can separate two groups of curves (IV and V). As it appears, they correspond to the zone of the intrinsic conductivity of olivines. This is also substantiated by the high activation energies, by the retention of the whole mechanism up to 1200°C, and by the reliable monitoring of these zones which can be done by the method of the inflection points (see Figure 34). It is still not clear why there are two groups of curves within the zone of intrinsic conductivity. It appears that these groups are defined by different amounts of fialite in olivine. On the other hand, it is possible that they reflect the thermodynamic parameters, in the presence of which the crystallization of minerals and the melt reconstitution took place. It is necessary to point out that at higher temperatures,

namely from 900 to 1100 and to 1200°C, one can isolate for olivinites another group - the group of curves VI. As one can see from the histogram, the E_0 and σ_0 parameters in this group have no clear distribution on the basis of which the curves could be verified. It is likely that the position of the curves in the case of the above-mentioned temperatures may be explained by the oxidation processes and by some other changes in the samples, in the free oxygen surrounding. The points of inflection of the lg σ=f(1/T) curves which are grouped within a narrow temperature range, and also the rapid increase of electrical conductivity as a function of temperature substantiate to some degree this proposition. However, one should be reminded that the rapid increase of electrical conductivity may be due also to some other transformations in olivine. We shall present below the parameters of E_0 and σ_0, determined on the basis of the histogram for each group of the curves (Table 17). /105

TABLE 17. ELECTRICAL PARAMETERS OF OLIVINITES AND OLIVINES

Group	Temperature range t, °C	E_0, eV	σ_0, $ohm^{-1} \cdot cm^{-1}$	Assumed mechanism of conductivity
I	100—500	0,62	10^{-4}	Impurity-related ionic and semiconducting
II	100—600	0,80	$8 \cdot 10^{-4}$	
III	100—750	1,0	10^{-2}	
IV *	500—1200	1,8	$5 \cdot 10^{3}$	Intrinsic-ionic
V *	800—1200	2,55	$2 \cdot 10^{4}$	
VI **	900—1200	3,2—3,8	10^{10}—10^{12}	
	100—500 (at 20 кбар)	0,75	$5 \cdot 10^{-3}$ $2 \cdot 10^{-2}$	Impurity-related ionic
	500—700 (at 20 кбар)	2,0	10^{5}—10^{6}	Intrinsic-ionic

* Defined by a clear point of inflection.
** No clear point of inflection.

[Commas in tabulated material are equivalent to decimal points.]

Figure 34, together with our comprehensive experimental results, shows also the results for synthetic olivines and for peridotite. One can see from Figure 34 that the curves for synthetic olivines, containing from 1 to 15% fialite, fall well within the region of the first three groups of curves. The conductivity parameters of synthetic olivine in the temperature

range from 100 to 300-500°C, in which E_0=0.7-0.75 eV and σ_0= =10^{-2}-10^{-3} ohm^{-1}·cm^{-1}, correlate well with the parameters of the second group of natural olivines. This group, just like the first one, seems to correspond to the impurity-related ionic conductivity case. In the case of other synthetic olivines, in the temperature range 300-500 to 750-900°C E_0 is 019-0.95 eV and σ_0 is 10-10^{-2} ohm^{-1}· ·cm^{-1}, which corresponds to the parameters of the olivines in the third group. Bradley et al. have shown that in this case [42], the synthetic olivines display the semiconducting type of conductivity.

Generally, the parameters of the IV group correspond to the parameters of intrinsic conductivity of forsterite, but do not completely coincide (see Figure 34). This is not by accident, since we were involved here not with pure forsterite. It appears that in order to calculated the electrical conductivity in the mantle at great depths, one could utilize the parameters of conductivity E_0 and σ_0 from the groups IV and V. However, one should recognize that the parameters of the V group will produce, at greater depth, somewhat higher figures. Therefore, the calculations, by using the parameters from group IV, may be assumed to be the nominal at great depth. /106

6. Pyroxenites

The pyroxenites are typical ultrabasic rocks, which are encountered only in the intrusive forms. The opinion has been expressed that in the lower part of the continental crust, one may encounter rocks,rich with pyroxene because of the instability of the mineral association of the olivine gabbro [104]. The study of the physical properties of pyroxenites is of substantial interest, since the pyroxene, togehter with olivine, is one of the major components of the mantle material.

The studies of the electrical properties were carried out by using the samples selected at the Russian plateau, Cola peninsula, the Soviet Far East and Kazakhstan. The results of measurements are attached in Appendix 7 and are shown in Figure 36.

The pyroxenite 2492 is the cataclistic rock, with the features of plastic deformation. The deformed grains of pyroxene (monocline) in the rock are oriented in different directions. Between the grains, one finds the chlorotactinolite material of magnesium composition. In conjunction with this, the samples which were cut out in two perpendicular directions have displayed a weak anisotropy of electrical conductivity within the structurally-sensitive region, in other words, approximately up to 600°C. At higher temperatures, similar electrical conductivities were obtained.

The pyroxenite 2497 which is 80% diopside, in terms of its electrical conductivity, differs only slightly from pyroxenite 2492, although the activation energy is somewhat less. It is possible that the activation energy of pyroxenite 2492 is higher because of the plastic deformations, the greatest of which can be found in the microsection samples of this rock, and one should also not exclude the effect of chlorite of magnesium composition. The pyroxenite 2497, just like pyroxenite 2492, becomes cataclistic, but is affected to a lesser degree by the secondary processes. The pyroxenites 2482 and 2500 are approximately of the same mineral composition and display the same degree of alterations with the resulting similar electrical parameters. In conjunction with the replacement of pyroxene by uralite, as a function of temperature, the electrical conductivity of one rock, in the temperature range 800-900°C, and in the case of the other rock - 820-940°C, displays the disruption of linear dependence of $\lg \sigma = f(1/T)$ because of the evolution of the hydroxyl group $(OH)^{1-}$ from uralite. /107

In parallel with the pyroxenites which have low electrical conductivity, one encounters high conducting pyroxenites. The electrical conductivity of pyroxenite 2501, for example, at 200°C reaches 10^{-5}-10^{-4} $ohm^{-1} \cdot cm^{-1}$. The high σ in this sample is due to the enrichment by ore material, which is located at the grain boundaries.

The olivine pyroxenites from the Cola peninsula, 340, 591 and 469, differ from the pyroxenites of the Russian plateau by having lower electrical conductivity (see Appendix 7). This is related to the considerably smaller degree of alterations in it, and also to the presence in it of the rhombic pyroxene - enstatite, instead of diopside.

Of particular interest are the pyroxenites from Koksharov plateau (USSR maritime region) which is about 140 million years old. These are extensively found in this area, and are the major component here. The pyroxenites from this region are characterized by the following mineral composition: titanium augite, titanium magnetite, eugirite-augite, perovskite, apatite, sphene and malanite. The secondary minerals are represented by biotite, vermiculite and iron hydroxides. The five pyroxenites of this origin which we have investigated in terms of the electrical properties are divided into two groups. The first one includes the pyroxenite 1004 and 1001 which display extremely high electrical conductivity, and this is connected in the first place with the high quantities (about 25%) of the ore material - titanium magnetite, which is located along the tiny cracks and at the grain boundaries as the extended chains. Because of such geometry of titanium magnetite grains, one observes the current-conducting channels which enhance appreciably the electrical conductivity of the rocks. The second mineral which also features high electrical conductivity is the titanium augite (Table 18).

The second group of pyroxenites (1002, 1006 and 1003) is characterized by lower electrical conductivity across the whole temperature range of 200-1100°C. The petrographic analysis of these rocks indicates that in the samples 1002 and 1006, the ore mineral is in lesser quantity than in the first group of pyroxenites. The amounts of eugirite-augite and of eugirite in the pyroxene in these rocks facilitates the increased electrical conductivity in the pyroxenite. Table 18 shows the chemical composition of the minerals obtained from the rocks of Koksharov plateau. According to the data in this table, in the eugirite-augite, one finds the following oxides Fe_2O_3, FeO and Na_2O, while the pure eugirite, as has been pointed out earlier, is itself a conducting mineral within the pyroxene group. Therefore, the highly conducting properties of pyroxenites within the alkaline formations of Koksharov plateau are due to a considerable concentration in them of the Fe^{2+}, Fe^{3+}, Na^{1+} and Ti^{4+} cations. /108

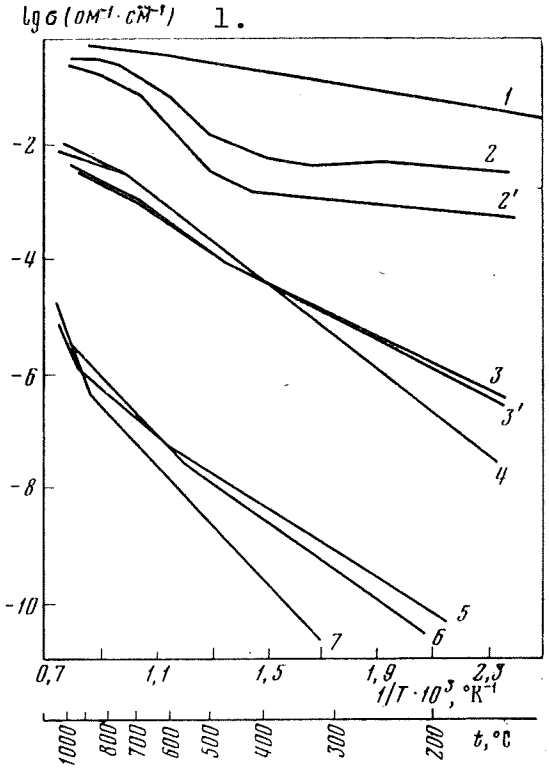

Figure 36. Electrical conductivity of pyroxenites as a function of temperature.

1 - sample 1004; 2,2' - sample 1001; 3,3' - sample 1006; 4 - sample 1002; 5 - sample 2482; 6 - sample 2492; 7 - sample 591.

Key: 1. $ohm^{-1} \cdot cm^{-1}$

The pyroxenite 1003, obtained from the oreless part of the Koksharov plateau, features low electrical conductivity and low activation energy, which are typical for this type of rocks.

The presented graphic material indicates the broad range within which the electrical parameters of pyroxenite may vary, depending on the type of pyroxene, on the amounts of the ore mineral and on the character of its distribution within the rock.

In addition, the secondary changes which are in the form of uralitization result in the disruption of linear dependence of lg σ=f(1/T), affecting only slightly the absolute values of electrical conductivity.

In the case of pyroxenites which have been affected only slightly by the secondary processes, the following values of E_0 and σ_0 are quite characteristic:

Temperature range	E_0, eV	lg σ_0, ohm$^{-1}\cdot$cm^{-1}
Up to 500-600	0.60	-4.2
600-900	1.0	-1.1 ÷ 2.6
900-1100	2.2-2.55	3.0-4.5

TABLE 18. CHEMICAL COMPOSITION OF MINERALS IN THE ULTRABASIC ROCKS OF KOKSHAROV COMPLEX [105]

Rock	SiO_2	TiO_2	Al_2O_3	Fe_2O_3	FeO	MnO	MgO	CaO	Na_2O	K_2O
Titanium augite from pyroxenite	41,85	2,72	9,74	5,97	8,26	0,33	7,26	21,91	0,93	0,12
Titanium augite from the ore pyroxenite	48,13	1,88	3,65	3,67	4,08	0,88	14,32	23,42	0,50	0,02
Eugirite-augite	51,31	0,83	2,76	12,49	5,38	1,1	5,92	13,99	5,99	0,15
Titanium magnetite from the ore pyroxenite	1,8	15,5	0,48	45,42	28,27	0,28	5,26	1,92	—	—

[Commas in tabulated material are equivalent to decimal points.]

The inflection point in the straight lines of lg σ=f(1/T), which is ordinarily observed at the temperature of about 900°C, may be due to the polymorphous transition of pyroxene, as per data presented in the studies [96, 97]. /109

The investigated xenolith from pyroxenite 1508* from the ophite lava of a volcano in Kamchatka in the temperature range of 150-700°C displays high σ with the anomalous variation at 600-700°C. At the temperatures above 700° it features parameters which are typical for rhombic pyroxenites of the Cola peninsula.

7. Effect of Serpentinization on the Ultrabasic Complex of Rocks

The ultrabasic complex of rocks without feldspar, depending on the mineral composition, may be subdivided into olivinites, pyroxenites, peridotites and dunites. All of these are characterized by small quantities of silicic acid - about 45%. The rock-forming minerals in this case are the olivine and pyroxene. The ultrabasic rocks are affected quite appreciably by the metamorphic change of serpentization type. The most intensive process occurs within the zones of fragmentation. The opinion has been expressed that one of the reasons for inhomogeneity at the lower boundary of the Earth's crust is the serpentization of the olivine material, which occurs at 500-600°C [106]. Let us consider the effect of serpentization on the electrical parameters of the basic rock groups.

The electrical properties of olivinites at high temperature were investigated by using the rock samples (583, 6014 - from the Cola peninsula, 1381 from Avachinsk inactive volcano mound, 5683, 6013 - from the south Ural mountains) which were affected to a different degree by serpentization. All rocks within the temperature range of 200-1100°C feature low electrical conductivity - from $9.1 \cdot 10^{-13}$ to $5.9 \cdot 10^{-4}$ $ohm^{-1} \cdot cm^{-1}$ (Appendix 8). In this case, in terms of the electrical conductivity within the structurally-sensitive region (approximately up to t=600°C), they are close to granites and at higher temperatures, their electrical conductivity is, as a rule, higher.

The curves of $\lg \sigma = f(1/T)$ depict sufficiently clearly the three temperature regions, with the inflection points within the temperature range of 500-600 and 800-900°C. The range of activation energies in the low temperature regions is 0.7-0.86 eV. In the intermediate and high temperature range, it increases, reaching 1.1-1.46 and 2.1-2.6 eV, respectively. In the case of four olivinites (583, 6014, 5683 and 6013), one observes an insignificant increase of electrical conductivity with the decrease of the level of serpentinization. Such relationship contradicts the data obtained for the other types of rocks. As it appears, the inverse relationship between the serpentinization and the magnitude of electrical conductivity for the above-mentioned rocks is due to the differt amounts of fialite present.

On the basis of the obtained data, one may claim that the display of serpentinization up to the level of 10%, has no effect on the electrical conductivity in olivinites. The decisive role here is played by the amount of fialites. The second probable /110

cause of increased electrical conductivity in olivinites may be the appearance of polymorphous transition.

The dunites, just like the olivinites, consist predominantly of olivine, but differ from the latter by the amounts of chromite in the quantities of up to 3%. In the chromite-containing dunites, its quantities are much greater. In addition to the chromite in dunites, one encounters also the magnetite. The electrical conductivity of chromite-containing dunites in the absence of magnetites is quite low, for example, at t=200°C, it is about 10^{-12} $ohm^{-1} \cdot cm^{-1}$. The effect of chromium oxide resulting in the decrease of electrical conductivity in the compounds of Fe_3O_4 type have been considered in the first chapter. The dunites which we have investigated were affected to a greater degree by serpentinization than the olivinites. Appendix 9 shows the experimental data for ten dunites of different origin, with the percentages of serpentine found. The major feature of these dunites is a broad range of electrical conductivities in the region of impurity-related conductivity and the presence of anomalous relationship between the electrical conductivity and temperature within the range of 400-900°C (Figure 37a). The dispersion of electrical conductivity within the range of intrinsic conductivities (800-1100°C) in the case of these dunites, as one can see from Figure 37a, will increase. For example, the dunite 5556 and 5577 which feature extremal values of electrical conductivity within the impurity-related region, in terms of σ quantity, differ only slightly at high temperatures. Somewhat lower dispersion of electrical conductivity in dunites at high temperatures is explained by the decreased effect of Fe ions on the intrinsic conductivity, as compared to their decisive role within the low temperature range. The significant role of iron ions in the mechanism of electrical conductivity at low temperatures is substantiated by low activation energy (E_0=0.1-1.34 eV) in the conducting dunites.

As one can see from the data shown in Appendix 9, there is no clearly defined relationship between the electrical conductivity and the degree of serpentinization. This is explained by the fact that the rocks having high percentage of serpentine do not always contain magnetite in the form of hair-thin inclusions, which bisect the serpentine grains or appear along the grain boundaries. The serpentine itself features a rather low electrical conductivity (see Appendix 1).

The anomalous change of electrical conductivity with the temperature increase within a specific temperature range is quite characteristic for the majority of dunites. The width of this temperature range for different rocks is not similar. In the case of dunite 5577, which features only slight serpentinization and which has the lowest electrical conductivity, the anomalous temperature range was not detected. In the case of a number of rocks /111

(7198), 6671, 6672, 6669) this range does not exceed the temperature of 200°C, and more often than not, it does not go beyond 100°C. The presence of such anomalous change in σ may be caused by two phenomena: the conversion of serpentine into olivine, in the course of which dehydration takes place, and the oxidation of iron.

The study [44], by employing the X-ray analysis, has convincingly shown the presence of such conversion. On the other hand, in the case of the serpentines which had different quantities of water, one was able to obtain the direct relationship between the width of the anomalous zone of σ change as a function of temperature and the function of the amounts of water [107]. One should also not exclude the possibility of the effect of transition from the ferromagnetic state into the paramagnetic state and the related electrical conductivity, something which has been pointed out by a number of researchers [32, 108-111].

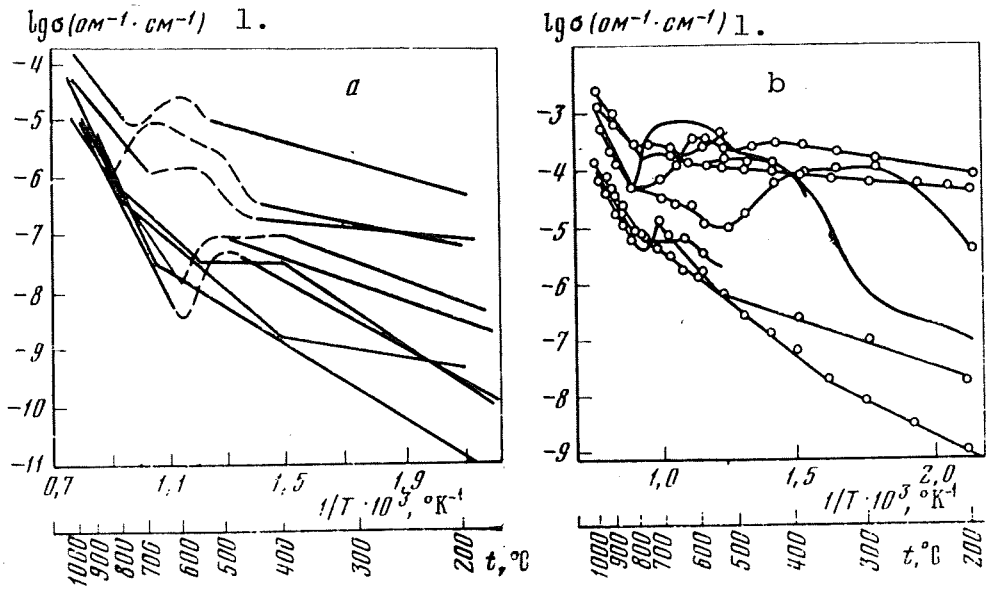

Figure 37. Electrical conductivity in dunites (a) and in peridotite (b) as a function of temperature, having different levels of serpentinization.
Key: 1. $ohm^{-1} \cdot cm^{-1}$

The electrical conductivity as a function of activation energy has been noted in the case of serpentinized dunites. As can be seen in Appendix 9, as one decreases the electrical conductivity one observes the increased activation energy. As a result of such relationship, in parallel with the broad range of electrical conductivities at low temperatures, one observes a broad range of

activation energies (from 0.1-0.7 eV). In the region of high temperatures (t>800°C), the activation energies of the current carriers in dunites are within the range of 1.42-2.14 eV. In this case, the most conducting dunites are characterized by the activation energy of 1.42-1.7 eV, and in the case of high resistivity dunites it is somewhat higher, comprising E_0=2.0-2.14 eV. Since the variation in the levels of electrical conductivity are due to the quantity and character of the magnetite distribution, it appears that this is also the main cause of variations in terms of the activation energy within the region of intrinsic conductivity. The dunites are the /112 most probable components of the upper mantle, and therefore the knowledge of their electrical parameters is quite important to define the limits of change in the electrical conductivity of the Earth's interior.

The peridotites are primarily made of olivine and bisilicate (pyroxene). The olivine crystals in them are ordinarily idiomorphous, and are frequently serpentinized. The pyroxene may be represented as a monocline diallog, diopside and rhombic pyroxene (either enstatite or bronzite). The studied peridotites, just like the dunites which we have considered earlier, are strongly serpentinized. On the whole, in the case of serpentinized peridotites, a higher electrical conductivity is typical as compared to dunites, because of their higher iron content and the absence of chromium oxide, which is partially neutralizing the electron transfer which is being observed in the presence of bi and trivalent iron. In the case of peridotites, just like in the case of dunites, one observes a stronger dispersion of electrical conductivities at lower temperatures than at higher temperatures. If, for example, at t=200°C, the electrical conductivity changes from 10^{-5} to 10^{-12} $ohm^{-1}\cdot cm^{-1}$, at t=1000°, this range will narrow down to one order of magnitude, in other words, it will correspond to $4.0\cdot10^{-5}$-$7.0\cdot10^{-6}$ $ohm^{-1}\cdot cm^{-1}$ (Appendix 10). The similarity between dunites and peridotites is also displayed in terms of the anomalous electrical conductivity as a function of temperature (Figure 37b). In this case, for peridotites, the lower temperature boundary of the anomalous region, in a number of cases, will drop to 200-300°C and the upper range will reach 900°C. The activation energy, in both the impurity-related region and in the intrinsic conductivity region is small and changes between 0.1 and 0.75 eV in the first case, and from 1.1 to 1.4 eV in the second case, and in four rocks of the 14 studied, it fluctuates between 2 and 3 eV.

The peridotite 2511 features the greatest electrical conductivity among all 5 rocks from the Russian plateau which have been investigated. This is related to the fact that its serpentinized mass is 70% mineralized. As a result of this, the rock contains about 20% of sulfides, and approximately 10% of magnetite. In such case, the ore minerals form a cellular texture, replacing the serpentine. One observes clearly defined anisotropy of σ in two directions.

The peridotite 2502 contains less of ore minerals than the peridotite 2511, but the character of the evolution of the ore mineral facilitates the increased electrical conductivity. The elongated grains of magnetite form some discontinuous chains with a well-defined orientation along the grain boundaries.

The peridotites 6871 and 5375 feature low electrical conductivity because of small quantities of magnetite present and its appearance in the form of isolated grains.

The electrical properties of Voronezh syneclise of the Mamonov tract are being considered separately since they feature not only the serpentinization, but also some other changes: the amphibolization, the talcum deposits and also hydrothermal and other exposure at a somewhat later time. /113

The apodunite 2606 has the highest electrical conductivity which increases only slightly with temperature. The linear relationship between lg σ and 1/T is observed in two temperature ranges: 200-380 and 820-1100°C. These regions are characterized by small E_0 and lg σ_0. The high electrical conductivity of apodunite 2606 is due to the evolution of the secondary magnetite along the grain boundaries, thus creating the current-conducting channels which increase considerably the electrical conductivity of the rock.

The apodunite 2614 differs from the samples considered above by featuring the low electrical conductivity at the temperature of up to 600°C, and with the further increase of temperature, the differences in σ values will decrease. The somewhat higher insulation properties of apodunite 2614 are due to the uniform distribution of the conducting ore mineral grains across the whole rock, and the absence at the boundaries, of the olivine and serpentine grains. Because of this, the conducting components are electrically insulated and will not affect the electrical conductivity of the rock. In addition, the quantities of magnetite (about 10%) in this rock are smaller than in the apodunite 2606 (about 20%).

Of the peridotite group, the greatest electrical conductivity is featured by the apoperidotite 2604, in which one observes the traces of cataclasis and of the weathering process. The effect of these two factors, as has been mentioned already, results in the increased electrical conductivity in the rocks. The ore mineral is distributed within the rock unevenly and is found sometimes along the tiny cracks and the grain boundaries, which also facilitates the increase in electrical conductivity.

The apoperidotite 2611, just like the 2604 rock, has high electrical conductivity. The apoperidotite 2611 and 2604, which feature the maximum electrical conductivity, are at the same time

the most serpentinized as compared to the 2606, 2610 and 2614 rocks.

The high temperature and low temperature ranges are characterized by somewhat lower activation energy in the current carriers, the magnitude of which is also affected by the presence of magnetite. The activation energy in these rocks fluctuates between 1.0 and 1.24 eV, the activation energy of the current carrier which is also characterized in the iron oxide (α-Fe_2O_3).

The somewhat higher electrical conductivity of dunites and peridotites within the Mamonov tract, and also small E_0 and σ_0 are due not only to the high degree of serpentization, the result of which is the evolution of specific grains of magnetite also, but also by some secondary changes.

The serpentinites are the products of change in the ultrabasic rocks, but in terms of physical properties, they are similar to peridotites and dunites, which were affected by metamorphosis. /114
In conjunction with this, the electrical parameters of these rocks will be considered in this section. The serpentinite 2494 has the highest electrical conductivity of all ten serpentinite samples which we shall consider below (Appendix 11). It contains magnetite which is found at the grain boundaries and as powdery isolated inclusions. The serpentinites 2512 and 2514 were obtained from the same drill hole. The serpentinite 2512 contains considerably greater quantities of sulfides and magnetite, as compared to the serpentinite 2514, which results in its somewhat greater electrical conductivity. The serpentinite 2488 is characterized by the specific evolution of magnetite in the shape of rings around the pyroxene grains, consisting of isolated, elongated magnetite grains. Because of the sparse distribution of the magnetite grains, the electrical conductivity of it is lower, although it contains much greater quantities of magnetite than the serpentinite 2494. The serpentinite 2185 and 2183, in terms of their mineral composition and electrical properties (see Appendix 11) are quite similar. These samples feature extensive magnetite rectilinear inclusions, placed at an angle of 30-45°.

In the serpentinites AV-45, 2519 and 2518, the serpentine is in the form of chrysotile. These serpentinites, according to the data in Appendix 11, differ from the preceding ones by the lower electrical conductivity. The absence of free magnetite along the grain boundaries is also one of the major reasons of the relatively low electrical conductivity.

The common feature of all serpentinites which we have investigated is the disruption of linear dependence in lg σ as a function of 1/T. In the case of serpentinites with high conductivity, the σ anomaly is observed in a broader temperature range than in the case of serpentinites with low electrical conductivity, which is in accordance with the results obtained for the

peridotites and dunites. The activation energy of the current carriers in the region of intrinsic electrical conductivity is within the range of 1.0-2.2 eV. In this case, one observes the tendency for the increased activation energy with the increase of the amounts of chrysotile in the rocks.

In conclusion, let us note the following.

1. The olivinite and pyroxenite, in the presence of typical quantities in them of oxides FeO, Fe_2O_3, Na_2O and K_2O are characterized approximately by the same electrical conductivities. The electrical conductivity of pyroxenites from the ore zone with high amounts of the above-mentioned oxides is considerably higher and at the temperature of 1000°C, reaching 10^{-1}-10^{-2} $ohm^{-1}.cm^{-1}$.

2. The dunites and peridotites display extremely broad range of electrical conductivities in the low temperature range, which, as the temperature increases, narrows down and as it becomes apparent, the electrical conductivity of these rocks at high temperature may be less than in the case of olivinites and pyroxenites. Among the highly conducting dunites and peridotites /115
are the rocks which were affected by serpentinization process and which contain the ore material in the quantities of 10 and more percents. In the case when the serpentinization of the rock is not accompanied by the evolution of ore material, the electrical conductivity of the rock remains low and is similar to the electrical conductivity of unaltered dunite or peridotite.

3. According to the chemical composition of dunites, the total quantities in them of high resistivity oxides (MgO, Al_2O_3 and SiO_2) is considerably greater (88%) than in the peridotites and serpentinites (77%) and the amounts of iron oxides are less by 4-6%. In addition, the dunites which contain chromium oxide feature the decreased electrical conductivity. All this results in the lowered electrical conductivity of dunites. Therefore, among the dunites, one encounters most frequently, the high resistivity samples, as compared to the other rocks of the ultrabasic nature. In the course of serpentinization and during various secondary changes, as the ore minerals evolve along the grain boundaries, there is very little difference between dunites and peridotites, particularly at low temperatures. Figure 38 shows the electrical conductivities at t=200 and 1000°C in the ultrabasic rocks, as a function of the amounts of ore mineral. As one can see, a clearly defined increase of electrical conductivity in the rocks is shown as a function of the quantities of ore mineral.

4. The comparison of investigated ultrabasic rocks in terms of the activation energy and $\lg \sigma_0$ shows that there is a certain differentiation here. In the case of olivinites, pyroxenites and

TABLE 19. ELECTRICAL PARAMETERS E_0 and $\lg \sigma_0 (ohm^{-1} \cdot cm^{-1})$ IN THE ULTRABASIC ROCKS

Group of rocks		1st region (from 500-600°C)		2nd region (from 500 to 900°C)		3rd region (above 900°C)	
		E_0, eV	$\lg \sigma_0$	E_0, eV	$\lg \sigma_0$	E_0, eV	$\lg \sigma_0$
Olivinites		0,6÷0,8	—4,4÷—2,5	1,0÷1,5	—0,5÷2,0	1,5÷2,6	5,0÷6,0
Pyroxenites	I	0,44÷0,8	—9,7÷—2,2	0,8÷1,0	—1,0÷2,6	2,0÷2,6	2,0÷5,0
	II	0,17÷0,76	—2,3÷1,1	0,36÷0,8	—1,2÷2,5	0,4÷1,05	—1,75÷1,6
Dunites	I	0,64÷0,7	—5,5÷—3,0	Anomaly,	500—600	1,9÷2,14	2,0÷3,5
	II	0,1÷0,52	—5,5÷—4,0	Anomaly,	500—800	1,42÷1,7	1,5÷2,5
Peridotites	I	0,34÷0,75	—7,5÷—4,5	Anomaly,	400—700	1,6÷2,8	—1,5÷8,0
	II	0,16÷0,5	—4,0	Anomaly,	500—800	1,1÷1,4	—1,5÷2,0
Serpentinites	I	0,54÷0,6	—5,2÷—3,0	Anomaly,	700—820	1,66÷2,0	1,5÷3,0
	II	0,1	—5,5	Anomaly		1,0÷2,2	—1,5÷4,7

[Note: commas in tabulated material are equivalent to decimal points.]

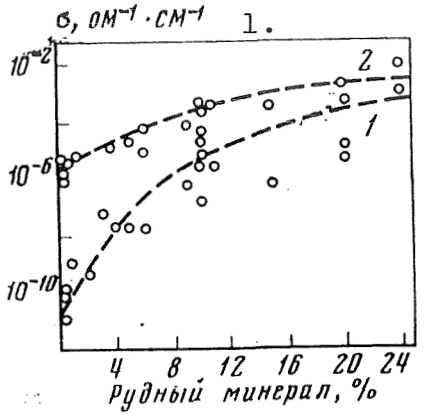

Figure 38. Electrical conductivity in the ultrabasic rocks as a function of the amounts of ore mineral at 200° (1) and 1000°C (2).
Key: 1. $ohm^{-1} \cdot cm^{-1}$
2. ore mineral

other rocks, one observes three temperature ranges with different mechanisms of electrical conductivity (Table 19).

It should be noted that in the olivinites, the E_0 values for all three regions is found within a narrow range, while in the case of pyroxenites, one observes considerable fluctuation in the activation energies. It follows from Table 19, that the average E_0 in pyroxenite and the first and second regions are somewhat lower, and at high temperatures, somewhat higher than in the case of olivinites.

The dunites feature a considerable dispersion of electrical conductivity and of activation energy. The dunites which are characterized by lower E_0 in the low temperature range, also have lower E_0 in the region of intrinsic conductivity, and vice versa. The peridotites, just like dunites, may be separated into two groups. In the case /117
of the dunite group with high electrical conductivity, one observes the disruption of linear dependence in $\lg \sigma = f(1/T)$ in a broad temperature range and low activation energy, while in the case of the other group, one observes somewhat narrower temperature ranges for the anomalous σ and even its absence and also high activation energies.

5. The above-mentioned similarity, and differences in electrical parameters of the ultrabasic rocks which we have studied are due not only to the mineral and chemical composition, but also to the secondary changes to which these rocks were subjected.

8. Electrical Conductivity of Eclogites in the Earth's Crust

At the present time, the majority of researchers have come to the conclusion that the eclogites which are found in the metamorphic rocks of the green shale and amphibolite facial zonalities were formed in the Earth's crust during the metamorphism of the basic rocks. In addition, the ecologites are encountered here primarily in the localized tectonic zones of increased pressure. The crust eclogites differ from the mantle ecolgites in terms of a number of petrochemical features. In particular the mineral composition of the former includes garnet-almandine and in the case of the second, up to 50% garnet-pyrope. They are also characterized by dissimilar electrical properties at different thermodynamic conditions. The electrical conductivity of the crust

eclogites at high temperatures and pressures was investigated primarily by using rocks from the Kokchetava basin (Kazakhstan) and the samles from the Ural mountains. Within this basin in Kazakhstan, one observes deep-lying rocks of the young epiherschian formations. These are primarily single type formations of eclogites which are found among the muscovite-garnet gneiss, and other rocks. Up to the present time the question as to the origin of Kokchetava eclogites has not been unanimously resolved [112-114]. The most probable is the point of view according to which, eclogites were formed within the gabbro-diabase structures, during metamorphism of the precipitative, volcano-originated geocline series, at the high temperature of the amphibolite facial formations at elevated pressure [112]. In investigating the electrical conductivity of the crust eclogites in Kazakhstan and of the mantle eclogites, at high temperatures, it has been established that these two groups of rocks differ distinctly in terms of this parameter (Figure 39a). However, the crust eclogites of the South Ural mountains, in terms of their electrical conductivity, occupy an intermediate position, and their upper and lower values are overlapping on one hand, with the mantle eclogites, and on the other hand with the crust eclogites.

/118

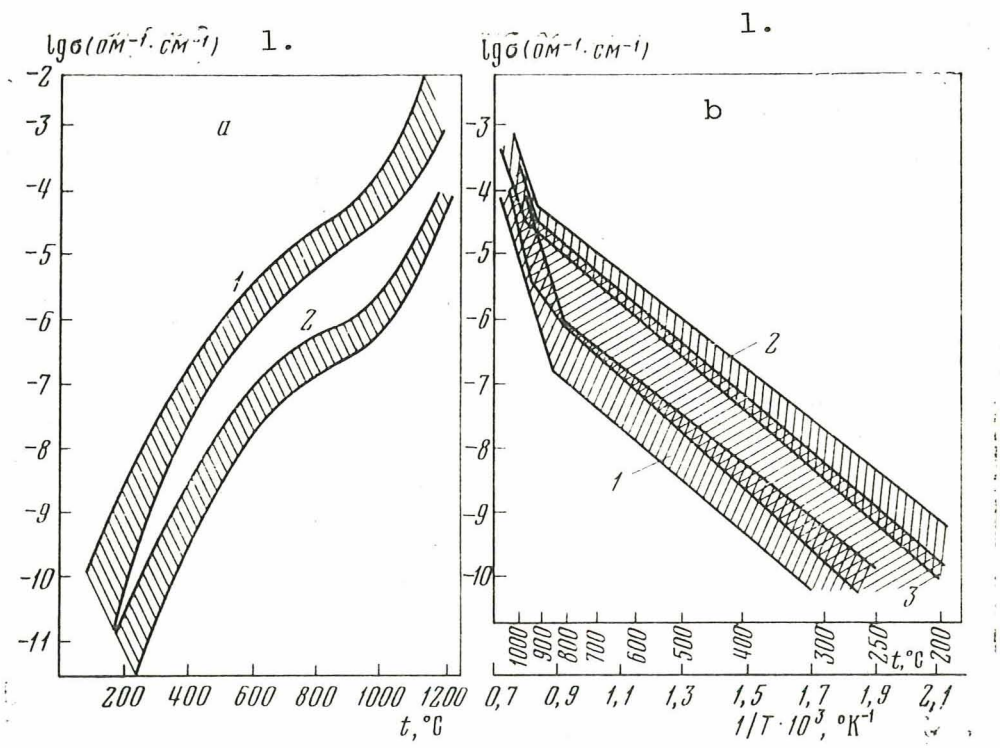

Figure 39. Areas of dependent relationship between the electrical conductivities and temperature.
a - crust eclogites in Kazakhstan (1) and mantle eclogites from kimberlites (2); b - mantle eclogites (1), eclogites from the Ural mountains (2) and eclogites from Kazakhstan (3).

Key: 1. $ohm^{-1} \cdot cm^{-1}$

This is explained primarily by the mineralogical composition and by the degree of metamorphism. As one can see in Figure 39b, these regions, as compared to the regions for other types of rocks, are somewhat narrower and are well maintained across the whole temperature range. In addition, on the basis of this drawing, one can come to the conclusion that the electrical conductivity of the Kazakhstan crust eclogites, as compared to the mantle eclogites, is higher by two orders of magnitude. The activation energy in the majority of the crust eclogites in the temperature range of 900-1200°C, as one can see in Table 20, is within the range of 2.1-2.4 eV, and in the case of the mantle, E_0=3.0-3.4 eV. As it appears, this data has a relationship to the thermodynamic conditions of the eclogite formation. As it appears, the obtained experimental E_0 may be used as an auxiliary criterion in determining the thermodynamic parameters, in the presence of which the specific rocks were formed. The Kazakhstan crust eclogites, in terms of their electrical conductivity, are quite similar to continental basalts (Appendix 12). The range is partially overlapping, but on the average, the σ in the case of eclogites is somewhat lower than in the case of basalts. In basalts, the E_0 values are within the range 1.6-2.0 eV, in other words, it is lower than in the case of eclogites. Probably this is not accidental, since the eclogites were formed at higher pressures and temperatures.

The electrical parameters of mantle eclogites are presented /119
in Appendix 6. It should be noted that the behavior of lg σ=f(1/T) in some rocks which have a special mineralogical composition and the conditions of formation, would not fit within the range of any specific region, and therefore they should be considered separately. Such rock within the Kokchetava mound in Kazakhstan is the pyrope serpentinite KKK 674. This is an extremely rare rock which has no mineralogical analogues and which is similar only to the deep-lying derivatives of the kimberlite tunnel formations. The sample which was studied was obtained from a drilled hole at the depth of 134 m, and had the following mineralogical composition (in %): pyrope - 60, titanium-olivine - /120
25, spinel - 2-3, serpentine - 10, ore mineral - 1-2. The pyrope in this rock is, according to I. A. Efimov, of the following composition (in %): pyrope - 59.8, almandine - 24.1, grossular - 7-8, and andradite - 8.3. The serpentine is evolving here within the separate zones of the rock. Sometimes it is observed that it primarily replaces augite and on rare occasions - titanium-olivine. Within the same zone, one observes the development of spinelite-tremolite scales. The formation of this rock is associated, by A. I. Efimov, with the gravitational differentiation within the magmatic source which occurred within the contact zone between the granite foundation and the mantle [113]. The majority of garnet-pyrope which is found in the mineral composition of this rock, the high levels of magnesium and the presence of Cr_2O_3 as an impurity (Table 21) have

TABLE 20. ELECTRICAL PARAMETERS σ, E_0 AND σ_0 OF THE KAZAKHSTAN CRUST ECLOGITES

/119

Rock	Temperature range t, °C	σ ($ohm^{-1} \cdot cm^{-1}$) at the beginning and at the end of the interval	E_0, eV	lg σ_0, $ohm^{-1} \cdot cm^{-1}$
I Small grain eclogite KKK 676	150—150	$9 \cdot 10^{-11}$	0,6	$7 \cdot 10^{-2}$
	950—1150	$7 \cdot 10^{-5}$	2,28	$5 \cdot 10^{13}$
		$4 \cdot 10^{-2}$		
II. Large grain eclogite KTS 672	150—800	$6 \cdot 10^{-11}$	0,62	10^{-1}
	800—950	$4 \cdot 10^{-5}$	Anomalous region	
	950—1150	$9 \cdot 10^{-6}$		
		$9 \cdot 10^{-4}$	4,2	10^{15}
III. Chianti eclogite AMB 672	150—1000	$2 \cdot 10^{-12}$	0,76	10^{-1}
	1000—1150	$5 \cdot 10^{-5}$	2,18	$5 \cdot 10^{-14}$
		$5 \cdot 10^{-4}$		
IV. AMB 6613	150—700	$3 \cdot 10^{-11}$	0,64	$7 \cdot 10^{-2}$
	700—800	$6 \cdot 10^{-6}$	1,55	$6 \cdot 10^{4}$
	800—1000	$6 \cdot 10^{-5}$	0,38	$8 \cdot 10^{-3}$
	1000—1150	$9 \cdot 10^{-5}$	2,4	$8 \cdot 10^{8}$
		$2 \cdot 10^{-3}$		
V. Pyrope serpentinite KKK 674	200—900	$1 \cdot 10^{-11}$	0,76	10^{-1}
	900—1100	$7 \cdot 10^{-6}$	2,18	$2 \cdot 10^{6}$
		$5 \cdot 10^{-4}$		
VI. Garnet ampibolite AMB 674	150—950	$1 \cdot 10^{-11}$	0,72	1,0
	950—1200	$4 \cdot 10^{-4}$	2,4	$8 \cdot 10^{8}$
		$2 \cdot 10^{-2}$		
VII. Garnet druzite KTE 671	150—700	$1 \cdot 10^{-11}$	0,7	0,2
	700—900	$7 \cdot 10^{-6}$	Anomalous region	
	900—1150	$2 \cdot 10^{-6}$	3,6	10^{14}
		$8 \cdot 10^{-3}$		

[Commas in tabulated material are equivalent to decimal points.]

defined its low σ in the region of low and high temperatures (see Appendix 12). The electrical conductivity in the range of 850-1200°C corresponds to the pyrope eclogites from kimberlites, but the activation energy (1.72 eV) is considerably lower than in the case of the latter (see Appendix 7). This is explained by the fact that this rock has been altered by the serpentinization which decreases E_0. Somewhat higher σ in the temperature range of 150-850°C, than in the case of the pyrope eclogites from kimberlites, was caused by the conducting titanium-olivine and primarily - by serpentinization. However, the serpentinized eclogite from Czechoslovakia is characterized by the electrical parameters which are typical for the crust eclogites (see Appendix 12).

One should discuss at this time also the eclogite 9152, which has the highest electrical conductivity of all the samples which were surveyed. The relatively high conducting properties of this eclogite are due to the amounts of omphacite (30%) and of hornblende (15%). The first mineral, due to the quantities of Fe and Na cations and also due to the presence of the hydroxal group $(OH)^{1-}$ must have high conducting properties and the hornblende, according to our experimental data, displays a sufficiently high conductivity in the structurally-sensitive region.

The electrical conductivity of eclogites from the Ural mountains, according to the joint studies with S. M Kireenkova, is characterized by somewhat lower values than the electrical conductivity of the Kazakhstan eclogites. The E_0 at 200-1100°C in them is the same as in the case of the Kazakhstan eclogites (see Appendix 12). It should be noted that more often than not, in the case of the rocks which, at 850-900°C, display anomalous σ, one observes in the region of the intrinsic electrical conductivity the high E_0 (3.0-4.0 eV). As it appears, they are defined by the polymorphous conversions in the pyroxenes or in the amphiboles and also by the partial melting of the rocks.

The Ural mountain eclogites, in terms of their electrical properties, are primarily subdivided into three groups, which correspond to three stages of metamorphism: the progressive metamorphism within the eclogite facial structure, the "deep underground diaphtorite", which is the facial structure of glaucophene slates, and the diaphtorites which are the facial structures of green shales. Within the first group are the rocks which are represented by the rock-forming minerals garnet-almandine and pyroxene, which together comprise 95%. The muscovite, quartz, ruthenium and sphene are found as the secondary minerals. The second group consists of rocks which were affected by the glaucophenization and muscovitization. In conjunction with this, one finds, in addition to the garnet (50-60%), some amphiboles which are almost completely replaced by the pyroxene. The eclogites of /121

the third group are affected by the green rock alterations and contain chlorite- 20-40% and about 50% of garnet. The rocks of this group were not subjected to the second stage of metamorphosis. The eclogites of the first group have lower electrical conductivity than the eclogites of the second group which includes the amphibole (see Appendix 12). They are characterized by three regions of lg $\sigma=f(1/T)$, differing by the charge carrier type, and have E_0 of 0.8-0.9 eV at up to 600-750°C, 1.0-1.4 eV at 600-900° and sometimes at 1000°C, respectively. At t>1000°C, E_0 reaches an anomalously high level of 3.0 eV, and more. From the data as presented, and also keeping in mind the data with respect to the minerals (see Chapter 1) one may assume that the character of lg $\sigma=f(1/T)$ is defined by the quantitative relationship between the diopside and garnet minerals. The low temperature region corresponds to the diopside component and the presence of the inflection point at 900-1000°C is due to the processes which take place within the garnet.

TABLE 21. CHEMICAL COMPOSITION OF THE ROCKS AND MINERALS WITHIN THE GRANULITE-BASITE GROUP FROM KAZAKHSTAN
(see Table 20)

Oxides	I	II	III	IV	V	VI	VII
SiO_2	39,86	48,20	41,25	42,00	49,74	55,74	47,28
TiO_2	1,83	1,83	0,74	0,46	1,38	1,58	1,45
Al_2O_3	18,91	12,80	20,54	21,22	15,53	12,70	16,23
Fe_2O_3	2,04	1,86	2,45	2,94	2,09	4,15	2,72
FeO	11,65	14,33	15,29	11,21	7,83	10,5	11,25
MnO	0,11	0,22	0,41	0,09	0,07	0,21	0,16
MgO	20,72	5,36	12,74	15,63	7,80	4,20	6,86
CaO	4,69	11,40	5,92	5,46	9,94	5,67	10,63
Na_2O	0,28	1,85	0,21	0,25	1,95	2,61	1,92
K_2O	0,32	0,37	0,31	0,31	1,10	1,22	0,67
H_2O^+	0,97	0,40	—	—	—	0,11	0,40
H_2O^-	0,21	0,70	0,12	0,22	0,20	0,88	0,18
P_2O_5	0,13	0,13	0,14	0,07	0,09	0,17	0,15

[Commas in tabulated material are equivalent to decimal points.]

The second group of eclogites is characterized by high σ at high temperatures and by high E_0 (3.0 eV). In addition, in conjunction with the presence of amphibole, one notices the new temperature regions, as well as the anomalous changes in electrical conductivity. It is possible that the amphibole plays a major role in defining the high σ within this group of rocks. It should be noted that the eclogites which contain muscovite have somewhat lower electrical conductivity than those which contain none of it (see Appendix 12). /122

The electrical conductivity in the eclogites of the third group is frequently overlapping with the values of σ in the preceding groups. However, one should note that the chlorite, which within this group of rocks reaches levels of up to 40%, is also causing the anomaly at high temperatures, in conjunction with the evolution of the hydroxal group $(OH)^{1-}$.

It follows on the basis of all this data that the degree of the effect of metamorphism on the electrical parameters of eclogites is defined by the character of the change in mineralogical composition. The appearance of muscovite during metamorphism has practically no affect on σ, while the amphibolization as a result of which the omphacite, hornblende and other minerals are being formed, facilitates the increased electrical conductivity.

9. Magmatic Alkaline Sodium and Potassium Rocks

The magmatic alkaline sodium and potassium rocks are found extensively within the basic rock formations. They attract more and more attention because of the specificity of the conditions of their formation and the useful minerals which are found in them. The crystallization of the alkaline rocks depends on the volatile components, and therefore, different varieties may be formed at different thermodynamic conditions at the depth between 5 and 45 km and at the temperatures on the order of 600°C [116, 117]. In terms of the mineral composition, the sodium rocks contain large quantities of nephelite which contains aluminum, there are also alkaline feldspar, eugirite, eudialyte, sphene, lamprophillite, apatite, lepidomelane, titanomagnetite and other materials. In the case of potassium rocks, the predominant minerals are the pseudoleucite, the potassium feldspar, pyroxene and also sodalite, amphibole, muscovite, carbonite and in the shape of isolated grains - nephelite. We have investigated the electrical conductivity of the sodium rocks in Khibin and Lovozero land masses on the Cola peninsula and also the ultrapotassium formations of pseudoleucites which were first discovered in Synnyra pluton of the northern Baikal region [118].

We can see in Table 22 and in Figure 40 that the electrical conductivity of the alkaline rocks is closely related to the mineral composition. With the increase in the rocks of feldspar and nephelite, the electrical conductivity across the whole temperature range will decrease. This is due to the fact that the /124
mineral nephelite, as one can see in Figure 40 (curves 1 and 2) has considerably lower electrical conductivity than the rocks in which it is incorporated.

The eudialyte and eugirite, just like the rock in which these minerals are in large quantities, will have, on the other hand, the highest conductivity (curves 5 and 6). In the case of these rocks and of eugirite at high temperatures, one observes frequently

TABLE 22. AVERAGE VALUES OF ELECTRICAL PARAMETERS σ, E_0 (THEIR LIMITING VALUES) AND σ_0 of ALKALINE ROCKS

Rocks	σ (ohm^{-1}.cm^{-1}) at t, °C							Temperature range t, °C	E_0, eV	$\lg \sigma_0$, (ohm^{-1}.cm^{-1})
	200	400	600	700	900	1000	1100			
Alkaline rocks Khibin formation	$4 \cdot 10^{-9}$	10^{-7}	10^{-6}	$1{,}8 \cdot 10^{-6}$	$1{,}8 \cdot 10^{-4}$	$9 \cdot 10^{-4}$	$4 \cdot 10^{-3}$	50—700	0,48 (0,4—0,63)	—4,7
	$4 \cdot 10^{-11}$	$3{,}2 \cdot 10^{-8}$	$1{,}2 \cdot 10^{-7}$	$1 \cdot 10^{-7}$	$1 \cdot 10^{-6}$	$3 \cdot 10^{-5}$	$2{,}2 \cdot 10^{-3}$			
	$5 \cdot 10^{-8}$	$9{,}3 \cdot 10^{-7}$	$9{,}4 \cdot 10^{-6}$	$2 \cdot 10^{-5}$	$1 \cdot 10^{-3}$	$5 \cdot 10^{-3}$	$2{,}4 \cdot 10^{-2}$	700—1200	2,0 (1,1—2,9)	5,0
Lovozero formation	$6{,}4 \cdot 10^{-8}$	$1{,}2 \cdot 10^{-6}$	$9{,}6 \cdot 10^{-6}$	$1{,}8 \cdot 10^{-5}$	$2{,}6 \cdot 10^{-4}$	$1{,}2 \cdot 10^{-3}$	$5{,}2 \cdot 10^{-3}$	50—800	0,45 (0,4—0,7)	—3,5
	$6 \cdot 10^{-9}$	$1{,}2 \cdot 10^{-7}$	$1{,}2 \cdot 10^{-6}$	$3 \cdot 10^{-6}$	$1 \cdot 10^{-5}$	$1 \cdot 10^{-4}$	$4{,}2 \cdot 10^{-3}$			
	$3 \cdot 10^{-7}$	$9{,}6 \cdot 10^{-6}$	$4{,}8 \cdot 10^{-5}$	$9 \cdot 10^{-5}$	$4 \cdot 10^{-3}$	$1 \cdot 10^{-2}$	$8{,}9 \cdot 10^{-2}$	800—1200	2,1 (1,3—3,1)	5,5
Potassium rocks Synnyra formation	10^{-10}	$1{,}6 \cdot 10^{-8}$	$3 \cdot 10^{-7}$	10^{-6}	$8 \cdot 10^{-6}$	$4 \cdot 10^{-5}$	10^{-3}	100—850	0,74 (0,66—0,86)	—3,7
	$6 \cdot 10^{-12}$	$3 \cdot 10^{-9}$	$1{,}6 \cdot 10^{-7}$	$6 \cdot 10^{-7}$	$4 \cdot 10^{-6}$	$2 \cdot 10^{-5}$	$6 \cdot 10^{-4}$			
	$3 \cdot 10^{-10}$	$3 \cdot 10^{-8}$	10^{-6}	$2{,}6 \cdot 10^{-6}$	$1{,}6 \cdot 10^{-5}$	10^{-4}	$1{,}2 \cdot 10^{-3}$	850—1100	2,2 (1,1—2,8)	—4,0

[Note: Commas in tabulated material are equivalent to decimal points.]

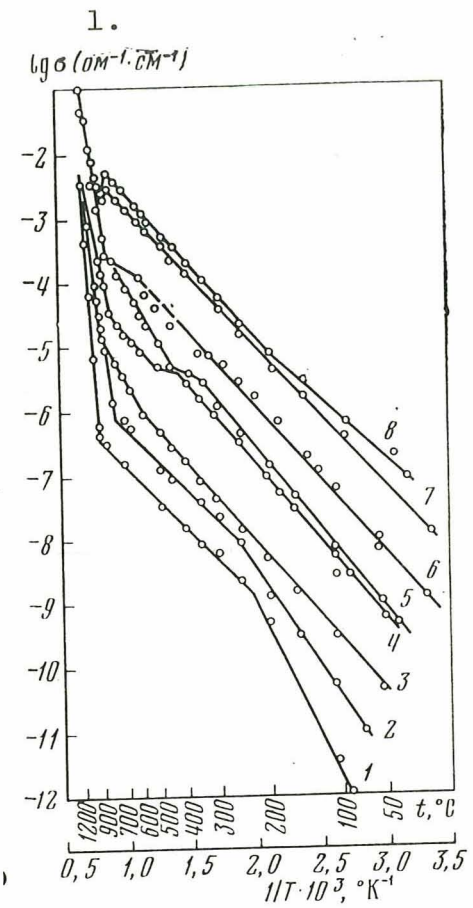

Figure 40. Electrical conductivity of the alkaline rocks and minerals as a function of temperature.

1 - nephelite ⊥ to the planes of cleavage; 2 - nephelite || to the planes of cleavage; 3 - foyalite 1441; 4 - urtite 1475; 5 - eudialyte; 6-8 - eugirite during three repeat tests.

Key: 1. $ohm^{-1} \cdot cm^{-1}$

the anomalous change of electrical conductivity with the increase of temperature (Figure 40, curves 7 and 8).

After 3 measurements of σ in eugirite at the same temperatures and identical conditions without disruption of the electrical contacts, the figures obtained in our test assembly agreed in terms of σ values, during the second and third measurements.

At high temperatures in the region of intrinsic conductivity, regardless of the number of repeat tests, the lines of $\lg \sigma_0 = f(1/T)$ will, as a rule, coincide.

The high values of $E_0 =$ $=2.3-6.2$ eV in the temperature range of 700-1200°C (Table 22 and Appendix 13) were obtained for the alkaline rocks and minerals. In the case of all studied alkaline rocks, with the exception of nephelite, one observes at these temperatures the traces of melting, causing the rapid increase of electrical conductivity and high E_0. We have constructed a curve of intrinsic conductivity for these alkaline rocks and minerals in terms of σ at the inflection points of $\lg \sigma = f(1/T)$ curves. Figure 41 shows that all these points are within a narrow region which corresponds to the intrinsic conductivity. The computed activation energies, on the basis of this curve, turned out to be, just like in the case of the other rocks, considerably lower than the values obtained for some alkaline rocks and minerals and are within the range of 2.3-2.5 eV. Therefore, the computed activation energies and the calculated pre-exponential coefficients based on the curves

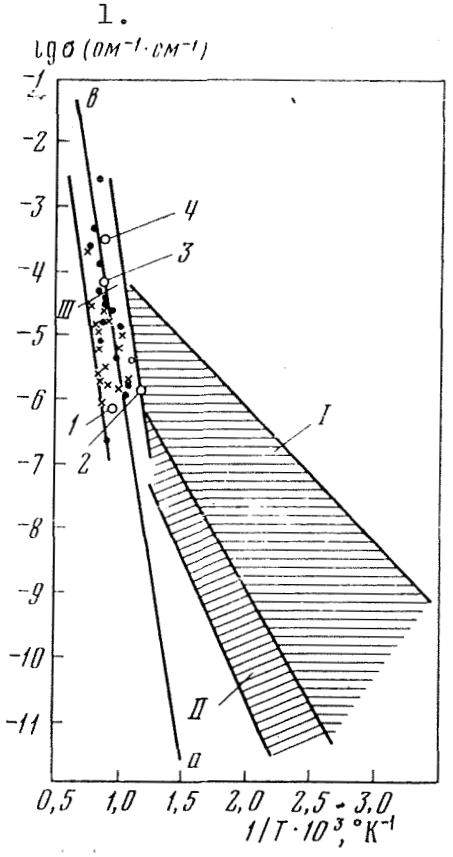

Figure 41. Electrical conductivity of the basic sodium rocks and minerals as a function of inversed temperature.

I - area of impurity-related conductivity of sodium rocks; II - of potassium rocks from Synnyra; III - region of intrinsic conductivity, constructed on the basis of the points of inflection in the curve of lg σ=f(1/T). The circles are the inflection points of electrical conductivity in the rocks and in the minerals: 1 - nephelite, 2 - sphene, 3 - potassium feldspar; 4 - eudialyte, a and b are the averaged-out curves of the intrinsic electrical conductivity.

Key: 1. $ohm^{-1} \cdot cm^{-1}$

constructed in two different ways, namely, using the averaged-out curve (Figure 42) and using the curve obtained by the method of the point of inflection (see Figure 41) turn out to be quite similar. Therefore, this data characterizes the intrinsic conductivity for this type of rocks and minerals, with the exception of such alkaline rocks and minerals in which one observes the melt-out of the material or in which the polymorphous conversions take place (this is the case of nephelite).

In analyzing the comprehensive curves, shown in Figure 42, one can see that in the region of impurity-related conductivity, the Lovozero rocks are of higher mean electrical conductivity and the electrical conductivity point of inflection is observed at higher temperatures. In the case of Lovozero alkaline rocks, this inflection point occurs at 800-825°C, and in the case of Khibin rocks - at 700°C. In the high temperature region, both averaged-curves of electrical conductivity coincide (see Figure 42). Such behavior of electrical conductivity in the alkaline rocks of Lovozero basin, as will be shown below, is due to the high quantities of Na and iron oxides which are found in Lovozero rocks, and also to the presence of some quantities of rare earth metals. In the case of potassium rocks, the point of inflection in lg σ as a function of 1/T is observed /126

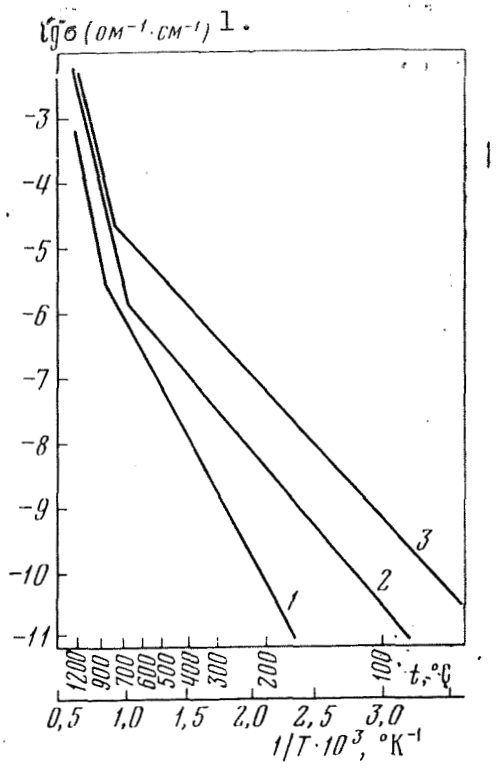

Figure 42. Averaged-out electrical conductivity in the alkaline rocks as a function of temperature.

1 - for rocks from Synnyra; 2 - Khibin; 3 - Lovozero

Key: 1. $ohm^{-1} \cdot cm^{-1}$

at 850-900°C. These rocks, when compared to the sodium rocks, are characterized by the lowest electrical conductivity and high activation energy in the region of impurity-related conductivity. In the region of intrinsic conductivity, the difference between σ, σ_0 and E_0 parameters are insignificant (see Figure 42). As we can see, on the basis of the comprehensive curves (see Figure 42) which show the electrical conductivity as a function of temperature, it becomes clear that the alkaline rocks of these formations are clearly differentiated in terms of σ quantities. The Lovozero rocks are displaying the highest electrical conductivity. The potassium rocks from Synnyra basin have the electrical conductivity which is lower by two orders of magnitude. However, the levels of σ in the sodium rocks of Khibin pluton, within a broad temperature range, occupies an intermediate position (see Table 22). This differentiation, in terms of the electrical conductivity of the alkaline rocks for the above-mentioned formations is defined by the specifics of chemical composition of these rocks (Table 23) and primarily, by the amounts of oxides of Na, K and Fe [118-121]. The highly conducting Lovozero rocks are characterized by the maximum amounts of sodium and iron oxides and in the low conducting rocks of Synnyra basin, one finds the prevailing potassium oxides which contain considerably smaller quantities of sodium and iron. The electrical conductivity as a function of temperature depends quite clearly on the (Na) coefficient of internal adhesion in $Na_2O/Al_2O_3-K_2O$, introduced by /127 B. I. Zlobin [122]. The formula to determine the coefficient of internal adhesion makes it possible to calculate the relationship between the total sum of alkalis and aluminum, and the ratio of sodium and potassium. The low coefficient in Synnyra rocks (Figure 43) corresponds to the low σ, and the high coefficient corresponds to the highly conducting sodium rocks from Lovozero pluton. The

points corresponding to Khibin rocks occupy the intermediate position on the curve for $\sigma=f(Na)$. In addition, the increased electrical conductivity of Lovozero alkaline rocks corresponds to high quantities of iron oxide present.

Figure 44 shows the electrical conductivity of alkaline rocks as a function of the total iron oxides. One can see that the potassium rocks which contain the least quantities of iron oxides will have the lowest electrical conductivity.

TABLE 23. AVERAGE CHEMICAL COMPOSITION OF THE MAGMATIC SODIUM ROCKS FROM KOLA PENINSULA AND POTASSIUM ROCKS FROM SYNNYRA FORMATIONS

Oxides	Quantities of oxides (in %) within the formations			Oxides	Quantities of oxides (in %) within the formations		
	Synnyra	Khibin	Lovozero		Synnyra	Khibin	Lovozero
SiO_2	55,70	53,23	53,62	Na_2O	3,00	9,32	10,97
TiO_2	0,40	1,04	1,12	K_2O	12,70	5,99	5,86
ZrO_2	—	0,10	0,48	H_2O^+	—	0,68	0,99
Al_2O_3	20,70	21,42	17,39	H_2O^-	—	0,22	0,14
Fe_2O_3	1,50	2,99	4,93	P_2O_5	0,18	0,24	0,20
FeO	1,50	1,60	1,01	SO_2	—	0,015	0,10
MnO	0,03	0,20	0,34	Cl	—	0,16	0,16
MgO	0,80	0,67	0,98	F	—	0,11	0,14
CaO	1,60	—	—	*Na*	0,9	1,02	1,40
SrO	—	1,69	1,22	Na/K	0,23	1,39	1,67

[Commas in tabulated material are equivalent to decimal points.]

The electrical conductivity as a function of chemical composition of the alkaline rocks is also established within the framework of each formation. Figure 45 shows the electrical conductivities as a function of temperature for potassium rocks from Synnyra formation with different amounts of Na, K and Fe, in which the curve 1 characterizes $\sigma=f(1/T)$ for the pseudoleucite syenite (sample 8995), 2 is the curve for pyroxene-horblende syenite (pulaskite sample 9007) and curve 3 - for the pyroxene, biotite shonkinite (sample 8822). One can see from Table 24, and in Figure 45, that the electrical conductivity decreases with the increase of quantities of K and decrease of Fe and vice versa. /128

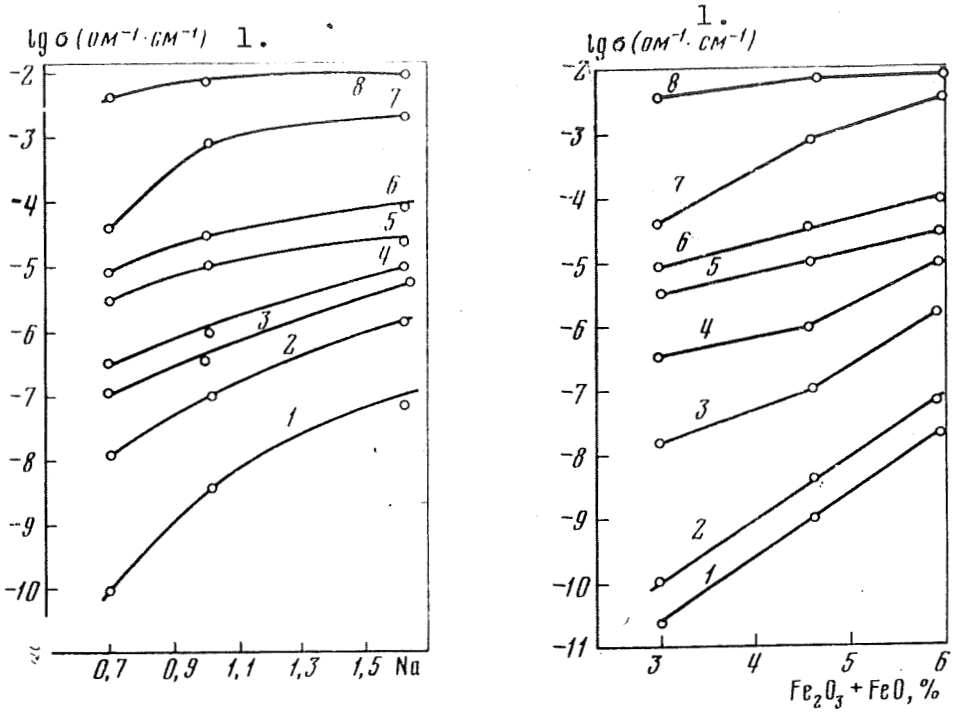

Figure 43. Electrical conductivity of the alkaline rocks as a function of the coefficient of internal adhesion for (Na) at different temperatures.

At t,°C: 1-8 - 200, 400, 500, 600, 800, 900, 1000, 1200, respectively.

Figure 44. Electrical condictivity of the alkaline rocks from Synnyra, Khibin and Lovozero as a function of the total iron oxides at different temperatures.

At t, °C: 1-8 - 150, 200, 400, 600, 700, 900, 1000, 1200, respectively.

Key: 1. $ohm^{-1} \cdot cm^{-1}$

10. Metamorphic Rocks

The metamorphic rocks are igneous or stratified rocks which were subjected to structural, textural and mineralogical changes, being affected by pressure, temperature and by stress [123]. In the course of metamorphosis, one observes the recrystallization of the primary minerals within the rock. In the case of some minerals, as for example in the case of quartz, feldspar and calcite, this is accompanied by a simple increase in the grain size, and by the change in orientation. Some rocks which underwent metamorphosis are recrystallized and new minerals are being formed without a

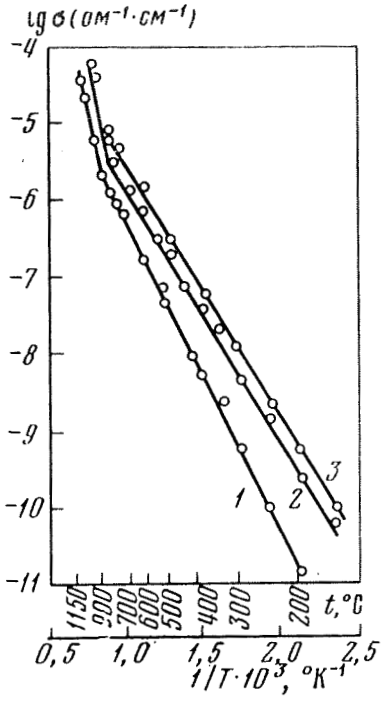

Figure 45. Electrical conductivity of Synnyra potassium rocks, containing different amounts of alkali and iron as a function of temperature.

1 - pseudoleucite syenite 8895; 2 - pyroxene syenite 9007; 3 - pyroxene shonkenite 8822.

Key: 1. $ohm^{-1} \cdot cm^{-1}$

TABLE 24. ELECTRICAL CONDUCTIVITY AND CHEMICAL COMPOSITION OF ALKALINE ROCKS

Rock	oxides, %					lg σ, $ohm^{-1} \cdot cm^{-1}$		
	K_2O	Na_2O	Fe_2O_3	FeO	MgO	200° C	500° C	700° C
Pseudoleucite syenite (sam. 8995)	15,22	1,71	0,93	1,46	0,76	$2 \cdot 10^{-11}$	$7 \cdot 10^{-8}$	$8 \cdot 10^{-7}$
Pyroxene-hornblende syenite (sam. 9007)	7,02	6,31	2,98	2,22	1,55	$3 \cdot 10^{-10}$	$3 \cdot 10^{-7}$	$2 \cdot 10^{-6}$
Pyroxene-biotite shonkinite (sam. 8822)	7,50	1,70	4,96	5,52	5,09	$8 \cdot 10^{-10}$	$5 \cdot 10^{-7}$	$4 \cdot 10^{-6}$

[Commas in tabulated material are equivalent to decimal points.]

general change of composition. However, in the majority of the rocks which underwent metamorphosis, one observes either the addition or removal of some material, in other words, the so-called matasomatosis takes place. The major factors which define the nature of metamorphism is the composition, temperature, hydrostatic pressure and stress. The increase of temperature /129
facilitates the crystallization of minerals with less dense packing, while pressure results in the formation of minerals of greater density. The stress affects the structure and texture of the rocks which underwent metamorphosis [123].

Let us consider in this section only the electrical conductivity of gneiss, amphibolites and shales. Such metamorphic rocks as the crust eclogites and serpentinites were described earlier, while we have considered the crust eclogites and the effect of serpentinization on the electrical properties of rocks. Gneisses are represented by the samples selected from the Caucasus region, from the amphibolite-gneiss Oboyansk late archeozoic region and from the Gor'kiy region. All of them differ in terms of the geological features and minerals which are found in the rocks. The comparison of the measured results, presented in Appendix 14, indicate the following.

It was possible to substantiate a significant increase of electrical conductivity in the rocks as a result of cataclasis by using the gneiss 2792 (Gor'kiy formation) and gneiss 2575 (Oboyansk formation). It is interesting that the increase in electrical conductivity of the rock is not accompanied by changes in the activation energy E_0 and σ_0 which are found to be in the range typical for this group of rocks. The four other gneisses differ by somewhat lower electrical conductivity which is due to a considerable degree to large quantities of quartz found in them (from 30 to 50%).

However, one should point out that the garnet gneiss 2578, in spite of rather high amounts of quartz (40-50%) at t=200-500°C, possesses electrical conductivity which is ten times greater than in the other gneisses, with analogous amounts of quartz (2565 and 2581). The increased electrical conductivity of gneiss 2578 in the low temperature range is apparently associated with the presence in it of garnet-almandine, with the correlated higher quantities of iron oxide.

The temperature relationship for all rocks is described by a broken line, consisting of two or three segments, in other words, one observes either two or three temperature ranges which are characterized by different electrical parameters. In terms of the values of these parameters in the low temperature range, in which the current carriers are the impurity ions, the

gneisses should be subdivided into two groups. The first group includes the gneiss 2578 and 2575, and the second group - 2792, 2575, 2796 and 2581.

In the gneisses 2578 and 2565, the first replacement of the current carriers occurs at a relatively low temperature, namely at 300°C. Within this region, one observes low activation energy (E_0=0.20-0.30). The reason for this is the presence of Fe ions, which account for the decreased activation energy, down to 0.1 eV. /130
As it appears, the presence of iron ions had a certain effect on the mechanism of electrical conductivity also in the subsequent temperature range, which extends up to 900°, where the activation energy and lg σ_0 for the rocks of the first group is lower than for the second group of rocks, namely 0.72-0.74 eV, instead of 0.84-1.0 eV.

For the two gneisses with high electrical conductivity, the disruption of the linear relationship between lg σ and 1/T is expressed in the irregular decrease of electrical conductivity as a function of the temperature increase in the range of 500-900°C. It is assumed that this anomaly is associated with the high amounts of micas and the resulting evolution of water. On the other hand, the anomaly of electrical conductivity and lower activation energy in gneiss 865 is due to the presence of chlorite.

The high temperature break of the curve in lg σ=5(1/T) relationship occurs almost always at the same temperature in the case of all gneisses, namely at about 900°C. The presence of such a break, and consequently the change in the activation energy, is probably related to the polymorphous transition in the potassium feldspar at t=900°C. The temperature range above 900°C for all rocks is characterized by higher activation energies which are in the range of 2.5-3.2 eV, and in addition, just like in the case of garnets, the majority of rocks have E_0=3.0 eV.

The amphibolites belong to the regionally widely found metamorphic rocks in the Earth's crust. They are formed at somewhat higher pressures and temperatures than gneiss. According to the experimental data, the pressure of 10-15 kbar, and t=800-1100°C, are the maximum for the existence of amphibolites. The amphibolites are the result of metamorphism in the limestone and dolomite stratified formations and the amphibolization of the basic lava and basic intrusive rocks. They differ only slightly from each other in terms of their chemical composition, but can be differentiated on the basis of petrographic features. The difference in structure and in mineral composition of amphibolites of different genesis must be reflected also in their electrical parameters.

TABLE 25. ELECTRICAL CONDUCTIVITY OF SHALES

Shale, No. of the sample	Electrical conductivity ($ohm^{-1} \cdot cm^{-1}$) at t, °C								
	200	300	400	500	600	700	800	900	1000
Chlorite-containing 1145	$5,9 \cdot 10^{-9}$	$7,6 \cdot 10^{-8}$	$4,9 \cdot 10^{-7}$	$1,9 \cdot 10^{-6}$	$9,8 \cdot 10^{-6}$	$3,1 \cdot 10^{-5}$	$7,6 \cdot 10^{-5}$	$1,6 \cdot 10^{-4}$	$3,7 \cdot 10^{-4}$
Magmatized (10% magnetite) 2563	$1,7 \cdot 10^{-5}$	$2,5 \cdot 10^{-5}$	$5,0 \cdot 10^{-5}$	$1,2 \cdot 10^{-4}$	$5,0 \cdot 10^{-3}$	$2,2 \cdot 10^{-2}$	$2,9 \cdot 10^{-2}$	$1,2 \cdot 10^{-2}$	$5,0 \cdot 10^{-2}$
Graphitized 2599	$5,5 \cdot 10^{-9}$	$5,5 \cdot 10^{-8}$	$6,9 \cdot 10^{-7}$	$2,5 \cdot 10^{-6}$	$1,2 \cdot 10^{-5}$	$6,5 \cdot 10^{-5}$	$1,2 \cdot 10^{-4}$	$2,7 \cdot 10^{-4}$	$6,0 \cdot 10^{-4}$
Garnet-biotite 59-12	$7,6 \cdot 10^{-12}$	$1,1 \cdot 10^{-10}$	$2,5 \cdot 10^{-9}$	$2,2 \cdot 10^{-8}$	$1,3 \cdot 10^{-7}$	$4,0 \cdot 10^{-6}$	$1,9 \cdot 10^{-5}$	$6,2 \cdot 10^{-5}$	$3,2 \cdot 10^{-4}$
Diostene-mica-quartz 5836	$2,7 \cdot 10^{-11}$	$6,2 \cdot 10^{-10}$	$1,0 \cdot 10^{-9}$	$8,3 \cdot 10^{-8}$	$9,8 \cdot 10^{-7}$	$4,7 \cdot 10^{-6}$	$1,4 \cdot 10^{-5}$	$2,2 \cdot 10^{-5}$	—

[Commas in tabulated material are equivalent to decimal points.]

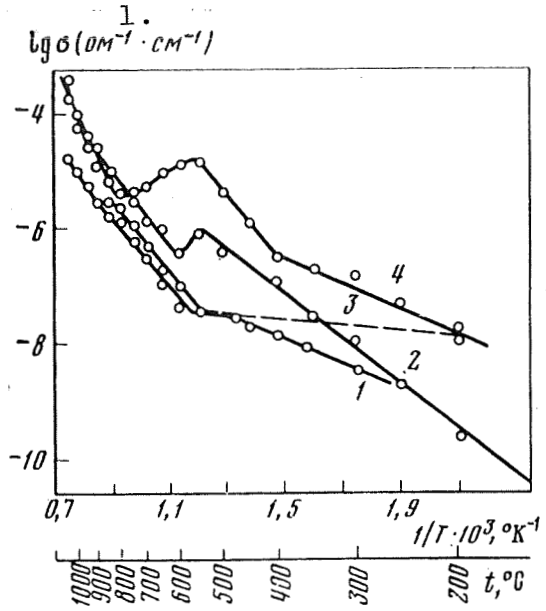

Figure 46. Electrical conductivity as a function of temperature for the rocks

1 - amphibolites; 2,4 - ortho-amphibolites; 3 - chlorite-amphibolite 2490.

Key: 1. $ohm^{-1} \cdot cm^{-1}$

This is a problem which is to be investigated further. The study of the electrical properties of the amphibolite rocks is rather important, since these formations include a number of the most likely representatives of the rocks of which the high conductivity layer is composed, and this layer is found in the intermediate part of the Earth's crust in some regions. /132

The data obtained by us with respect to $\lg \sigma = f(1/T)$ relationships indicate that this group differs from gneiss, garnet and gabbro by having a considerably higher conductivity and lower activation energies and $\lg \sigma_0$ (see Appendix 13). In addition, all amphibolites, just like the other petrographic formations, contain the minerals of the amphibole group, which indicates the disruption of the linear relationship between $\lg \sigma$ and $1/T$. The curves, shown in Figure 46, indicate that the anomalous behavior of electrical conductivity is displayed at 700-900°C. In conjunction with the fact that the sodium amphiboles (ribecite) possess the greatest electrical conductivity among all silicates, their prevalent role in amphibolites will naturally result in higher conductivity of the rock.

Shales. The investigated shales featured considerable variety of mineral composition, which was reflected in a certain fashion in the electrical properties. The highest electrical conductivity, as can be seen in Table 25, is characterized by the shale 2563, because of considerable quantities of magnetite. The chlorite shale 1145, and to a lesser degree the graphitized 2599 have approximately the same electrical conductivity, although the conducting mineral in the first one is chlorite and in the second one - graphite. The two last shales in Table 25 have rather low electrcial conductivity because of the prevalence in them of such minerals as quartz, mica and garnet.

CHAPTER FOUR. FOUR MAJOR FACTORS WHICH DEFINE THE ELECTRICAL CONDUCTIVITY IN ROCKS

1. Effect of Mineral Composition on the Electrical Parameters of Rocks /133

The experimental material on electrical conductivity of rocks, which we have presented earlier, gives us merely a general concept as to the possible changes in electrical conductivities for the most widely found types of rocks. On the other hand, in addition to the rocks which we have considered, there are a number of other rocks which may form large tracts, intrusions and veins, consequently their electrical parameters are also of great interest. It is therefore of great importance to know the relationship between the electrical parameters of the rocks and of the minerals of which these rocks are composed, taking into account the structure of the rock. Let us first of all consider the possibility of calculating the electrical conductivity in the isotropic rocks at high temperatures, on the basis of σ in the minerals. In considering the relationship of change in electrcial conductivity of the rocks as a function of mineral composition, and the proper selection of the calculation formula, it is necessary first of all to know exactly the structure of the rock. All rocks, depending on the character of the mineral distribution, are divided into two major classes - the isotropic and anisotropic. The isotropic rocks, in turn, may be represented as the matrix systems and the statistical mixtures. In the matrix system, one component discharges the function of inclusion medium, and the second one is represented as the inclusions, isolated from each other. In the isotropic matrix system, the inclusions are in the shape of spheres. Let us consider first of all the possibility of calculating the electrical conductivity in isotropic rocks in the form of both matrix systems, and statistical mixtures at high temperatures, on the basis of electrical conductivity data for the minerals involved, using the examples of the most widely found rocks. In addition, let us simulaneously generalize the experimental results, pertaining to the relationship between the electrical conductivity of the rocks, and the mineral composition. The formulas for matrix systems have been worked with most extensively. It is assumed in this case that the electrical conductivity of the inclusion medium σ is considerably greater than /134
the electrical conductivity of the inclusions themselves σ_1 and σ_2.

For the mixtures, a sufficiently well defined agreement between the experimental data and the calculated data is given by the Lichtenecker formula

$$\lg \sigma = \theta_1 \lg \sigma_1 + \theta_2 \lg \sigma_2. \qquad (4.1)$$

It is also recommended to use the Odelevskiy formula

$$\sigma = B + \sqrt{B^2 + \frac{\sigma_1 \sigma_2}{2}}, \tag{4.2}$$

where

$$B = \frac{(3\theta_1 - 1)\sigma_1 + (3\theta_2 - 1)\sigma_2}{4}.$$

For the matrix systems, the following formulas are known:

Maxwell formula

$$\sigma = \sigma_0 \frac{2\sigma_0 + \sigma_1 - 2\theta_1(\sigma_0 - \sigma_1)}{2\sigma_0 + \sigma_1 + \theta_1(\sigma_0 - \sigma_1)}, \tag{4.3}$$

and Riley formula which has been derived by taking into account the interaction between the inclusions which are in the form of spheres of any size

$$\sigma = \sigma_0 \left(1 - \frac{3\theta_1}{\theta_1 + \frac{2\sigma_0 + \sigma_1}{\sigma_0 - \sigma_1} - 0{,}525 \frac{\sigma_0 - \sigma_1}{4/3\sigma_0 + \sigma_1} \theta_1^{10/3}}\right), \tag{4.4}$$

where θ_1, θ_2 are the volume concentration of the first and second component, σ_1, σ_2, σ_0 are the electrical conductivity of the first, second and inclusion-filling components, respectively. By obtaining this data, describing the electrical conductivity of the rock of a specific mineral composition, as a function of temperature, by using one of the above-mentioned formulas, it becomes possible to calculate the electrical conductivity of the rock for any assigned temperature. For the simplification of calculations, if it is possible, it would be more desirable to consider the rock as a two-component system. For example, the garnet in which the major minerals are quartz, mica and feldspar. At t=100-200°C, the quartz and mica differ only slightly in terms of σ, and therefore they may be assumed to be one component and the feldspar - the other component. The minerals are electrically anisotropic materials, and therefore, one should use the averaged-out electrical conductivities in the above-mentioned formulas (4.1)-(4.4), and these electrical conductivities must be calculated on the basis of the measured data, along the major

crystallographic directions. Let us note that the rocks of garnet type belong to the isotropic statistical systems. The example of isotropic matrix systems are the rocks in which one observes the evolution of the ore conducting mineral along the grain boundaries (these are some of the pyroxenites, peridotites, dunites and serpentinites).

In determining by the above-mentioned method the electrical conductivities of the rocks at different temperatures, it becomes possible, on the basis of calculated data, to construct the $\lg \sigma = f(1/T)$ relationship, and on this basis, to determine the E_0, and /135 $\lg \sigma_0$. The comparison of experimental data with the calculated one makes it possible to elucidate the role of the surface conductivity, of the porosity and of a number of other features which reflect the electrical conductivity in the real rocks, and also to determine on the basis of mineralogical composition, the electrical conductivity of presumed rock formations at the depths of interest. We have considered above one of the possible ways of determining the electrical conductivity of the rock of given composition as a function of temperature. The second method is to establish experimentally the relationship of σ change in the rock as a function of one or two similar (in terms of σ) rock-forming minerals at different temperatures. As has been shown in Figure 22, the rocks of garnet-diorite group have a well-defined relationship between σ and the amounts of quartz for a broad temperature range. For the gabbro group, there is insufficient statistical material to show the change of σ as a function of the amounts in it of hyperstene, or of minerals from the amphibole group. With the increase in gabbro of the above-mentioned minerals, one must observe the corresponding increase of their electrical conductivity.

In the case of ultrabasic rocks - olivinite, peridotite and dunite, the mineral which affects strongly the electrical parameters is the ore mineral which must be represented in them by magnetite, titanium-magnetite and chromite. Figure 38 gives us a general idea as to the character of this relationship at t=200 and 1000°C. As one can see, there is a considerable scattering of the points, since in parallel with the amounts of the ore material, of great importance here is the structural factor - the geometry of the ore mineral evolution. At high temperature, the effect of the ore component, although noticeable, is not as pronounced. A sufficiently extensive material, with respect to the ultrabasic rocks which are affected to a different degree by serpentinization, indicates that in the majority of cases, this processs is accompanied by the evolution of the ore component, which results in the increased electrical conductivity. The monocrystal of serpentine itself, however (see Appendix 1) has a low electrical conductivity. For the group of alkaline rocks, one also traces out a clearly defined relationship between the electrical conductivity within a broad temperature range and the amounts of such relatively highly conducting minerals as eugirite and eudialyte. With the increase of the total amount of these minerals, from 5 to 40%, the electrical conductivity at

200°C will increase from 10^{-11} to 10^{-7} ohm$^{-1}\cdot$cm^{-1} (Appendix 13). The electrical conductivity of the eclogite group depends on the type of garnet (the pyrope will decrease and almandine will increase its level) and in addition, of significance here is the degree of amphibolization in eclogites. Particularly, the electrical conductivity will increase with the presence of omphacite.

In addition to the effect of the mineral composition on the electrical conductivity, it was also possible to establish the relationship between the activation energy and the mineral composition of the rocks. For the garnet diorite series, we have obtained the decrease in these parameters in the region of impurity-related and intrinsic conductivities, as a function of /136

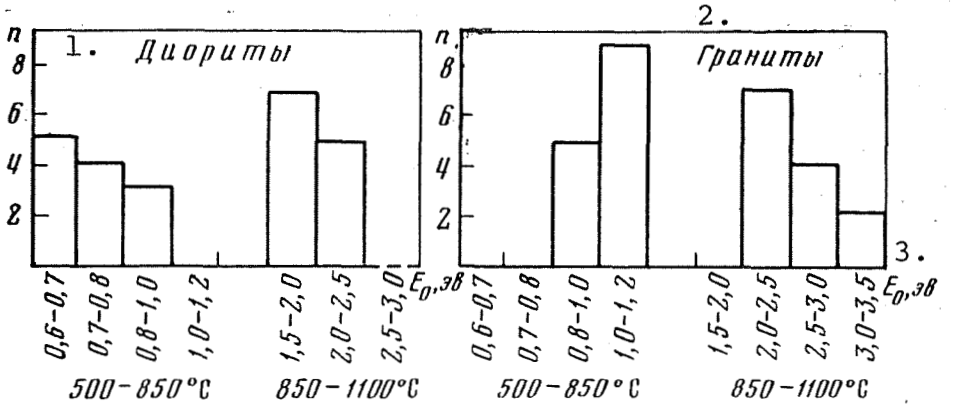

Figure 47. Effect of the rock composition on the magnitude of activation energy.

Key: 1. Diorites; 2. Granites; 3. E_0, eV

the increase in quantities of ferrous minerals, and decrease of quartz (Figure 47). In addition, in the case of gabbro and some other rocks, one observes the decreased activation energy with the increase of amounts of minerals from the amphibole group, which have high amounts of iron cations. The presence of the ore mineral in the form of magnetite and titanium magnetite also is reflected on E_0 and σ_0 parameters. According to Figure 48, the activation energy decreases particularly intensively with the increase of the ore mineral in the temperature range which corresponds to the impurity-related electrical conductivity, since the impurity-related conductivity is brought about in this case by the electron transfer from the bivalent iron ions to the trivalent, and vice versa. Therefore, just like in the case of electrical conductivity, by knowing the mineral composition of the rock, it is possible on the basis of this data to make an assumption as to the limiting values of electrical parameters.

2. Effect of Chemical Composition on the Electrical Parameters of Rocks

In analyzing above the electrical properties of minerals it has been established that the major factor which defines the electrical conductivity in minerals is their chemical composition and in particular, the relationship between the amounts of oxides which facilitate the increase in electrical conductivity and the oxides which cause its decrease. Let us remind the reader that the greatest role in developing electrical conductivity is played by the following two groups of oxides: Fe_2O_3, FeO, Na_2O, K_2O and MgO, Al_2O_3, SiO_2.

For the minerals (see Figure 19) one finds a specific relationship between σ quantity and the total amounts of the following oxides Na_2O, K_2O, Fe_2O_3 and FeO. Figure 49 shows that in the case of rocks, one also observes a relationship between the electrical conductivity and the amounts of the above-mentioned oxides. Since the quantity of these oxides and the /137
conductivity fluctuates within a certain range, this data is represented in the form of rectangles. A large scattering of σ values in this case is due to the fact that the structure of the rock and lack of homogeneity in terms of its composition, plays an important role. In analyzing the electrical conductivity of the rock as a function of the high resistivity oxide MgO, which is one of the mandatory components, one also observes a certain relationship between σ and amounts of MgO, but in this case it is of reverse character. With the increase of high resistivity oxide MgO, the electrical conductivity will decrease.

In considering the specific groups of rocks, one should note the following. Within the garnet-diorite series, one notes similar character of the electrical conductivity as a function of the total amounts of SiO_2 and the amounts of quartz. The alkaline group of rocks clearly defines the importance of Na_2O and K_2O oxides in the electrical conductivity. For the alkaline rocks of loevrite and uvite type, the highest total amounts of Na_2O and K_2O oxides is most characteristic. In this case, the rocks in which the Na_2O prevails, display higher electrical conductivity at $t=200^{\circ}C$ (approximately by three - four orders of magnitude) than the rocks which higher amounts of K_2O. The effect of these oxides has been described in detail earlier (see Chapter 3).

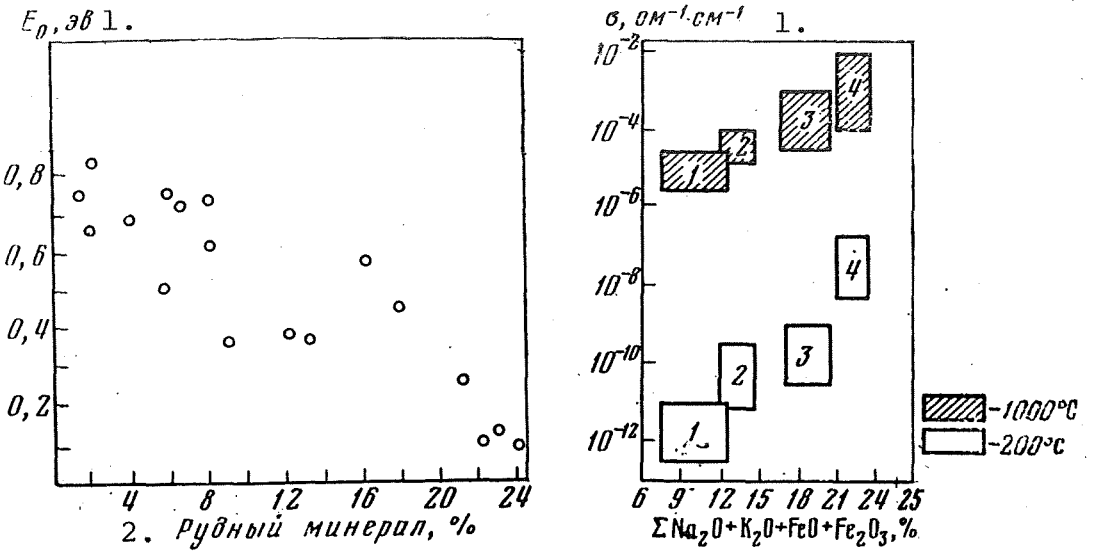

Figure 48. Activation energy in the region of impurity-related conductivity in the ultrabasic rocks as a function of the amount of ore mineral.

Key: 1. eV; 2. Ore mineral

Figure 49. Electrical conductivity in the rocks as a function of the total amount of oxides.

1 - Granites; 2 - diorites; 3 - dolorites and basalts; 4 - alkaline rocks

Key: 1. $ohm^{-1} \cdot cm^{-1}$

The alkaline rocks of other types, as for example the basalts and pyroxenites, in contrast to their ordinary analogues, also differ in terms of increased electrical conductivity. The excess of Na_2O by 2-3%, when compared to K_2O quantities, and generally, a somewhat larger total amount of these minerals, separates the /138 alkaline basalts into a group of higher conductivity. An analogous picture is observed in the case of pyroxenites. The eugirite-augite pyroxenites have considerably higher electrical conductivity (by approximately a factor of $10^2 - 10^3$ at t=200°C) when compared to the diopside pyroxenites. As it appears, the ribecite rocks must also have higher electrical conductivity.

One must once again consider the effect of iron oxides on the magnitude of electrical conductivity in the minerals and in the rocks. Of great significance in electrical conductivity of the olivinites, and consequently in the ultrabasic rocks as a whole, are the iron oxides. According to the studies [43, 103], Figure 50 shows the electrical conductivity of olivine as a function of the amounts of fialite in it. With increased quantities of fialite, one observes a sharp increase of electrical conductivity.

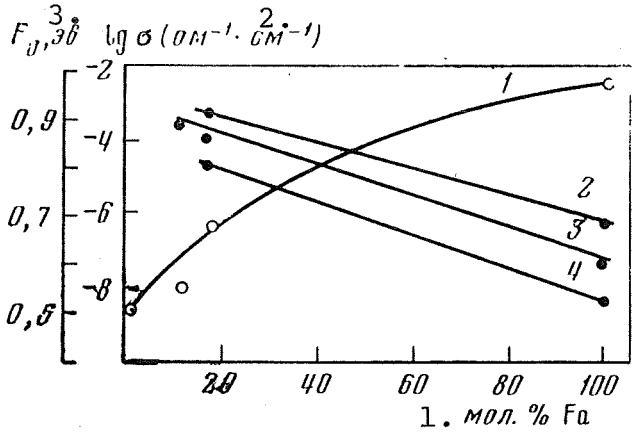

Figure 50. Electrical conductivity (1) and activation energy (2-4) in the olivines as a function of amounts of fialite.

At p, kbar:
2 - 12;
3 - 22;
4 - 33

Key: 1. mol % Fa; 2. $ohm^{-1}.cm^{-1}$
3. eV

In addition, fialite lowers the activation energy of the rocks (see Figure 50). Such relationship is observed while investigating the $\sigma=f(t)$ in the case of the forsterite inclusions in kimberlites, in basaltoids and in the volcanic lava. At the present time, the basic oxides have been defined which influence to the greatest degree the electrical conductivity in the rocks. On the basis of available material, it is still rather difficult to judge the role in electrical conductivity of the oxides in the rocks such as CaO, MnO and TiO_2.

Of great interest also is to investigate the effect of the hydroxyl group.

3. Effect of Structure and Texture on the Electrical Parameters of the Rocks

In parallel with the mineral and chemical composition of the rocks, as they affect the electrical parameters, of significance also is the structure and porosity. By structure we shall understand here the shape and size of the mineral grains, the relationship between the decrystallized and glassy material. The effect of the size and shape of the grain on the character of the change in electrical conductivity as a function of temperature has not been investigated separately. In investigating the basalts, as one observes the increased grain size, one also observes the decrease of electrical conductivity and increase of the activation energy. On the basis of the fact that at the grain boundary, the crystalline lattice is disrupted, and therefore, the ions at the grain boundary are in a somewhat different energy state than the ions further removed from the grain boundary, one should expect that the activation energy needed for displacement of the boundary ions will be lower than required for the displacement of the bulk of the ions. On the basis of data which indicates the increased diffusion of the metal atoms at the grain boundaries, one may also assume that they are more mobile. All this must result in the increased electrical conductivity of the low crystalline material, as compared to the large crystalline material, in other words, an inverse relationship

/139

must exist between the grain size and electrical conductivity.

In addition, as it appears, the grain size must play an important role in the region of impurity-related conductivity. As we can see, the obtained experimental results for basalt are in total agreement with such considerations. Here one should also mention that for all types of rock (basalts, pyroxenites, peridotites, etc.) which are characterized by fine dispersion (powdery) and evolution of the ore mineral, one also notes a rather significant increase in electrical conductivity, as compared to the rocks in which these grains are of large size. Of greatest interest in conjunction with the problem of the origin of the conducting layer in the upper part of the mantle, is the study of the effects of the amorphous phase. Therefore, we have investigated the most widely found intrusive rocks and their effusive analogues. Figure 51 shows the range of electrical conductivities for each pair of rocks at t=300 and 1000°C. In addition, for the basalts with low and high percentages of amorphous phase, we are presenting the activation energies separately, and the range of electrical conductivities. It is quite clear that all effusive analogues differ from intrusive rocks by having higher electrical conductivity in spite of the identical chemical composition. In terms of the electrical conductivity as a function of the amorphous phase, the basalts differentiation is also clearly manifested. The presence of amorphous phase and of smaller crystalline structures in the effusive rocks is reflected in the E_0 and σ_0 levels, which are lower. The decrease of activation energy and increase of electrical conductivity are two phenomena which accompany the transition of material from its crystalline state into amorphous state, and this has been noted by a number of researchers in the study of glass crystallization [68]. The change of activation energy and also of σ_0 is of great interest from the point of view of the physics of the electrical conductivity mechanism. Such phase transition is not accompanied by the composition change, and therefore the energy of dissociation must not be significantly changed since the electrostatic attraction does not decrease appreciably. In conjunction with this, the observed change in E_0 and σ_0 parameters should be due to the change in the energy of the already dissociated ion, in other words, as it appears, this must be due to the decrease in the ion mobility. In the geometrically properly arranged crystalline lattice which features denser packing than the amorphous one, the ion mobility must be much lower. /140

Here one should note an interesting relationship which is observed in the case of the alkaline glasses: during the complete crystallization of the alkaline glass, the lower is the resistivity of the initial glass, the higher will be its resistivity during complete crystallization.

In addition to the rocks which have no clearly defined relationship in terms of the position of the mineral components, there are a number of rocks which display a specific orientation of the minerals, in other words, which display a textural arrangement. The texture, depending on the degree of orientation of the minerals, may either be complete or constrained. The higher is the degree of orientation of the minerals, in other words, the less diffusion one observes, the more clearly defined will be the anisotropy of the rock. However, the anisotropy in structure is not always extended to the anisotropy of electrical parameters, since it is not as clearly defined in all minerals.

The structural anisotropy is more frequently encountered in the metamorphic rock (gneiss, quartzite, shale, marble, amphibolite, etc.) and also in some igneous rocks, the texture of which is being formed during the magma cooling. In considering the texture, one should keep in mind that it may be the result of orientation of minerals not only in terms of their internal arrangement, but also in terms of the shape. There are cases known when the orientation has been observed only in terms of the shape, and as far as the crystallographic axes are concerned, there were no definite relationships. There are some opposite cases. For example, in the quartz vein, quartzite, the grains which are of isometric shape display a strict internal orientation.

We have investigated the electrical anisotropy of different types of rocks because, according to what has been said so far, the presence of it in one of the groups of rocks does not mean, necessarily, its manifestation in all others. /141

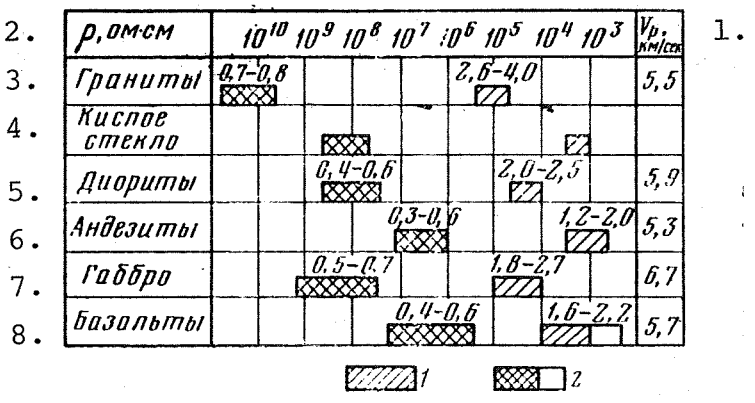

Figure 51. Amorphous phase as a function of electrical conductivity in different types of rocks.

At t, °C:
1 - 1000;
2 - 300

Key: 1. km/s; 2. ohm-cm; 3.Granites; 4. Acidic glass; 5. Diorites; 6. Andecites; 7. Gabbro 8. Basalts

[Commas in the above figure are equivalent to decimal points.]

Appendix 10 shows the experimental data regarding the electrical conductivity which was measured laterally and longitudinally with respect to the layers, in the representative samples of different types of rocks. The anisotropy in electrical conductivity has not been established for the monomineral amphibolites. As it appears, in this case, we have the grain orientation in terms of the shape which, due to the monomineral composition of the rock, has not been reflected in the electrical conductivities in two mutually perpendicular directions or this type of amphibole does not display anisotropy in electrical conductivity.

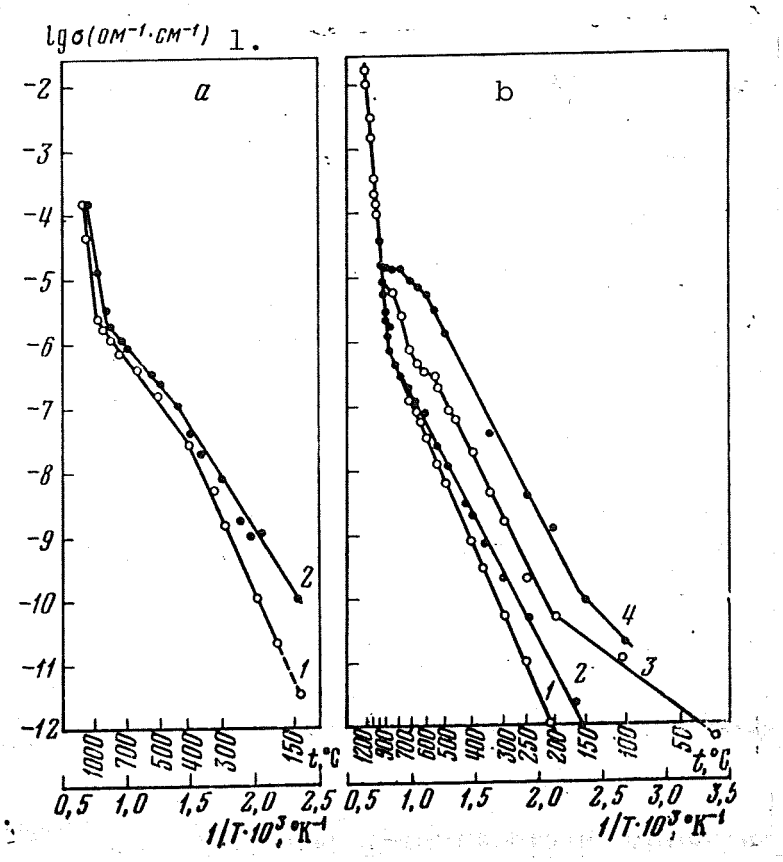

Figure 52. Electrical conductivity as a function of the anisotropy in the rock.
a - kyanite-biotite-amphibole gneiss 968: 1 - perpendicular to the layer; 2 - parallel to the layer; b - gabbro: 1,2 - slated gabbro 1472; 3,4 - striated gabbro 1474, along and across the layer, respectively

Key: 1. $ohm^{-1}.cm^{-1}$

The kyanite-biotite amphibole gneiss 968 is characterized by a thin slated structure with a well developed linearity. At low temperatures, as one can see in Figure 52a, one observes a considerable anisotropy in electrical conductivity. With the temperature increase, this anisotropy decreases and is not manifested at all at 850-1100°C. The anisotropy in σ correlates well with the considerable anisotropy of the dielectric penetrability and of the longitudinal wave velocities V_p [124, 125]. In the case /142 of gabbro 1474, of thin-slated linear structure, in which plageoclase is interspersed with horblende, biotite and chlorite, in the temperature range of 100-950°C, one observes the anisotropy in σ in the range of one order of magnitude (Figure 52b). In the course of further temperature increase, it practically disappears. A qualitatively analogous picture is observed also for the other gabbro 1472. The anisotropy in σ of elastically deformed pyroxenite is less pronounced ($\frac{\sigma_{\parallel}}{\sigma_{\perp}} \approx 3$) and is observed only up to 600°C and it is correlated with the anisotropy of the longitudinal wave velocities V_p. In some serpentinites, which display anisotropy in V_p, one also observes the anisotropy in electrical conductivity ($\frac{\sigma_{\parallel}}{\sigma_{\perp}} < 4$). The low anisotropy in σ in seprentinites and diopside pyroxenites is explained by its weak manifestation in serpentine and diopside. Therefore, on the basis of experimental data, in the case of the rocks which display anisotropy, one can see that the anisotropy across the grain and along it will have different $\sigma = f(1/T)$. In the temperature range t=20-800°C, where the impurity-related type of conductivity dominates, the electrical conductivity will always be greater along the layers than across them. The question of the structural effect on the electrical parameter has not been investigated sufficiently well. It appears, in investigating the relationship between the electrical conductivity in rocks, and the structure of these rocks, the greatest attention must be devoted to the study of the character of change in σ, namely, within the structurally-sensitive region, in other words, the region of relatively low temperatures.

4. Mechanism of Electrical Conductivity in Rocks within a Broad Temperature Range

The systematic studies of the mechanism of electrical conductivity in rocks at high temperatures by setting up special experiments and determining the thermal emf, the Hall effect, or the amount of transferred material, according to the Farraday law, have not been conducted. The basic data in determining the mechanism of electrical conductivity in rocks are the experimental

curves lg σ=f(1/T) for different types of rocks. In addition, the study of the effect of the minerals and the chemical composition, as well as of the structure, on the electrical conductivity in rocks at high temperatures have helped to a considerable degree in explaining the mechanism of electrical conductivity. The study of the character of the relationship between the electrical conductivity and temperature for different rocks makes it possible to define the following specifics. As a rule the lg σ as a function of 1/T is characterized by not less than one break in the curve, frequently, by two breaks and less often, by three.

The linear dependence of lg σ=f(1/T) for some types of rocks /143
is disrupted by the anomalous change of σ, with the temperature increase, with the manifested decrease of electrical conductivity within a specific temperature range. For some rocks and minerals, one observes a sharp increase of σ with the concurrent extremely high E_0 and σ_0.

All the above-mentioned specifics in lg σ=f(1/T) relationship points to a complex mechanism of electrical conductivity in rocks.

In the physics of dielectrics and semiconductors, the electrical conductiivty, depending on the fact , whether it is accomplished by means of the impurity-related defects or the major defects, is divided into two types. On the basis of such general postulates, let us consider the mechanism of electrical conductivity in rocks. For the majority of rocks, the first break in the curve is observed at the temperature range of 500-700°C and the activation energy of particles which are the charge carriers fluctuates between 0.5 and 0.8 eV. In this low temperature (impurity-related) region of conductivity, the following possible sources of the charge carriers are: defects which are due to the presence of impurity-related ions, the boundary ions and also the defects in crystalline lattice in the basic material. To bring about the appearance of the current because of the above-mentioned defects, the necessary activation energy must be merely equal to the energy which is to be expended for the displacement of a vacancy, and the defect of the heat of formation in this case is not incorporated into the level of activation energy. It follows from this that at the low temperatures, because of the impurity-related, boundary ions and disruptions, the number of current carriers will be much higher than the concentration of the current carriers which have been formed within the crystal because of the thermal fluctuations. In conjunction with this, the activation energy in the region of the impurity-related conductivity is always considerably lower than in the region of intrinsic conductivity. Since the concentration of the current carriers which is due to the presence of defects is much smaller than the concentration of current carriers which are the result of the thermal vibrations of the ions in the basic material, the pre-exponential coefficient σ_0', which incorporates the number of current carriers, is always

less than σ''_0. The concentration of impurity-related defects is also reflected in the level of E_0 and the temperature at which the electrical conductivity curve will have the point of inflection. The higher is the concentration of such defects, the lower will be E_0 quantity, but the temperature of the break point for a given material and for a given impurity will be higher.

It should be noted that depending, whether the electrical conductivity is due to the ionic movement between the lattice points, or the holes, the presence of impurities has different effect on the electrical properties of the material. In the first case, because of the small number of vacancies at the lattice points, the introduction of impurities results in a sharply increased number of current carriers, since the impurities will be located within the interpoint spaces. If, however, the whole mechanism predominates, then the introduction of small amounts of impurities, part of which will occupy the existing vacancies, will not significantly change the magnitude of electrical conductivity. /144

Even one single piece of a rock is characterized by the inhomogeneous composition and structure, and therefore, the variations in σ and E_0, and also the temperature at which the point of inflection will be displayed, are defined by the number of defects and by the type of defect. The presence of one straight line $\lg \sigma = f(1/T)$ is note a clear indication that there is just one type of mechanism which is involved in the current transfer within a rock and it is more likely that there are several current carriers with similar activation energies within a specific temperature range which simultaneously are involved. If however, one type of current carriers may be singled out in terms of the number of carriers, and in terms of E_0 magnitude, the curve of $\lg \alpha = f(1/T)$ within the region of impurity-related conductivity will display another point of inflection. Such points of inflection or breaks in the curve for rocks are sometimes defined at t=300-400°C. In such case, at the lowest temperature range, the activation energy is ordinarily quite small, comprising 0.1-0.3 eV. The low level of activation energy makes it possible to assume that in this case, one is faced with the contribution to the electron conductivity associated with the presence of iron oxides. Within the region of the impurity-related conductivity, according to the relationship between the electrical conductivity in the minerals and in the rocks, and the total amounts of oxides Na_2O, K_2O, Fe_2O_3 and FeO, the major current carriers must be the Na^{1+} and K^{1+} cations. Depending on the Fe_2O_3/FeO ratio, and on their amounts, the electron mechanism of conductivity will manifest itself. With the increase of the electron conductivity, one should expect a decrease in the activation energy, something which does take place in the ultrabasic rocks.

The high electrical conductivity in the minerals and in the rocks, in the presence of iron oxides is due to the following. The iron oxides, such as NiO, Mn_2O_3 and CuO, are the oxides of transition metals which are characterized by specific mechanism of electrical conductivity. For these compounds the appearance of such structure is possible when the electrons are transferred from the ion of one valence to the an ion of another valence, Fe^{2+}-electron $\rightleftarrows$ Fe^{3+} + electron. In this case, the energy to overcome this barrier is only 0.1 eV.

The leading role of Na^+ and K^+ cations in electrical conductivity is due to their small charge and to a relatively small radius, the result is that the ionization potential of these cations is small. These parameters of Na^+ and K^+ cations define their low bonding energy within the crystalline lattice points. Therefore, within a specific temperature range, both potassium and sodium are comparatively easily removed from the crystalline lattice points, causing greater ionization and consequently, greater conductivity in the material under investigation. In addition, Na and K are always combined with somewhat larger silicate anion, for example $K_2Si_4O_9$ and $Na_2Si_2O_5$. This results in the decrease of valence bonding. And the weaker are the valence bonds, the more "ionic" will be the material, and the higher will be the alkaline properties of the elements under consideration [118].

The major rock-forming potassium minerals are the feldspar /145
and the micas. The major sodium-containing minerals are the acidic and neutral plageoclase, to some extent the potassium-sodium shales and amphiboles. These minerals have different degrees of stability with respect to different types of environment, and consequently, they display different bonding of potassium and sodium within the crystalline lattices. The experimental studies within the framework of reactions of the mineral formation indicate that in the case of sodium, it is more easily removed from the feldspar than potassium [126]. The sodium ions also are more easily replaced by isomorphous impurities. Therefore, the plageoclase lattice is less stable, and the bonding energy of sodium is considerably lower than that of potassium within the lattice of the potassium feldspar [127]. The higher energy in the crystalline lattice of the potassium feldspar and the activation energy of potassium ions as compared to the sodium ions in the sodium-containing minerals will also indicate the high E_0 and somewhat lower σ_0, which are obtained while investigating the temperature-related electrical conductivity for these types of minerals (see Appendix 1).

In the high temperature region, the concentration of vacancies which were formed as a result of the thermal fluctuations is considerably higher since they are the result of the basic material ion removal from the crystalline lattice point. The activation energy in this case is a summary quantity, one part of which is

being expended on the formation of the defect, and another one - on its displacement. It follows from this that $E'_0 < E''_0$ always and that $E'_0 \approx E''_0/2$, according to [16]. The number of particles which participate in the charge transfer within the region of the internal conductivity is large and therefore, σ''_0 may exceed σ'_0 by a factor of one million. At high temperatures, the Na^{1+} and K^{1+} cations, it appears, are by far not the major charge carriers, since, according to Figure 19, within the region of intrinsic conductivity, the value of σ as a function of the total amounts of conducting oxides, is not as strongly pronounced. Therefore, the most probable current carriers at high temperatures, in parallel with Na^{1+} and K^{1+}, may be Ca^{2+}, Mg^{2+} and Al^{3+} cations. The complex anion SiO_2^{4-} and also possibly the anion in the form of oxygen, because of a large charge and size, do not take part in the electrical conductivity. In having considerable amounts of iron oxides, some contribution of the electron component is also possible.

One should also consider the effect of the thermochemical conversions within the rocks as they affect the electrical conductivity as a function of temperature. A number of rocks feature an anomalous change in electrical conductivities within a specific temperature range and the character of it cannot be reproduced during the repeat heating and cooling. One of the major reasons for such anomalous change in electrical conductivity as a function of temperature may be evolution of water in different phases. The molecules of the water of crystallization increase the effective radius of the anion, which lowers the energy of the crystalline lattice and the evolution of such /146
water results in the reverse effect, which can be manifested by the increase in resistivity within a specific temperature range.

The investigations have established that olivine and pyroxene incorporate water within the defects of the crystalline lattices, and also that magnetite and titanium magnetite at high temperatures, undergo physical and chemical conversions [67, 128]. It was shown that the removal of the water from the lattice in the above-mentioned minerals, the decomposition of volcanic glass in basalts, and transition of bivalent iron into trivalent iron during the oxidation process at 700-900°C, are accompanied, probably, by the partial destruction of the crystalline lattice [67]. These processes affect the general character of electrical conductivity as a function of temperature in the rocks, and the absolute quantities of electrical parameters. They may also affect partially the inflection point in the curve of $\lg \sigma = f(1/T)$. /147
It is possible that the intensity of these irreversible physical-chemical processes and also their general character define the magnitude in hysteresis in the direct and reverse behavior of the $\lg \sigma = f(1/T)$ curves (Figure 53).

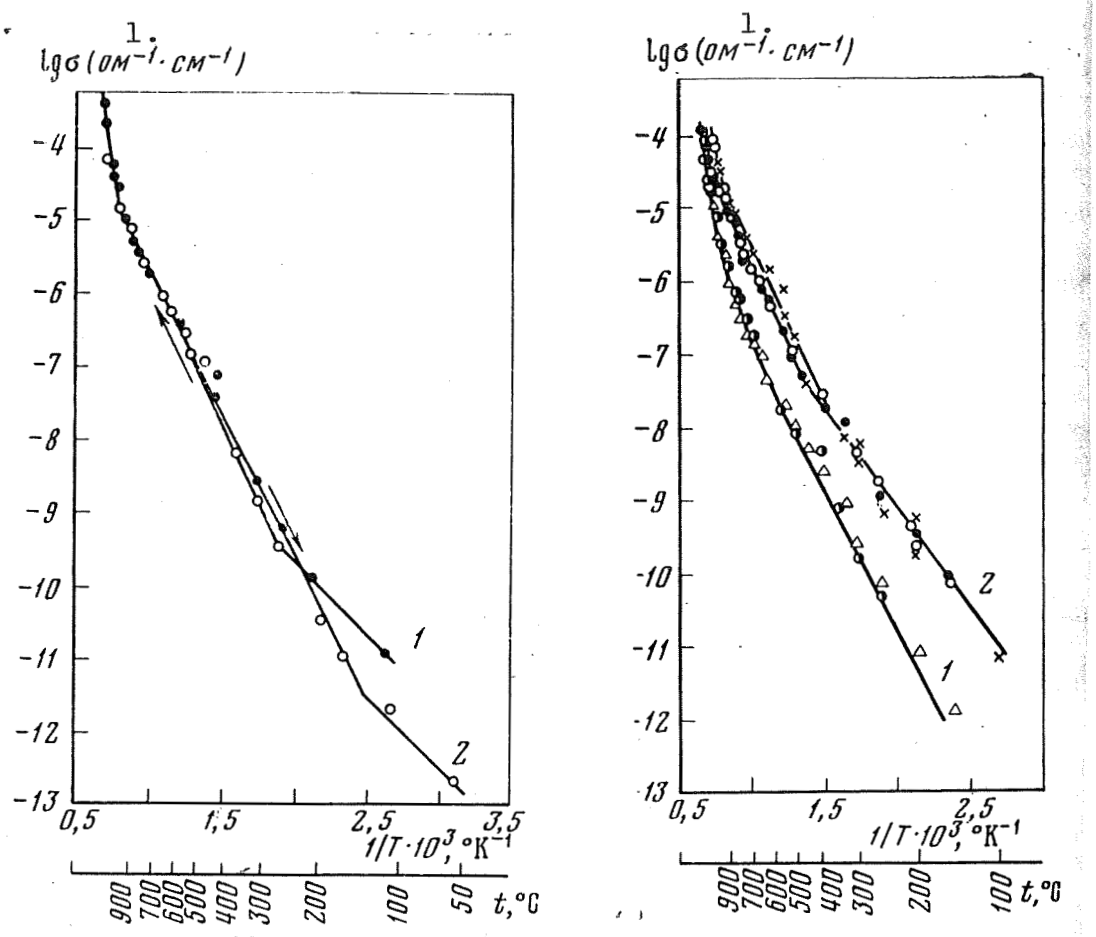

Figure 53. Electrical conductivity of gabbro 1450 as a function of temperature.

1 - forward development; 2 - reverse development.

Key: 1. $ohm^{-1} \cdot cm^{-1}$

Figure 54. Electrical conductivity of the pyrope eclogite 2259 as a function of temperature.

1 - the two samples during the first test;
2 - the three repeat tests.

Key: 1. $ohm^{-1} \cdot cm^{-1}$

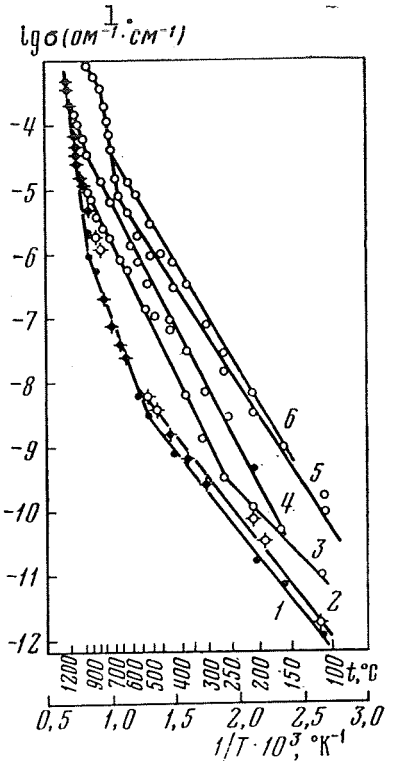

Figure 55. Electrical conductivity of gabbro as a function of temperature.

1-3 are the repeat measurements of gabbro 1450, 4-6 are the measurements of three samples of gabbro 462.

Key: 1. $ohm^{-1} \cdot cm^{-1}$

The electrical conductivity as a function of temperature in the magmatic eclogite 2259 within the tunneled formation "Obanzhennaya" which was subjected to four repeat measurements, is shown in Figure 54. In this figure, the curve 1 shows quite well the agreement in the curves for two eclogite samples during the first measuring cycle. The curve 2 shows the same eclogite during the subsequent three repeat tests. In the region of impurity-related condictivity (100-800°C) the disagreement in σ between the first and three subsequent tests, as one can see in Figure 54, is quite considerable. Within the region of intrinsic conductivity however, in other words at 800-1200°C, the σ values are quite similar. The experimental points for the repeat tests all fall within a narrow zone. Therefore, the electrical conductivity for the region of impurity-related conductivity, when the sample undergoes irreversible changes, should be taken on the basis of the first tests.

The repeat measurements of electrical conductivity were also taken in identical conditions by using the samples of gabbro 1450 (Figure 55, curves 1-3). These tests have shown that for several heating cycles, the data scattering is within the observation errors for different gabbro samples, made of the same rock (curves 4-6). As one can see, the reproducibility of results depends on both the irreversible physical-chemical phenomena which take place at high temperatures within the rocks, and on different conducting inclusions and defects in different samples, which were made from the same rock. A significant disagreement in the values of σ during the repeat tests is the partial melt-out of the minerals. It should be pointed out that the hysteresis of electrical conductivity within the region of impurity-related conductivity is due primarily to the removal of the volatile components and the conversion to a solid phase of the ore and other minerals. It should be pointed out however, that this disagreement in electrical conductivities is observed primarily at the temperature range of 100-850°C only, and at higher temperatures, no scattering

of the readings was observed. The obtained scattering of σ, as one goes from one sample to another in the same type of rock, and also the hysteresis during the repeat measurements, indicate that it is necessary to generate the average values of electrical parameters for each type of rock. /148

To better understand the mechanism of electrical conductivity in rocks, one should consider the relationship between the electrical conductivity and activation energy, and the dielectric penetrability of different types of rocks, and also the general character of the relationship between E_0 and σ_0.

The theoretical calculations indicate that the displacement of cations from the lattice point to the interpoint space requires considerable energy. For example, to displace the cation of silver Ag in the compound AgBr in such manner, the energy of 10 eV is needed. In reality however, in order to form a defect, a considerably less energy is required because of the lattice weakening which is the result of polarization. The higher is the polarization of cations and anions, the less energy would be required for their displacement.

According to [16], the energy gained, which is due to the lattice polarization around the vacancy, and the interpoint space ion, are defined by the following expressions, respectively:

$$W_1' = \frac{q^2}{2R_a}\left(1-\frac{1}{\varepsilon}\right), \qquad W_2'' = \frac{q^2}{2R_C}\left(1-\frac{1}{\varepsilon}\right),$$

where q is the ion charge, R_a and R_C are the radii of the anions and cations. In the case of AgBr, the total polarization energy turnes out to be less than 10 eV, in other words, it is comparable to the energy which is needed in developing the defect, according to Frenkel.

Keeping in mind the significant effect of polarization obtained theoretically, on the magnitude of the energy required to move the ion, we have conducted the comparison for a number of rocks, of the dielectric penetrability, the activation energy levels and the electrical conductivity [129, 130]. Figure 56 shows the average activation energies for different types of rocks as a function of dielectric penetrability. It is known that E_0 within the region of intrinisic conductivity of rocks is a stable quantity. Therefore, this curve was constructed on the principle of the activation energy related to the intrinsic conductivity within the temperature range 700-1200°C, as a function of dielectric penetrability. The values of dielectric penetrability in

this case were obtained at the frequency of 500 kHz, when ε is practically independent of frequency. The horizontal lines give us the intervals of change in dielectric penetrability in different samples of the rocks. It should be noted that in the case of the rocks having high dielectric penetrability, the relationship between ε and E_0 is disrupted. It is likely that it is due to the fact that at the 500 kHz frequency, the dielectric penetrability has not reached its maximum high frequency level, in other words, in the rock polarization, the ionic-relaxation or structural polarization are still playing some role. One can also trace out here the relationship between the electric conductivity and dielectric penetrability (Figure 57), something which should be expected, on the basis of the effect of polarizability on the energy of the current carriers. We have already considered earlier (Chapter III) the relationship between the pre-exponential coefficient σ_0 and the activation energy of the particles which are involved in the conductivity in the rocks and in minerals. It should only be pointed out here that one obtains a straight linear relationship between σ_0 and E_0, for various groups of rocks. Analytically, this relationship may be expressed by the following formuala

/149

$$\sigma_0 = ae^{bE_0},$$

where a and b are the constant coefficients which are approximately of the same value for all rocks within the region of intrinsic conductivity.

However, the impurity related conductivity is characterized by other figures, which are greater for b than for a. Below are the limits of a and b for intrinsic conductivity:
$a=-4.0- -6.3$ ohm$^{-1}\cdot$cm^{-1}, $b=0.25-0.32$ eV^{-1}.

Such difference in the values indicates that in the region of impurity-related conductivity, the increase in the number of current carriers is accompanied by a larger increase in the activation energy than in the case of intrinsic conductivity. The values of activation energies for the defects, in conjunction with dissimilar physical nature of them, have considerably greater range than in the case of carriers of charged particles in the basic material.

/150

In order to refine our general concepts as to the mechanism of electrical conductivity, it is necessary to organize special experiments and determine the type of the current carriers and the contribution of presumable current carriers to the total electrical conductivity.

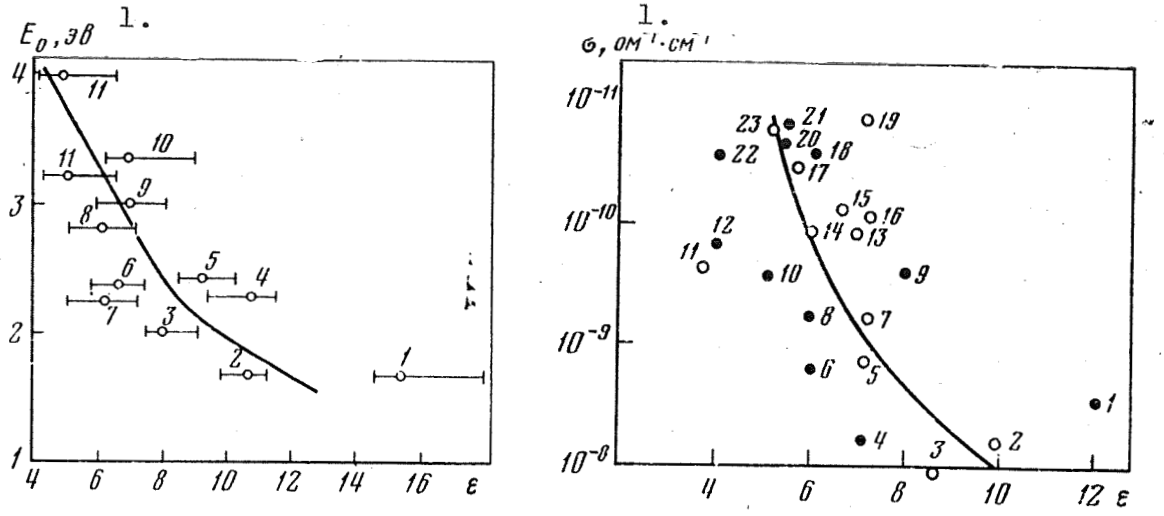

Figure 56. Relationship between activation energy E_0, intrinsic electrical conductivity and dielectric penetrability ε in the rocks, at the frequency of 500 kHz.

1 - peridotites; 2 - diabase; 3 - dunites; 4 - basalts; 5, 6 - gneisses; 7,8 - alakline rocks; 9 - amphibolites; 10 - gabbro; 11 - granites.

Key: 1. E_0, eV

Figure 57. Relationship between σ by employing the d.c. current, and at f=10 MHz, in the case of alkaline rocks.

1 - eugirite; 2 - luiarite; 3 - uvite; 4 - eugirite of second generation; 5, 7, 8 - urtites; 6 - loevrite, trachetoid $\perp$; 9 - nephelite syenite; 10 - loevrite, trachetoid $\parallel$; 11, 17, 23 - rhizchorites; 12 - uvite; 13 - iolite; 14 - urtite; 15 - nepheline syenite; 16 - veined rock; 18 - nepheline; 19 - nepheline iolite; 20, 21 - foyanite; 22 - udalite

Key: 1. $ohm^{-1} \cdot cm^{-1}$

CHAPTER FIVE. ELECTRICAL CONDUCTIVITY IN MINERALS AND ROCKS AT HIGH PRESSURES AND TEMPERATURES

1. General Information about the Effect of Pressure on the Electrical Conductivity in Different Materials /151

Before we shall present our experimental data on the effect of pressure on electrical conductivity in minerals and rocks, it is necessary first to consider briefly all available data for semiconductors and dielectrics.

The electrical conductivity of the majority of metals and semiconductors increases with increase of pressure, something which is due primarily to the change in the electron mobility. The opposite relationship is observed rather rarely, and it is associated with the increase of the effective mass of the current carriers.

The dominating effect on the electrical conductivity in semiconductors as a function of pressure is the change in activation energy. It has been established that the extent of the forbidden zone, and consequently, the activation energy, as one decreases the interatomic distances, may either increase or decrease. In conjunction with this, the hydrostatic pressure in some semiconductors results in the increase and in some others - in the decrease of electrical conductivity, or its minimization. Such variety in the character of the behavior of electrical conductivity as a function of pressure is explained by the complex distribution of the energy levels in the semiconductors.

One should also not exclude the change in electrical conductivity as a function of pressure, associated with the increase in mobility of the current carriers. The shortened distances between atoms which is the result of pressure bring about a decrease in the amplitude of their thermal vibrations. As a result, the thermal scattering in the current carriers decreases and one observes an increase in the mobility of the current carriers.

P. B. Bridgeman, in the study [131], investigating the electrical resistivity of different materials, pointed out that there is no theory which would explain the correlational relationship between the resistivity, the resistivity sign change during the phase transitions, and the change in the volume of the material. /152
At a later time, the expression for the isothermic process was obtained by Lacam and Lallemand [132] by differentiating with respect to pressure, the equations of ionic electrical conductivity. In utilizing this expression, Kurnick [133] has shown that in the

AgBr, with some added CdBr, the conductivity is accomplished across the defects, as per Frenkel. The formation of defects, as per Schottky, is slowed down by the pressure because the defects require high activation energy.

V. N. Zharkov [134] emphasizes the great importance of investigating the electrical conductivity as a function of pressure in determining the general character of the effect of pressure on E_0 and σ_0 parameters. He has developed the equation which describes the electrical conductivity as a function of pressure by employing the integral compressibility which takes also into account the number of the carriers and their mobility. These equations make it possible to determine the electrical conductivity in the lower part of the mantle.

Bardeen, Paul and Shockley et al. [135-137] have considered the theoretical questions of the pressure effect on electrical conductivity in a semiconductor, disregarding the mobility of the charge carriers, which during the process of this kind is of significance [138-139]. In parallel with such studies, some other researchers have investigated the effect of pressure on E_0 and σ_0 and also the mobility of the charge carriers in the materials with semiconducting conductivity [140-148]. It was discovered in experimental studies with germanium and silicon that, depending whether they are semiconductors of n or p type, the relationship of σ change as a function of pressure, is different. For example, the electrical conductivity in germanium with the hole conductivity, exposed to the pressure of 30,000 kg/cm^2, will decrease by a factor of 4.5, while in the case of germanium with electron conductivity - it increases by several percentage points. The hydrostatic pressure of the same magnitude to which silicon is exposed has the opposite effect, in other words the σ of silicon of n type increases by a factor of two, while in the case of the silicon of p type - it decreases by several dozen percentage points. Particularly strong effect on the electrical conductivity as a function of pressure increase is observed in the case of tellurium and selenium. In the case of the first, the electrical conductivity increases by more than two orders of magnitude as one increases pressure up to 30,000 kg/cm^2, and in the case of the second one, as one increases the pressure up to 100,000 kg/cm^2, the conductivity will increase by a factor of 10^4.

The effect of pressure on electrical conductivity in materials with ionic conductance has been investigated by using the haloids of alkaline metals [149-151]. It has been established that with the pressure increase, the electrical conductivity in these ionic dielectrics will decrease. At low pressures one observes sometimes the increase of electrical conductivity, which is associated with improved contact between the grains.

The first experiments in investigating the electrical conductivities of rocks at the pressures of up to 10,000 kg/cm^2 and temperatures up to 1240°C were carried out by Hughes [102], who investigated the peridotites.

Bradley, Jamil and Munro [42-43] present the data which shows /153 that in the presence of quasihydrostatic pressures and increased temperatures, one observes the decreased E_0 and σ_0 in the case of fialite (Fe_2SiO_4) and the increased E_0 and σ_0 in the case of forsterite ($MgSiO_4$). They have also determined the character of E_0 change with the pressure, depending on the percentage amounts of fialite present. Hamilton [103], while measuring σ of periclase (MgO) and of olivine up to the pressure of 45 kbar and the temperature of 900°C, has discovered their electrical conductivity increase and activation energy decrease, within this range of pressures. The activation energy of olivine has decreased from 0.9 to 0.8 eV. This is associated with the fact that in this case, not all impurity-related levels are occupied by electrons. Akimoto and Fujisawa [152] have determined the electrical resistivitiy of synthetic fialite of olivine structure as a function of temperature at the pressures of 31 and 59.5 kbar. By using the isobar of 59.5 kbar at the temperature of about 630°C, they have established a jump in σ by two orders of magnitude. The sharp increase in the electrical conductivity was associated with the transition of fialite from its olivine structure to the spinel structure, with the corresponding decrease in E_0 parameter.

As we can see from this brief review, at higher temperatures and pressures, olivine, fialite and periclase display the increased electrical conductivity, and E_0 may either decrease or remain constant. It should be noted that the question of the effect of pressure and temperature on the electrical conductivity in different types of rocks, of which the Earth's crust is composed, and of the upper layers of mantle, practically have not been investigated.

2. Equipment and Methods Used to Measure the Electrical Conductivity in Minerals and Rocks at High Pressures and Temperatures

The investigation of the effect of pressure and temperature on the electrical conductivity in rocks has been proceeding along two avenues. The first direction is associated with the problem of industrial geophysics. In this case one ordinarily limits oneself to the pressures of up to 1500 kg/cm^2 and temperatures of up to 200-300°C. For the second approach, one needs the data regarding the electrical conductivity in the igneous, deep-lying rocks, at pressures of up to several dozens and hundred thousands of atmospheres, and the temperatures of up to 1000-1400°C. The study of electrical conductivity in the rocks-collectors, as a

function of pressure and disregarding temperature has been undertaken by numerous Soviet and foreign scientists [153-156]. In investigating rocks, the need arises to create not only an all-around, external pressure which simulates the pressure to which the rocks are exposed, but also to simulate the internal pressure which corresponds to the internal rock pressure as a porous medium. There are only a few studies which present the experimental results by measuring the electrical conductivity in stratified rocks, with the simultaneous investigation of the effects of pressure and temperature [160, 161]. They have made use of chambers with external heating in which one may generate the temperatures of 300°C. The ordinary alloyed steel undergoes fatigue above this temperature. /154

The rock samples in such chambers are separated from the pressurized liquid by the heat-resistant resin.

To study the physical properties of crystalline rocks, it is necessary to develop pressures of more than 5-10 kbar and the temperature >300°C. Pressures of up to 10 kbar may be attained by using both the gas and liquid assemblies [162-164].

In the assemblies to develop pressures above 20 kbar, one makes use of solid material. The utilization of solid material as a medium which transmits pressure simplifies considerably the design of the assembly. The main drawback of this type of assembly is the ability to create pressure which is only similar to hydrostatic, in other words, which is quasihydrostatic. The sample in this case is in the enclosure, made of indium or lead, when one measures the mechanical parameters, and is surrounded by pyrophillite or talcum, for the study of electrical parameters. The heating elements in such chambers are in the form of pipes, made of graphite or platinum. Various modifications of this type of assembly are considered in greater detail in [165-170].

The assembly, the principle design of which is shown in Figure 58, has been developed to investigate the electrical conductivities of rocks at pressures of up to 40 kbar and room temperatures, and also for the pressures of up to 20 kbar and temperatures of up to 650-700°C. The assembly consists of four main components: the plunger 1, the sample matrices 2, and the two supporting holders. The plunger and matrix are made of the special tool steel R-18, thermally treated to have the hardness R_s=61-63, and the supporting holders are made of alloyed steel 40X or 35XGSA. These support holders are heat treated also, but only to the hardness of not more than R_s=40. The upper part of the assembly is used as one electrode and the lower part as the other electrode. In conjunction with this, they must be electrically insulated from one another, and therefore the plunger diameter is less by 0.3-0.4 mm than the sample matrix. This makes it possible to put a ring of high resistivity on the plunger, made of either plexiglass, fluoroplastic, ebonite or mica. The ring thickness is /155

0.15-0.2 mm. Therefore, the ring and a small air gap between the walls of the plunger and the sample matrix create a reliable insulation between the two parts of the assembly. The fluoroplastic material is used as a medium which transmits the pressure, while measuring the moisture-containing rocks, and in the case of dry rocks and high temperature, the pyrophillite is used.

The cut rings are of about 1.0 mm thickness. The plunger pressure is transmitted not only to the sample, but also to the sealing ring, thus creating the triaxial, uneven compression, similar to the compression all around, since the friction between the plunger and matrix is practically absent and the friction of the sample against the enclosing medium is small because of the small height of the sample (3-4 mm). The standardization of the assembly (standards based on bismuth) in having the pyrophillite filling, in the case of the polymorphous transition Bi I - Bi II occuring at the pressure which is quite close to the calculated one, with respect to the force, as read-off from the dial, measures the effective surface area of the plunger.

The above-mentioned polymorphous transition at $t=20^{\circ}C$, was recorded at the pressure of 27-28 kbar. According to the data in the literature, this transition occurs at 25 kbar. Therefore, the difference between the pressure, as calculated on the basis of the plunger surface area and on the basis of bismuth transition, was 2000-3000 kg/cm^2.

The axial force F was brought about by the standard hydraulic test unit, developing 30 tons of pressure. The upper and lower parts of the assembly were insulated from the press by mica or by a film made of fluoroplastic material.

In conducting the experiments at high temperatures, the whole assembly was placed into a vertical non-magnetic oven, 20 cm high (see Figure 58). The cylinder in the oven which was wound bifiliarly by nichrome wire, was made of quartz tubing, 70 mm in diameter. To transmit the pressure in this case, we have utilized the auxiliary plungers of 40 mm diameter, made of steel R-18, and thermally treated up to $R_S=40-45$.

The temperature was measured by the platinum-rhodium thermocouple and the accuracy was $\pm 5^{\circ}C$. The thermocouple was built-in into the metallic enclosure of the assembly. The large mass of the metal in the assembly ensured the uniform temperature of the sample. The experiments have shown that the difference between readings of two thermocouples was not more than $15^{\circ}C$. The above-described assembly makes it possible to develop the pressures of up to 25 kbar at the temperatures of up to $650-700^{\circ}C$.

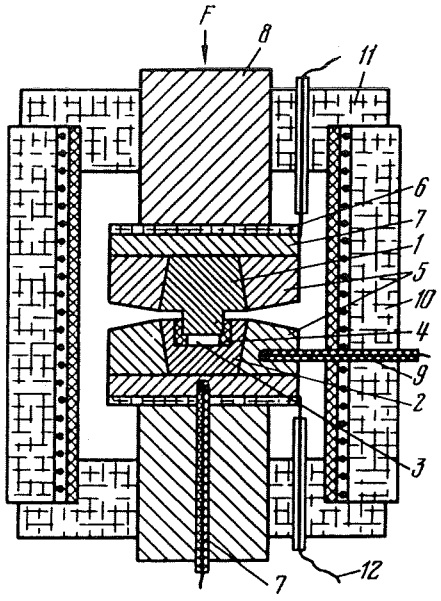

1 - plunger
2 - sample matrix
3 - sample
4 - pyrophillite ring
5 - supporting holders
6 - insulation
7 - electrode
8 - metallic cylinder
9 - thermocouple
10 - asbestos
11 - insulating enclosure
12 - electrodes terminals

Figure 58. Schematic diagram of the high pressure assembly for the study of electrical properties of rocks, featuring the exterior heating.

The high pressure assemblies similar in design were used /156
while investigating the electrical conductivity of the rocks by Moiseyenko [171] and by Bradley [143]. One should also mention here the Bridgman assembly, in which the samples were of 0.025 to 0.16 cm in thickness and 0.3 cm in diameter. In using this assembly, one almost attains the hydrostatic pressure. The adjustment deviations based on bismuth readings from the hydrostatic pressure does not exceed several percentage points. However, one observes some pressure gradient along the horizontal. If we are to assume that the rock resistivity, in its first approximation, changes with the pressure linearly, this has no basic importance [172].

3. Electrical Conductivity of Minerals at High Pressures and Temperatures

The electrical conductivity of moisture-free rocks as a function of temperature and pressure is determined primarily on the basis of the general behavior of the rock-forming minerals under such thermodynamic conditions. We shall consider below the experimental electrical conductivity data for different minerals, obtained by the authors at pressures of up to 20 kbar, at the elevated temperatures (200-650°C).

Quartz. Figure 59a shows the curves indicating the change of σ as a function of pressure for the quartz sample along the optical axis C. One can see that the magnitude of σ as one increases the pressure up to 20,000 kg/cm^2, increases several fold. In addition, /157 the inverse behavior of $\sigma=f(p,t)$ coincides. After the experiments, it was not possible to detect any change in the linear dimensions of the samples, and in the case of the microsections, there is no residual deformation and destruction. The last fact indicates that the sample was within the elastic area. A considerable increase of σ as a function of pressure is explained by the fact that the quartz displays a considerable compressibility in this direction [51] and this increases the density of particles which carry the electrical charges. The quartz activation energy along the C axis in the range of pressures between 600 and 20,000 kg/cm^2 changes by 23%:

Pressure, kg/cm^2	Temperature range t, °C	E_0, eV	lg σ_0, ohm$^{-1}\cdot$cm^{-1}
600	100-600	1.3	2.60
10,000	100-600	1.1	1.75
20,000	100-600	1.0	1.25

In measuring σ in the samples of quartz monocrystal perpendicular to C axis, one observes different behavior of $\sigma=f(p,t)$. As one can see in Figure 59b, in this case the isotherms display a maximum. The maximum which is observed in the pressure area of 3000-4000 kg/cm^2, as one increases the temperature, is displaced toward the lower pressure. It should be noted that in addition to the maximum on the isotherm 600°, one observes the σ minimum at the pressure of 14,000-16,000 kg/cm^2 and reversibility of the observed processes is also observed (see Figure 59b). The remaining four cycles which were conducted at the same temperature totally superimpose on these curves, and therefore are not presented. The minimum electrical conductivity of quartz in this case is likely due to the reversible polymorphous transition $\alpha-\beta$ quartz. The different behavior of $\sigma=f(p,t)$ for the monocrystalline quartz in two major crystallographic directions, as it appears, is due to the dissimilar density of ionic packing and to the ion mobility.

Olivine. The experimental data on the change of electrical conductivity and of E_0 and σ_0 quantities in the magnesium-rich olivine (8% fialite) which was obtained from the spinel dunite 2162-xenolith in kimberlite, is shown in Figure 60. As one can see, with the increase of pressure, the electrical conductivity decreases quite significantly. The pressure also affects quite appreciably the E_0 and σ_0 parameters in the region of impurity-related conductivity. However, in the region of intrinsic electrical conductivity, and in the pressure range of 500-20,000 kg/cm^2, the

activation energy hardly changes at all. However, if compared to the E_0 quantity for the intrinsic conductivity and at the atmospheric pressure, it has decreased by a factor of two. The intensive change of electrical conductivity and of the activation energy as a funciton of pressure is probably due to the impurities found in the sample of olivine spinel.

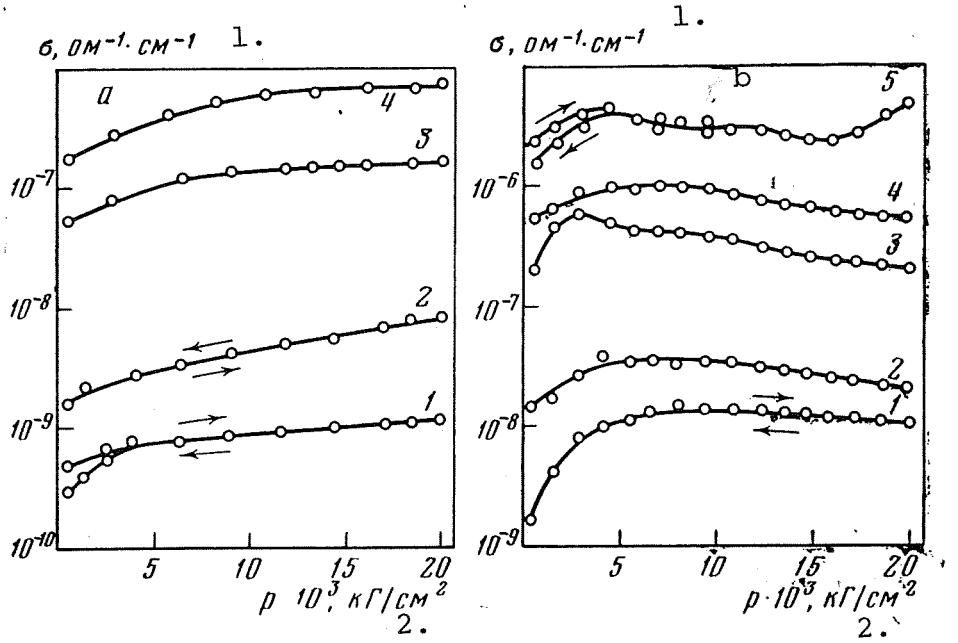

Figure 59. Electrical conductivity of quartz as a function of pressure at different temperatures.

a - along the optical axis C at t,°C, respectively: 1-4 - 320, 400, 500, 530; b - perpendicularly to C axis at t,°C, respectively: 1-5 - 200, 300, 400, 500, 600.

Key: 1. $ohm^{-1} \cdot cm^{-1}$; 2. kg/cm^2

It was also possible to obtain the data for $\sigma=f(p)$ for the monocrystalline olivine along the optical axis. In the case of this monocrystal, one observes the decreased growth of electrical conductivity as a function of pressure at the elevated temperature, so that practically σ=constant in the pressure range of 3000-20,000 kg/cm^2 at t=520°C. As a result of 20,000 kg/cm^2 pressure, the activation energy in the region of impurity-related conductivity decreases from 1.15 to 0.85 eV. The relatively high electrical conductivity of this monocrystal indicates that the amount of fialite in it is not more than 10%. /158

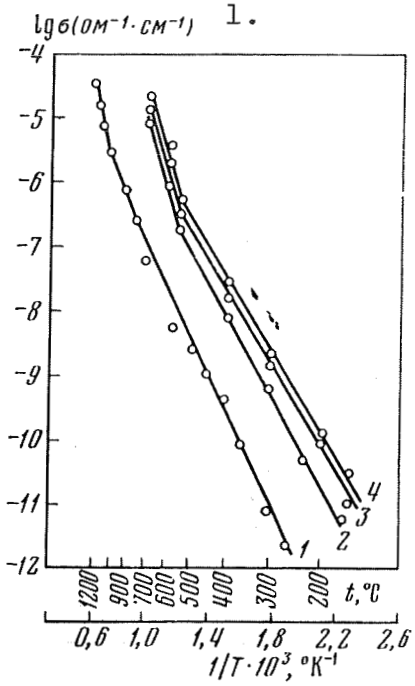

1 - atmospheric
2 - 500
3 - 6000
4 - 20,000 kg/cm^2
1 atmosphere - E_0=1.1 eV,
$\sigma_0=10^{-2}$ ohm$^{-1}\cdot$cm^{-1};
20,000 kg/cm^2 - E_0=0.83,
$\sigma_0=5\cdot10^{-2}$ (200-550°C);
E_0=1.64,
$\sigma_0=6\cdot10^{3}$ (550-700°C)

Figure 60. Electrical conductivity of olivine from dunite 2162 as a function of temperature at different pressures.
Key: 1. ohm$^{-1}\cdot$cm^{-1}

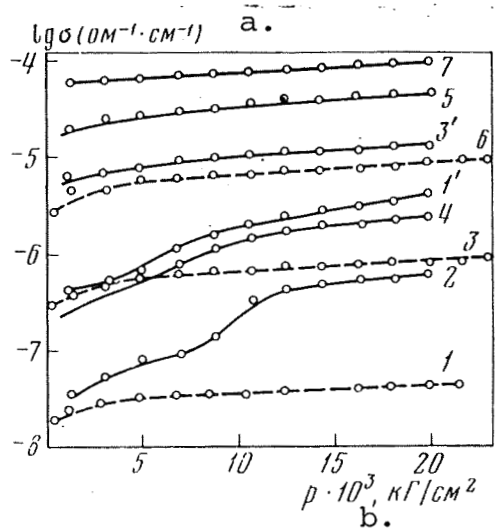

At t, °C:
1, 1' -400;
2 - 150;
3,3' - 500;
4 - 300;
5 - 600;
6 - 620;
7 - 650

Figure 61. Electrical conductivity of almandine garnet 2182 and of garnet-pyrope from the rocks 1497 (dotted line) as a function of pressure and temperature.
Key: a. ohm$^{-1}\cdot$cm^{-1}; b. pressure in kg/cm^2

The studies [143, 173, 174] also indicate the increased electrical conductivity in olivine and fialite as a function of pressure. These studies also present approximately analogous results in terms of $E_0=f(p)$ relationship. They also point out that the activation energy and the intensity of its change as a function of pressure depend on the amount of fialite present. With the increase of these amounts, the activation energy decreases and the intensity of the change as a function of pressure increases. It is of importance to substantiate this relationship by using larger amounts of material.

Garnet. The change of σ as a function of pressure and temperature in the case of mantle garnet-pyrope $Mg_3Al_2Si_3O_{12}$ and the garnet almandine $Fe_3Al_2Si_3O_{12}$ of metamorphic origin is shown in Figures 61 and 62. This data makes it possible to conclude that the chemical composition and thermodynamic conditions of this garnet formation affect quite strongly the magnitudes of σ, E_0 and σ_0 parameters and the general character of this relationship as a function of pressure. The intensive change of electrical conductivity in the pressure range of 1-20,000 kg/cm^2 is observed in the case of garnet almandine (see Figures 61 and 62), in the case of garnet-pyrope the electrical conductivity as a function of pressure is displayed only slightly (see Figure 61). Figure 62 and /159 the table below indicate the change in E_0 and lg σ_0 parameters in pyrope and almandine in the pressure range of 1-20,000 kg/cm^2 and in the temperature range of 150-700°C.

Minerals	Pressure, kg/cm^2	Temperature range t, °C	E_0, eV	lg σ_0, ohm$^{-1}\cdot$cm^{-1}
Garnet-pyrope	500	150—700	1,06	0,3
Garnet-almandine	20 000	150—700	0,96	0,2
	1	150—700	1,02	—2,6
		700—1000	1,54	1,6
	970	150—400	0,30	—5,7
		400—650	0,90	0,7
	5 000	150—400	0,22	—5,8
		400—650	0,76	—1,7
	20 000	150—400	0,20	—4,2
		400—600	0,66	—1,6

[Commas in tabulated material are equivalent to decimal points.]

This data indicates that the pressure here affects the electrical conductivity of garnets considerably less than the temperature.

Diopside. The results of electrical conductivity measurements in diopside at high pressures and temperatures are shown in Figure 63. By looking at the curves, one can see the changes in the electrical conductivity of diopside as a function of pressure and somewhat decreased slope of the curves. In addition, one observes at high pressures the point of inflection which, as has been shown earlier, has not been observed at the ordinary pressure. The change in the activation energy of diopside as a function of pressure in the temperature range 150-550°C is shown below:

Pressure, kg/cm^2	Temperature range t,°C	E_0, ev	lg σ_0, $ohm^{-1} \cdot cm^{-1}$
1	150—1200	0,89	—3,7
450	150—550	0,74	—3,7
	550—650	1,40	—1,9
2 000	150—450	0,70	—3,6
	450—650	1,40	—
22 000	150—450	0,64	—3,4
	450—650	1,40	—2,10

/160

[Commas in tabulated material are equivalent to decimal points.]

On this curve, the $E_0=f(t)$ relationship within the pressure range of 2-20 kbar is of linear character. The inflection point of the straight line lg $\sigma=f(1/T)$ at high pressures is probably associated with the contribution of the intrinsic conductivity which is very insignificant within a broad temperature range at atmospheric pressure. This is substantiated by low activation energy of 0.74-0.8 eV, and by the behavior of lg $\sigma=f(1/T)$ which is a straight line without any inflection point. However, as it is known, the pressure shifts the temperature, above which the other mechanism of conductivity will be manifested and this is the case at hand.

Eugirite. Figure 64a shows the $\sigma=f(p,t)$ relationship for eugirite 640, cut out in an arbitrary direction. One can see from the curves that the electrical conductivity of eugirite sharply increases with pressure of up to 5000-7000 kg/cm^2 and then continues increasing rectilinearly in terms of a small quantity (3-4%). Within the pressure range from atmospheric to 20,000 kg/cm^2 E_0 decreases from 0.5 to 0.4 eV.

/162

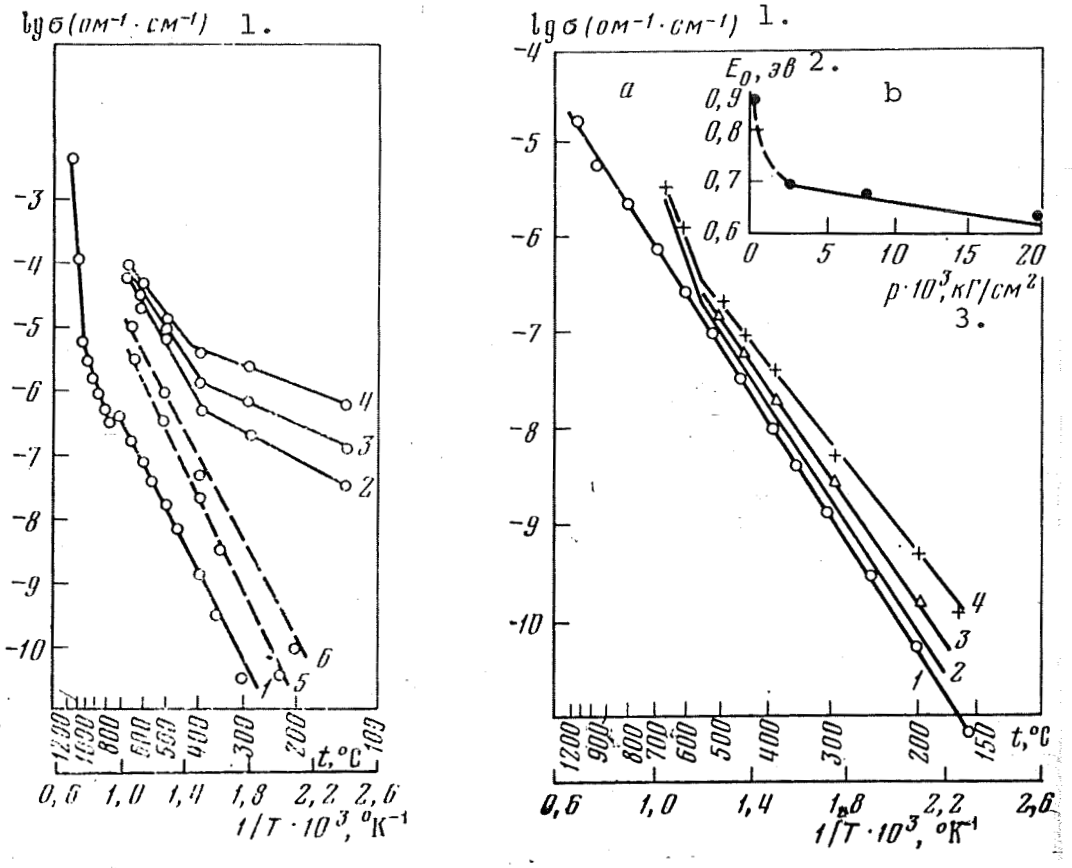

Figure 62. Electrical conductivity of almandine garnet and of garnet-pyrope (dotted lines) as function of temperature at different pressures.

1 - atmospheric pressure; 2 - 970; 3 - 5000; 4 - 20,000; 5 - 500; 6 - 20,000 kg/cm^2.

Figure 63. Electrical conductivity in diopside as a function of temperature at different pressures (a) and the activation energy within the temperature range of 150-700°C (b).

1 - atmospheric pressure; 2 - 1000; 3 - 5000; 4 - 20,000 kg/cm^2

Key: 1. ohm^{-1}·cm^{-1}; 2. E_0, eV; 3. kg/cm^2

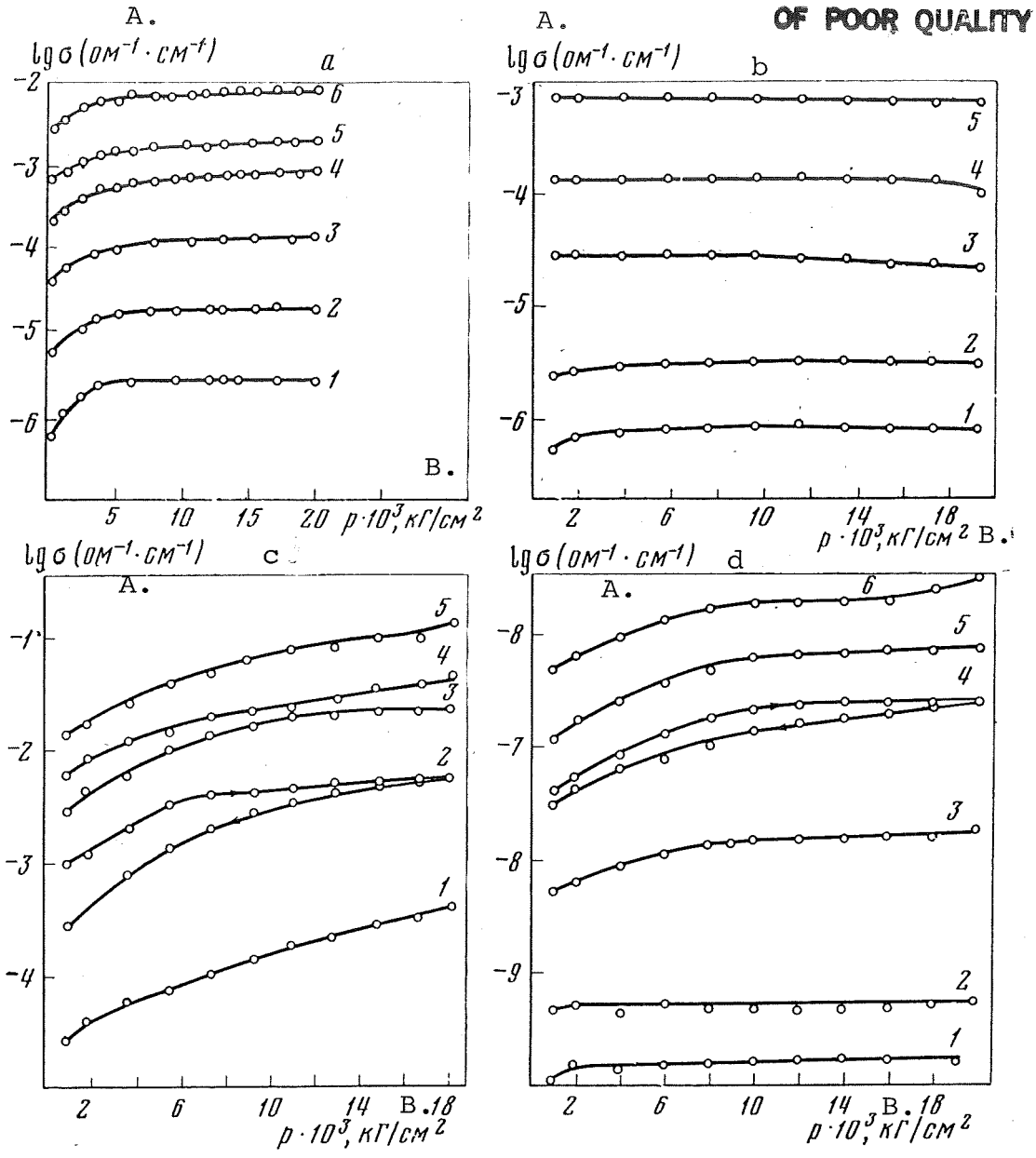

Figure 64. Electrical conductivity as a function of pressure and temperature.

a - eugirite 640 at t,°C, respectively: 1-6 - 110, 200, 300, 400, 500, 650; b - jadeite: 1-5 - 260, 300, 400, 500, 610; c - rubecite; 1-5 - 100,200, 300, 550, 600; d - serpentine: 1-6 - 200,300, 400, 500, 600.

Key: A. $ohm^{-1} \cdot cm^{-1}$; B. kg/cm^2

Jadeite. The electrical conductivity of polycrystalline jadeite as a function of pressure, just like that of the other pyroxenes, will increase. However, at the temperature above 400°C, the isotherms of electrical conductivity indicate an insignificant increase of σ only up to the pressure of 14,000 kg/cm^2, and then one observes its decrease (Figure 64b). The activation energy of jadeite is practically unchanged with the pressure increase, and is about 1.0 eV.

Rubecite. This mineral at high pressures and temperatures was investigated in four crystallographic directions. As has been noted already (Chapter I), this mineral is characterized at elevated temperatures by the highest electrical conductivity of all silicates within the group. The results of this study indicates that it displays also the greatest change of electrical conductivity (Figure 64c). The activation energy in the range of 1000-18,000 kg/cm^2 decreases only slightly. According to the experimental data, as the temperature increases, one observes less intense increase of electrical conductivity as a function of pressure increase.

Serpentine. The electrical conductivity of serpentine was investigated by using the samples cut out of two monomineral rocks from different regions. One sample is of faintly greenish color, and is characterized by low σ within the temperature range of 200-600°C and displays the increase of electrical conductivity only as a function of pressure. It is interesting that in the low temperature range (200-400°C), one observes an insignificant increase of electrical conductivity. As can be seen in Figure 64d, at p>2000 kg/cm^2 the electrical conductivity is practically independent of pressure. During a further increase of temperature, one observes increased intensity in the electrical conductivity change as a function of pressure, in other words there is a relationship which is inverse to the one obtained for olivine. The character of forward and reverse temperature change coincides quantitatively. The values of σ, as one increases and decreases the pressure, differ only slightly. The activation energy is 1.09-1.18 eV. In the case of the second serpentine sample, one observes approximately the analogous behavior of $\sigma=f(p,t)$ but with somewhat sharper increase of change in electrical conductivity as a function of p increase (in kg/cm^2) at the temperatures above 400°C:

t, °C	$1\cdot10^3$	$4\cdot10^3$	$10\cdot10^3$	$16\cdot10^3$	$20\cdot10^3$
400	$4{,}2\cdot10^{-8}$	$5{,}2\cdot10^{-8}$	$6{,}8\cdot10^{-8}$	$8{,}7\cdot10^{-8}$	$1{,}0\cdot10^{-7}$
500	$1{,}7\cdot10^{-7}$	$2{,}5\cdot10^{-7}$	$5{,}3\cdot10^{-7}$	$6{,}7\cdot10^{-7}$	$9{,}8\cdot10^{-7}$
600	$1{,}2\cdot10^{-6}$	$1{,}8\cdot10^{-6}$	$1{,}9\cdot10^{-6}$	$2{,}6\cdot10^{-6}$	$1{,}4\cdot10^{-5}$

[Commas in tabulated material are equivalent to decimal points.]

The increase of $d\sigma/dp$ on the isotherm 600°C at the pressures above 16,000 kg/cm^2 is explained by the polymorphous transformations in serpentine [175]. The activation energy in this pressure range decreases from 0.9 to 0.8 eV. /163

The group of feldspar, in terms of the change in electrical conductivity as a function of pressure differs from all the above-considered minerals, with the exception of quartz. For the albite, oligoclase, microcline and orthoclase minerals, just like in the case of x-microsection quartz, one observes the maxima of electrical conductivity at increased pressure, but they are less pronounced.

In the case of albite (Figure 65a) the behavior of $\sigma=f(p)$ for the two mutually-perpendicular directions is approximately the same, namely, almost at all temperatures one observes a gently sloping σ maxima.

A considerable decrease in electrical conductivity was obtained in the study [176] while investigating it in albite and increasing the pressure, operating at higher temperatures.

In the case of the oligoclase, with the temperature increase, the σ maximum is displaced toward lower pressures and at t>400°C, the σ is monotonically decreasing (Figure 65b). There is no noticeable change in the activation energy in this case and it is about 0.84 eV. The electrical conductivity of oligoclase was investigated by using two different monocrystals, but there is no fundamental difference in the $\sigma=f(p)$ relationship, although the crystallographic directions do not coincide.

The orthoclase, which was measured in one direction only, displays the same character in σ change as a function of pressure, as the oligoclase. The difference is only that the decrease of σ in orthoclase with the pressure increase begins at somewhat lower temperatures than in the case of the oligoclase (Figure 65c).

Microcline. The electrical conductivity of microcline was investigated by using three samples, cut out from the same monocrystal and the measurements were taken in three different crystallographic directions. Another sample which was used was cut from another monocrystal, perpendicularly to the planes of the layers. In the latter case, for the two samples of different monocrystals, the identical behavior of $\sigma=f(p,t)$ was obtained. The electrical conductivity peak maxima as a function of temperature increase, are shifted toward lower pressures. In the other two crystallographic directions, the electrical conductivity, with pressures of up to 10,000 kg/cm^2, increases more intensively than in the first case. At p>1000 kg/cm^2, the electrical conductivity at all temperatures, with the pressure increase, practically does not change and has a tendency to decrease (Figure 65d).

Nepheline. The changes in the electrical conductivity of nepheline by using the sample cut out along the optical axis, with the accuracy of 5-6°C, have shown along the curve which defines the electrical conductivity as function or pressure the observable maximum which is analogous to quartz and feldspar. Figure 65e /165
shows that this maximum, with the temperature increase, will also be shifted toward lower pressures. With the temperature increase, the magnitude of σ in nepheline, after the maximum, decreases more intensively with the pressure. For example, on the isotherm 210°C, the electrical conductivity of nepheline decreased with the pressure by 13%, and on the isotherm 600°C, it has decreased several fold.

Eudialyte. The electrical conductivity was measured on the powdery samples, in the pressure range of 500-20,000 kg/cm^2, and at t=200, 400, 500 and 600°C. The σ increases by 10-12%. The activation energy in the region of impurity-related and in the region of intrinsic conductivities does not change and is equal to 0.74 and 1.28 eV, respectively.

In generalizing this data, let us note that in terms of the character of $\sigma=f(p,t)$ relationship, the investigated minerals may be divided into two groups. In the case of one group, the garnet-olivine, diopside, eudialyte, rubecite and serpentine, in the pressure range of 1000-20,000 kg/cm^2 at t=100-700°C, one observes only the increased electrical conductivity and in the case of the second group, the feldspar and quartz, a more complex relationship as a function of pressure is characteristic, which depends on the experimental temperature and on the crystallographic directions. To elucidate the physical nature of the observed difference, one should consider the specifics of the physical parameters of each group. First of all, one should note that the feldspars are characterized by the greatest mean atomic volume and V_k volume per each oxygen ion and also the least density of ion packing. In terms of the magnitude of these parameters, the closest to these is quartz. The studies [51, 52] shows that in the case of silicates, one can see a definite relationship between the V_k and the volumetric compression k, the d and k parameters and also between the V_k and the "mean" standard entropy S^0_{298}. In addition, in all curves and in all cases, the feldspars and quartz occupy the extreme upper and lower positions. Figure 66 shows the decremental volumes $\Delta V/V_0$ in oxides and silicates as a function of pressure. As one can see, the quartz and the feldspar group feature the greatest volumetric decrement which is due to their relative porous structure. For the densely packed minerals - bromellite stishovite, this quantity is minimal. Therefore, the quartz and feldspar differ not only in terms of different $\sigma=f(p,t)$, but in terms of other physical parameters.

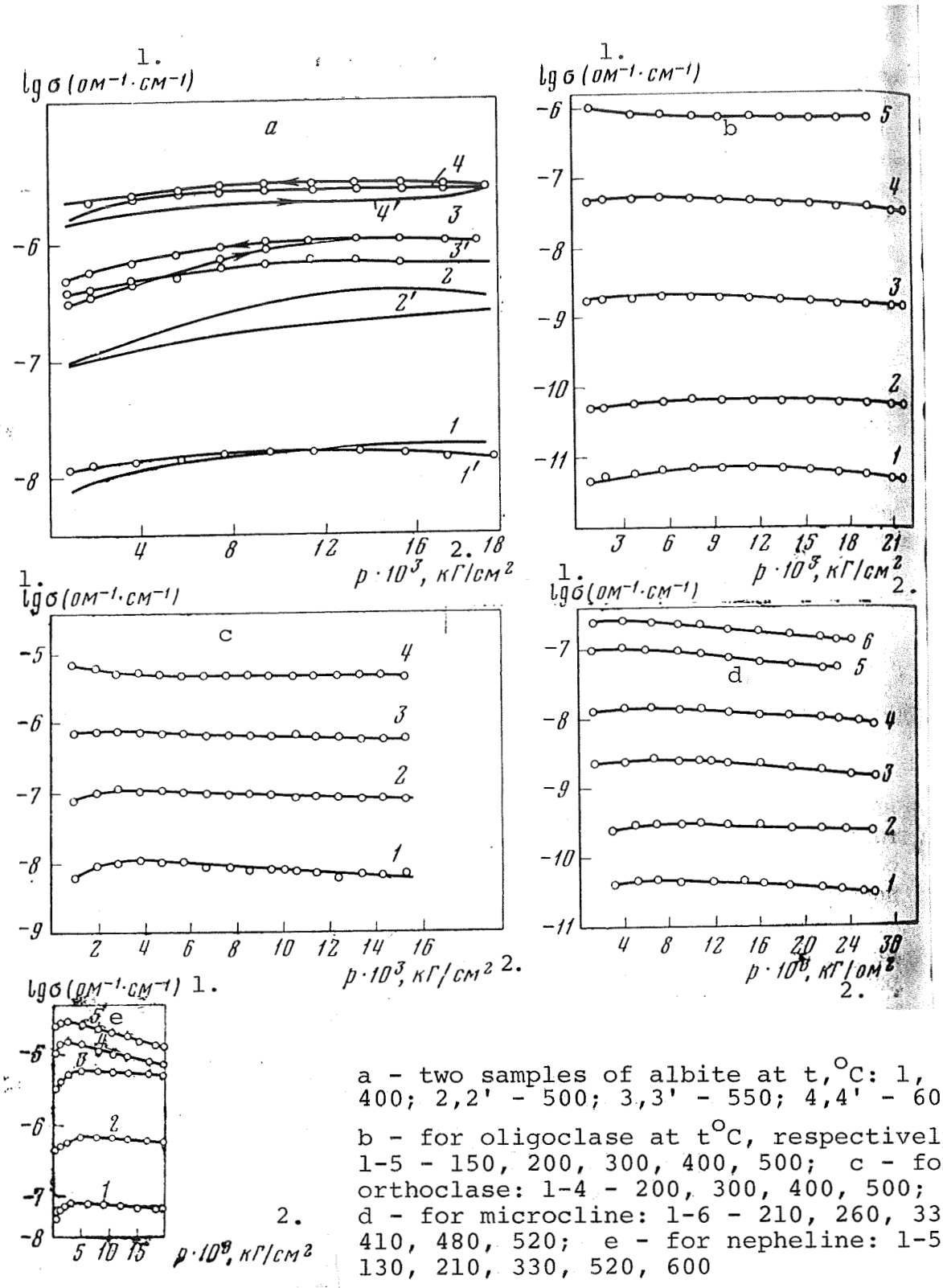

a - two samples of albite at t,°C: 1, 1' - 400; 2,2' - 500; 3,3' - 550; 4,4' - 600;

b - for oligoclase at t°C, respectively: 1-5 - 150, 200, 300, 400, 500; c - for orthoclase: 1-4 - 200, 300, 400, 500; d - for microcline: 1-6 - 210, 260, 330, 410, 480, 520; e - for nepheline: 1-5 - 130, 210, 330, 520, 600

Figure 65. Electrical conductivity as a function of pressure and temperature.

Key: 1. $ohm^{-1}.cm^{-1}$; 2. kg/cm^2

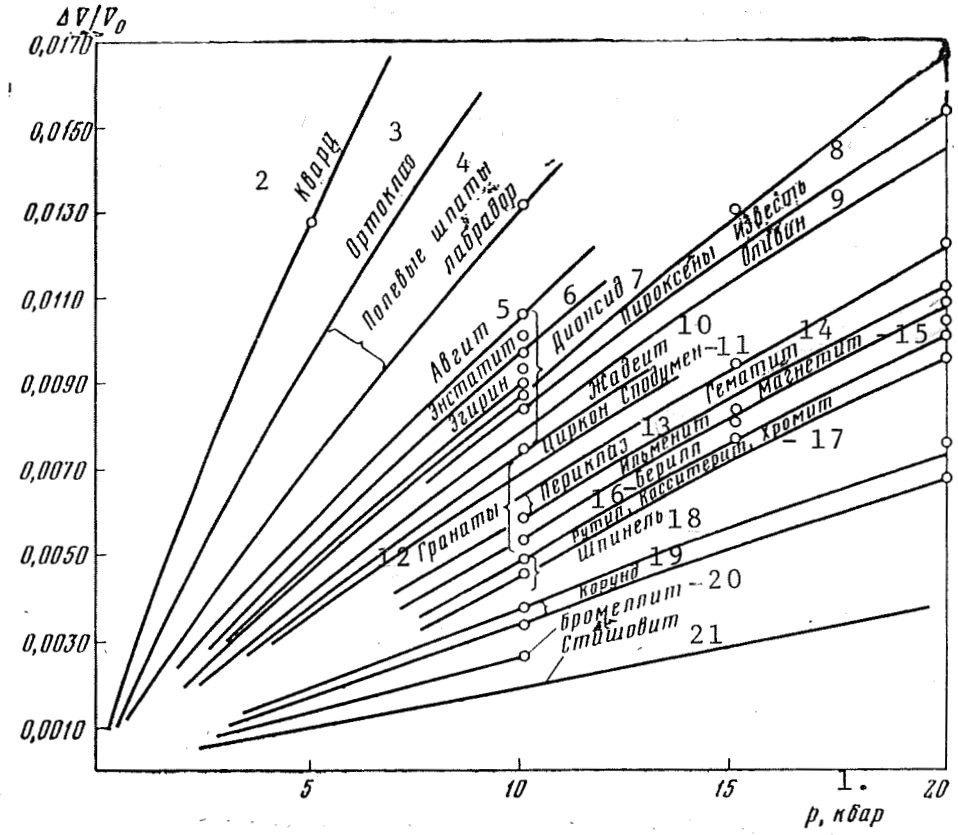

Figure 66. Volumetric decrement $\Delta V/V_0$ of oxides and silicates as a function of pressure.

Key: 1. kbar; 2. Quartz; 3. Orthoclase; 4. Feldspar,Labradorite; 5. Augite; 6. Enstatite; 7. Eugirite,diopside; 8. Pyroxenes,Lime; 9. Olivine; 10. Jadeite; 11. Zircon,Spodumene; 12. Garnets; 13. Periclase; 14. Hematite; 15. Ilmenite, Magnetite; 16. Beryl; 17. Rutile, Cassiterite, Chromite; 18. Spinel; 19. Corundum; 20. Bromellite; 21. Stishovite

Keeping in mind the values of the physical parameters and also the behavior of k=f(p) one may assume that because of their relative greater porosity, as one increases the pressure, the more intense density increase takes place, and as a result of this, the energy of the crystalline lattice may also increase. In addition, because of the decrease in the distances between the tetrahedrons of SiO_2, with the pressure increase, the movement of K and Na ions, /166 having a large ionic radii, becomes more hindered and these ions are employed in this group of minerals as the charge carriers.

In olivine, diopside and garnet, the volumetric decrement is incomparably smaller, and consequently the density increase as a function of pressure increase is small, having no significant effect on the electrical conductivity.

At somewhat higher pressures than were generated in our tests, and also at temperatures which correspond to the region of intrinsic conductivities, one can observe the decrease of electrical conductivity which also follows from the following equation

$$q_F=U_F+PV_F-TS_p,$$

where q_F is the free energy, according to Gibbs, necessary to remove the arbitrarily assigned ion from its normal position within the lattice and to place it at the arbitrarily chosen interpoint space at the constant temperature T and constant pressure p, S_p is the entropy and U_F and V_F are the internal energy and free volume of the formation.

One should also consider here such phenomenon as the displacement of maximum in $\sigma=f(p,t)$ with the temperature increase. It appears that this phenomenon may be observed in conjunction with /167 the increase of the anion effective radius, (and also possible that of the cation radius) with the temperature increase, which naturally will accelerate the pressure increase at which the ion mobility decreases. The other cause may be the increase of the volumetric decrement as a function of the temperature increase.

4. Electrical Conductivity of the Crystalline Rock Foundation at High Pressures and Temperatures

The electrical conductivity of the crystalline rocks was investigated at high pressures, up to 20,000 kg/cm^2 in the temperature range of 100-700°C. The measurements under such conditions were brought about by using dry samples, in other words the behavior of $\sigma=f(p,t)$ relationship could be affected only by the structure of the rock and by the properties of the minerals incorporated in the rock. Some data related to this question are presented in the studies [173, 174, 177-179].

TABLE 26. ELECTRICAL PARAMETERS OF GARNETS AND DIORITES

Rock	$p \cdot 10^3$, kg/cm^2	Temperature range t, °C	E_0, eV	$\lg \sigma_0$, ohm^{-1}.cm^{-1}
Garnet 304-9	1,0	150—270	0,50	—6,6
	20,0	150—290	0,30	—8,75
	1,0	270—500	0,85	—4,1
	20,0	200—500	1,00	—4,5
266-1	1,0	100—500	0,9	—5,6
	20,0	100—500	0,8	—5,5
Grano- 54-440 diorite	1,0	200—500	1,0	—3,2
	20,0	200—500	0,8	—2,75
Diorite 250-12	1,0	150—280	0,65	—4,2
	20,0	150—200	0,70	—4,0
	1,0	280—500	1,20	—2,75
	20,0	200—500	1,00	—2,25
89-1	1,0	150—300	0,55	—4,4
	20,0	150—300	0,60	—3,7

[Commas in tabulated material are equivalent to decimal points.]

The obtained electrical conductivities for garnets, granodiorite and diorite are shown in Table 26. For the rocks which display different intenstity and character of change in $\sigma=f(p,t)$, the curves were constructed and are shown in Figure 67 a,b,c. It should be noted that the studied garnets differed from each other in terms of the intensity of electrical conductivity change as a function of pressure, and the garnet 77-3 had even different type of $\sigma=f(p)$ function. In the case of the latter (see Figure 67c), at t=200-300°C, the electrical conductivity was increased only sightly, but at 400°C it practically has no change and during further temperature increase, it becomes even lower with the pressure increase.

Such behavior of electrical conductivity in this garnet at high pressures and temperatures is related to the predominance in the rock of quartz (48-50%) and of feldspar (~50%). The quartz and the minerals of the feldspar group, as has been shown earlier, differ from the majority of the silicate minerals in having fundamentally different relationship of σ change as a function of pressure, in other words, it either displays the σ maximum, or has the decreased electrical conductivity as a function of pressure increase. Since this rock is composed of these minerals, and its

porosity is small (K=1.6%), naturally, the character of this relationship is reflected in the total change of electrical conductivity in the garnet components as a function of pressure.

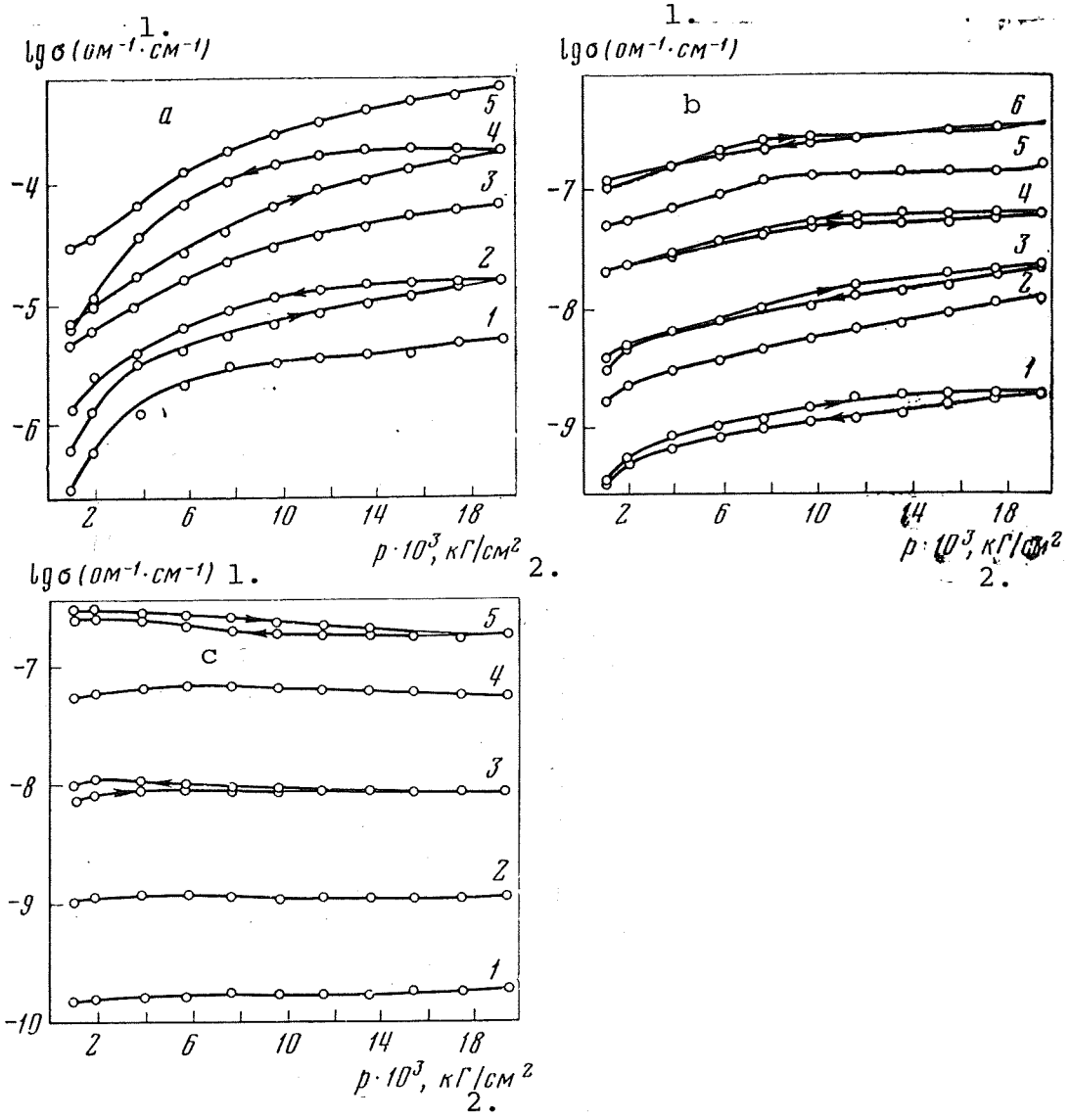

Figure 67. Electrical conductivity as a function of pressure and temperature.
a - for garnet 768-246 at t, °C, respectively: 1-5 - 150, 200, 300, 400, 500; b - for amphibole garnet 85-3: 1-6 - 200, 250, 300, 400, 450, 500; c - for garnet 77-3: 1-5 - 200, 300, 350, 400, 500.

Key: 1. $ohm^{-1} \cdot cm^{-1}$; 2. kg/cm^2

The garnets 266-1, 206-21 and 303-1 have similar mineral composition with lower quantities of quartz, and display only the increase of electrical conductivity with the increase of pressure. The higest rate of change in electrical conductivity as a function of the pressure increase is characterized by the garnets which underwent secondary changes. For example, the pelitic garnet 85-3 displays a considerable increase of σ across the whole pressure range. Even to a greater degree the electrical conductivity increases in the other garnet - 768-246 which underwent intense cataclasis and the corresponding secondary changes. The secondary processes of seritization and carbonatization significantly change the structure of the primary minerals, making them more porous, which results in a considerable increase in the number of defective ions with low bonding energy. This is reflected not only in the values of all electrical parameters, but to a certain degree, changes the electrical conductivity as a function of pressure. /169

The quartz diorite 206-21 and diorite 250-12 and 89-1 contain smaller amounts of quartz. In conjunction with this, they feature larger electrical conductivity but, just like garnets, are characterized by a broad range of $\frac{\Delta\sigma}{\sigma}\cdot 100\%$ ratio. The higher electrical conductivity of diorites as compared to garnets is due to the presence in them of dark colored minerals from the amphibole group. All these rocks are affected in one way or another by the secondary processes. The studies have shown that the intensity in increase of the electrical conductivity is directly related to the degree of alterations which occurred within the rock.

The greatest $\frac{\Delta\sigma}{\sigma}\cdot 100\%$ ratio is displayed by diorite 89-1, which is most affected by the secondary processes. In contrast to some garnets, the intermediate rocks across the whole temperature range show only the increase of electrical conductivity as a function of pressure. In addition, in the case of all four rocks which were investigated, as the temperature was increased, the intensity of change in electrical conductivity as a function of pressure has decreased. Approximately the same relationship is observed in the case of garnets. We shall present below the E_0 and σ_0 values for some of these rocks.

It follows from all this data that the pre-exponential coefficients, being affected by pressure, may either decrease or increase. This behavior is due to the physical nature of the changes in electrical conductivity. When the activation energy does not change and the electrical conductivity increases considerably, σ_0 may increase because of the increase in mobility and in the number of current carriers. As the activation energy decreases, σ_0 ordinarily drops somewhat. In the case of a number of samples (266-1, 304-9, 303-1, 206-21 and 89-1), the change in

activation energy is within the range of the measuring error. At the same time, in the granodiorite 54-440, in the amphibolite garnet 85-3, in the plageogarnet, it decreases by 40%, while the pressure is increased from 1000 to 20,000 kg/cm^2. In addition, in the case of some rocks, one observes the change in the position of the point of inflection, as we change the temperature from 20 to 100°C, with the point being lower as a result of pressure. /170

In parallel with the study of igneous rocks, we have investigated the other possible representatives of the crystalline base - the amphibolites and gneisses. The electrical conductivity of some amphibolites increases by approximately a factor of 10, with the pressure increase from 600 to 20,000 kg/cm^2 at the temperatures of up to 400°C, and at 500°C $\Delta\sigma/\sigma=0.1$ (Figure 68), the activation energy will decrease from 0.67 to 0.48 eV. The electrical conductivity of crystalline shales within this pressure range and at the temperature of up to 695°C will increase by 40-60%. The results of investigation of gneisses show that their electrical conductivity increases within the pressure range of 1-20,000 kg/cm^2 by more than one order of magnitude (Table 27) and that the activation energy drops from 0.6to 0.45 eV, while the pre-exponential coefficient changes from $2\cdot10^{-2}$ to $6\cdot10^{-2}$ ohm$^{-1}\cdot$cm^{-1}. For the garnet gneiss, one notes an insignificant increase of electrical conductivity as a function of pressure, which may be due to high amounts of quartz and also to high amounts of garnet.

Gabbro. In all gabbros which were investigated the electrical conductivity increased with pressure. Gabbro differs from granite, gneiss and diorite by having less intense change of σ with pressure. The maximum increase of electrical conductivity ($N=\Delta\sigma/\sigma\approx8$) at t=400°C, in the pressure range of $1\text{-}20\cdot10^3$ kg/cm^2, was in the case of gabbro 28-52. Within the temperature range of 200-300°C, N was also large (N=7.1). In the remaining cases, N fluctuates between 0.45 and 1.5. The electrical conductivity change as a function of pressure is displayed to the least degree in the case of gabbro-norite 75-26 (see Table 27). It should be noted that the maximum change of electrical conductivity for the majority of gabbros corresponds to a temperature of about 500°C, at which one observes the inflection point on the lg σ=f(1/T) curve. The isotherms (Figure 69a,b) are located parallel to each other and the relationship is close to linear. In the case of all gabbro, one observes a good agreement in σ in both directions of the parameter changes. The specific features of gabbros which were studied are the similar activation energies (E_0=0.75 eV) within the temperature range of 150-500°C. With the increase of pressure from 1000 to 20,000 kg/cm^2, the E_0 has a tendency to increase only slightly. The shift in the inflection point on the lg σ=f(1/T) as a result of pressure is barely observed, and the maximum shift of 30-40°C has been observed only in the case of one gabbro of seven. /174

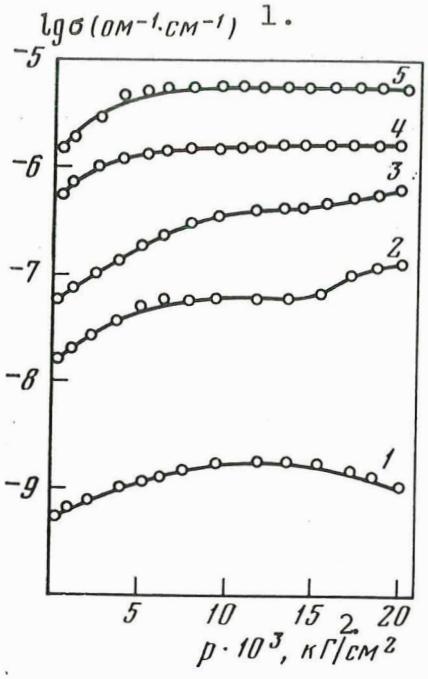

Figure 68. Electrical conductivity of amphibolite 220 as a function of pressure and temperature.

At t, °C, respectively: 1-5 - 20, 220, 320, 420, 500.

Key: 1. $ohm^{-1} \cdot cm^{-1}$; 2. kg/cm^2

5. Electrical Conductivity of Basalts and Dolerites

The basalts, just like gabbros, are characterized by the decreased electrical conductivity as a function of the pressure increase. According to the data presented below, the intensity of this change in the area of relatively low pressures (up to 10,000 kg/cm^2) depends to a considerable degree on the structure of the pores and on the coefficient of porosity. The highly porous basalt 5/22 is characterized by the increased electrical conductivity, by the lower activation energy and by the shift of the curve inflection point toward lower temperatures. In addition, the greatest change of σ takes place before the inflection point (Figure 70). Such sharp increase of σ should be associated with the decrease of porosity and improved contact between small grains of the rock and the thinly dispersed ore mineral. This may be substantiated by looking at the nonlinear segment of $\sigma=f(p,t)$ before the pressures of 8000 kg/cm^2 are attained (Figure 71, curve 7). However, after that, the electrical conductivity of basalt 5/22 continues to increase linearly, probably because of the change in activation energy (see Figure 71) which is due to the elastic compression of the crystalline environment of minerals. The appearance of new rectilinear segments in the curves of $\lg \sigma=f(1/T)$ indicates the appearance of another mechanism of electrical conductivity as a result of pressure. The dolerite 61-b (Table 28) behaves analogously, except for the decrease of E_0 quantity in the region of intrinsic conductivity (Table 29). On the other hand, the basalt 602, in contrast to the basalts 5-22 and 61-b, displays only insignificant change of σ as a function of pressure, a small decrease of E_0 and the temperature-related points of inflection are not shifting. The electrical conductivity of basalts 161 and 313, which were taken from the rift zone of the Indian Ocean, display the relationship as a function of pressure which is analogous to the continental basalts. The activation energy of basalt 313 at the pressures of up to 25,000 kg/cm^2 did not change and E_0 in basalt 161, as the pressure

/175

TABLE 27. ELECTRICAL CONDUCTIVITY OF ROCKS AT HIGH PRESSURES AND TEMPERATURES

Rock	Mineral composition	t, °C	$p \cdot 10^3$, kg/cm^2 1	5	10	15	20	$\frac{\Delta\sigma}{\sigma} \cdot 100\%$
Granite 77-3	Plageoclase -45 quartz-50, hornblende -3-4	200	$1,3 \cdot 10^{-10}$	$1,64 \cdot 10^{-10}$	$1,7 \cdot 10^{-10}$	$1,76 \cdot 10^{-10}$	$1,8 \cdot 10^{-10}$	38,4
		300	$1,26 \cdot 10^{-9}$	$1,14 \cdot 10^{-9}$	$1,11 \cdot 10^{-9}$	$1,03 \cdot 10^{-9}$	$1,2 \cdot 10^{-9}$	—4,7
		400	$5,3 \cdot 10^{-8}$	$6,64 \cdot 10^{-8}$	$6,3 \cdot 10^{-8}$	$5,56 \cdot 10^{-8}$	$5,3 \cdot 10^{-8}$	0
		500	$2,84 \cdot 10^{-7}$	$2,88 \cdot 10^{-7}$	$2,28 \cdot 10^{-7}$	$1,84 \cdot 10^{-7}$	$1,74 \cdot 10^{-7}$	—38,7
		550	$6,38 \cdot 10^{-7}$	$6,4 \cdot 10^{-7}$	$5,74 \cdot 10^{-7}$	$5,62 \cdot 10^{-7}$	$7,7 \cdot 10^{-7}$	20,3
Alaskite granite 266-1	Albite-35, calcspar-30, quartz-35	200	$5,6 \cdot 10^{-10}$	$4,76 \cdot 10^{-9}$	$6,94 \cdot 10^{-10}$	$7,15 \cdot 10^{-10}$	$8,8 \cdot 10^{-10}$	57,0
		300	$8,3 \cdot 10^{-10}$	$1,04 \cdot 10^{-10}$	$1,53 \cdot 10^{-9}$	$1,45 \cdot 10^{-9}$	$1,4 \cdot 10^{-9}$	69,0
		400	$1,3 \cdot 10^{-8}$	$1,52 \cdot 10^{-8}$	$1,45 \cdot 10^{-8}$	$1,62 \cdot 10^{-8}$	$1,7 \cdot 10^{-8}$	30,4
		500	$8,3 \cdot 10^{-8}$	$9,8 \cdot 10^{-8}$	$1,01 \cdot 10^{-7}$	$1,1 \cdot 10^{-7}$	$1,10 \cdot 10^{-9}$	32,2
		550	$2,3 \cdot 10^{-7}$	$2,63 \cdot 10^{-7}$	$2,95 \cdot 10^{-7}$	$2,78 \cdot 10^{-7}$	$3,3 \cdot 10^{-7}$	43,5
Quartz diorite 206-21	Plageoclase-55, hornblende-25, quartz-15	200	$2,1 \cdot 10^{-9}$	$2,9 \cdot 10^{-9}$	$3,14 \cdot 10^{-9}$	$3,08 \cdot 10^{-9}$	$3,0 \cdot 10^{-9}$	43,0
		300	$1,3 \cdot 10^{-8}$	$2,33 \cdot 10^{-8}$	$3,22 \cdot 10^{-8}$	$3,82 \cdot 10^{-8}$	$4,2 \cdot 10^{-8}$	22,0
		400	$4,4 \cdot 10^{-7}$	$5,75 \cdot 10^{-7}$	$7,65 \cdot 10^{-7}$	$8,41 \cdot 10^{-7}$	$9,8 \cdot 10^{-7}$	12,0
		500	$1,7 \cdot 10^{-5}$	$2,78 \cdot 10^{-5}$	$3,84 \cdot 10^{-5}$	$4,55 \cdot 10^{-5}$	$5,0 \cdot 10^{-5}$	29,4
Muscovite-biotite granite 303-1	Albite-35, calcspar-30, quartz-32-30, biotite, muscovite-2.5	200	$3,0 \cdot 10^{-10}$	$7,0 \cdot 10^{-10}$	$7,35 \cdot 10^{-10}$	$6,72 \cdot 10^{-10}$	$6,7 \cdot 10^{-10}$	123,0
		300	$4,5 \cdot 10^{-10}$	$7,2 \cdot 10^{-10}$	$8,32 \cdot 10^{-10}$	$9,51 \cdot 10^{-10}$	$1,05 \cdot 10^{-9}$	145,0
		400	$1,9 \cdot 10^{-8}$	$3,72 \cdot 10^{-8}$	$4,92 \cdot 10^{-8}$	$5,56 \cdot 10^{-8}$	$5,9 \cdot 10^{-8}$	210,0
		500	$1,1 \cdot 10^{-7}$	$2,23 \cdot 10^{-7}$	$3,94 \cdot 10^{-7}$	$4,64 \cdot 10^{-7}$	$4,7 \cdot 10^{-7}$	327,0
		550	$3,2 \cdot 10^{-7}$	$4,86 \cdot 10^{-7}$	$9,52 \cdot 10^{-7}$	$1,32 \cdot 10^{-6}$	$1,5 \cdot 10^{-6}$	400,0

[Commas in tabulated material are equivalent to decimal points.]

(Table 27 is continued on the following page)

TABLE 27 (continued)

Rock	Mineral composition	t, °C	$p \cdot 10^3$, kg/cm^2 1	5	10	15	20	$\frac{\Delta\sigma}{\sigma} \cdot 100\%$
Hornblende plageoclase 85.3	Plageoclase-65, quartz-28-30, hornblende-5-6	200	$3,2 \cdot 10^{-10}$	$6,24 \cdot 10^{-10}$	$1,1 \cdot 10^{-9}$	$1,52 \cdot 10^{-9}$	$1,2 \cdot 10^{-9}$	270,0
		300	$2,9 \cdot 10^{-9}$	$6,24 \cdot 10^{-9}$	$1,04 \cdot 10^{-8}$	$1,56 \cdot 10^{-8}$	$2,2 \cdot 10^{-8}$	660,0
		400	$2,0 \cdot 10^{-8}$	$2,7 \cdot 10^{-8}$	$2,18 \cdot 10^{-8}$	$3,57 \cdot 10^{-8}$	$6,2 \cdot 10^{-8}$	209,0
		500	$1,0 \cdot 10^{-7}$	$1,52 \cdot 10^{-7}$	$2,71 \cdot 10^{-7}$	$2,95 \cdot 10^{-7}$	$3,7 \cdot 10^{-7}$	206,0
Granite 768-246	Plageoclase-55, quartz-42 (underwent cataclasis)	200	$5,9 \cdot 10^{-7}$	$3,21 \cdot 10^{-6}$	$6,1 \cdot 10^{-6}$	$1,13 \cdot 10^{-5}$	$1,5 \cdot 10^{-5}$	2440,0
		300	$4,4 \cdot 10^{-6}$	$9,64 \cdot 10^{-6}$	$2,96 \cdot 10^{-5}$	$5,32 \cdot 10^{-5}$	$8,7 \cdot 10^{-5}$	1880,0
		400	$5,1 \cdot 10^{-6}$	$1,75 \cdot 10^{-5}$	$6,42 \cdot 10^{-5}$	$1,28 \cdot 10^{-4}$	$1,9 \cdot 10^{-4}$	3610,0
		500	$2,9 \cdot 10^{-5}$	$6,41 \cdot 10^{-5}$	$2,57 \cdot 10^{-4}$	$4,77 \cdot 10^{-4}$	$6,3 \cdot 10^{-4}$	2030,0
Diorite 250-12		200	$4,1 \cdot 10^{-9}$	$1,44 \cdot 10^{-8}$	$2,26 \cdot 10^{-8}$	$2,65 \cdot 10^{-8}$	$3,0 \cdot 10^{-8}$	630,0
		300	$7,4 \cdot 10^{-8}$	$2,04 \cdot 10^{-7}$	$3,21 \cdot 10^{-7}$	$3,85 \cdot 10^{-7}$	$4,4 \cdot 10^{-7}$	495,0
		400	$2,4 \cdot 10^{-6}$	$4,17 \cdot 10^{-6}$	$6,67 \cdot 10^{-6}$	$7,94 \cdot 10^{-6}$	$8,5 \cdot 10^{-6}$	252,0
		500	$3,8 \cdot 10^{-5}$	$7,82 \cdot 10^{-5}$	$8,2 \cdot 10^{-5}$	$8,2 \cdot 10^{-5}$	$8,2 \cdot 10^{-5}$	195,0
Diorite amphibolite 89-1	Plageoclase-65-70, quartz-15, amphibole-10-12, magnetite-3-4, zircon-2	200	$2,4 \cdot 10^{-8}$	$4,54 \cdot 10^{-8}$	$9,6 \cdot 10^{-8}$	$1,67 \cdot 10^{-7}$	$2,4 \cdot 10^{-7}$	900,0
		300	$2,0 \cdot 10^{-7}$	$4,05 \cdot 10^{-7}$	$9,02 \cdot 10^{-7}$	$1,62 \cdot 10^{-6}$	$2,4 \cdot 10^{-6}$	1100,0
		400	$6,5 \cdot 10^{-7}$	$1,5 \cdot 10^{-6}$	$4,10 \cdot 10^{-6}$	$6,94 \cdot 10^{-6}$	$9,4 \cdot 10^{-6}$	1350,0
		500	$5,2 \cdot 10^{-7}$	$8,34 \cdot 10^{-7}$	$1,54 \cdot 10^{-6}$	$3,33 \cdot 10^{-6}$	$3,2 \cdot 10^{-6}$	515,0

(Table 27 is continued on the following page)

Table 27 (continued)

Rock	Mineral composition	t, °C	p·10, kg/cm²					$\frac{\Delta\sigma}{\sigma}\cdot 100\%$
			1	5	10	15	20	
Andradite-salite-gneiss* 1410	Quartz-77-72, plageoclase -10 scapolite -18-20, pyrope - 1-2	200	$4,6\cdot10^{-8}$	$1,3\cdot10^{-7}$	$2,1\cdot10^{-7}$	$2,5\cdot10^{-7}$	$3,0\cdot10^{-7}$	550,0
		300	$8,0\cdot10^{-7}$	$1,8\cdot10^{-6}$	$2,6\cdot10^{-6}$	$3,2\cdot10^{-6}$	$3,9\cdot10^{-6}$	387,0
		400	$1,8\cdot10^{-6}$	$5,4\cdot10^{-6}$	$8,9\cdot10^{-6}$	$1,2\cdot10^{-5}$	$1,7\cdot10^{-5}$	844,0
		500	$4,9\cdot10^{-6}$	$1,4\cdot10^{-5}$	$2,0\cdot10^{-5}$	$2,7\cdot10^{-5}$	$3,6\cdot10^{-5}$	634,0
		600	$1,2\cdot10^{-5}$	$3,3\cdot10^{-5}$	$4,0\cdot10^{-5}$	$5,9\cdot10^{-5}$	$7,7\cdot10^{-5}$	640,0
Olivine gabbro 844-3	Labrodorite-55, olivine-22-25, pyroxene-17-18, clinpyroxene-7-10	200	$8,3\cdot10^{-10}$	$1,32\cdot10^{-9}$	$1,54\cdot10^{-9}$	$1,67\cdot10^{-9}$	$1,7\cdot10^{-9}$	104,0
		300	$1,0\cdot10^{-8}$	$1,57\cdot10^{-8}$	$1,97\cdot10^{-8}$	$2,33\cdot10^{-8}$	$2,6\cdot10^{-8}$	157,0
		400	$1,8\cdot10^{-7}$	$2,63\cdot10^{-7}$	$3,4\cdot10^{-7}$	$3,71\cdot10^{-7}$	$4,0\cdot10^{-7}$	122,0
		500	$1,0\cdot10^{-6}$	$1,48\cdot10^{-6}$	$2,09\cdot10^{-6}$	$2,44\cdot10^{-6}$	$2,5\cdot10^{-6}$	150,0
		600	$7,0\cdot10^{-6}$	$1,2\cdot10^{-5}$	$1,46\cdot10^{-5}$	$1,5\cdot10^{-5}$	$1,5\cdot10^{-5}$	114,0
Gabbro-norite 74-26	Labrodorite - 50, olivine-10, pyroxine- 25, monoclinpyroxene, rhombic -12, ore mineral -1.0-1.5	200	$7,8\cdot10^{-11}$	$1,04\cdot10^{-10}$	$1,16\cdot10^{-10}$	$1,16\cdot10^{-10}$	$1,3\cdot10^{-10}$	67,5
		300	$1,1\cdot10^{-9}$	$1,36\cdot10^{-9}$	$1,51\cdot10^{-9}$	$1,56\cdot10^{-9}$	$1,6\cdot10^{-9}$	45,0
		400	$1,4\cdot10^{-8}$	$1,82\cdot10^{-8}$	$2,04\cdot10^{-8}$	$2,13\cdot10^{-8}$	$2,1\cdot10^{-8}$	50,0
		500	$1,2\cdot10^{-7}$	$1,61\cdot10^{-7}$	$1,93\cdot10^{-7}$	$2,13\cdot10^{-7}$	$2,3\cdot10^{-7}$	92,0
		600	$2,0\cdot10^{-6}$	$2,35\cdot10^{-6}$	$2,67\cdot10^{-6}$	$2,9\cdot10^{-6}$	$2,9\cdot10^{-6}$	45,0
Gabbro hornblende 95-1	Plageoclase - 40, hornblende-53 sulfides 6-7	200	$3,1\cdot10^{-8}$	$4,84\cdot10^{-8}$	$6,0\cdot10^{-8}$	$6,85\cdot10^{-8}$	$7,5\cdot10^{-8}$	142,0
		300	$5,0\cdot10^{-7}$	$7,15\cdot10^{-7}$	$9,5\cdot10^{-7}$	$1,08\cdot10^{-6}$	$1,1\cdot10^{-6}$	120,0
		400	$8,4\cdot10^{-6}$	$1,12\cdot10^{-5}$	$1,61\cdot10^{-5}$	$1,86\cdot10^{-5}$	$2,0\cdot10^{-5}$	138,0
		500	$3,6\cdot10^{-5}$	$6,06\cdot10^{-5}$	$9,7\cdot10^{-5}$	$1,18\cdot10^{-4}$	$1,3\cdot10^{-4}$	260,0
		560	$5,7\cdot10^{-3}$	$1,08\cdot10^{-4}$	$1,75\cdot10^{-4}$	$2,21\cdot10^{-4}$	$2,4\cdot10^{-4}$	41,6

[Commas in tabulated material are equivalent to decimal points.]

Remark. The rock samples were made available by A. K. Kurskeyev, and the measurements were done by A. Dauylbayev.

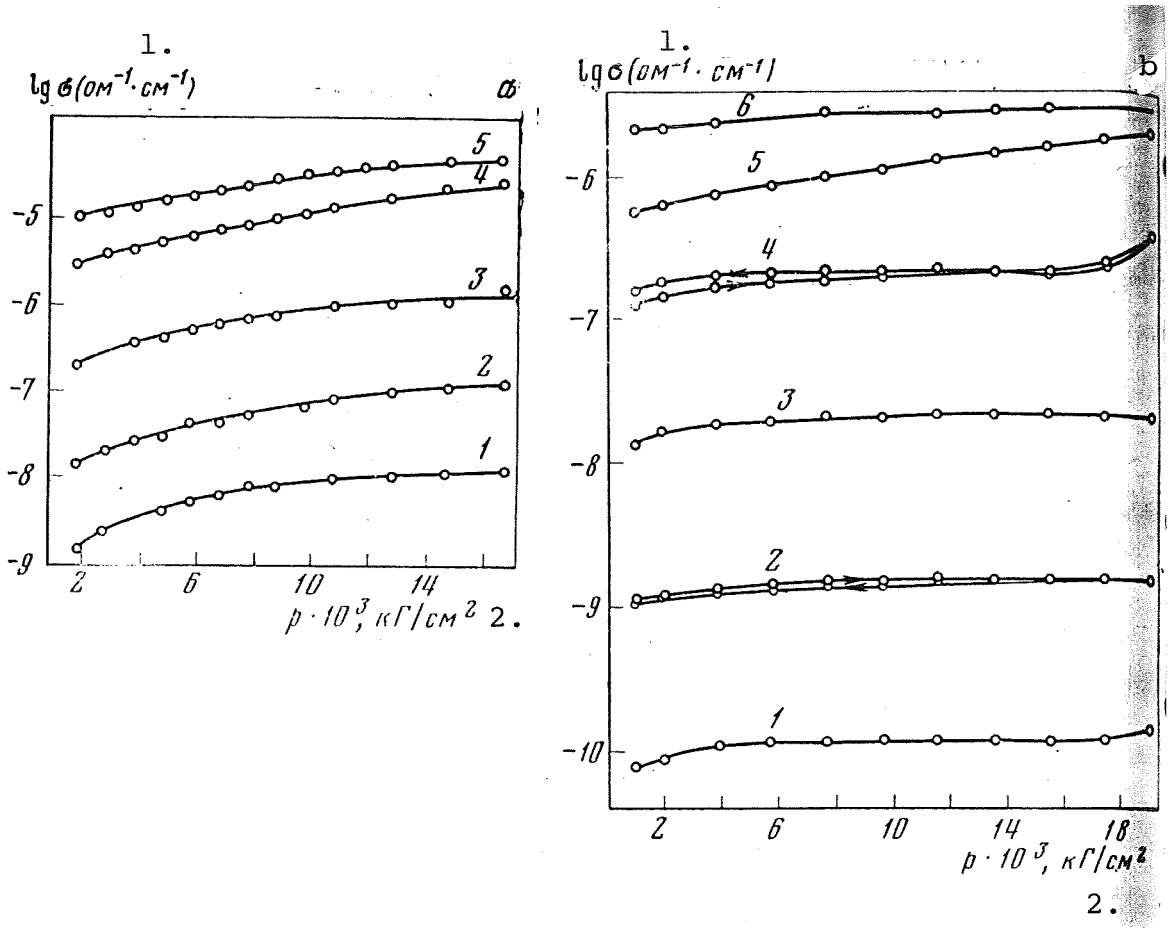

Figure 69. Electrical conductivity as a function of pressure and temperature.

a - for gabbro 28-52 at t, ^{o}C, respectively: 1-5 - 100, 200, 300, 400, 450; b - for gabbro-norite: 1-6 - 200, 300, 400, 500, 550, 600.

Key: 1. ohm^{-1}·cm^{-1}; 2. kg/cm^{2}

was increased from 960 to 22,000 kg/cm^2, has correspondingly decreased from 0.625 to 0.45 eV (see Table 29). It is interesting to note that in the olivine basalt 1483, the point of inflection on the curve which is the result of the pressure change, has been shifted toward somewhat lower temperatures, from 650 to 550°C. /176

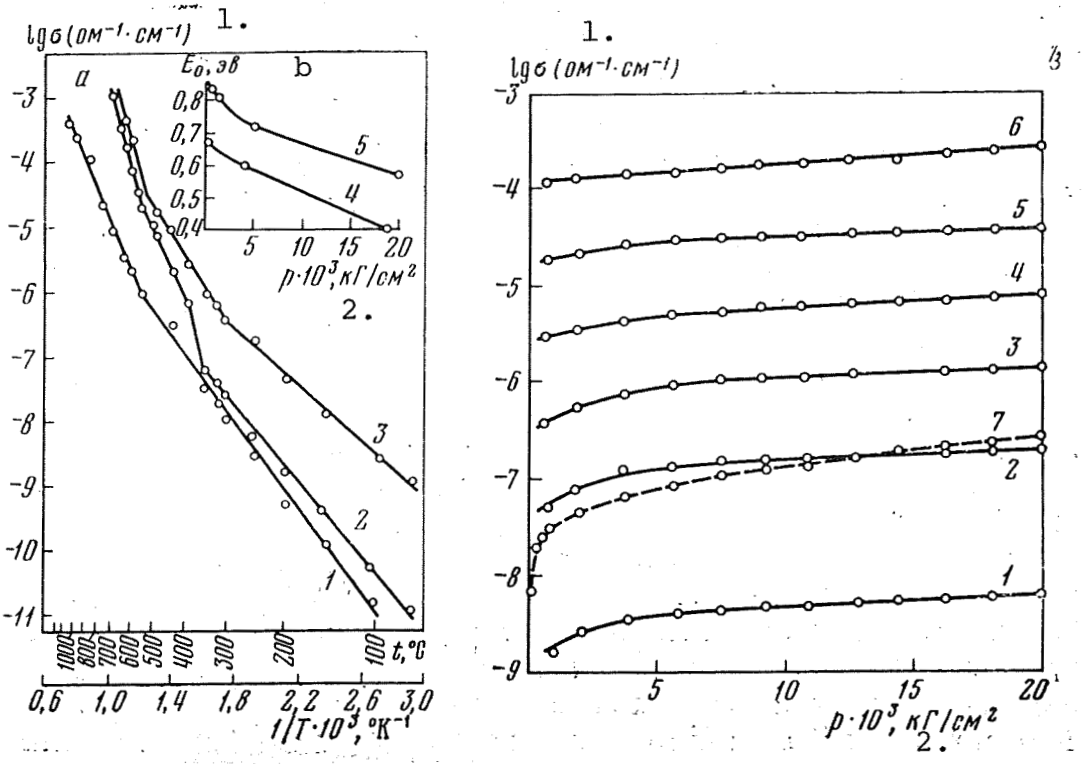

Figure 70. Electrical conductivity (a) and activation energy (b) in basalt 5/22 as a function of temperature at different pressures.

1 - atmospheric pressure; 2 - 5000; 3 - 12,000 kg/cm^2; 4 - change of E_0 for basalt 5/22; 5 - E_0 for basalt 21 within the temperature range of t=100-700°C.

Figure 71. Electrical conductivity of basalt as a function of pressure at different temperatures.

1-6 basalt 21 at t, °C, respectively: 200, 300, 400, 500, 600 and 680; 7 - basalt 5/22 at 350.

Key: 1. ohm^{-1}.cm^{-1}; 2. kg/cm^2

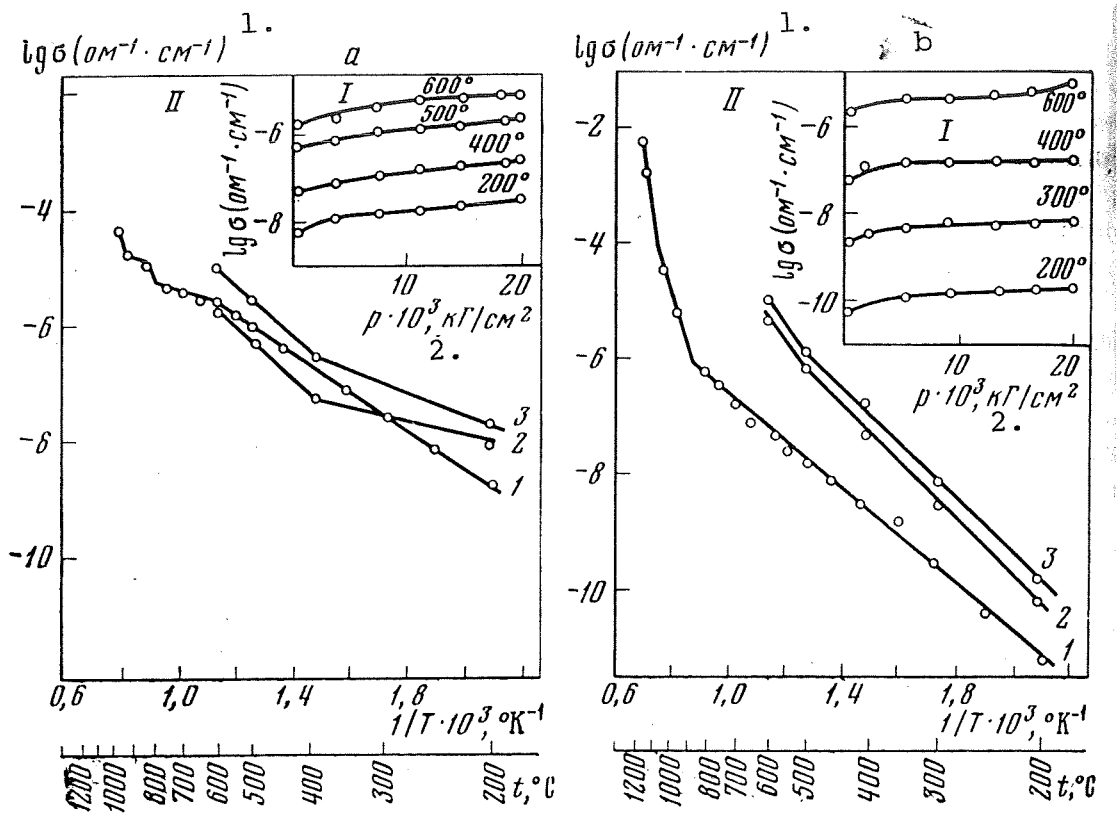

Figure 72. Electrical conductivity of basalts as a function of pressure (I) and of temperature (II).

a - basalt 1295: 1 - atmospheric pressure; 2 - 500; 3 - 20,000 kg/cm^2;
b - basalt 1114: 1 - atmospheric pressure; 2 - 500; 3 - 20,000 kg/cm^2.

Key: 1. ohm^{-1}·cm^{-1}; 2. kg/cm^2

The shift of such point of inflection for basalts which contain no olivines occurs before 400°C (see Table 29). The activation energy in the region of impurity-related (extrinsic) and intrinsic σ in basalt 1483, as a function of pressure, does not change and is 0.7 and 1.4 eV, respectively. In the case of basalt 21, the activation energy, in the presence of pressures within the intrinsic conductivity range remains constant (1.4 eV) and within the region of impurity-related conductivity, it decreases from 0.83 to 0.57 eV. The basalts from the Caucasus which were studied, utilizing the sample 1295 (porosity of 0.6%) (Figure 72a) and 1114 (porosity 26.8%) (Figure 72b) have indicated a significant relationship between the electrical conductivity and pressure. In the case of highly porous basalt 1114, as one can see in Figure 72b, the electrical conductivity changes less than in the case of basalt 1295. This may be explained by the fact that in the presence of all-around pressure exposure, the highly porous samples

of basalts undergo inelastic deformation, while the sample is exposed to the preliminary pressure of 500-800 kg/cm^2. Therefore, the electrical conductivity, as one removes this pressure, does not revert to the initial state of the unloaded sample. Because of this, the isobar of electrical conductivity in the case of basalt 1114 at the pressure of 800 kg/cm^2 adjoins the isobar of 20,000 kg/cm^2, while in the presence of atmospheric pressure, /178 when the sample is not deformed, it is shifted quite a ways down. The temperature- related inflection point on the curve has shifted from 850 to 500°C and E_0 changed from 0.82 to 0.98 eV, and from 3.58 to 1.36 eV, in other words, in the region of impurity-related conductivity, E_0 has increased and in the intrinsic conductivity region - it has decreased quite considerably. In addition, the isobar slope at 500° and 20,000 kg/cm^2 area, within the region of intrinsic conductivity has not changed (see Figure 72b, curves 2 and 3), and therefore the E_0 quantity which is equal to 1.36 eV probably is defining the intrinsic conductivity of basalts at the appropriate pressures. The high E_0=3.58 eV for the 850-1050°C /179 segment, at atmospheric pressure, may not be due to the intrinsic conductivity, and therefore it defines the physical and chemical processes which take place within the rock in this temperature range. These results indicate that in the presence of pressures, the mechanism of intrinsic electrical conductivity is manifested much more at lower temperatures and is characterized by lower E_0.

As we can see, one can draw the conclusion that the high electrical conductivities which are found at atmospheric pressure are complicated by various types of structural disruptions which, generally speaking, are not characteristic for the rocks which /181 are found at greater depth.

The change in electrical conductivity as a function of pressure in the Caucasus dolerites 511, 527 and 490 which have the porosity of 5.0, 9.4 and 11.7%, respectively (Figure 73a,b,c) is of the same character as in the case of some basalts, in other words in the case of dolerites which have less porosity, the electrical conductivity as a function of pressure will increase more than in the case of dolerites which have high porosity. It is of interest here that in the dolerite 511 (Figure 73a) the isobars at 500 and 20,000 kg/cm^2 do not have the inflection point, while in the case of dolerite 490, we do have such inflection point, and it is being shifted towards lower temperatures, down to 300°C. At the present time it is difficult to explain the different behavior of $\sigma=f(p,t)$ function, but on the basis of mineral composition, it is quite likely that the shift of the inflection point in the case of dolerite 490, down to 300°C, is due to the high amounts of volcanic glass and of the ore minerals (9.8%). The dolerite 511

TABLE 28. ELECTRICAL CONDUCTIVITY IN BASALTS AND DOLERITES AS A FUNCTION OF PRESSURE AND TEMPERATURE

/177

Rock, No. of sample	Porosity %	Temperature °C	σ(ohm^{-1}·cm^{-1}) at p, kg/cm^2 950	5000	10 000	15 000	20 000
Siberian traps							
Small grain dolerite, porphyrous, 61-b	0,52	200	—	$2,2\cdot10^{-9}$	$9,1\cdot10^{-9}$	$1,1\cdot10^{-8}$	$1,3\cdot10^{-8}$
		400	—	$1,3\cdot10^{-6}$	$2\cdot10^{-6}$	$2,6\cdot10^{-6}$	$2,8\cdot10^{-6}$
		500	$3,2\cdot10^{-5}$	$4,9\cdot10^{-5}$	$6,4\cdot10^{-5}$	$7,1\cdot10^{-5}$	$7,7\cdot10^{-5}$
		600	—	$1,7\cdot10^{-4}$	$2,5\cdot10^{-4}$	$3,2\cdot10^{-4}$	$3,6\cdot10^{-4}$
Intermediate grain dolerite 108-b		650	$1,5\cdot10^{-4}$	$3,7\cdot10^{-4}$	$6\cdot10^{-4}$	$6,7\cdot10^{-4}$	$7,7\cdot10^{-4}$
	—	200	$2,9\cdot10^{-9}$	$5,3\cdot10^{-9}$	$6,2\cdot10^{-9}$	$6,9\cdot10^{-9}$	$7,4\cdot10^{-9}$
		300	$3,9\cdot10^{-8}$	$7,1\cdot10^{-8}$	$8,5\cdot10^{-8}$	$8,5\cdot10^{-8}$	$8,5\cdot10^{-8}$
		400	$3,2\cdot10^{-7}$	$6,3\cdot10^{-7}$	$7,4\cdot10^{-7}$	$8,1\cdot10^{-7}$	$8,8\cdot10^{-7}$
		500	$8,5\cdot10^{-7}$	$1,9\cdot10^{-7}$	$2,1\cdot10^{-6}$	$2,2\cdot10^{-6}$	$2,7\cdot10^{-6}$
		600	$3,6\cdot10^{-5}$	$4,3\cdot10^{-5}$	$5,4\cdot10^{-5}$	$5,7\cdot10^{-5}$	$6,5\cdot10^{-5}$
		700	$1,5\cdot10^{-4}$	$1,7\cdot10^{-4}$	$2,4\cdot10^{-4}$	$2,5\cdot10^{-4}$	$3,2\cdot10^{-4}$
Indian Ocean							
Small grain basalt 161	—	100	$3,1\cdot10^{-10}$	$7,9\cdot10^{-10}$	$1,1\cdot10^{-9}$	$1,2\cdot10^{-9}$	$1,3\cdot10^{-9}$
		200	$1,4\cdot10^{-8}$	$3,1\cdot10^{-8}$	$3,7\cdot10^{-8}$	$4,3\cdot10^{-8}$	$4,6\cdot10^{-8}$
		300	$2,1\cdot10^{-7}$	$3,3\cdot10^{-7}$	$3,7\cdot10^{-7}$	$4,1\cdot10^{-7}$	$4,2\cdot10^{-7}$
		400	$1,1\cdot10^{-6}$	$2,0\cdot10^{-6}$	$2,4\cdot10^{-6}$	$2,9\cdot10^{-6}$	$3,2\cdot10^{-6}$
		520	$1,1\cdot10^{-5}$	$1,3\cdot10^{-5}$	$1,6\cdot10^{-5}$	$1,7\cdot10^{-5}$	$1,8\cdot10^{-5}$
		600	$6,6\cdot10^{-5}$	$7,5\cdot10^{-5}$	$8,1\cdot10^{-5}$	$8,3\cdot10^{-5}$	$8,9\cdot10^{-5}$
Small grain basalt 313	—	200	$5,5\cdot10^{-9}$	$1,03\cdot10^{-8}$	$1,2\cdot10^{-8}$	$1,4\cdot10^{-8}$	$1,6\cdot10^{-8}$
		300	$4,7\cdot10^{-8}$	$7,4\cdot10^{-8}$	$1,1\cdot10^{-7}$	$1,2\cdot10^{-7}$	$1,5\cdot10^{-7}$
		400	$4,7\cdot10^{-7}$	$6,7\cdot10^{-7}$	$9,1\cdot10^{-7}$	$1,1\cdot10^{-6}$	$1,4\cdot10^{-6}$
		500	$2,4\cdot10^{-6}$	$3\cdot10^{-6}$	$3,7\cdot10^{-6}$	$4,1\cdot10^{-6}$	$4,7\cdot10^{-6}$
		650	$9,5\cdot10^{-5}$	$1,2\cdot10^{-4}$	$1,5\cdot10^{-4}$	$1,8\cdot10^{-4}$	$1,9\cdot10^{-4}$
Olivine basalt-oceanite 1483	—	250	$3,9\cdot10^{-9}$	$6,5\cdot10^{-9}$	$8,6\cdot10^{-9}$	$1,1\cdot10^{-8}$	$1,3\cdot10^{-8}$
		300	$1,4\cdot10^{-8}$	$2,9\cdot10^{-8}$	$3,7\cdot10^{-8}$	$5\cdot10^{-8}$	$6\cdot10^{-8}$
		400	$6,2\cdot10^{-8}$	$1,2\cdot10^{-7}$	$1,7\cdot10^{-7}$	$1,9\cdot10^{-7}$	$2,3\cdot10^{-7}$
		500	$3,5\cdot10^{-7}$	$6,8\cdot10^{-7}$	$6,8\cdot10^{-7}$	$9,6\cdot10^{-7}$	$1,1\cdot10^{-6}$
		600	$2,5\cdot10^{-6}$	$2,9\cdot10^{-6}$	$4\cdot10^{-6}$	$5,9\cdot10^{-6}$	$6,1\cdot10^{-6}$
		650	$4,9\cdot10^{-6}$	$6,6\cdot10^{-6}$	$1,1\cdot10^{-5}$	$1,12\cdot10^{-5}$	$1,13\cdot10^{-5}$
Caucasus							
Basalt 1295	0,6	200	$6,2\cdot10^{-9}$	$1,1\cdot10^{-8}$	$1,8\cdot10^{-8}$	$2,3\cdot10^{-8}$	$2,6\cdot10^{-8}$
		300	$1,6\cdot10^{-8}$	$3,4\cdot10^{-8}$	$5,1\cdot10^{-8}$	$7\cdot10^{-8}$	$7,8\cdot10^{-8}$
		400	$5,1\cdot10^{-8}$	$1\cdot10^{-7}$	$1,5\cdot10^{-7}$	$1,9\cdot10^{-7}$	$2,3\cdot10^{-7}$
		500	$5,2\cdot10^{-7}$	$5,7\cdot10^{-7}$	$1,3\cdot10^{-6}$	$1,7\cdot10^{-6}$	$4,1\cdot10^{-6}$
		600	$1,6\cdot10^{-6}$	$3,4\cdot10^{-6}$	$5,6\cdot10^{-6}$	$7,1\cdot10^{-6}$	$8,1\cdot10^{-6}$

Table 28 is continued on the following page

Table 28 (continued)

Rock, No. of sample	Porosity %	Temperature °C	σ (ohm^{-1}·cm^{-1}) at p, kg/cm^2 950	5000	10 000	15 000	20 000
			Caucasus				
Basalt 1114	26,8	200	$5,5\cdot10^{-11}$	$6,6\cdot10^{-11}$	$1,2\cdot10^{-10}$	$1,6\cdot10^{-10}$	$1,6\cdot10^{-10}$
		300	$2,1\cdot10^{-9}$	$3,1\cdot10^{-9}$	$5,1\cdot10^{-9}$	$6,2\cdot10^{-9}$	$7,3\cdot10^{-9}$
		400	$5,9\cdot10^{-8}$	$1,2\cdot10^{-7}$	$1,4\cdot10^{-7}$	$1,6\cdot10^{-7}$	$1,7\cdot10^{-7}$
		500	$5,5\cdot10^{-7}$	$7,4\cdot10^{-7}$	$1,06\cdot10^{-6}$	$1,2\cdot10^{-6}$	$1,3\cdot10^{-6}$
		600	$3,8\cdot10^{-6}$	$4,3\cdot10^{-6}$	$5,2\cdot10^{-6}$	$6,7\cdot10^{-6}$	$1,1\cdot10^{-5}$
Dolerite 511	5	200	$6,4\cdot10^{-9}$	$2,5\cdot10^{-8}$	$5,2\cdot10^{-8}$	$8,2\cdot10^{-8}$	$1,2\cdot10^{-7}$
		300	$1,8\cdot10^{-7}$	$7,2\cdot10^{-7}$	$1,4\cdot10^{-6}$	$1,9\cdot10^{-6}$	$2,6\cdot10^{-6}$
		400	$3,9\cdot10^{-6}$	$1,6\cdot10^{-6}$	$6,9\cdot10^{-6}$	$1,4\cdot10^{-5}$	$1,7\cdot10^{-5}$
		500	$1,1\cdot10^{-5}$	$1,6\cdot10^{-5}$	$2,3\cdot10^{-5}$	$3,7\cdot10^{-5}$	$3,9\cdot10^{-5}$
		600	$1,6\cdot10^{-5}$	$3,8\cdot10^{-5}$	$4,6\cdot10^{-5}$	$6,5\cdot10^{-5}$	$7,3\cdot10^{-5}$
			Sichote-Alin (alkaline) series				
Nepheline basalt, 7	13,1	220	$1,12\cdot10^{-8}$	$2,45\cdot10^{-8}$	$3,78\cdot10^{-8}$	$4,64\cdot10^{-8}$	$6,42\cdot10^{-8}$
		400	$1,66\cdot10^{-6}$	$1,92\cdot10^{-6}$	$2,37\cdot10^{-6}$	$2,77\cdot10^{-6}$	$3,04\cdot10^{-6}$
		500	$5,56\cdot10^{-6}$	$1,04\cdot10^{-5}$	$1,24\cdot10^{-5}$	—	$1,38\cdot10^{-5}$
		600	$4,95\cdot10^{-5}$	$7,24\cdot10^{-5}$	$7,58\cdot10^{-5}$	—	$8,47\cdot10^{-5}$
		700	$5,18\cdot10^{-4}$	$5,56\cdot10^{-4}$	$5,56\cdot10^{-4}$	$5,62\cdot10^{-4}$	$7,0\cdot10^{-4}$
Porous basalt, 602	15–21	200	$1,7\cdot10^{-8}$	$2,4\cdot10^{-8}$	$2,7\cdot10^{-8}$	$3,2\cdot10^{-8}$	$3,8\cdot10^{-8}$
		300	$2,2\cdot10^{-7}$	$3,4\cdot10^{-7}$	$4,3\cdot10^{-7}$	$4,3\cdot10^{-7}$	$4,8\cdot10^{-7}$
		420	$3,9\cdot10^{-6}$	$4,5\cdot10^{-6}$	$5,2\cdot10^{-6}$	$5,9\cdot10^{-6}$	$6,6\cdot10^{-6}$
		500	$1,3\cdot10^{-5}$	$2,2\cdot10^{-5}$	$2,8\cdot10^{-5}$	$3\cdot10^{-5}$	$3,1\cdot10^{-5}$
		600	$1,1\cdot10^{-4}$	$1,3\cdot10^{-4}$	$1,4\cdot10^{-4}$	$1,5\cdot10^{-4}$	$1,6\cdot10^{-4}$
Spinel-olivine basalts 271 (high clay-Earth series)	3,6	150	$9,1\cdot10^{-9}$	$1,77\cdot10^{-8}$	$1,84\cdot10^{-8}$	$2,13\cdot10^{-8}$	$2,43\cdot10^{-8}$
		300	$2,04\cdot10^{-8}$	$5,0\cdot10^{-8}$	$7,75\cdot10^{-8}$	$9,44\cdot10^{-8}$	$1,02\cdot10^{-7}$
		400	$6,67\cdot10^{-8}$	$1,55\cdot10^{-7}$	$2,57\cdot10^{-7}$	$2,9\cdot10^{-7}$	$3,42\cdot10^{-7}$
		500	$3,7\cdot10^{-7}$	$9,34\cdot10^{-7}$	$1,35\cdot10^{-6}$	$1,55\cdot10^{-6}$	$1,59\cdot10^{-6}$
		600	$8,83\cdot10^{-6}$	$1,07\cdot10^{-5}$	$1,16\cdot10^{-5}$	$1,19\cdot10^{-5}$	$1,25\cdot10^{-5}$

[Commas in tabulated material are equivalent to decimal points.]

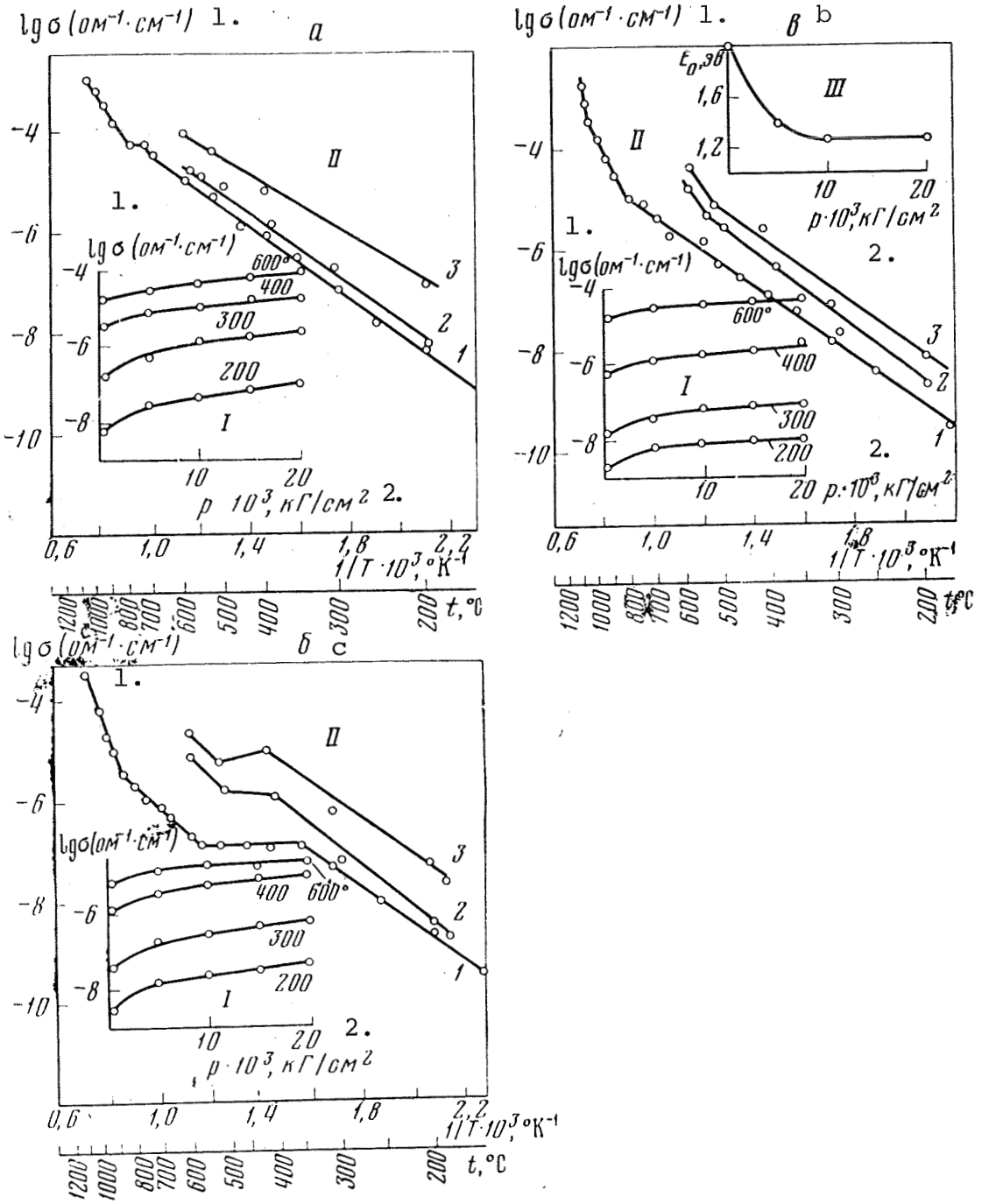

Figure 73. Electrical conductivity of Caucasus dolerites 511 (a), 527 (b), 490 (c) as a function of pressure (I), temperature (II) and the activation energy as a function of pressure (III). 1 - atmospheric pressure, 2 - 500, 3 - 20,000 kg/cm^2.

Key: 1. ohm^{-1}·cm^{-1}; 2. kg/cm^2

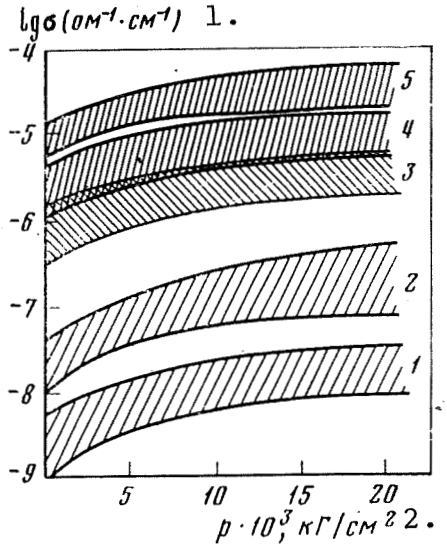

Figure 74. Regions of electrical conductivity curve extension for dolerite and dolerite basalt as a function of pressure at different temperatures.

At t, ^{o}C respectively:
1-5 - 200, 300, 400, 500, 600.

Key: 1. ohm^{-1}·cm^{-1}; 2. kg/cm^{2}

contains two times less of the ore mineral and the bulk of the rock is made of plageoclase (67.3%). In addition, it contains significantly large number of diopside molecules. It is shown in Chapter I that diopside has higher σ than a number of other minerals, and up to the temperature of 1200^{o}C, does not show any inflection point on the curve. Therefore, the electrical conductivity in the dolerite 511 is much higher than in the dolerite 490. It is necessary to point out that the temperature range of the anomalous curve behavior in the case of basalts as a function of pressures is narrowing down, and that the temperature-related inflection point as a function of pressure is shifted toward higher temperatures (Figure 73b). Figure 74 shows the areas in which the isotherms of electrical conductivity of dolerites and dolerite basalts from the Caucasus folding strata are found within a narrower range and these isotherms were obtained at the pressures of up to 20,000 kg/cm^{2} and the temperatures of up to 600^{o}C. The isotherms of σ in basalts which do not incorporate volcanic glass and thinly dispersed ore material would not fit into this area because they have higher σ.

The extensive experimental material which we have presented, /182 describing the relationship between electrical conductivity in basalts of different mineral composition as a function of pressure indicates that within the investigated range of pressures and temperatures, one observes only the increase of σ, and the intensity of this increase decreases with the pressure increase. The activation energy for a number of basalts within the region of impurity-related (extrinsic) conductivity decreases, while for some of these rocks, it remains constant, which is defined to a considerable degree by the character and extent of porosity. As a rule, within the region of intrinsic conductivity, E_0 does not increase.

TABLE 29. ELECTRICAL CONDUCTIVITY AS A FUNCTION OF TEMPERATURE AND PRESSURE

/180

Rock, No. of sample	Pressure, kg/cm^2	Temperature range, t, °C	E_a, eV	$\lg \sigma_0$, ohm^{-1} · cm^{-1}
Low grain dolerite, 61 b	1 atm	150—500	0,70	—2,2
	1 atm	500—900	0,98	0,4
	1 atm	900—1100	3,54	14,5
	12000	150—350	0,54	—2,4
	12000	350—600	0,82	0,9
	12000	600—700	3,20	13,0
Intermediate grain dolerite, 108	200	200—550	0,70	—2,6
	200	550—690	2,84	7,2
	1000	200—550	0,65	—2,4
	1000	550—690	2,84	7,2
	20000	200—550	0,64	—1,2
	20000	550—690	2,84	7,2
Porous basalt, 602	200	100—300	0,47	—2,2
	200	300—550	2,84	7,2
	200	550—690	0,90	0,8
	5000	100—300	0,35	—3,4
	5000	300—650	0,90	0,9
	10000	100—300	0,35	—3,6
	10000	300—650	0,9	2,2
Highly porous basalt, 5/22	1 atm	100—550	0,66	—3,9
	1 atm	550—1100	1,22	1,0
	5000	100—350	0,6	—3,2
	5000	350—550	1,06	—2,6
	5000	550—700	1,8	6,3
	12000	100—310	0,48	—3,3
	12000	310—550	0,8	0,2
	12000	550—700	1,8	6,6
Intermediate porous basalt, 161	960	100—580	0,625	—1,0
	960	580—700	1,4	4,7
	10000	100—580	0,55	—1,1
	10000	580—700	1,4	4,9
	20000	100—580	0,45	—2,7
	20000	580—700	1,4	4,2
Basalt, 1295	1 atm	150—600	0,55	0,3
	1 atm	600—800	0,32	—4,2
	1 atm	800—875	2,6	5,3
	500	200—400	0,28	—6,3
Basalt, 1295	500	400—650	0,90	—1,5
	20000	200—400	0,40	—4,5
	20000	400—650	0,90	—1,9
Dolerite, 511	1 atm	150—875	0,74	0,2
	1 atm	875—1050	1,50	2,9
	20000	200—600	0,60	—3,5

/181

[Commas in tabulated material are equivalent to decimal points.]

According to the data of N. I. Khitarov and A. B. Slutskiy [176], at the temperatures above 700°, the electrical conductivity of basalt will decrease with the pressure increase.

6. Electrical Conductivity in Ultrabasic Rocks, in the Xenoliths of Ultrabasic Composition and the Mantle Eclogites

In the course of study of the electrical conductivity distribution in the upper mantle, of great interest is the data which shows the effect of pressure on the electrical parameters of the ultrabasic rocks. The generalized and comprehensive parameters of electrical conductivity obtained at the atmospheric and high pressures in the case of olivines, olivinites and pyrope peridotites, are presented in Tables 17, 30 and in Figure 75.

The investigated pyrope peridotite 2163 is a xenolith of the kimberlite formations, which contain minerals found at great depth (olivine, garnet-pyrope, chromium-diopside). Figure 75 shows the shift of the inflection point in the curve for $\lg \sigma = f(1/T)$ toward the lower temperatures which is the result of pressure. Because of the fact that the isobars display the inflection point on the curve at the same temperature (600°), one should assume that this shift of the temperature inflection point on the curves is due to closure of pores at comparatively low /184
pressures, and also to the improvement of contact between the electrode and sample. It should be noted that if by using some preliminary pressure, one is to remove these structural defects which do not characterize the physical properties of the rocks at greater depth [2], then the intrinsic electrical conductivity will be contributing at somewhat lower temperatures, and the earlier activation of the mechanism of intrinsic conductivity at greater depth will produce higher electrical conductivities. This becomes quite apparent by looking at the isobars 1-2 in Figure 75. The activation energy in the pressure range of 1000-20,000 kg/cm^2 is 0.64-0.62 eV, and in the region of intrinsic conductivity it is 1.78-2.0 eV. As we can see, if referenced against the atmospheric pressure, this type of rock is characterized by lower E_0. Therefore, one may assume that the E_0 quantity, as presented, characterizes the region of electrical conductivity in the magnesium-rich material of the mantle.

Change of electrical conductivity and of the activation /185
energies during polymorphous transitions in olivines and eclogites.

The experiments have shown that in the course of polymorphous transitions, the electrical conductivity may increase by a factor of 1.5-2. For example, as one can see in Figure 76, the electrical conductivities as a function of temperature and

TABLE 30. ELECTRICAL CONDUCTIVITY σ (ohm$^{-1}\cdot$cm^{-1}) IN THE ULTRABASIC ROCKS AS A FUNCTION OF PRESSURE AND TEMPERATURE

Rock, No. of sample	Temperature, °C	$p\cdot10^3$, kg/cm^2 0,95	5	10	15	20
Pyrope eclogite, 2259	200	$4,5\cdot10^{-11}$	$7\cdot10^{-11}$	$9\cdot10^{-11}$	10^{-10}	$1,3\cdot10^{-10}$
	400	10^{-8}	$1,5\cdot10^{-8}$	$1,8\cdot10^{-8}$	$2,1\cdot10^{-8}$	$2,6\cdot10^{-8}$
	500	$1,2\cdot10^{-7}$	$1,4\cdot10^{-7}$	$1,6\cdot10^{-7}$	$1,9\cdot10^{-7}$	$2,2\cdot10^{-7}$
	600	$4\cdot10^{-7}$	$6,8\cdot10^{-7}$	10^{-6}	$1,5\cdot10^{-6}$	$2\cdot10^{-6}$
	650	$5,1\cdot10^{-6}$	$6,4\cdot10^{-6}$	$6,9\cdot10^{-6}$	$8\cdot10^{-6}$	$8,6\cdot10^{-6}$
Olivinite 1482	300	$1,8\cdot10^{-10}$	$2,6\cdot10^{-10}$	$3,3\cdot10^{-10}$	$3,8\cdot10^{-10}$	$4,4\cdot10^{-10}$
	400	$1,7\cdot10^{-9}$	$2,4\cdot10^{-9}$	$2,9\cdot10^{-9}$	$3,3\cdot10^{-9}$	$4,1\cdot10^{-9}$
	500	$6,2\cdot10^{-8}$	$1,05\cdot10^{-7}$	$1,5\cdot10^{-7}$	$1,7\cdot10^{-7}$	$1,9\cdot10^{-7}$
	600	$9,2\cdot10^{-7}$	$1,4\cdot10^{-6}$	$1,9\cdot10^{-6}$	$2,2\cdot10^{-6}$	$2,4\cdot10^{-6}$
	650	$2,9\cdot10^{-6}$	$4,2\cdot10^{-6}$	$7,6\cdot10^{-6}$	$7,9\cdot10^{-6}$	$9,3\cdot10^{-6}$
Almandine eclogite 1320	150	$3,6\cdot10^{-9}$	$5,8\cdot10^{-9}$	$7,5\cdot10^{-9}$	$8,3\cdot10^{-9}$	$9,1\cdot10^{-9}$
	350	$1,1\cdot10^{-6}$	$1,66\cdot10^{-6}$	$1,8\cdot10^{-6}$	$2,0\cdot10^{-6}$	$2,1\cdot10^{-6}$
	400	$2,5\cdot10^{-6}$	$5\cdot10^{-6}$	$5,5\cdot10^{-6}$	$5,9\cdot10^{-6}$	$7,2\cdot10^{-6}$
	500	$9,2\cdot10^{-6}$	$1,4\cdot10^{-5}$	$1,7\cdot10^{-5}$	$1,8\cdot10^{-5}$	$1,86\cdot10^{-5}$
	600	$3,1\cdot10^{-5}$	$5,1\cdot10^{-5}$	$5,2\cdot10^{-5}$	$5,3\cdot10^{-5}$	$5,4\cdot10^{-5}$
Spinel dunite, 2162	200	$4\cdot10^{-10}$	$8,3\cdot10^{-10}$	$9,2\cdot10^{-10}$	$9,8\cdot10^{-10}$	$1,07\cdot10^{-9}$
	400	$7,4\cdot10^{-8}$	$1,6\cdot10^{-7}$	$1,8\cdot10^{-7}$	$1,9\cdot10^{-7}$	$2,1\cdot10^{-7}$
	550	$1,7\cdot10^{-7}$	$3\cdot10^{-7}$	$3,7\cdot10^{-7}$	$4\cdot10^{-7}$	$4,6\cdot10^{-7}$
	680	$6,8\cdot10^{-6}$	$1,1\cdot10^{-5}$	$1,4\cdot10^{-5}$	$1,6\cdot10^{-5}$	$1,8\cdot10^{-5}$
Pyrope peridotite, 2163	200	$1,5\cdot10^{-11}$	$1,6\cdot10^{-11}$	$2\cdot10^{-11}$	$2,1\cdot10^{-11}$	$2,2\cdot10^{-11}$
	400	$6,7\cdot10^{-9}$	$2,5\cdot10^{-8}$	$3,2\cdot10^{-8}$	$3,7\cdot10^{-8}$	$4,1\cdot10^{-8}$
	570	$1,1\cdot10^{-7}$	$2,4\cdot10^{-7}$	$2,6\cdot10^{-7}$	$2,8\cdot10^{-7}$	$3,2\cdot10^{-7}$
	620	$3,9\cdot10^{-7}$	$6,9\cdot10^{-7}$	$7,1\cdot10^{-7}$	$7,1\cdot10^{-7}$	$9,8\cdot10^{-7}$
Olivine nodule from the basaltoid Baikal region (green)	250	$1,2\cdot10^{-10}$	$2,27\cdot10^{-10}$	$3,35\cdot10^{-10}$	$3,88\cdot10^{-10}$	$4,0\cdot10^{-10}$
	300	$9,45\cdot10^{-10}$	$1,6\cdot10^{-9}$	$2,03\cdot10^{-9}$	$2,31\cdot10^{-9}$	$3,13\cdot10^{-9}$
	400	$1,73\cdot10^{-8}$	$3,88\cdot10^{-8}$	$4,6\cdot10^{-8}$	$5,0\cdot10^{-8}$	$5,71\cdot10^{-8}$
	500	$8,8\cdot10^{-6}$	$1,18\cdot10^{-5}$	$1,61\cdot10^{-5}$	$1,88\cdot10^{-5}$	$2,14\cdot10^{-5}$
	600	$3,78\cdot10^{-5}$	$5,05\cdot10^{-5}$	$6,6\cdot10^{-5}$	$7,3\cdot10^{-5}$	$7,3\cdot10^{-5}$
	690	$1,08\cdot10^{-4}$	$1,24\cdot10^{-4}$	$1,43\cdot10^{-4}$	$1,47\cdot10^{-4}$	$1,57\cdot10^{-4}$

[Commas in tabulated material are equivalent to decimal points.]

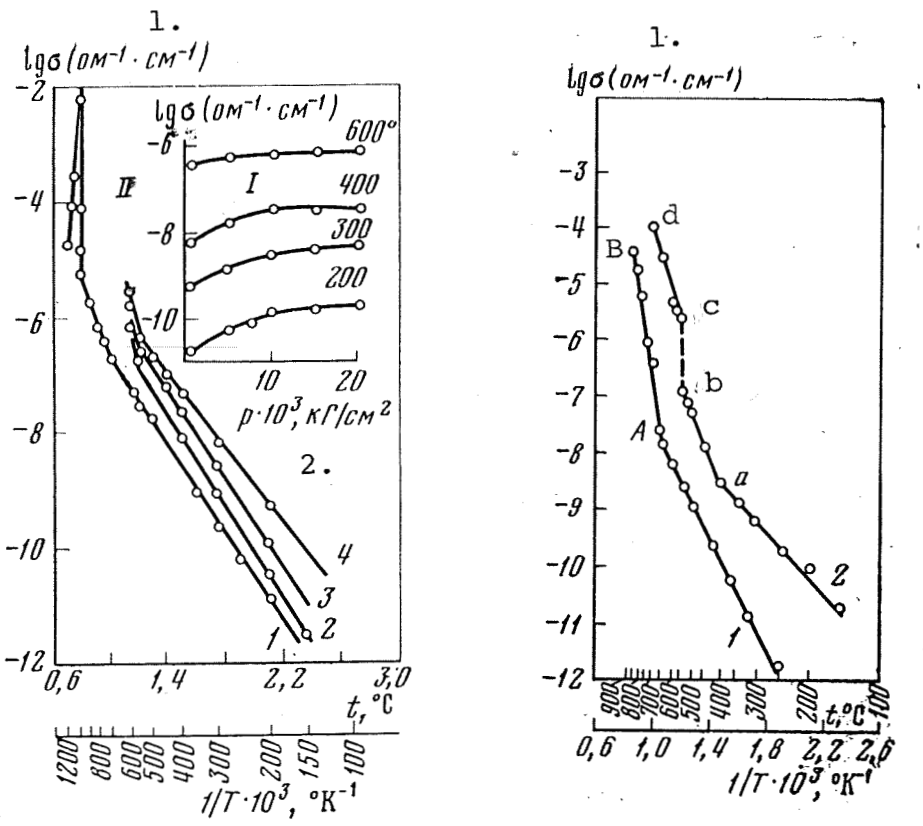

Figure 75. Electrical conductivity of pyrope peridotite 2163 as a function of pressure (I) and of temperature (II).

1 - atmospheric pressure; 2 - 950; 3 - 5750; 4 - 20,000 kg/cm^2.

Figure 76. Electrical conductivity in olivinite 1423 as a function of temperature at different pressures.

1 - atmospheric pressure; 2 - 12,000 kg/cm^2

Key: 1. ohm^{-1}.cm^{-1}; 2. kg/cm^2

pressure of 12,000 kg/cm^2 and the atmospheric pressure, differ quite significantly. The general appearance and slope of the curves with respect to the temperature has also changed. In atmospheric conditions, the first inflection point on the curve is observed at 650-700°C, after which, one observes the second inflection point at t=900°C, which is characterized by E_0=2.0 eV. The relatively high

E_0 indicates a significant contribution of the intrinsic conductivity. At the pressure of 12,000 kg/cm^2, the inflection point on the curve which defines the impurity-related (extrinsic) conductivity has shifted toward lower temperatures (t=400°C). After the point of inflection and up to the temperature 550°C, the slope of the straight line is less (E_0=1.24 eV) than in the case of the atmospheric pressure and at 550°C, one observes a sharp jump, with the magnitude increase on the order of 1.5. At the constant temperature, this jump is observed during 20 minutes, after which the electrical conductivity, with the inrease of the temperature up to 600°C, was increasing only slightly and then the rate of σ growth was again the same as before the sharp jump. It is not excluded that the reduced rate of the change of electrical conducivity prior to the jump is associated with the evolution of iron oxides along the grain boundaries of the minerals and is also due to mircocracks.

Figure 76 shows that the segements ab and cd on the curves at the pressures of 12,000 kg/cm^2 are separated by the polymorhpous tranistion region segment bc, corresponding the the segment of the AB curve for the atmospheric pressure. As we can see, according to our studies and on the basis of data in the literature [43] the pressure affects only slightly the electrical parameters of the rocks and of other materials. Since in this experiment the temperature in the test assembly for high pressures was developed by using external heating, this transition cannot be detected by sample annealing. However, one may suspect that the sharp increase in electrical conductivity may be due to the transition of the olivine modification Fe_2SiO_4 into the spinel modification, and also it is possible that this is due to the decomposition of fialite into $FeSiO_3$+FeO. The somewhat earlier transition of the olivine modification in these thermodynamic conditions, as compared to the data in the study [43], is apparently due to larger shear deformations in our sample, as it was exposed to all-around pressure.

Figure 77 shows the change in electrical conductivity of another sample for the same olivinite 1423 as a function of pressure which was up to 20,000 kg/cm^2 at different temperatures. The intensive increase of σ as a function of pressure at 600°C probably also indicates a polymorphous transition.

The analogous increase in electrical conductivity with the jump of the curve by one order of magnitude is also observed in the case of the mantle pyrope eclogite 2257 at the pressure of 15,000 kg/cm^2 and at the temperature of 575-600°C (Figure 78). The values of electrical conductivities for olivinite 1423 and eclogite 2257 are presented below: /186

	Pressure, kg/cm^2	Temperature range t, °C	E_0, eV	lg σ_0, $ohm^{-1} \cdot cm^{-1}$
Olivinite 1423	1	200—675	0,92	—2,7
		675—800	2,0	4,5
	12 000	150—400	0,5	—2,2
		400—550	1,24	2,2
		550—700	1,5	
Pyrope eclogite 2257	1	200—950	0,8	—3,3
		950—1200	3,0	6,0
	15 000	200—500	0,8	—2,2
		500—575	2,5	8,6
		575—700	1,22	2,2

[Commas in tabulated material are equivalent to decimal points.]

The pyroxenites, just like the rocks which we have considered above, display the increased electrical conductivity as a function of pressure at all temperatures (150-600°C). Figure 79 shows the data for two samples of pyroxenite which display different intensity of electrical conductivity change as a function of pressure. In the case of pyroxenite 1139, the activation energy decreases from o.92 to 0.72 eV, and lg σ_0 - from /187
0.3 to 0.5 $ohm^{-1} \cdot cm^{-1}$, and in the case of the rock 1133, E_0 changes somewhat less - from 0.9 to 0.8 eV. The clinopyroxenite is characterized by the intensive increase of electrical conductivity as a function of pressure at all temperatures, but its activation energy is practically the same (E_0=0.75-0.70 eV). This pyroxenite contains about 10% of titanium magnetite and it is possible that during the increase of pressure, one obtains an improved contact between the separate conducting layers and therefore, across the whole temperature range (150-500°C), it retains approximately the same intensity of the electrical conductivity change as a function of pressure. The other five pyroxenites which were selected from the Kola peninsula and in Kazakhstan, in terms of the change in electrical conductivity as a function of pressure, do not differ. Because of the insignificant change in electrical conductivity of diopside as a function of pressure, the pyroxenites with prevailing amounts of this mineral, must have an insignificant increase in σ as a function of pressure.

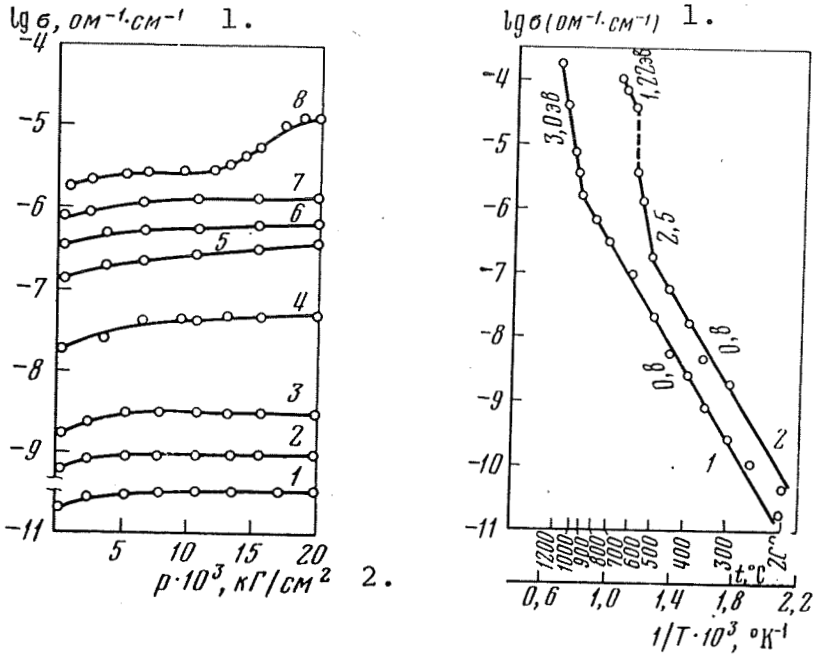

Figure 77. Electrical conductivity in the monomineral olivinite 1423 as a function of pressure and temperature.

At t,°C, respectively: 1-8 - 130,200,320,420,500,550,600,650.

Figure 78. Electrical conductivity in eclogite 2257 as a function of temperature at different pressures.

1 - atmospheric pressure; 2 - at 15,000 kg/cm^2

Key: 1. ohm^{-1}·cm^{-1}; 2. kg/cm^2

7. Electrical Conductivity in Crust Eclogites at High Pressures and Temperatures

The study of electrical conductivity in the crust eclogites by using the samples from two different origins, from Kokchetava formation (Kazakhstan) and from Shubino (Ural mountains) which were affected to a different degree by the regressive metamorphism, show no significant difference in behavior at higher temperatures and pressures. In both cases, one observes the increase of σ as a function of the pressure increase of up to 20,000 kg/cm^2 at all temperatures. However, in the case of one of the rocks, the isobars of σ are represented by one straight line and at p=10,000-20,000 kg/cm^2 are almost parallel to the isobar which corresponds to p=1000 kg/cm^2 with a small decrease of activation energy (Figure 80). In the case of other eclogites which were exposed to the pressure, one observes the inflection point on the straight lines which define lg σ=f(1/T) at considerably lower /188

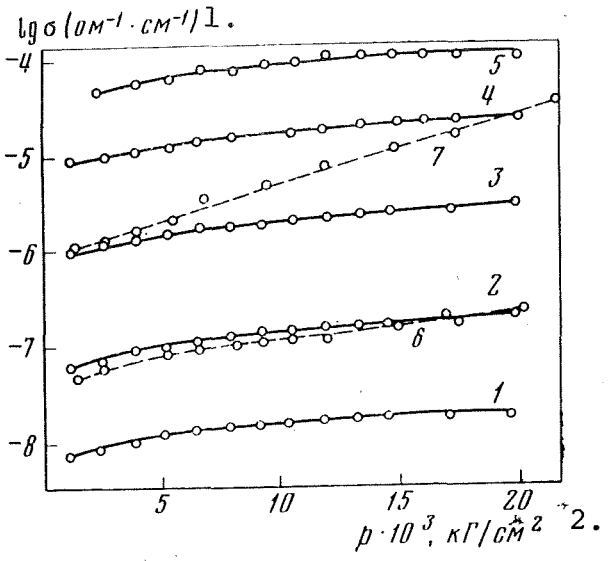

Figure 79. Electrical conductivity as a function of pressure and temperature

At t, °C, respectively, for pyroxenite 1139: 1-5 - 200, 300, 400, 500, 600; for pyroxenite 1133: 6 - 200; 7 - 300.

Data generated by E. I. Parkhomenko

Key: 1. $ohm^{-1} \cdot cm^{-1}$; 2. kg/cm^2

temperature than has been found at the atmospheric pressure. The isotherms of eclogites $\sigma=f(p)$ are of linear nature (Figure 81). The slope of the isotherms depends to a considerable degree on the porosity. The relationship in terms of the change in $\Delta\sigma/\sigma$ ratio as a function of effective porosity indicates a direct relationship between the parameters (Figure 82). Such relationship is observed in the case when the differential porosity predominates. This relationship has not been well established if a large number of spherical pores are present.

8. Influence of the Degree of Serpentinization on the Electrical Conductivity as a Function of Pressure in the Ultrabasic Rocks

The nature of change in $\sigma=f(p,t)$ relationship in the presence of different degrees of serpentinization has been investigated by usign the olivinites and dunites. The olivinite 1613 which has not been affected by metamorphism, just like the olivine xenoliths, displays within the pressure range of 1000-20,000 kg/cm^2 only slight change in electrical conductivity, on the order of 30-40% and a small shift of the temperature-related inflection point on the curve which defines the electrical conductivity (from 600 to 500°C).

In the case of olivinite 1614 (5% of serpentine) the electrical conductivity as a function of pressure of up to 20,000 kg/cm^2 and at the temperatures of up to 600°C changes considerably more. It is assumed that this is related to a higher degree of porosity in

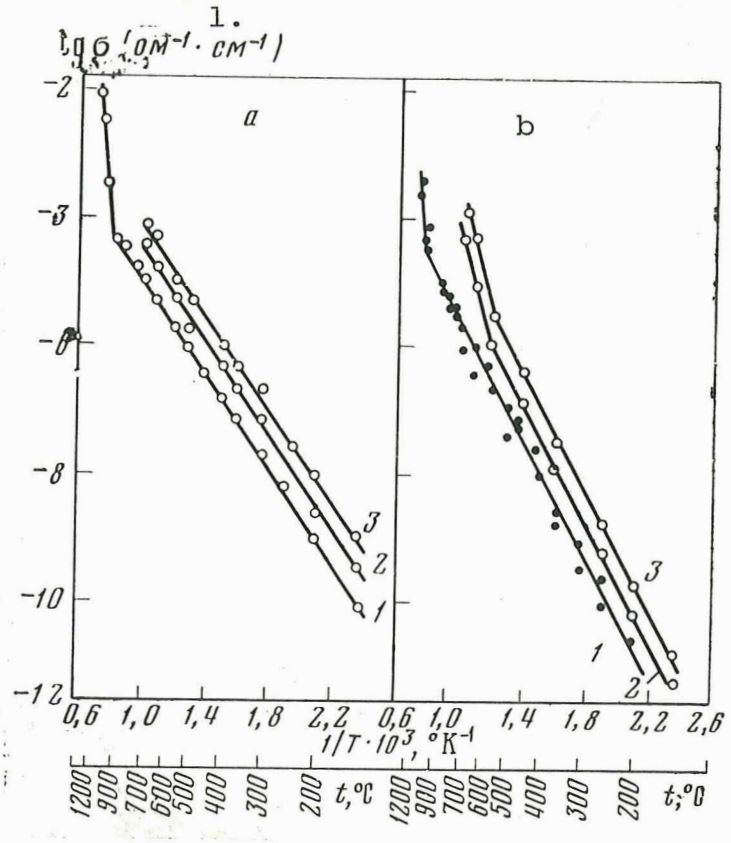

Figure 80. Electrical conductivity in the small grain eclogite KKK-676 (a) and in the mica eclogite AMB (b) as a function of temperture and pressure.

1 - atmospheric pressure; 2 - 1000; 3 - 20,000 kg/cm^2.

Key: ohm^{-1}·cm^{-1}

this olivinite, than in olivinite 1613, rather than serpentinization. In the case of the first sample, the coefficient of volumetric porosity is 1.07% and in the case of the second one - 0.54%. As it appears, a slight change in electrical conductivity at t=650°C, is due to the complete closure of the pores because of the pressure and because of the thermal expansion of minerals at the pressures of up to 1000 kg/cm^2 (see Figure 82).

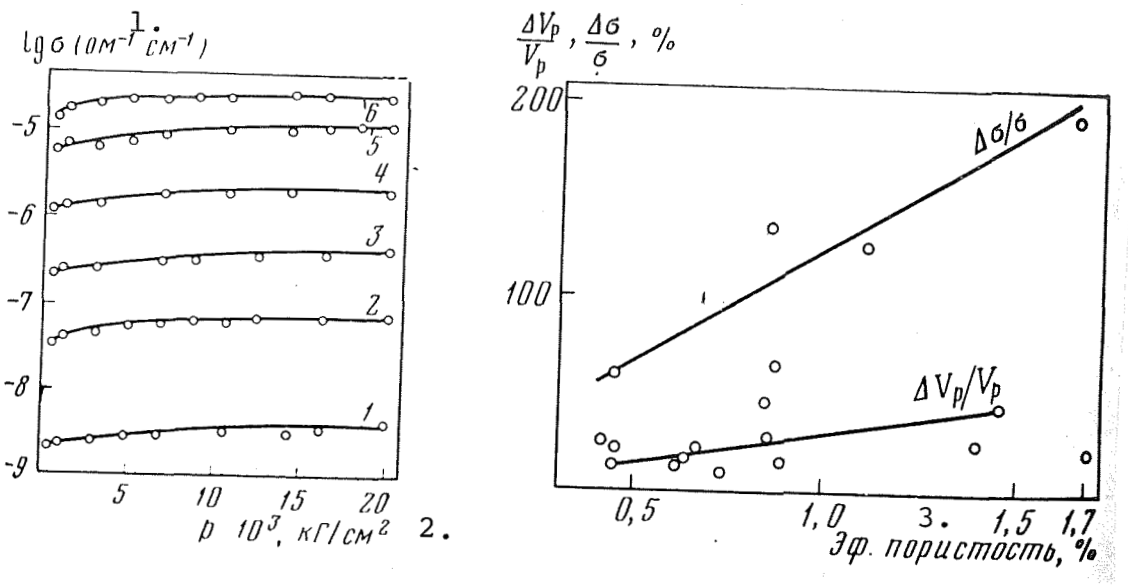

Figure 81. Electrical conductivity in the large grain eclogite KTS-672 as a function of pressure and temperature.
At t, ^{o}C, respectively: 1-6 - 200, 300, 400, 500, 600, 650.

Figure 82. $\Delta\sigma/\sigma$ and $\Delta V_p/V_p$ in eclogites as a function of the coefficient of effective porosity.
Key: 1. ohm$^{-1}\cdot$cm^{-1}; 2. kg/cm^2; 3. Effective porosity, %.

Table 31, and Figures 83, 84a and b, show the experimental data obtained for the olivinites and dunites which were affected by serpentinization to the extent of 30 to 90%. Let us note the following specifics in the change of electrical conductivity in dunites. As one increases the pressure from 1000 to 20,000 kg/cm^2, the dunites which were serpentinized to 30, 45 50 and 60%, display as a rule a small increase in electrical conductivity at the temperatures below 450^{o}C.

Within the same temperature range, the dunites which were serpentinized to 75 and 96%, and also the peridotites which contain 80% of serpentine, show the opposite relationship between σ and pressure. The electrical conductivity in the above-mentioned rocks, with the increase of pressure, will decrease (see Figure 84b). The decrease of electrical conductivity in this case reaches 80%. It should be noted that the rocks under consideration are characterized by a considerable degree of porosity (1.35-2.28%), and

therefore, one should expect the increase in electrical conductivity. At the present time, one might only surmise that the observed change in $\sigma=f(p)$ relationship within the temperature range of 400-500°C is associated with the conversion of serpentine into olivine. /190

At 600 and 650°C, in all rocks, regardless of the amounts of serpentine, one observes the increase in electrical conductivity as a function of the pressure increase, with the exception of dunite 4825 which displayed a sharp increase of σ at 600°C in the pressure range of 12,000-15,000 kg/cm^2.

As we can see, in such case when the larger part of the rock is affected by serpentinization, one observes a specific change in the electrical conductivity as a function of the pressure increase.

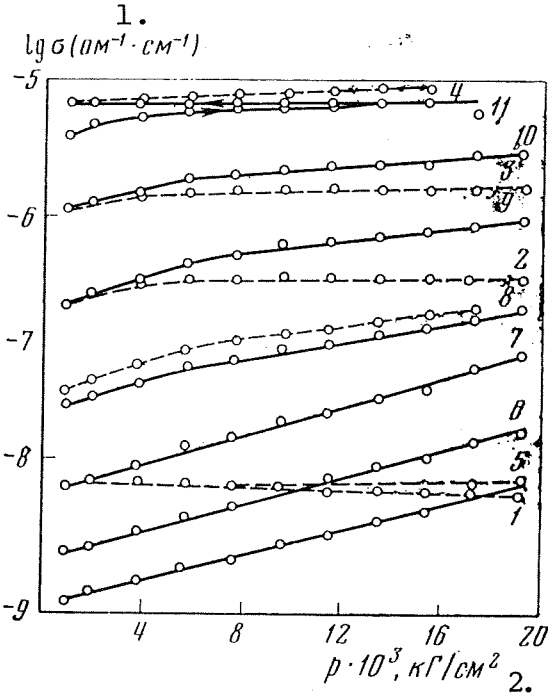

At t,°C, respectively: 1-4 - 300, 475, 550, 600; 5-11 - 250, 350, 400, 560, 600, 650.

Figure 83. Electrical conductivity in olivinites as a function of pressure and temperature, the olivinite 1614 (solid line and olivinite 1613 (dotted line).
Key: 1. ohm^{-1}·cm^{-1}; 2. kg/cm^2

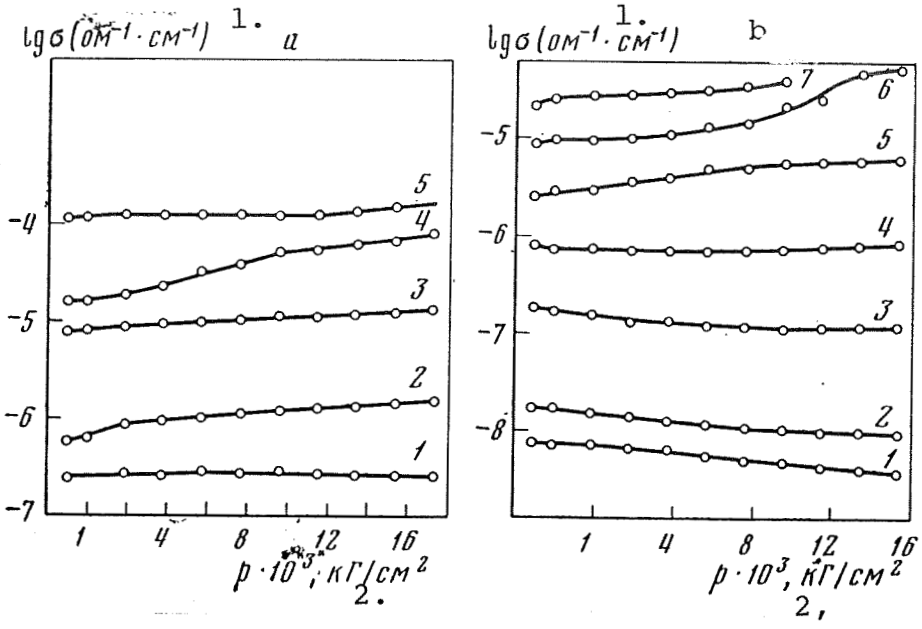

Figure 84. Electrical conductivity in dunite 7199, containing 30% of serpentine (a) and 7198 containing 90% of serpentine (b) as a function of pressure at different temperatures.

At t,°C, respectively: a. 1-5 - 260, 350, 450, 500, 600; b. 1-7 - 250, 300, 400, 460, 500, 600, 650.

Key: 1. $ohm^{-1} \cdot cm^{-1}$; 2. kg/cm^2

The second and also rather interesting feature of the serpentinized dunites is an extremely sharp temperature shift of the inflection point on the curve of $lg\ \sigma=f(1/T)$ toward the lower temperatures, which takes place in the case of some of the dunites at 300°C. The displacement of the inflection point is causing the decrease in the temperature range of anomalous change in electrical conductivity as a function of temperature, and the correlated decrease of temperature when the new mechanism of electrical conductivity begins to manifest itself. Figure 85a, b and c shows the character of change in isobars for some rocks which differ in terms of $lg\ \sigma=f(1/T)$ relationship. As a result of considerable temperature shift of the inflection point in the case of some dunites at 550-650°C, at the pressure of 20,000 kg/cm^2, the electrical conductivity, as compared to the conductivity at the atmospheric conditions, increases by a factor of one hundred and more. One should also mention the unusual character of change in the activation energy as a function of pressure. In the case of dunites which display at certain temperatures the decrease of

/191

/192

TABLE 31. ELECTRICAL CONDUCTIVITY ($ohm^{-1} \cdot cm^{-1}$) IN DUNITES AT HIGH PRESSURES

/191

Rocks, % of serpentine	Temperature, °C	Electrical conductivity, σ p=1000 kg/cm²	p=20,000 kg/cm²	$\frac{\Delta\sigma}{\sigma} \cdot 100\%$
Dunite				
5577, 30	250	$6,6 \cdot 10^{-10}$	$1,9 \cdot 10^{-9}$	190
	300	$5,1 \cdot 10^{-9}$	$6,2 \cdot 10^{-9}$	220
	400	$5,02 \cdot 10^{-8}$	$7 \cdot 10^{-8}$	40
	500	$1,1 \cdot 10^{-6}$	$2,5 \cdot 10^{-6}$	130
	600	$1,3 \cdot 10^{-6}$	$4,5 \cdot 10^{-6}$	250
5556, 50	250	$3,1 \cdot 10^{-8}$	$5,5 \cdot 10^{-8}$	78
	300	$1,8 \cdot 10^{-7}$	$1,8 \cdot 10^{-7}$	0
	400	$5,2 \cdot 10^{-6}$	$3,3 \cdot 10^{-6}$	—37
	500	$4,5 \cdot 10^{-5}$	$1,25 \cdot 10^{-5}$	180
	600	$3,0 \cdot 10^{-5}$	$2,6 \cdot 10^{-5}$	13
6672, 60	300	$9,5 \cdot 10^{-8}$	$1,1 \cdot 10^{-7}$	16
	440	$2,6 \cdot 10^{-6}$	$4,4 \cdot 10^{-6}$	69
	500	$4,3 \cdot 10^{-6}$	$8,3 \cdot 10^{-6}$	93
	600	$2,9 \cdot 10^{-5}$	$4,3 \cdot 10^{-5}$	48
4825, 75	260	$1,2 \cdot 10^{-7}$	$6,5 \cdot 10^{-8}$	—46
	300	$3,9 \cdot 10^{-7}$	$1,8 \cdot 10^{-7}$	—54
	400	$6,7 \cdot 10^{-6}$	$2,7 \cdot 10^{-3}$	—60
	500	$1,5 \cdot 10^{-4}$	$8,1 \cdot 10^{-5}$	—47
	600	$2,3 \cdot 10^{-4}$	$6,7 \cdot 10^{-4}$	190
7198, 90	250	$1,5 \cdot 10^{-9}$	$7,3 \cdot 10^{-9}$	—51
	300	$3,4 \cdot 10^{-8}$	$1,9 \cdot 10^{-8}$	—44
	400	$3,6 \cdot 10^{-7}$	$2,4 \cdot 10^{-7}$	—33
	500	$5,3 \cdot 10^{-6}$	$1,1 \cdot 10^{-5}$	170
	600	$6,8 \cdot 10^{-5}$	$1,2 \cdot 10^{-4}$	76

[Commas in tabulated material are equivalent to decimal points.]

electrical conductivity, the change of activation energy has not been observed. The isobars of electrical conductivity are practically parallel to each other. In the case of some other dunites (5577, 6672) within the region of impurity-related (extrinsic) and intrinsic electrical conductivity, one even observes the increase of activation energy. For example, in the peridotite 6871, the activation energy changes in an analogous fashion from 0.85 eV at the atmospheric pressure, to 1.25-1.35 eV at p=20,000 kg/cm^2. Such change in the activation energy

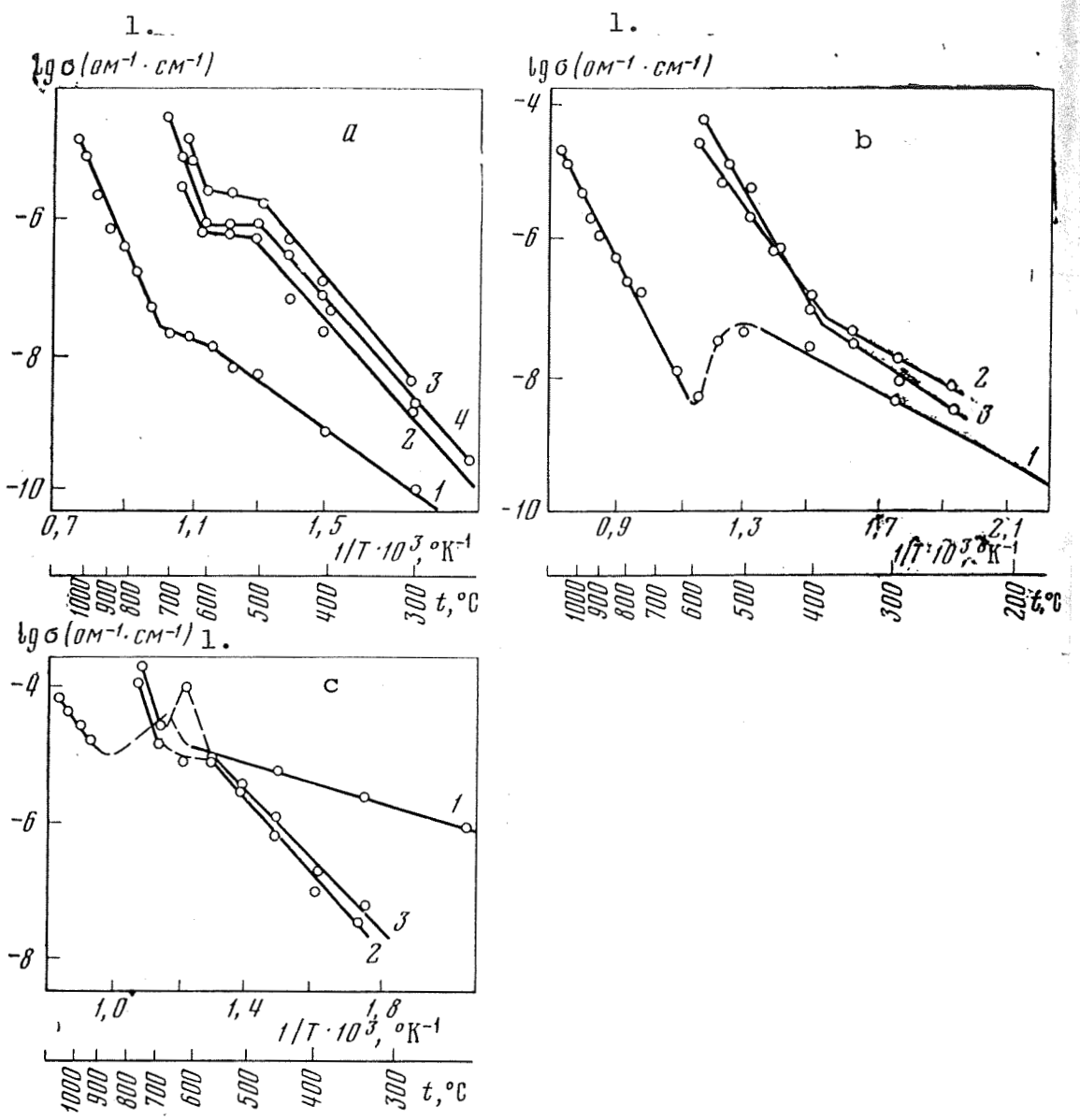

Figure 85. Isobars of electrical conductivity in dunite 5577 (a), 5556 (b) and 7198 (c) at different pressures (kg/cm^2).

1 - atmospheric pressure; 2 - 1000; 2 - 20,000; 4 - 10,000

Key: 1. ohm^{-1}·cm^{-1}

is related to the increase of the intensity in σ change as a function of pressure which may be the result of dehydration. It is possible that due to the uneven distribution of mechanical stresses, the beginning of this process is shifted toward lower temperature range, which is also indicated by the fact of the lowered temperature when the intrinsic electrical conductivity begins to manifest itself. /193

We have also studied several serpentinites which had a rather high electrical conductivity because of considerable quantities of the ore components and a favorable geometry for its evolution. In the case of two serpentinites with the initial electrical conductivity of 10^{-4} and 10^{-3} $ohm^{-1}.cm^{-1}$, the σ changes only by 10-20% and in the case of serpentinite KKK-672, in which $\sigma=8.6\cdot10^{-5}$ $ohm^{-1}\cdot cm^{-1}$, at 20°C, this change is considerably greater (Figure 86).

As we can see, the serpentinized dunites, peridotites and serpentinites which, at normal conditions, in a number of cases, display greater electrical conductivity [180], display even higher conductivity as a function of temperature and pressure [110, 111].

The areas of serpentinites, discovered in recent days, and extending for 350 km in the Eastern Carpathian mountains, substantiate the hypothesis of the extensive distribution of such rocks within the Earth's crust [62, 106, 181] and may be associated with the high electrical conductivity in the Earth's crust and in the upper mantle layers.

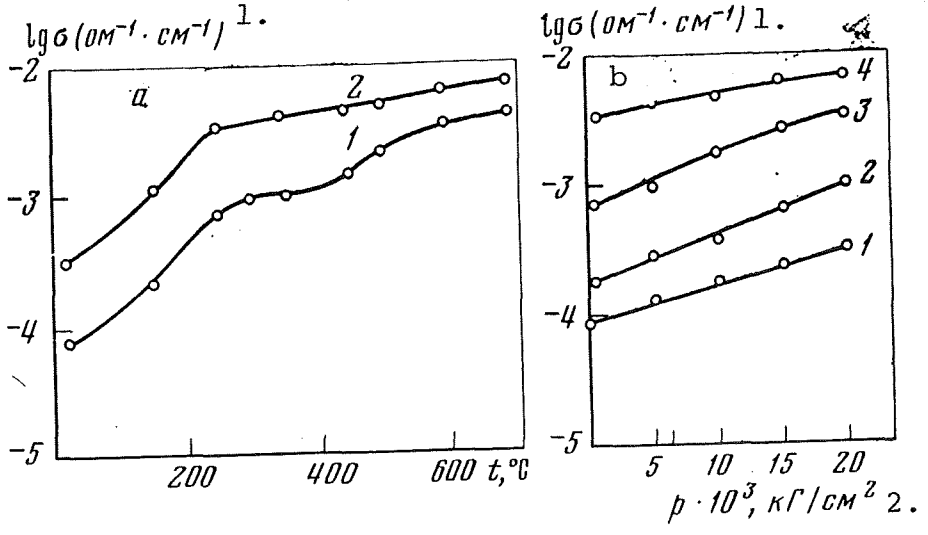

Figure 86. Electrical conductivity in the pyrope serpentinite KKK-672 as a function of temperature (a) and of pressure (b). a: 1 - 600; 2 - 20,000 kg/cm2; b: at t,°C, respectively: 1-4 - 20, 150, 250, 600.

Key: 1. $ohm^{-1}\cdot cm^{-1}$; 2. kg/cm^2

9. Electrical Conductivity of the Igneous Alkaline Rocks at High Pressures and Temperatures

The electrical conductivity of alkaline rocks at different pressures and temperatures was studied primarily by using the samples from the central part of the Khibin formation in which the amounts of nepheline varies between 35 and 80%.

The iolite 610 (nepheline - 66%, feldspar - 8, eugirine - 48, sphene - 6 and lepidomelane - 2%) indicate the change in σ by almost one order of magnitude as one increases the pressure up to 20,000 kg/cm^2 at 300 and 360°C (Figure 87a). A strong change is also observed at different temperatures. /194

The increase of σ is accompanied by a decrease in E_0, primarily up to p=15,000 kg/cm^2.

Figure 87b shows the isotherms for alkaline rocks - the trachetoidaliolite 615. This rock differs from the preceding one in that it contains 20% less nepheline mineral and 20% more of ferrous minerals eugirine and lamprophillite. Such difference in composition affects considerably the intensity of electrical conductivity change as a function of pressure with the increase of the former. Just like for some other rocks, in the case of iolite 615, one observes the shift of the point of inflection on lg σ=f(1/T) curves as a function of pressure increase, toward the region of lower temperatures. If we are to assume that prior to the point of inflection, the σ is impurity-related (extrinsic), the fact to which the lower E_0 points, and after the inflection point, of significance is the intrinsic conductivity, we can see that with the pressure increase and with somewhat lower temperatures, the mechanism of intrinsic conductivity in the rock begins to manifest itself.

It should be noted that E_0 decreases with the increase of p in both the low temperature and high temperature range (Table 32). /195

The euvite 639, which has large quantities of the ferrous minerals (nepheline - 30%, eugirine - 45, feldspar - 8, sphene and lamprophillite - 20%) displays a considerably more pronounced relationship between σ and pressure than iolite (Figure 88). In this case, E_0 changes from 0.54 eV at p=500 kg/cm^2 to 0.42 eV at p=5000 kg/cm^2, and then it remains constant.

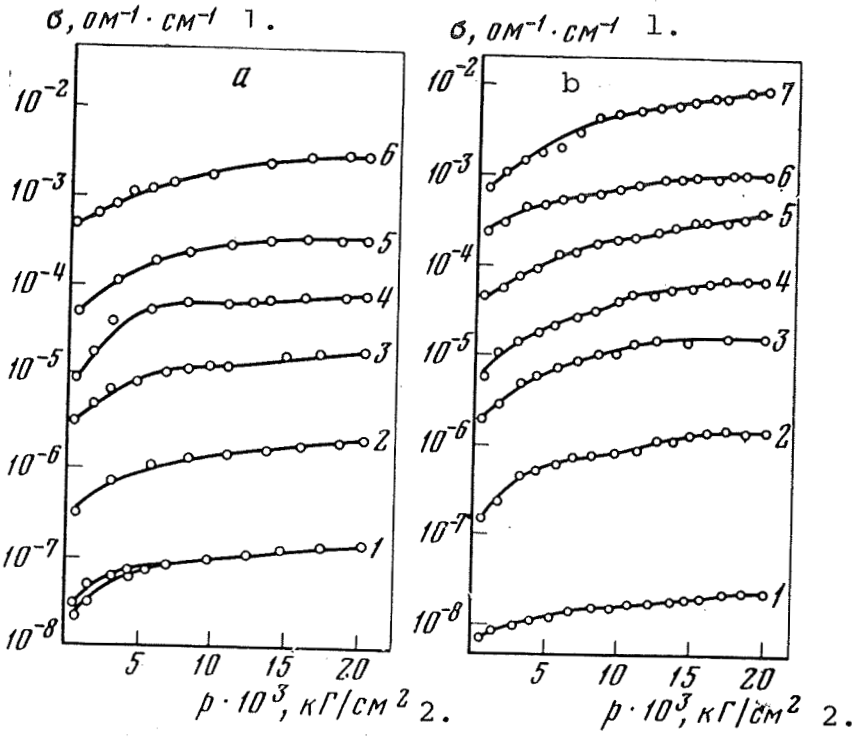

Figure 87. Electrical conductivity of the alkiline rocks iolite 610 (a) and 615 (b) as a function of pressure at different temperatures.

At t,°C, respectively: a. 1-6 - 20, 140, 300, 360, 490, 680; b. 1-7 - 20, 120, 300, 400, 520, 640, 680

Key: 1. $ohm^{-1} \cdot cm^{-1}$; 2. kg/cm^2

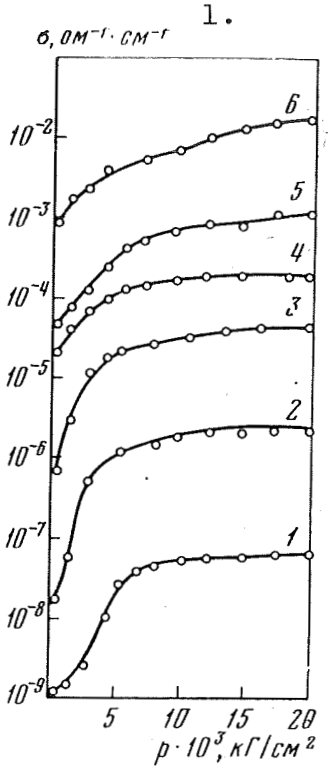

Figure 88. Electrical conductivity in euvite 639 as a function of pressure and temperature.

At t,°C, respectively:
1-6 - 20, 100, 200, 350, 420, 650.

Key: 1. $ohm^{-1} \cdot cm^{-1}$; 2. kg/cm^2

By looking at the data and measuring σ, $E_0=f(p)$ up to 20,000 kg/cm^2 and t=700°C in the case of euvite 639, which contains as a part of its composition more than one half of alkaline and ferrous minerals (65%) and by considering the analogous data for the alkaline-ferrous mineral rubecite, one may observe the same character of relationship between these parameters as a function of pressure. In addition, one observes in both cases the change of σ by 1.5-2 orders of magnitude and the unchanging E_0. One should conclude then, that this may be due to the increase in the mobility of electrons, in the presence of the iron cations of different valence and may also be due to the increase in the concentration of the current carriers, which are in the form of the sodium cations, the fact which has already been mentioned while considering the electrical conductivity of rubecite. /196

Conclusions

In trying to generalize the obtained experimental data related to the measurements of the electrical conductivity in rocks containing zero porous moisture, at the pressures within the range of 1-20 kbar and in the temperature range of up to 650°C, one might note the following.

1. The overwhelming majority of the rocks show the increased electrical conductivity as a function of the presure increase up to 20,000 kg/cm^2 within the temperature range of 100-650°C. In addition, the $\lg \sigma=f(p)$ relationship is frequently of linear character, something which has been observed predominantly at the pressures above 6000 kg/cm^2.

TABLE 32. ELECTRICAL CONDICTIVITY IN IOLITES AS A FUNCTION OF TEMPERATURE AND PRESSURE

p, kg/cm^2	Before the inflection point on the curve: Temperature range, t, °C	E_0, eV	$\lg \sigma_0$, ohm^{-1}·cm^{-1}	After the inflection point on the curve: Temperature range, t, °C	E_0, eV	$\lg \sigma_0$, ohm^{-1}·cm^{-1}
			Trachetoidaliolite 610			
1	100—600	0,76	—4,95	600—900	0,9	0,7
600	100—420	0,56	—4,97	420—700	0,65	0,2
10000	100—320	0,46	—4,81	320—700	0,51	—2,9
15000	100—320	0,46	—4,92	320—700	0,51	0,2
20000	100—320	0,42	—4,84	320—700	0,51	0,6
			Trachetoidaliolite 615			
600	100—420	0,3	—5,92	420—680	0,6	—2,9
5000	100—400	0,24	—4,00	400—680	0,55	—2,7
10000	100—380	0,24	—3,47	380—680	0,56	—2,9
15000	100—290	0,24	—3,54	290—680	0,49	—2,9
20000	100—290	0,24	—3,47	290—680	0,5	—1,1

[Commas in tabulated material are equivalent to decimal points.]

2. One notes the dissimilar intensity in the increase of electrical conductivity as a function of pressure, not only for different groups of rocks, but also for different representatives of the same petrographic type of rock. In a number of cases, some rocks are characterized by an intensive increase in electrical conductivity in the beginning of the pressure range, up to 8000 kg/cm^2. At higher pressures $d\sigma/dp$ becomes considerably less and may even acquire the levels close to zero.

3. In parallel with the prevailing number of rocks which display the increased electrical conductivity as a function of pressure, there are some rocks in which the electrical conductivity decreases with the pressure increase within a certain temperature range, and where one observes the maximum (in the case of some granites, in the intensely serpentinized ultrabasic rocks).

4. The intensity of change of σ as a function of pressure depends on the mineral composition and on porosity. With the increase of stratified porosity, the degree of electrical conductivity increase as a function of pressure will also increase. On the other hand, the presence of minerals, rich in Na^+ ions and Fe ions (rubecite) also facilitates the intensity of σ change as a function of pressure.

5. The rocks which were affected by the secondary changes - by cataclasis, serpentinization, etc., display different behavior of electrical conductivity as a function of pressure, when compared to the rocks which did not undergo these processes. The greatly altered rocks which underwent cataclasis show a considerable increase of electrical conductivity as a function of the pressure increase, which is due to the porous microstructure and a general increase in porosity. With the decrease in the changes which took place in the rocks, the intensity of σ increase as a function of pressure will be lower. The more extensive is serpentinization in the rock, the broader will be the temperature range in which the inverse relationship will be displayed - the decrease of electrical conductivity as a function of pressure. In having the small amounts of serpentine in the rock, only some isotherms of σ in the presence of relatively low temperatures (150-300°) will show the decreased electrical conductivity. When the amounts of serpentine are more than 70%, the decrease of electrical conductivity as a function of pressure occurs within a broader temperature range, namely, up to the temperatures at which the inflection point on the curve is observed, in other words, 450-500°C. As it appears, of great significance here is the dehydration of serpentine and possibly, the oxidation of iron. /197

6. In the presence of pressure, the rocks are characterized by the electrical conductivity hysteresis. The hysteresis of σ manifests itself to a different degree for petrographically different rocks. The best agreement for the two-way experiment has been found in the case of gabbro, the olivinites and some eclogites. A sufficiently good agreement in σ values, as one increases and then decreases pressures, is found in the case of some dunites.

7. It has been established that for a group of granite-diorite rocks, in the majority of cases, the activation energy practically remains constant. In the case of the rocks which were exposed to the secondary changes, the activation energy may decrease by 40% as one increases the pressure from 1 to 20 kbar. The values of E_0 and σ_0 change particularly intensively in the case of plageogranite, which is characterized by the most intensive change of σ as a function of pressure. As it appears, the above-mentioned decrease in E_0 is a fictional one, and it does not reflect the energy states of the current carrier. Among the

rocks which were investigated, one may isolate another two groups which differ in terms of the E_0 change as a function of pressure. In the case of one of these, the decrease of E_0 before the first inflection point on the lg σ=f(1/T) line is quite characteristic and in the case of another group - after the inflection point. As it appears, the difference is related to the mechanism of the electrical conductivity change as a function of pressure and namely, whether the process is due to the micro or to the macrostructural events which take place.

The gabbro group differs from the alkaline rock group by having a constant activation energy. The exception is olivine gabbro which display the increase of activation energy as a function of pressure rather than decreased or constant value, as is ordinarily the case.

8. In the case of a number of rocks, one observes the shift of the inflection point on the lg σ=f(1/T) curve toward lower temperatures. This manifests itself particularly strongly in the case of some dunites and basalts. As a result of this, one observes a much narrower region of anomalous change of electrical conductivity at high pressures with the temperature increase up to 600-650°C, or no anomalous change at all and the electrical conductivity, when compared to the measured values at the atmospheric conditions, increases by a factor of 100 and more. The shift of temperature-related inflection point on the lg σ=f(1/T) curve in the case of dunites may be explained in the following manner. It may be due to the uneven distribution of the mechanical, normal stress across the sample and also, possible shear stresses, creating the conditions which facilitate the lowering of dehydration temperature in serpentinites. As a result, the activated state is observed only at lower temperatures and as the tests show, is more pronounced. Because of this, the electrical conductivity with the temperature increase and at high pressure will increase much faster then at the atmospheric pressure. As it appears, in the presence of the activated state, the number of the current carriers and their mobility increase, and this fact is substantiated by high σ_0.

CHAPTER SIX. ELECTRICAL CONDUCTIVITY OF THE EARTH'S CRUST AND UPPER MANTLE, ON THE BASIS OF LABORATORY MEASUREMENTS

1. Electrical Conductivity of the "Granite" Layer Rocks, Based on Laboratory Data

/199

According to geological and geophysical data, the upper part of the Earth's crust, approximately down to the depth of 10 km, is composed of stratified rocks. The stratified rocks are characterized by high content of porous moisture, the quantity of which is defined by the coefficient of porosity K. In conjunction with great difference in electrical conductivities within the liquid and solid phase, the major factors which define the electrical parameters of stratified rocks are the amounts of pore solution, its concentration and the character of its distribution, which depend on the structural features of the rocks. Table 33 shows the electrical conductivities for a number of stratified rocks at two levels /200 of salt concentration which were obtained by the electrical probing method and the results of laboratory measurements of the air-dried samples are cited for comparison [182].

TABLE 33. EFFECT OF THE LIUQUID PHASE ON ELECTRICAL CONDUCTIVITY IN STRATIFIED ROCKS

Rock	Electrical conductivities, $ohm^{-1} \cdot cm^{-1}$		
	Air-dried samples	Saturated rocks	
		By fresh and brackish water (up to 3 g/l)	By salt water (above 3 g/l)
Clays	10^{-3}—10^{-5}	10—10^{-2}	1—10^{-1}
Clay shales	10^{-3}—10^{-5}	$2 \cdot 10^{-2}$—$2 \cdot 10^{-3}$	1—$2{,}0 \cdot 10^{-2}$
Sandstones			
porous	10^{-5}—10^{-6}	$3 \cdot 10^{-2}$—$5 \cdot 10^{-3}$	1—10^{-1}
high density	10^{-5}—10^{-6}	10^{-2}—10^{-3}	$2 \cdot 10^{-1}$—10^{-2}
Limestones			
fractured	10^{-4}—10^{-6}	10^{-2}—10^{-3}	$2 \cdot 10^{-2}$—10^{-2}
densely crystalline	10^{-4}—10^{-6}	10^{-3}—10^{-5}	10^{-2}—10^{-3}

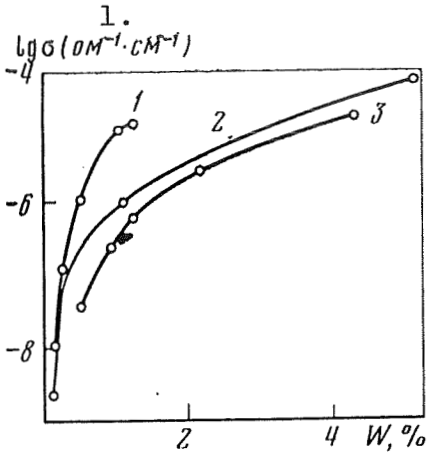

Figure 89. Electrical conductivity as a function of moisture content in rocks.
1 - albitophyre (3.0 g/l NaCl);
2 - gneiss (20 g/l NaCl)
3 - gneiss (10 g/l NaCl)
Key: 1. $ohm^{-1} \cdot cm^{-1}$

The electrical conductivity of stratified layer can be determined with sufficient reliability by the field electrical probing methods, and therefore there is no need to handle this question.

The structure of "granite" layer may include the granites, granodiorites, diorites and syenites, and also the rocks which underwent metamorphosis and which are represented by gneiss, slate and crystalline limestones. In addition, closer to the surface, one encounters extensive layers of basalts, of the serpentinized ultrabasic rocks and other geological formations. The porosity of these rocks does not exceed 3%. Therefore, the moisture capacity of these rocks is not significant.

In spite of the fact that there is much less moisture in the crystalline rocks than in stratified, the pore solutions also exert a significant effect on the electrical conductivity. The "granite" layer may be exposed to a broad range of thermodynamic parameters, from the ordinary atmospheric conditions (upper part of the top bed) and all the way to the pressures of 6000 kg/cm^2 and temperatures of 600°C (the lower boundary of the "granite" layer within the zone of folds). It is therefore of great interest to consider, in parallel with the effect of temperature and pressure on the electrical conductivity in rocks, within the granite layer, the major relationships reflecting the changes of electrical conductivity as a function of the amounts in the rocks of the pore solution W and its concentration c. The available information as to the relationship of electrical conductivity in the crystalline rocks, and the amounts and concentration of salts in the pore solution is quite limited [183-186]. Figure 89 shows the $\sigma=f(W)$ relationship for gneiss and albitophyre at different concentrations of solution. The averaged-out experimental data, calculated on the basis of measurement of three albitophyre samples, and the measured results for one of these samples, correlated quite well, which indicates a similar character of structure in these samples. According to the curve which is presented, with /201 the increase of humidity from 0.1 to 1.0-1.5%, one observes an intensive increase of electrical conductivity (by several orders of magnitude). As once increases further W to 5%, the electrical conductivity of gneiss increases by not more than one order of magnitude, regardless of the solution concentration. The $\lg \sigma=f(\lg W)$ relationship is of linear character

$$\lg \sigma = k \lg W + b,$$

where k and b are the coefficients which depend on the concentration of the electrolyte which saturates the rock, and on the structural features of the rock. In the case of three studied rocks, the b and k coefficients fluctuate within the following range: $b=-5.5-7.1$ ohm$^{-1}\cdot$cm^{-1}; $k=3-4.6$. For the straight line segment of the curve which corresponds to the humidity $W<0.3\%$, the range of these coefficients was not determined because of the lack of available data. In the presence of small amounts of moisture (0.1-0.2%) the slope of this segment of the straight line depends on the conducting properties of the basic rock and of the liquid phase. If the solid component is represented by high resistivity mineral, the liquid phase will be predominant and the straight line, after the inflection point, will show the increase of inclination angle. In the presence of conducting minerals, the slope of this line will decrease.

It should be noted that the type of predominant moisture in the rock plays an important role, just like the solid phase, in the electrical conductivity. According to the existing general concepts, the electrical conductivity of bound water may be either higher or lower than that of the free water [183]. If the electrical conductivity of the bound water is higher than that of the free water, within the region of low moisture content, the $\sigma=f(W)$ relationship, having a high resistivity rock, will be much more sharply pronounced than in the second case.

The second important factor in the level of electrical conductivity of the moisture-saturated rock is the concentration of the pore electrolyte. The concentration of mineralized waters in the central and to some extent in the northern parts of the USSR reaches 3 g/l. It is increasing as a function of depth [182]. In conjunction with this, the studied rock samples were saturated during the experiments with NaCl, in the quantities from 0 to 20 g/l. As has been expected, with the increase of concentration of the solution, the electrical conductivity of the rocks has increased. In addition, the most intensive change of electrical conductivity takes place when the electrolyte displays low mineralization (up to 1.5 g/l). For example, the electrical conductivity of albitophyre, as the amounts of sodium chloride has increased from several hundredths fractions to 1.5 g/l, in the presence of different moisture content within this rock, will increase by approximately 95% and by changing the concentration of sodium chloride from 1.5 to 3 g/l, it will increase only by 20%. The electrical conductivity of gneiss and basalt changes in an analogous fashion. The increase of electrical conductivity in the rocks with the increase of salt concentration up to 20 g/l may reach two orders of magnitude. /202

The dissimilar character of the effect on electrical conductivity of the concentration of the solution, from 0 to 20 g/l, which is associated to a great degree with the physical and chemical properties of basic rocks, the volume relationship between the bound and free water, and the specificity of electrical-chemical processes which occur at the interface between the solid and liquid phase. It is known that in the capillary systems, as they are being filled with the diluted solutions, of great importance is the surface conductivity which decreases with the increase of the concentration of the solution. This gives us grounds to assume that the intensive increase in electrical conductivity of the rocks, in the presence of weak electrolytes, is due to a large degree to the surface conductivity. This is also substantiated by a sharp increase of porosity $P_p=\sigma_{el}/\sigma_p$ (σ_{el} is the electrical conductivity of the electrolyte) in albitophyre, as one increases the concentration of electrolytes up to 1.5 g/l of NaCl. As one changes the concentration of the electrolyte from 1.5 to 3.0 g/l, however, the $P_p=f(c)$ curve remains parallel to the x-axis (Figure 90).

Effect of pressure. The igneous rocks, and the rocks which underwent metamorphosis in the Earth's interior, may be found at different stressed states.

In conjunction with this, it appeared to be quite important to elucidate the effect of the quantities and concentration of the pore solution on the electrical conductivity as a function of pressure by using the one-sided compression, the quasihydrostatic and hydrostatic pressures. The experimental data indicates that in the case of one-sided compression, according to the previously obtained data [19, 184], the granite samples of different origin, magmatite, albitophyre, gneiss and basalt, while being incompletely saturated with a weak electrolyte, display only insignificant in- /203
crease in electrical conductivity. The increase of electrical conductivity in such rocks is also observed in the presence of quasihydrostatic and hydrostatic pressures. The moisture-saturated rocks are characterized by different relationship between the electrical conductivity and pressure.

In the presence of quasihydrostatic pressure, it was possible to investigate four moisture-saturated rocks: granites (two samples), quartz sandstone and hematite quartzite. The first three samples within the range of quasihydrostatic pressure from 2 to 10 kbar, display a linear decrease of electrical conductivity as a function of pressure to a different degree. Figure 91 shows the electrical conductivity of granite, fully saturated, as a function of the quasihydrostatic pressure. However, in the case of hematite quartzite which has high electrical conductivity in its dry state, one observes the increase of σ, regardless of the concentration of the solution. Such type of relationship is due to the improved contact between the grains of ore minerals.

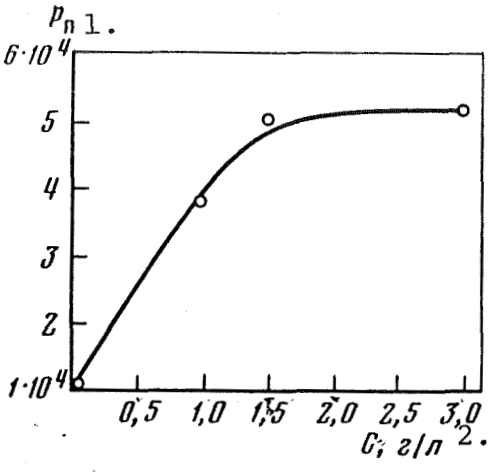

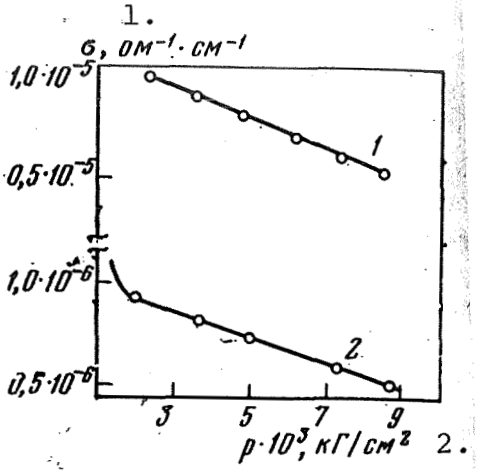

Figure 90. Porosity of albitophyre as a function of the electrolyte concentration.
Key: 1. P_p; 2. g/l

Figure 91. Electrical conductivity of the moisture-saturated granite as a function of pressure at different concentration of electrolyte.
NaCl, g/l: 1 - 20; 2 ~0.
Key: 1. ohm^{-1}·cm^{-1}; 2. kg/cm^2

By comparing the character of change in electrical conductivity as a function of pressure at different concentration of the pore solution, it was possible to establish the identical type of $\sigma=f(p)$ relationship, not only qualitatively but it was also possible to obtain quite similar $\Delta\sigma/\sigma$ values for two tests, with the samples which were saturated by the solution of NaCl of different concentrations [185]. As we can see, the obtained results indicate a different type of change of σ as a function of pressure, depending on the degree of saturation of the rock by electrolyte, and the conducting properties of the solid material, as well as the passive effect of the degree of pore solution mineralization (with the NaCl content from 0 to 20 g/l) and its total effect on $\sigma=f(p)$.

However, in the presence of hydrostatic pressure and complete saturation of the rock by the solution, one is faced with the decrease of cross sections of current-conducting channels and more complex geometry, which results in the decreased electrical conductivity as a function of pressure. In addition, while investigating these two samples, having different coefficients of porosity (in the granite K=0.48 and in the syenite K=2.22%), the coefficient of electrical conductivity as a function of pressure $k_p=\frac{1}{\sigma}\frac{d\sigma}{dp}$ is higher

in the case of granite than in the case of syenite. The observed inverse relationship between K_p and porosity may be due to the intensive closure of the fissured pores as a function of the pressure increase. Therefore, the more complex the current channels become, the more intense will be the decrease of electrical conductivity in the rock as a function of pressure. Analogous results were obtained by Brace et al. [157] for different moisture-containing igneous rocks, exposed to the hydrostatic pressure. /204
Table 34 shows the electrical conductivities for some of these rocks. On the basis of data in this table, one can see the degree of change in electrical conductivity as a function of all-around pressure increase, when the pore pressure is equal to zero. This data indicates that the intensity of the electrical conductivity decrease as a function of pressure is independent of the concentration of the pore solution, with the greatest change at 1000-2000 kg/cm^2.

The change of electrical conductivity in four rocks (granite, gabbro, granosyenite and syenite) saturated by the pore solution of 3 g/l of NaCl concentration has been investigated by increasing the temperature up to 260°C. The experimental data shown in Figure 92 was obtained in the presence of hydrostatic pressure p_h=500 kg/cm^2, and the pore pressure of the solution p_p=100 kg/cm^2. This data was obtained by the All-Union Scientific Research Institute for Geophysics.

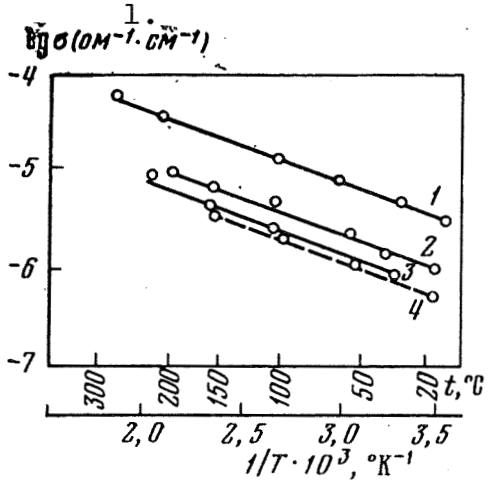

1 - granite 2400
2 - granite 2411
3 - gabbro 2413
4 - granite (at p=1500 kg/cm^2)

Figure 92. Electrical conductivity of moisture saturated rocks as a function of temperature.
Key: 1. ohm^{-1}·cm^{-1}

TABLE 34. ELECTRICAL CONDUCTIVITY OF IGNEOUS ROCKS, SATURATED BY SOLUTIONS WITH THE RESISTIVITY OF 50 (σ_1) AND 0.25 ohm·m (σ_2)

Rocks		p, kg/cm²			Rocks		p, kg/cm²		
		50	2000	10000			50	2000	10000
Granite	σ_2	$1{,}17\cdot10^{-6}$	$1{,}9\cdot10^{-7}$	$3{,}1\cdot10^{-8}$	Gabbro	σ_1	$3{,}0\cdot10^{-7}$	$1{,}6\cdot10^{-7}$	$7{,}7\cdot10^{-9}$
	σ_1	$7{,}8\cdot10^{-7}$	$1{,}78\cdot10^{-7}$	$6{,}9\cdot10^{-8}$		σ_2	$1{,}0\cdot10^{-6}$	$1{,}9\cdot10^{-7}$	$1{,}2\cdot10^{-8}$
White marble	σ_1	$5{,}8\cdot10^{-5}$	$4{,}3\cdot10^{-6}$	$1{,}15\cdot10^{-7}$	Peridotite	σ_1	$4{,}3\cdot10^{-9}$	$2{,}6\cdot10^{-9}$	$1{,}6\cdot10^{-9}$
Gabbro	σ_1	$7{,}6\cdot10^{-7}$	$3{,}1\cdot10^{-7}$	$2{,}9\cdot10^{-7}$	Dunite	σ_1	$4{,}1\cdot10^{-7}$	$1{,}2\cdot10^{-7}$	$9{,}0\cdot10^{-9}$
	σ_2	$7{,}7\cdot10^{-6}$	$6{,}5\cdot10^{-7}$	$8{,}0\cdot10^{-8}$		σ_2	$5{,}1\cdot10^{-6}$	$6{,}7\cdot10^{-7}$	$7{,}2\cdot10^{-8}$

TABLE 35. ELECTRICAL CONDUCTIVITY OF GRANITE AND SYENITE ($ohm^{-1}\cdot cm^{-1}$) AT HIGH PRESSURES AND TEMPERAURES*

t, °C	50	100	200	500	750	1000	1250	1500	$\frac{\sigma_{50}}{\sigma_{1500}}$
					Syenite				
20	$2{,}2\cdot10^{-6}$	$1{,}9\cdot10^{-6}$	$1{,}3\cdot10^{-6}$	$9{,}6\cdot10^{-7}$	$7{,}6\cdot10^{-7}$	$6{,}3\cdot10^{-7}$	$5{,}5\cdot10^{-7}$	$4{,}8\cdot10^{-7}$	4,58
50	$5{,}3\cdot10^{-6}$	$4{,}8\cdot10^{-6}$	$4{,}05\cdot10^{-6}$	$2{,}7\cdot10^{-6}$	$2{,}2\cdot10^{-6}$	$1{,}9\cdot10^{-6}$	$1{,}6\cdot10^{-6}$	$1{,}35\cdot10^{-6}$	3,93
100	$1{,}1\cdot10^{-5}$	$1{,}0\cdot10^{-5}$	$7{,}5\cdot10^{-6}$	$5{,}0\cdot10^{-6}$	$3{,}8\cdot10^{-6}$	$3{,}1\cdot10^{-6}$	$2{,}8\cdot10^{-6}$	$2{,}5\cdot10^{-6}$	4,41
150	$1{,}55\cdot10^{-5}$	$1{,}4\cdot10^{-5}$	$1{,}1\cdot10^{-5}$	$7{,}0\cdot10^{-6}$	$5{,}7\cdot10^{-6}$	$5{,}1\cdot10^{-6}$		—	—
					Granite				
20	$2{,}0\cdot10^{-6}$	$1{,}57\cdot10^{-6}$	$1{,}25\cdot10^{-6}$	10^{-6}	$7{,}5\cdot10^{-7}$	$5{,}9\cdot10^{-7}$	$5{,}1\cdot10^{-7}$	$4{,}4\cdot10^{-7}$	4,55
50	$5{,}5\cdot10^{-6}$	$3{,}9\cdot10^{-6}$	$2{,}7\cdot10^{-6}$	$2{,}1\cdot10^{-6}$	$1{,}75\cdot10^{-6}$	$1{,}50\cdot10^{-6}$	$1{,}35\cdot10^{-6}$	$1{,}2\cdot10^{-6}$	4,66
100	$1{,}6\cdot10^{-5}$	10^{-5}	$7{,}1\cdot10^{-6}$	$4{,}7\cdot10^{-6}$	$3{,}6\cdot10^{-6}$	$3{,}9\cdot10^{-6}$	$2{,}6\cdot10^{-6}$	$2{,}4\cdot10^{-6}$	6,67
150	$2{,}9\cdot10^{-5}$	$1{,}6\cdot10^{-5}$	$1{,}1\cdot10^{-5}$	$6{,}9\cdot10^{-6}$	$5{,}2\cdot10^{-6}$	$4{,}4\cdot10^{-6}$	$3{,}9\cdot10^{-6}$	$3{,}9\cdot10^{-6}$	8,06

*On the basis of data supplied by Z.S. Stefankevich and E.I. Parkhomenko

[Commas in tabulated material are equivalent to decimal points.]

One can see that the character of the change in electrical conductivity as a function of temperature is the same for all rocks. As we can see, the strongest change of σ with the increase of temperature occurs within the temperature range of 20-150°C and then the curve flattens out. Within the coordinate system lg σ and 1/T, the experimental points are all on a straight line. Consequently, in the moisture-saturated samples, the electrical conductivity depends exponentially on the temperature

$$\sigma = \sigma_0 e^{-\frac{E_0}{kT}},$$

where k is the Boltzman constant. The activation energy of the studied rocks fluctuates between 0.16-0.19 eV and in the case of water E_0=0.2 eV [186]. Somewhat similar activation energies for the rocks and for water indicate that the electrical conductivity is due primarily to the electrolyte which saturates the rock. The level of lg σ_0 in these rocks changes from -4.7 to -5.25 $ohm^{-1}.cm^{-1}$.

In addition, the electrical conductivity of the two rocks - granite and syenite, was studied as a function of pressure at elevated temperatures. Across the whole temperature range, one observes the decrease of electrical conductivity as a function of pressure increase (Table 35). One can see from this table that the intensity of change in electrical conductivity of granite, as one increases the pressure, will increase with the temperature increase and in the case of syenite - it will decrease somewhat. On the whole, the decrease in electrical conductivity in the case of one specific rock, because of the pressure, is quite significant, which to some degree may be compensated by the increase of temperature at a greater depth. The geoelectrical probing hole cross-cuts which are presented below are constructed by taking into account this experimental data, describing the behavior of moisture-saturated crystalline rock as a function of pressure and temperature. /206

2. Distribution of Electrical Conductivity as a Function of Depth for the "Granite" and "Basalt" Layers

As has already been mentioned, on the basis of the magnetic variation methods and of the magnetotellurium probing, it was possible to establish in many parts of the Earth the presence of conducting layers (zones of increased electrical conductivity) which are found at different depths within the Earth's crust and in the upper mantle. In accordance with the laboratory studies of electrical properties of rocks, on the basis of the general theoretical and acceptable representations, the nature of these

zones is different. Some of them which are located not very deep, should be associated with the nature of the rock within the Earth's crust, and are characterized by the increased electrical conductivity without any additional heating, in the course of the modern era, by thermal flows which are emerging from the interior. The other part of the conductivity zones is found in the regions where some other anomalies of geophysical fields are being manifested - the increased thermal flows (thermal maxima) and the magnetic, gravitational and seismic anomalies. This type of conducting layer is associated with geothermic activity in the upper mantle which is particularly intense within the rift zones. The classical examples of this are the Baikal rift and Viluy sineclase [187-195]. For example, in the case of the Baikal system of grabbens, the synchronous and stepwise elevation of the three conducting layers, with the anomalously minimal depth of these layers, on the order of 11-12, 30-40 and 80 km, one detects the most seismic activity, the largest thermal flow (among those which are known) and the lowest gravitational field minimum.

Figures 93 and 94 show the generalized curves which define the electrical resistivity of the Earth's crust and of the upper mantle with different modes of thermal flows, to the depth of 100-240 km. This structural diagram of the Earth's crust and of the upper mantle was borrowed from the study by V. V. Belousov and N. V. Sobolev [196, 72]. In constructing the temperature and geoelectrical cross sections, we have made use of the materials found in the studies [11, 197-199]. The curves of electrical /207
resistivity change as a function of depth, within the Earth's crust (see Figure 93), are constructed by extrapolating the data obtained for the moisture-saturated granites, seperately, at the pressure of up to 15,000 kg/cm^2 and t=150°C and up to t=260°C at a constant pressure of p_i=500 and p_p=100 kg/cm^2.

By considering the Figures 93 and 94, and analyzing the experimental data which describes the conductivity zone within the upper part of the Earth's crust (down to the depth of 10-20 km), one might say that in the majority of cases, this may be due to the following.

1. The presence of the rocks of amphibolite and gneiss type which underwent metamorphosis, with the rocks being saturated by the pore solution of high concentration. In this case, they will be found under the watertight layers of the rocks which limit the diffusion of moisture.

2. The presence of serpentinites or the formations of serpentinized rocks.

3. The time correlation with the tectonically disrupted

zones of the alkaline rocks, enriched with the following oxides FeO, Fe_2O_3, Na_2O and K_2O. The alkaline rocks, different in composition, are most frequently found within the base layer and upper bed layers [121, 116] as a result of intrusion into the upper layers of the Earth's crust, of large quantities of alkaline magma. The Kola peninsula is a classical area in which the alkaline rocks of nepheline-syenite and eurtite-iolite series are extensively found. The alkaline rocks are also widely distributed in the Siberian base formation, within the crystalline layer in the Ukraine and in other areas [200].

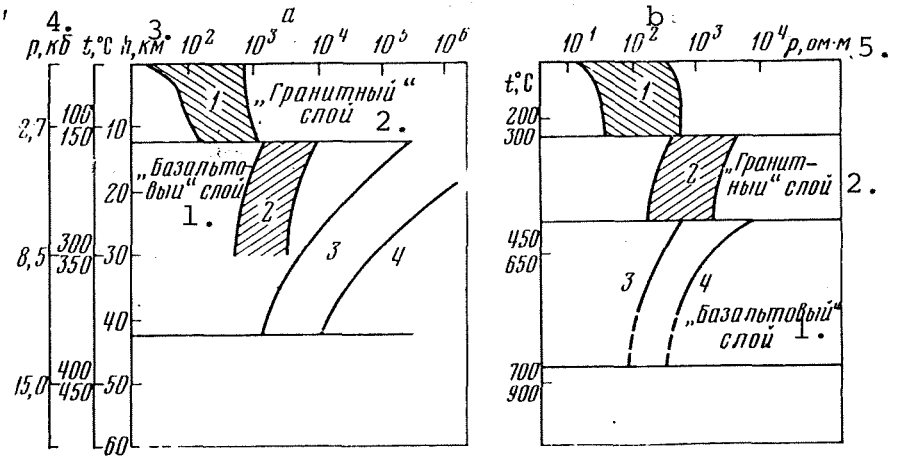

Figure 93. Distribution of electrical conductivity within the Earth's crust according to laboratory data for the upper bed layer (a) and for the fault zone (b).

1 - region of laboratory ρ values for the moisture-saturated stratified rocks and the data, based on the electrical probing; 2 - laboratory data for the moisture-saturated granites; 3 - averaged-out data for amphibolites; 4 - averaged-out data for gabbro.

Key: 1. "Basalt" layer; 2. "Granite" layer; 3. km; 4. kb 5. ohm·m

4. The dehydration processes in the rocks, in the course of which they are being enriched by the solution which conducts the electrical current well. It is known that the saturation of the solution with conducting compounds may be observed as the rocks undergo metamorphism [187, 196]. On the basis of the available data, in the first of the above-mentioned three cases, one must observe a sharp jump in the electrical conductivities, by about 2 or 3 orders of magnitude. /208

These conductivity zones may bisect the deep-lying fissures and disruptions, along which the thermal flows may enter from the interior into the Earth's crust. In conjunction with this, one should observe a faster increase in electrical conductivity not only within the regions which conduct the current well, but also within the top formations. As it appears, this is the reason for the high conductance upper layer in the southern part of the Siberian base formation, near Lake Baikal.

It has been established that the conductivity zones may be correlated with the regions of elastic waves within the Earth's crust, determined by the seismologists, which have lower velocities [201]. Such layers of lower velocities have been discovered in recent times in the Gharm region [202, 203]. The data for olivinites, spinel olivines, peridotites, pyrope-spinel dunites, pyrope eclogites and pyrope peridotites from kimberlite tunnel formations in Yakutiya, was used for the investigation down to the depth of 40 km. Figure 94,A, curve 1, the distribution of electrical conductivity, within the Earth's crust and in the upper mantle to depth on the order of 240 km, is shown for the base formations and for the upper bed formations. It is necessary to keep in mind that the experimental ρ correspond to the temperatures shown in this diagram. Therefore, if the depth-related temperatures for the geological regions of interest are distributed somewhat differently, then the ρ levels will correspondingly change. The electrical conductivities shown in Figure 94A, to the depth of 70-80 km, are cited, keeping in mind the simultaneous influence of p and t. In the case of greater depth, the effect of pressure on the elecrtrical conductivity was extrapolated. The horizontal shading shows the possible area of the electrical conductivity distribution as a funciton of the rock composition. With the increase of ferrous component in the ultrabasic rock, the conductivity will increase and the electrical conductivity distribution curve will shift to the left. In the case of magnesium composition with the admixture of chromium-spinelites and diopside, the electrical conductivity decreases and the curve will be in the extreme right position, within the shaded area, in Figure 94A.

One can see from Figure 94A that within the range of granite-gneiss, granulite-basite, granulite-eclogite formations, and in the upper mantle to the depth of 50 km, the electrical conductivity sharply increases. Then one observes very slow increase of σ as a function of depth. The rapid growth of electrical conductivity begins again at the depth of 150-160 km at 800-900°C. It appears that this increase is due to the conversion of the impurity-related (extrinsic) conductivity into the intrinsic conductivity. The increase of electrical conductivity at this depth may also occur because of the phase conversions in the olivines with a high percent of fialite. /209

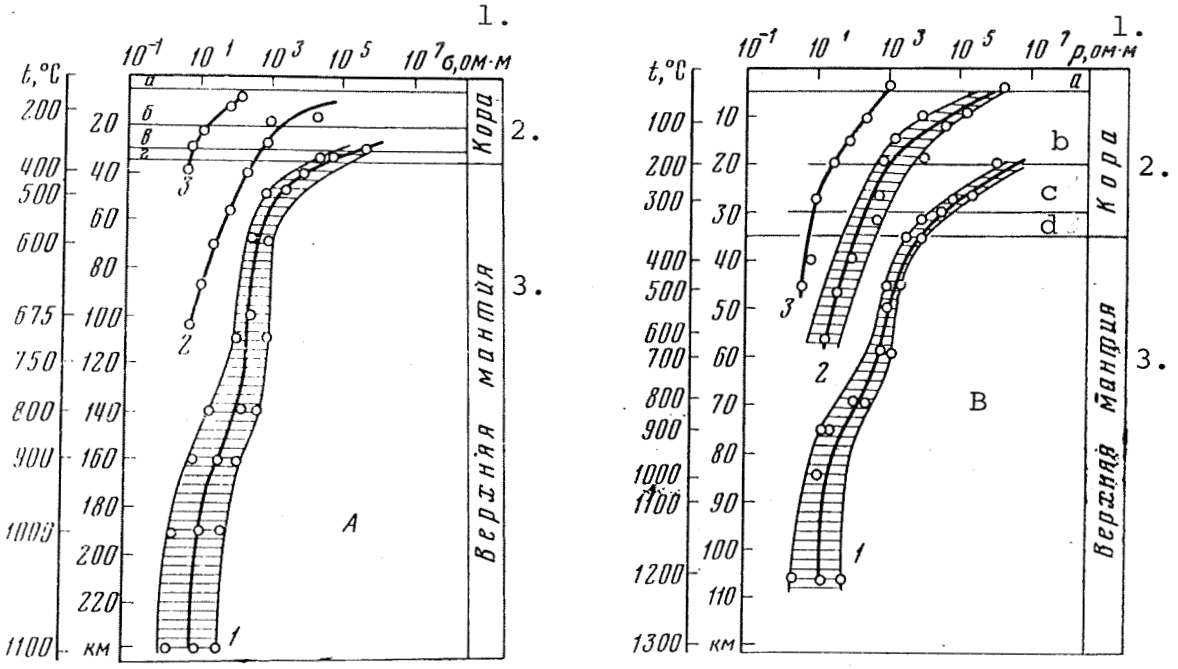

Figure 94. Distribution of electrical resistivity within the Earth's crust and in the upper mantle on the basis of experimental data within the base formations (A) and for Pechenga region of the Kola peninsula (B).

1 - area of electrical resistivity as a function of the rock composition; 2 - distribution of electrical resistivity in terms of the alkaline rocks; 3 - distribution of electrical resistivity in terms of the rock serpentinization; a - stratified layer; b - granite-gneiss layer; c - granulite-basite layer; d - granulite-eclogite layer.

Key: 1. ohm·m; 2. Crust; 3. Upper mantle.

3. Distribution of Electrical Resistivity as a Function of Depth in the Zones with Different Thermal Conditions

A number of studies have appeared in recent times in which the authors present the temperature distribution as a function of depth, for different generic parts of the Earth, taking into account the specific thermal flows [197-199].

Figure 95 shows the experimental data for the distribution of electrical resistivity to the depth on the order of 100 km for the regions with different structure and temperature distribution within the Earth's crust and in the upper mantle.

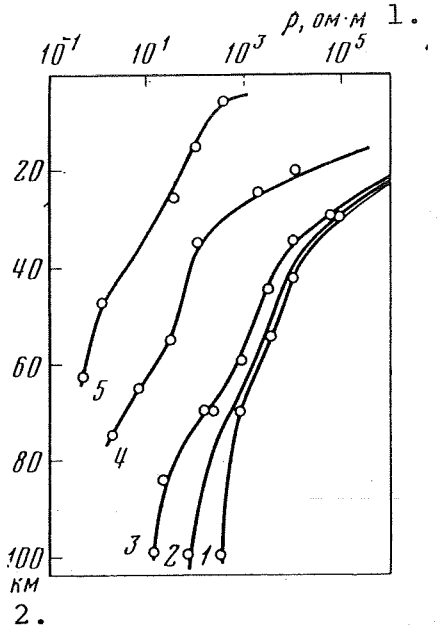

Figure 95. Electrical resistivity in the Earth's crust and in the upper mantle in different tectonic zones based on experimental data. The curves were constructed by taking into account the effect of temperature and pressure.

1 - beds; 2 - platforms; 3 - Pechenga region of Kola peninsula; 4 - areas of present-day volcanic activity; 5 - island arcs.

Key: 1. ohm·m; 2. km

On the basis of this new data, describing the temperature distribution in the Earth's interior, the electrical parameters of the rocks within the Earth's crust and in the mantle were estimated for the zones of low (0.8), normal (1.1), intermediate (1.3-1.5) and high ($2.0 \cdot 10^{-6}$ m·cal/cm^2·s) thermal flows (Table 36).

Distribution of the electrical resistivity as a function of depth in the Pechenga district of the Kola peninsula.

By taking into account the local thermal flows and structure of the Earth's crust, based on seismic data, E. A. Lubimova and V. K. Vlasov have calculated /210 the temperature distribution curve for Pechenga region of the Kola peninsula, to the depth of 100 km [11]. On the basis of this temperature distribution, the curves of electrical conductivity distribution in the Earth's crust and in the upper mantle were constructed, taking into account the effect of pressure on σ, to the depth of 100 km (Figure 94B). One can /211 also see in this figure that the electrical conductivity change in this region as a function of depth, and compared to the other platforms, is of different character. If we are to take into account the geothermal data [11] and the electrical conductivity of the rocks at the appropriate p and t, then the conducting layer which is at the depth of 120 km [202] probably corresponds to the reality.

Structure and possible explanation of the geoelectrical cross section, based on the laboratory experiments and electromagnetic probing on the Kola peninsula.

An attempt was made jointly with N. P. Vladimirov to interpret the probing curve, obtained in the area of Lovozero, by employing the geological and laboratory data.

The Lovozero region is located on the Kola peninsula, composed of displaced rocks and the rocks which underwent metamorphosis of the precambrian age. The crystalline base in this region features deep fractures of different lengths, along which one observes the incorporation of intrusions of the ultrabasic and alkaline rocks. The alkaline Lovozero mass is also found within the zone of the so-called extra deep and narrow fracture which bisects the Earth's crust, and probably reaches the mantle [204]. The specific resistivity of igneous rocks to the depth of several kilometers which was obtained by electrical probing, by using the d.c. current, is $5 \cdot 10^3 - 5 \cdot 10^4$ ohm·m [205-207].

The attempt was made to determine the degree of relationship between the interpretation results of the thermal flow distribution and the temperatures in this region. With this purpose in mind, some of the probable electrical conductivity distributions within the Earth's crust and in the upper mantle have been considered. The distribution curves were constructed by analyzing the temperature as a function of depth [11, 199, 208], and the electrical conductivity data for the rocks as a function of temperature and pressure [58, 88]. The electrical conductivity at temperature above 700°C was determined approximately by extrapolating the experimental results obtained at the pressures of 20,000 kg/cm^2 and the temperatures of up to 700°C as well as up to the temperature of 1200°C, but at atmospheric pressure. As an example, Figure 96 shows the measured $\lg \sigma = f(p,t)$ of the ultrabasic rocks of peridotite type with comparatively small quantities of iron in olivine (approximately 10-15%).

If one is to approximate the curve segments having a smooth change in σ by a stepwise curve, then the upper mantle may be represented as consisting of two layers, characterized by the specific resistance of 500-800 and 80 ohm·m.

According to Figure 96, the depth at which the rocks of the upper mantle are found is 45-50 km. The thickness of the upper layer of the mantle is established only approximately and may be equal to 25, 55, 90 km. The Earth's crust at the point of experimentation, according to the data from the magnetotelluric sounding, consists of two layers, 17 and 34 km thick, with the resistivity of about 6000 and 50,000 ohm·m. /212
The theoretical templets were calculated on the basis of the data by using the geoelectrical cross section analysis of the Earth's crust and of the upper mantle and are presented below:

No. of templets	Variant of temperature distribution	ν_2	μ_2	ν_3	μ_3	μ_4
1	[11]	2,0	7,3	1,49	0,094	0,0125
2	[208]	2,0	7,8	3,30	0,094	0,0125
3	[199]	2,0	7,8	5,40	0,094	0,0125

[Commas in tabulated material are equivalent to decimal points.]

$\nu_i=h_i/h_1$, $\mu=\rho_i/\rho_1$, where h_i and ρ_i is the thickness and resistivity of the i layer.

TABLE 36. ELECTRICAL PARAMETERS OF ROCKS WITHIN ZONES OF DIFFERENT THERMAL FLOWS

Depth, km	Temperature, °C	σ, ohm^{-1}·cm^{-1}	E_0, eV	σ_0', ohm^{-1}·cm^{-1}	Thermal flow
15	200	$2\cdot10^{-10}$	0,5—0,7	$2\cdot10^{-1}$	Low
	300	10^{-7}	0,5—0,7	$2\cdot10^{-1}$	Normal
	550	10^{-5}	1,2—2,0	$5\cdot10^{-1}$	Intermediate
	700	$1,6\cdot10^{-4}$	1,0—2,0	$5\cdot10^{-1}$	High
Boundary of the mantle					
40	400	$3\cdot10^{-9}$	1,2	$5\cdot10^{-1}$	Low
	550	$8\cdot10^{-8}$	1,2	$5\cdot10^{-1}$	Normal
	800	$2\cdot10^{-6}$	2,6	10^{6}	Intermediate
	1160	10^{-3}	2,6	10^{6}	High
Upper mantle					
90	1000	$3,4\cdot10^{-6}$	2,6—3,0	10^{4}—10^{6}	Normal
120	750	10^{-7}	0,8	10^{-4}	Low
190	1000	$3,4\cdot10^{-6}$	2,6—3,0	10^{4}—10^{6}	»
240	1100	$2\cdot10^{-5}$	2,6—3,0	10^{4}—10^{6}	»

[Commas in tabulated material are equivalent to decimal points.]

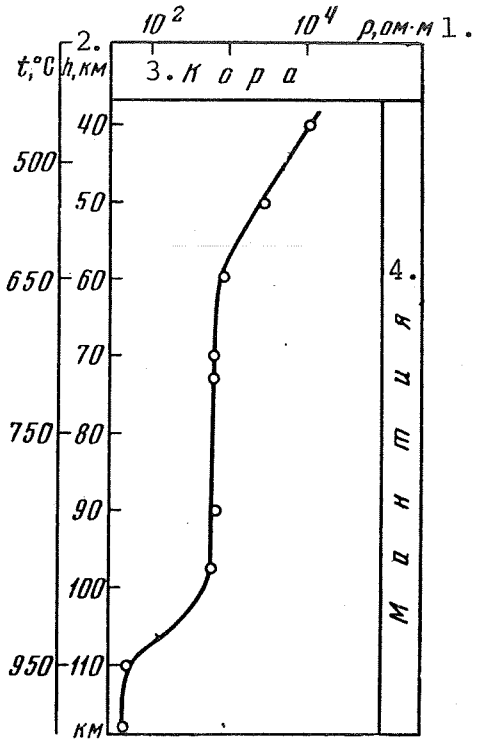

Figure 96. Distribution of specific resistance in the Earth's crust and in the upper mantle in the Lovozero region of the Kola peninsula, based on the laboratory data and on the electromagnetic probing.
Key: 1. ohm·m; 2. km; 3. crust; 4. mantle.

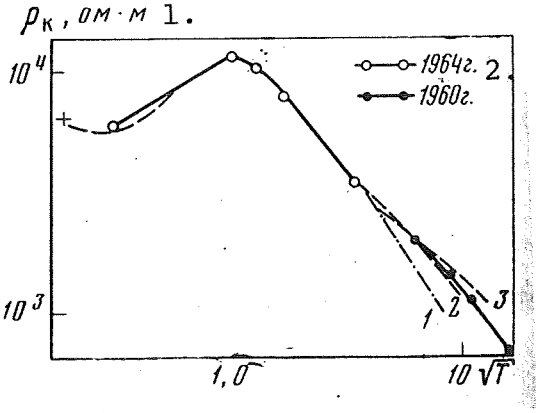

Figure 97. Probing curve, as compared to theoretical templets (1-3).
Key: 1. ohm·m; 2. year

In Figure 97, the experimental curve of probing superimposes in the best way with the templet 2, which corresponds to the temperature distribution presented in the studies [11, 199, 208]. Consequently, the interpretation of the curve gives us the following results: h_1=16.8 km, ρ_1=6400 ohm·m, h_2=33.6 km, ρ_2=50,000 ohm·m, h_3=55 km, ρ_3=600 ohm·m and $h_4=\infty$, ρ_4= 80 ohm·m.

The resistivity data obtained while interpreting the probing curve, in spite of some effect of the horizontal inhomogeneity of the cross section, also indicates the development under the Earth's crust, in the Lovozero region, of the ultrabasic rocks of peridotite type, containing small quantities of iron in the chemical composition of olivine. This conclusion agrees with the study in which, in the case of the upper mantle rocks, it is assumed that insignificant amount of iron is present. The Fe/Mg ratio fluctuates within the range of 1:9 and 1:4 [208]. /213

The preliminary studies presented here show the desirability of conducting the electromagnetic probing, while investigating the electrical conductivity in rocks at high pressures and temperatures. Such studies should be conducted in the regions in which the thermal flow has been well studied, and in which the temperature study as a function of depth has been determined. The geological structure of the Earth's crust in this area should also be thoroughly studied.

In our opinion, the promising regions for such studies are the Pechenga region on the Kola peninsula and Baikal rift, within the Baikal region [193, 11].

CONCLUSION /214

The material presented in this book (primarily on the basis of the studies by the authors) is the first comprehensive description of the study of electrical conductivity in minerals and rocks at high pressures and temperatures.

Because of the exceptional variety, and in a number of cases because of the rather complex chemical composition and structural peculiarities, the rocks and minerals are extremely complex physical objects which are to be investigated. Therefore, in order to obtain reliable data and probable limits in the parameters for a specific mineral or for a rock, it is quite important to have on one hand, the statistical, averaged-out data and on the other hand, to present the major factors which define the electrical conductivity in these natural objects.

Because of the fact that the data on minerals are based on the measurements of two-four samples, depending on variation in the amounts of impurities, it is likely that some deviations of electrical conductivity, shown in the tables, are possible. However, the data, even in such form, made it possible to draw a number of conclusions as to the effect of chemical composition and of the structure on the conducting properties of minerals. This information is needed to properly understand the relationship between the change in electrical properties of different rocks as a function of pressure and temperature.

The fact that the largest part of this book is devoted to the studies of electrical conductivities in rocks at high temperatures, but at atmospheric pressure, is due to much stronger effect of temperature on the electrical properties of the rocks than the temperatures within the range of 20-1100°C and the pressure of 1-20 kbar. At higher pressures and temperatures, the jump in the electrical conductivities because of the possible polymorphous transitions and melting should not be excluded.

It is necessary to point out that because of the thermochemical activity in a number of rocks, of great significance may be also the medium in which the experiment is being carried out. All measurements taken by us were at the atmospheric pressure, with the exception of mica, the electrical conductivity of which was measured in vacuum. The future work should involve the evaluation of the degree of effect of the surrounding medium on the electrical properties of the rocks and minerals by comparing the measurements at high temperatures in vacuum, in the helium atmosphere and in the air.

According to the general geological concepts, in the upper /215
part of the Earth's crust, down to 20-30 km, one should not exclude from the rock's composition the pore solutions which, as it is known, define the magnitude of related parameters. Because of a number of difficulties of technical nature, the study of moisture-saturated rocks at high pressures and temperatures were not carried out on the necessary scale and our investigations in this direction are limited by small experimental data. At the same time, the question of physical nature of the conducting layers in the Earth's crust without experimental data of such kind cannot be resolved satisfactorily. The study of a large variety of different samples, in terms of mineral composition and of the rock genesis, makes it possible at this time to state only that the rocks with the highest conductivity must be evaluated by the geologists from the point of view of their representativeness within the conducting layer of the Earth's crust.

The material presented in this book indicates that the electrical properties of ultrabasic rocks and the minerals contained in them, at pressures above 20 kbar and temperatures above 700°C, as well as the mechanism of electrical conductivity, have been investigated only slightly. It is necessary to set up some special studies and to determine the type of the current carriers and their mobility. Without experiments of such type, and the correspondingly generated data, the theoretical studies in these two directions, in determining the electrical conductivity in the lower part of the mantle, cannot be carried out and the temperature distributions as a function of depth cannot be obtained with the necessary degree of reliability. The study of electrical properties of rocks at high pressures and temperatures is quite important for the extensive geophysical probing and is also needed for the development of new and improved methods of rock destruction, the enrichment and utilization of the useful minerals and the determination of conditions for crystallization of minerals.

The authors take this opportunity to express their sincere gratitude to Professor M. P. Volarovich for the time he has spent in editing and advice, while this book was being written, to the senior scientific researcher S. N. Kondrashov for the valuable suggestions, while reading the manuscript, and to the senior laboratory assistant L. S Skvortsova for handling all graphic representations.

APPENDIX 1. Electrical conductivity ($ohm^{-1} \cdot cm^{-1}$) in minerals at high temperatures, the activation energies (E_0, eV) and the preexponential coefficient (σ_0, $ohm^{-1} \cdot cm^{-1}$) in the region of intrinsic conductivity.

Mineral and its chemical formula	Temperature, °C					Temperautre, °C				Temperature range t, °C	E_0, eV	$\lg \sigma_0$, $ohm^{-1}cm^{-1}$
	200	300	400	500	600	700	800	900	1000			
Halite NaCl	—	$1,0 \cdot 10^{-11}$	10^{-8}	—	10^{-5}	—	10^{-3}	Melting		200—800	1,7—2,6	—
Sylvene KCl	—	$5,0 \cdot 10^{-12}$	10^{-9}	—	$7 \cdot 10^{-6}$	Melting				200—750	1,9—2,06	—
Fluorite CaF_2	$4,0 \cdot 10^{-11}$	$2,4 \cdot 10^{-9}$	10^{-7}	$1,5 \cdot 10^{-6}$	$4,9 \cdot 10^{-5}$	$8,0 \cdot 10^{-5}$	$3,3 \cdot 10^{-4}$	$3,4 \cdot 10^{-3}$	—	200—1000	1,4	3,75
Fluorite	—	—	10^{-8}	$6,5 \cdot 10^{-8}$	—	10^{-6}	$6,5 \cdot 10^{-6}$	—	—	up to 500 500—800	0,54 0,87	—
Forsterite Mg_2SiO_4	—	—	—	—	—	$3,3 \cdot 10^{-7}$	—	$1,6 \cdot 10^{-6}$	—	up to 900 900—1300	0,8—1,0 2,2—2,4	—2,4 5,0
Fialite Fe_2SiO_4	10^{-2} $1,5 \cdot 10^{-4}$	$6,0 \cdot 10^{-2}$ $2,0 \cdot 10^{-3}$	— —	— $6,5 \cdot 10^{-2}$	— —	— —	— —	— —	— —	— 200—500	— 0,18—0,3	— —
Olivine $(Mg, Fe)_2SiO_4$	—	$3,1 \cdot 10^{-10}$	$4,0 \cdot 10^{-9}$	$3,1 \cdot 10^{-8}$	$3,0 \cdot 10^{-7}$	$2,5 \cdot 10^{-6}$	$6,3 \cdot 10^{-6}$	$4,0 \cdot 10^{-5}$	$2,0 \cdot 10^{-3}$	up to 470 470—620 620—1050	0,66 1,0 1,64	—3,8 —1,4 2,3
(Parallel to the optical axis)	—	$3,2 \cdot 10^{-8}$	$3,1 \cdot 10^{-7}$	$1,5 \cdot 10^{-6}$	$5,6 \cdot 10^{-6}$	$2,2 \cdot 10^{-5}$	$2,2 \cdot 10^{-5}$	$2,5 \cdot 10^{-4}$	$6,5 \cdot 10^{-3}$	up to 480 480—630 630—1050	0,64 0,8 1,2	—2,0 —0,9 1,3
(Perpendicular to the optical axis)	—	10^{-7}	$6,3 \cdot 10^{-7}$	$2,5 \cdot 10^{-6}$	$1,0 \cdot 10^{-5}$	$4,5 \cdot 10^{-5}$	10^{-4}	10^{-3}	$6,5 \cdot 10^{-3}$	up to 490 490—650 650—1020 1020—1120	0,64 0,83 1,3 3,2	—1,8 —0,7 1,5 9,4
Danburite $CaB_2[SiO_4]$	$2,1 \cdot 10^{-10}$	$6,5 \cdot 10^{-10}$	$3,5 \cdot 10^{-8}$	$5,4 \cdot 10^{-7}$	$3,8 \cdot 10^{-7}$	$6,7 \cdot 10^{-7}$	$1,5 \cdot 10^{-6}$	$1,9 \cdot 10^{-6}$	Melting	up to 500 500—600 600—950	1,20 Anomaly 0,7	1,5 —3,4
	—	$1,7 \cdot 10^{-10}$	$5,4 \cdot 10^{-9}$	$3,0 \cdot 10^{-8}$	$4,2 \cdot 10^{-8}$	$9,5 \cdot 10^{-8}$	$2,4 \cdot 10^{-7}$	$5,4 \cdot 10^{-7}$	Melting	up to 500 500—650 650—950	1,1 Anomaly 0,65	0,1 —3,2
	—	$1,3 \cdot 10^{-11}$	$5,1 \cdot 10^{-10}$	$2,5 \cdot 10^{-8}$	$4,2 \cdot 10^{-9}$	$1,9 \cdot 10^{-8}$	$4,7 \cdot 10^{-8}$	$5,3 \cdot 10^{-8}$	Melting	up to 500 500—600 600—950	1,4 Anomaly 0,66	0,5 —4,0
Garnet $A_3B_2[SiO_4]_3$	$2,9 \cdot 10^{-11}$	$2,4 \cdot 10^{-9}$	$1,1 \cdot 10^{-7}$	$1,1 \cdot 10^{-6}$	$4,1 \cdot 10^{-6}$	10^{-6}	$3,4 \cdot 10^{-5}$	$1,2 \cdot 10^{-4}$	$9,0 \cdot 10^{-4}$	up to 300 300—750 >750	1,0 0,8 1,42	1,0 —1,2 2,8
	$1,7 \cdot 10^{-11}$	$2,4 \cdot 10^{-10}$	$4,6 \cdot 10^{-8}$	$2,1 \cdot 10^{-7}$	$1,4 \cdot 10^{-6}$	$5,0 \cdot 10^{-6}$	$1,4 \cdot 10^{-5}$	$5,9 \cdot 10^{-5}$	$6,0 \cdot 10^{-4}$	up to 350 350—800 >800	0,76 1,0 2,0	—3,8 —1,5 4,4
	$2,4 \cdot 10^{-11}$	$6,2 \cdot 10^{-10}$	$1,3 \cdot 10^{-7}$	$2,1 \cdot 10^{-6}$	$8,9 \cdot 10^{-6}$	$1,3 \cdot 10^{-5}$	$2,6 \cdot 10^{-4}$	$4,0 \cdot 10^{-4}$	—	up to 350 350—780 >750	0,8 0,92 1,7—2,0	—1,8 3,6 —
Sphene CaTi[SiO$_4$]O	$1,1 \cdot 10^{-10}$	$1,8 \cdot 10^{-9}$	$3,3 \cdot 10^{-8}$	$2,8 \cdot 10^{-7}$	$9,5 \cdot 10^{-7}$	$1,8 \cdot 10^{-6}$	$7,1 \cdot 10^{-6}$	$7,2 \cdot 10^{-5}$	$9,8 \cdot 10^{-5}$	100—750 750—1000 1000—1200	0,9 1,3 3,2	—1,0 —1,3 8,01

[Appendix 1 is continued on the next page.]

APPENDIX 1 (continued)

Mineral and its chemical formula	Temperature, °C									Temperature range t°C	E_0, eV	$\lg \sigma_0$, $ohm^{-1} \cdot cm^{-1}$
	200	300	400	500	600	700	800	900	1000			
Beryl $Be_3Al[Si_6O_8]$	—	$5,6 \cdot 10^{-11}$	$7,6 \cdot 10^{-10}$	$4,2 \cdot 10^{-9}$	10^{-8}	$2,7 \cdot 10^{-8}$	$7,6 \cdot 10^{-8}$	$4,1 \cdot 10^{-7}$	$2,0 \cdot 10^{-6}$	up to 830	0,82	−4,3
	10^{-11}	$5,3 \cdot 10^{-9}$	$7,6 \cdot 10^{-9}$	$7,6 \cdot 10^{-8}$	$2,7 \cdot 10^{-7}$	$1,3 \cdot 10^{-6}$	$2,5 \cdot 10^{-6}$	$4,2 \cdot 10^{-6}$	$6,3 \cdot 10^{-6}$	>830	2,6	5,0
Eudialyte $(Na, Ca)_6 \cdot ZiSi_6[OH, Cl]$	$1,1 \cdot 10^{-7}$	$1,0 \cdot 10^{-6}$	$3,2 \cdot 10^{-6}$	$1,0 \cdot 10^{-5}$	$2,8 \cdot 10^{-5}$	$6,8 \cdot 10^{-5}$	$1,2 \cdot 10^{-4}$	$1,6 \cdot 10^{-3}$	$8,2 \cdot 10^{-3}$	200—950	0,80	−2,2
										150—450	0,5	−2,6
										450—800	0,7	−1,6
										800—1200	2,4	7,5
Diopside $CaMg[Si_2O_6]$	$1,1 \cdot 10^{-10}$	$6,3 \cdot 10^{-10}$	$7,5 \cdot 10^{-9}$	$1,2 \cdot 10^{-7}$	$5,3 \cdot 10^{-7}$	$2,2 \cdot 10^{-6}$	$1,5 \cdot 10^{-6}$	$3,4 \cdot 10^{-6}$	$4,7 \cdot 10^{-6}$	up to 700	0,98	−2,25
										700—850	Anomaly	
										850—1050	1,0	−3,6
	$1,2 \cdot 10^{-10}$	10^{-10}	$2,6 \cdot 10^{-9}$	$3,2 \cdot 10^{-8}$	$2,3 \cdot 10^{-7}$	$6,3 \cdot 10^{-7}$	$1,0 \cdot 10^{-6}$	$1,3 \cdot 10^{-6}$	$2,4 \cdot 10^{-6}$	up to 700	0,98	−3,75
										700—850	Anomaly	
										850—1050	1,0	−3,25
Eugirite $NaFe^{3+}[Si_2O_6]$	$2,6 \cdot 10^{-7}$	$1,3 \cdot 10^{-5}$	$1,5 \cdot 10^{-5}$	$3,2 \cdot 10^{-5}$	$1,0 \cdot 10^{-5}$	$1,4 \cdot 10^{-5}$	$1,6 \cdot 10^{-4}$	$5,9 \cdot 10^{-4}$	$1,0 \cdot 10^{-2}$	100—775	0,46	−2,9
										775—850	Anomaly	
										850—1100	2,4	8,95
Jadeite $NaAl[Si_2O_6]$	$3,4 \cdot 10^{-9}$	$3,4 \cdot 10^{-8}$	$3,9 \cdot 10^{-8}$	$1,3 \cdot 10^{-7}$	$1,9 \cdot 10^{-7}$	$3,3 \cdot 10^{-7}$	$2,3 \cdot 10^{-6}$	—	—	up to 700	0,4	−5,75
										700—850	(2,0)?	(3,0)?
	—	$1,3 \cdot 10^{-7}$	$1,7 \cdot 10^{-7}$	$5,5 \cdot 10^{-7}$	$1,0 \cdot 10^{-6}$	$3,9 \cdot 10^{-5}$	$4,7 \cdot 10^{-5}$	$1,5 \cdot 10^{-4}$	$1,2 \cdot 10^{-3}$	up to 500	0,36	−4,1
										900—1050	(2,8)?	(7,5)?
Hornblende $Ca_2Na(Mg, Fe^{2+})_4(Al, Fe^{3+})[(Si, Al)_4 \cdot O_{11}]_2[OH]_2$	—	$6,4 \cdot 10^{-8}$	$1,9 \cdot 10^{-7}$	$4,7 \cdot 10^{-7}$	$9,4 \cdot 10^{-6}$	$5,4 \cdot 10^{-6}$	$1,8 \cdot 10^{-5}$	$6,3 \cdot 10^{-6}$	$1,8 \cdot 10^{-5}$	up to 600	0,66	2,9
										600—850	Anomaly	
										850—1050	1,3	−1,7
	$4,2 \cdot 10^{-10}$	$2,1 \cdot 10^{-9}$	$1,9 \cdot 10^{-8}$	$2,7 \cdot 10^{-7}$	$8,2 \cdot 10^{-7}$	$1,3 \cdot 10^{-6}$	$5,0 \cdot 10^{-6}$	$5,5 \cdot 10^{-6}$	$7,6 \cdot 10^{-6}$	up to 750	0,69	−3,4
										750—900	Anomaly	
										900—1050	1,46	1,5
Actinolite $Ca_2(Mg, Fe^{2+})_5 \cdot [Si_4O_{11}]_2[OH]_2$	$2,1 \cdot 10^{-10}$	$2,9 \cdot 10^{-9}$	$4,8 \cdot 10^{-8}$	$2,1 \cdot 10^{-7}$	$5,2 \cdot 10^{-6}$	$3,9 \cdot 10^{-6}$	$4,0 \cdot 10^{-7}$	$5,1 \cdot 10^{-7}$	$2,4 \cdot 10^{-6}$	200—500	0,83	2,6
										500—630	2,18	6,64
										630—830	Anomaly	
										830—1100	1,65	0,75
Rubecite $Na_2Fe_2[Si_4O_{11}]_2 \cdot [O, OH]_2$	$1,9 \cdot 10^{-4}$	$4,8 \cdot 10^{-4}$	$2,6 \cdot 10^{-3}$	$1,1 \cdot 10^{-2}$	$1,5 \cdot 10^{-2}$	$3,8 \cdot 10^{-2}$	$8,5 \cdot 10^{-2}$	$1,9 \cdot 10^{-1}$	$3,8 \cdot 10^{-1}$	up to 750	0,42	0,75
										750—1050	0,9	—
											Melting	
										up to 750	0,2	−3,75
										750—1050	2,6	—
											Melting	
Talcum $Mg_3[Si_4O_{10}][OH]_2$	10^{-11}	$2,8 \cdot 10^{-10}$	$1,4 \cdot 10^{-9}$	$1,1 \cdot 10^{-8}$	$5,6 \cdot 10^{-8}$	$6,3 \cdot 10^{-7}$	$6,2 \cdot 10^{-7}$	$2,1 \cdot 10^{-6}$	$2,2 \cdot 10^{-6}$	300—950	0,94	−1,8
										>950	2,5	8,0
Pyrophillite $Al_2[Si_4O_{10}] \cdot [OH]_2$	10^{-12}	$6,2 \cdot 10^{-11}$	$1,1 \cdot 10^{-9}$	$9,2 \cdot 10^{-8}$	$4,0 \cdot 10^{-7}$	$1,3 \cdot 10^{-6}$	$5,6 \cdot 10^{-6}$	—	—	280—900	1,1	0,2
Phlogopite $KMg_3[Si_3AlO_{10} \cdot [OH, F]_2$	$3,3 \cdot 10^{-12}$	$2,0 \cdot 10^{-11}$	$3,6 \cdot 10^{-10}$	$9,4 \cdot 10^{-10}$	$2,5 \cdot 10^{-9}$	$6,1 \cdot 10^{-9}$	$2,3 \cdot 10^{-8}$	$1,1 \cdot 10^{-7}$	$4,0 \cdot 10^{-7}$	100—350	0,5	−6,6
										350—400	1,5	2,4
										400—750	0,5	−5,7
										750—950	2,4	3,0

(Appendix 1 is continued on the following page)

APPENDIX 1 (continued)

Mineral and its chemical formula	Temperature, °C									Temperature range t, °C	E_a, eV	$\lg \sigma_0$, $ohm^{-1} \cdot cm^{-1}$
	200	300	400	500	600	700	800	900	1000			
Biotite $K(Mg, Fe)_3 \cdot [Si_3AlO_{12}]$ [OH, F]	$3,2 \cdot 10^{-14}$	$3,3 \cdot 10^{-12}$	$5,8 \cdot 10^{-11}$	$5,5 \cdot 10^{-10}$	$7,1 \cdot 10^{-8}$	$1,6 \cdot 10^{-7}$	—	—	—	100—500	1,0	—2,4
										500—700	Anomaly	
										700—950	2,0	3,35
Muscovite $KAl_2[AlSi_3O_{10}] \cdot [OH]_2$	$9,1 \cdot 10^{-13}$	$1,8 \cdot 10^{-11}$	$1,7 \cdot 10^{-10}$	$1,3 \cdot 10^{-9}$	$4,5 \cdot 10^{-9}$	$2,3 \cdot 10^{-9}$	$2,2 \cdot 10^{-8}$	$2,3 \cdot 10^{-7}$	—	150—450	0,8	—3,75
										450—700	Anomaly	
										700—950	2,25	2,9
	$5,8 \cdot 10^{-15}$	$2,3 \cdot 10^{-12}$	$4,8 \cdot 10^{-11}$	$2,6 \cdot 10^{-9}$	$1,2 \cdot 10^{-8}$	$1,4 \cdot 10^{-9}$	$7,8 \cdot 10^{-9}$	$5,1 \cdot 10^{-8}$	$6,0 \cdot 10^{-7}$	150—400	0,95	—3,0
										400—700	Anomaly	
										700—950	2,2	—2,7
Serpentine $Mg_6[Si_4O_{10}] \cdot [OH]_8$	$1,3 \cdot 10^{-10}$	$9,4 \cdot 10^{-10}$	$1,1 \cdot 10^{-9}$	$3,5 \cdot 10^{-9}$	$1,3 \cdot 10^{-8}$	$3,2 \cdot 10^{-8}$	$9,4 \cdot 10^{-7}$	$2,5 \cdot 10^{-7}$	$1,3 \cdot 10^{-6}$	up to 400	0,21	—9,7
										400—900	0,8	—5,6
										900—1050	2,0	1,25
	$2,3 \cdot 10^{-10}$	$9,5 \cdot 10^{-10}$	$6,5 \cdot 10^{-9}$	$1,3 \cdot 10^{-8}$	$4,5 \cdot 10^{-8}$	$2,7 \cdot 10^{-7}$	$8,5 \cdot 10^{-8}$	$3,8 \cdot 10^{-7}$	$9,5 \cdot 10^{-7}$	up to 600	0,6	—3,0
										600—750	Anomaly	
										750—850	1,4	—1,3
										850—1050	1,8	1,0
Albite $Na[AlSi_3O_8]$	$9,5 \cdot 10^{-11}$	$2,0 \cdot 10^{-10}$	$5,5 \cdot 10^{-9}$	$6,3 \cdot 10^{-8}$	$1,4 \cdot 10^{-7}$	$2,9 \cdot 10^{-7}$	$5,5 \cdot 10^{-7}$	$9,5 \cdot 10^{-7}$	$4,8 \cdot 10^{-6}$	450—860	0,54	—4,2
										860—1050	1,60	0,5
	—	$2,3 \cdot 10^{-10}$	$3,8 \cdot 10^{-9}$	$4,2 \cdot 10^{-8}$	$4,8 \cdot 10^{-8}$	$3,3 \cdot 10^{-7}$	$4,5 \cdot 10^{-7}$	$7,6 \cdot 10^{-7}$	$3,8 \cdot 10^{-6}$	200—790	0,54	—5,7
										790—1050	1,76	1,1
	—	$9,5 \cdot 10^{-10}$	$4,8 \cdot 10^{-8}$	$1,5 \cdot 10^{-7}$	$7,6 \cdot 10^{-7}$	$3,5 \cdot 10^{-6}$	$7,6 \cdot 10^{-6}$	$1,9 \cdot 10^{-5}$	—	350—950	0,86	—2,7
Oligoclase	—	$5,6 \cdot 10^{-10}$	$5,0 \cdot 10^{-9}$	$2,5 \cdot 10^{-8}$	$5,0 \cdot 10^{-8}$	$1,6 \cdot 10^{-7}$	$1,0 \cdot 10^{-6}$	$5,6 \cdot 10^{-6}$	—	300—700	0,54	—4,2
										700—900	1,8	1,5
	10^{-11}	10^{-9}	$1,6 \cdot 10^{-8}$	$1,0 \cdot 10^{-7}$	$3,2 \cdot 10^{-7}$	$1,0 \cdot 10^{-6}$	$2,5 \cdot 10^{-6}$	$5,6 \cdot 10^{-6}$	$1,0 \cdot 10^{-5}$	up to 900	0,8	—2,0
										900—1050	2,0	1,0
Labrodorite	$1,8 \cdot 10^{-9}$	$2,2 \cdot 10^{-8}$	$7,4 \cdot 10^{-8}$	$3,3 \cdot 10^{-7}$	$9,0 \cdot 10^{-7}$	$1,5 \cdot 10^{-6}$	$3,5 \cdot 10^{-6}$	$8,7 \cdot 10^{-6}$	$2,7 \cdot 10^{-5}$	100—800	0,53	—4,8
										800—1000	0,93	2,9
										1000—1100	3,5	5,2
Microcline $K[AlSi_3O_8]$	10^{-12}	$3,2 \cdot 10^{-11}$	$2,6 \cdot 10^{-10}$	$1,4 \cdot 10^{-9}$	$5,9 \cdot 10^{-9}$	$4,0 \cdot 10^{-8}$	$1,1 \cdot 10^{-7}$	$3,2 \cdot 10^{-7}$	$6,2 \cdot 10^{-6}$	up to 550	0,72	—6,6
										550—900	1,13	—1,6
										900—1090	3,7	9,4
Orthoclase	10^{-12}	$4,2 \cdot 10^{-11}$	$7,7 \cdot 10^{-10}$	$3,6 \cdot 10^{-9}$	$1,6 \cdot 10^{-8}$	$7,1 \cdot 10^{-8}$	$1,2 \cdot 10^{-7}$	$3,0 \cdot 10^{-7}$	$7,1 \cdot 10^{-6}$	up to 300	0,6	—5,1
										300—900	0,85	—2,8
										900—1050	3,72	9,4
Nepheline $Na[AlSiO_4]$	$2,7 \cdot 10^{-9}$	$4,3 \cdot 10^{-9}$	$1,4 \cdot 10^{-8}$	$3,5 \cdot 10^{-8}$	$1,4 \cdot 10^{-7}$	$3,5 \cdot 10^{-7}$	$6,8 \cdot 10^{-7}$	$2,7 \cdot 10^{-6}$	$1,6 \cdot 10^{-5}$	200—450	0,2	—6,0
										450—700	0,66	—4,7
										700—1050	1,6	1,4
	$3,3 \cdot 10^{-10}$	$4,0 \cdot 10^{-9}$	$2,3 \cdot 10^{-8}$	$4,5 \cdot 10^{-8}$	$1,4 \cdot 10^{-7}$	$4,5 \cdot 10^{-7}$	$1,6 \cdot 10^{-6}$	$5,4 \cdot 10^{-6}$	$2,7 \cdot 10^{-5}$	150—700	0,4	—4,1
										700—1050	1,6	1,2

[Commas in tabulated material are equivalent to decimal points.]

APPENDIX 2. Electrical conductivity σ, activation energy E_0 and the preexponential coefficient σ_0 of acidic and intermediate rocks at high temperatures.

Rock, origin	Mineral composition, %	σ (ohm^{-1}·cm^{-1}) at t, °C				σ (ohm^{-1}·cm^{-1}) at t, °C					Temperature range t°C	E_0, eV	lg σ_0, ohm^{-1}·cm^{-1}
		200	300	400	500	600	700	800	900	1000			
Garnet 1779, Kazakhstan*	Quartz-30, Oligoclase-50-55, muscovite-8-10	$7,0\cdot10^{-12}$	$1,5\cdot10^{-10}$	$2,3\cdot10^{-9}$	$1,9\cdot10^{-8}$	$8,3\cdot10^{-8}$	$3,7\cdot10^{-7}$	$1,4\cdot10^{-6}$	$7,1\cdot10^{-6}$	10^{-5}	up to 450 450—850 850—1050	0,79 1,03 2,6	—2,6 —1,0 6,5
Garnet 1785, Kazakhstan*	Quartz-35 feldspar-60-63, biotite-2-5	—	$3,4\cdot10^{-11}$	$8,3\cdot10^{-10}$	$1,1\cdot10^{-8}$	$5,6\cdot10^{-8}$	$1,5\cdot10^{-7}$	$5,5\cdot10^{-7}$	$1,5\cdot10^{-6}$	$9,1\cdot10^{-6}$	up to 700 700—850 850—1050	0,8 0,9 1,5—2,0	—2,0 0,5
Garnet-porphyr 1794, Kazakhstan*	Quartz, potassium-containing feldsper, biotite, hornblende and micropertite	10^{-12}	$1,3\cdot10^{-11}$	$7,8\cdot10^{-10}$	$7,8\cdot10^{-9}$	$5,3\cdot10^{-8}$	$1,3\cdot10^{-7}$	$4,8\cdot10^{-7}$	$2,2\cdot10^{-6}$	$1,6\cdot10^{-5}$	up to 420 420—850 >850	0,92 1,0 2,2	—4,0 2,5 3,5
Garnet 566, Caucasus	—	$2,3\cdot10^{-12}$	$1,2\cdot10^{-10}$	$2,0\cdot10^{-9}$	$1,3\cdot10^{-8}$	$5,5\cdot10^{-8}$	$2,2\cdot10^{-7}$	$5,5\cdot10^{-7}$	$1,9\cdot10^{-6}$	10^{-5}	up to 900 900—1050	0,91 2,4	—2,1 4,1
Garnet 2039, Caucasus	—	10^{-12}	$2,0\cdot10^{-11}$	$7,0\cdot10^{-11}$	$6,2\cdot10^{-10}$	$4,7\cdot10^{-9}$	$1,5\cdot10^{-8}$	$5,5\cdot10^{-8}$	$2,5\cdot10^{-7}$	$1,5\cdot10^{-6}$	up to 400 400—800 800—1050	0,4 1,0 2,2	—8,9 —2,5 4,0
Garnet 251, North Karelia	—	$9,1\cdot10^{-12}$	$7,1\cdot10^{-11}$	$5,9\cdot10^{-10}$	$4,5\cdot10^{-9}$	$2,6\cdot10^{-8}$	$1,6\cdot10^{-7}$	$5,6\cdot10^{-7}$	$1,4\cdot10^{-6}$	$7,1\cdot10^{-6}$	up to 550 550—900 900—1050	0,73 1,18 1,8	—5,6 —1,2 2,75
Garnet 2862, Saltykov**	Plageoclase-20 Microcline-25, Quartz-20-25, Biotite-10-15	$1,7\cdot10^{-8}$	$9,1\cdot10^{-7}$	$6,3\cdot10^{-7}$	$2,6\cdot10^{-8}$	$3,1\cdot10^{-8}$	$7,1\cdot10^{-8}$	$2,6\cdot10^{-7}$	$1,1\cdot10^{-6}$	$5,0\cdot10^{-6}$	up to 300 300—670 670—900 900—1050	0,1 Anomaly 1,5 3,0	—3,5 —2,7 7,0
Plageogarnet-2585, Saltykov**	Plageoclase-50-60 (andesine-oligoclase), quartz-25-30, biotite-5-8	$3,6\cdot10^{-9}$	$3,8\cdot10^{-8}$	$2,5\cdot10^{-8}$	$5,2\cdot10^{-7}$	$7,1\cdot10^{-7}$	$3,3\cdot10^{-6}$	$4,9\cdot10^{-6}$	$4,7\cdot10^{-6}$	$3,6\cdot10^{-5}$	up to 400 400—900 900—1050	0,6 Anomaly 3,0	—2,0 7,0
Magmatite 2572, Oskoletsk**	Plageoclase-30-50, microcline-10-15, quartz-20-25, biotite-7-10	$1,0\cdot10^{-10}$	$2,8\cdot10^{-10}$	$1,8\cdot10^{-9}$	$5,2\cdot10^{-8}$	$8,3\cdot10^{-8}$	$2,7\cdot10^{-7}$	$5,3\cdot10^{-7}$	$2,3\cdot10^{-6}$	$2,5\cdot10^{-5}$	up to 350 350—820 820—1050	0,28 0,52 2,2	—7,0 —2,0 4,7
Magmatite 2797, Oskoletsk**	Plageoclase-50-60, quartz-20-25, biotite-10-15	$7,1\cdot10^{-11}$	$1,8\cdot10^{-9}$	$1,8\cdot10^{-8}$	$5,5\cdot10^{-8}$	$1,2\cdot10^{-7}$	$5,0\cdot10^{-7}$	$1,9\cdot10^{-6}$	$3,1\cdot10^{-6}$	$1,5\cdot10^{-5}$	220—860 860—1050	0,72 2,3	—3,6 3,1
Garnet 2198, Oskoletsk**	Plageoclase-20-30, microcline-30-35, quartz-25-30, biotite and muscovite -10	$2,9\cdot10^{-12}$	$3,3\cdot10^{-11}$	$3,7\cdot10^{-10}$	$4,3\cdot10^{-9}$	$1,1\cdot10^{-8}$	$5,9\cdot10^{-8}$	$1,6\cdot10^{-7}$	$4,7\cdot10^{-7}$	$1,1\cdot10^{-6}$	up to 900 900—1050	0,88 2,0	—3,25 2,75

Appendix 2 is continued on the following page.

APPENDIX 2 (continued)

Rock, origin	Mineral composition, %	σ (ohm^{-1}·cm^{-1}) at t, °C				σ (ohm^{-1}·cm^{-1}) at t °C					Temperature range t, °C	E_a, eV	lg σ_0, ohm^{-1}·cm^{-1}
		200	300	400	500	600	700	800	900	1000			
Plageomigmatite 2193, Pavlovsk**	Plageoclase-50-60 (oligoclase, andesine), microcline -10, quartz - 25, muscovite, biotite - 15-20	$5,9\cdot10^{-10}$	$2,6\cdot10^{-9}$	$1,1\cdot10^{-8}$	$7,8\cdot10^{-8}$	$1,5\cdot10^{-7}$	$2,1\cdot10^{-7}$	$2,1\cdot10^{-6}$	$2,3\cdot10^{-6}$	$2,3\cdot10^{-5}$	up to 780 780—1050	0,48 2,2	—5,5 4,7
Metasomatic garnet 2573, Pavlovsk**	Plageoclase - 20-25, potassium-containing feldspar -30, quartz-30-35, biotite-5-10	$3,3\cdot10^{-10}$	$3,6\cdot10^{-9}$	$8,3\cdot10^{-9}$	$2,1\cdot10^{-8}$	$6,7\cdot10^{-8}$	$2,8\cdot10^{-7}$	$8,7\cdot10^{-7}$	—	$1,2\cdot10^{-5}$	up to 500 500—900 900—1050	0,3 0,92 2,8	—6,8 —3,5 5,2
Polymigmatite 2187, Pavlovsk**	Plageoclase-40-50, microcline-15-20, quartz-25	$5,9\cdot10^{-11}$	$6,2\cdot10^{-10}$	$4,0\cdot10^{-9}$	$1,5\cdot10^{-8}$	$4,3\cdot10^{-8}$	$1,8\cdot10^{-7}$	$6,7\cdot10^{-7}$	$1,1\cdot10^{-6}$	$9,0\cdot10^{-6}$	up to 600 600—900 >900	0,6 0,94 3,0	—4,8 —1,0 9,8
Garnet 2577 Pavlovsk**	Muscovitized plageoclase-40-45, potassium-containing feldspar-10-15, quartz-25-30, biotite, muscovite- 5-7	$4,1\cdot10^{-12}$	$7,1\cdot10^{-11}$	$1,4\cdot10^{-9}$	$7,1\cdot10^{-8}$	$3,8\cdot10^{-8}$	$1,5\cdot10^{-7}$	$1,3\cdot10^{-6}$	$3,6\cdot10^{-6}$	$1,3\cdot10^{-5}$	up to 700 700—850 850—1050	0,9 Anomaly 1,7	—3,7 1,8
Quartz diorite (porphyroid) 80-160, Kazakhstan*	Plageoclase- 80, quartz-20	—	$4,8\cdot10^{-11}$	$1,4\cdot10^{-9}$	$1,1\cdot10^{-8}$	$5,0\cdot10^{-8}$	$2,4\cdot10^{-7}$	$9,1\cdot10^{-7}$	$3,4\cdot10^{-6}$	$1,9\cdot10^{-5}$	up to 840 840—1050	0,94 2,0	—2,3 2,4
Quartz diorite, Kazakhstan*	Plageoclase-60, chlorite, epidote-20, quartz-20	$6,7\cdot10^{-12}$	$1,2\cdot10^{-10}$	$1,0\cdot10^{-9}$	$2,6\cdot10^{-9}$	$1,1\cdot10^{-8}$	$8,3\cdot10^{-8}$	$1,7\cdot10^{-7}$	$7,7\cdot10^{-7}$	$2,1\cdot10^{-5}$	up to 600 600—900 900—1050	0,64 1,2 3,4	—6,7 —1,1 6,0
Quartz diorite 2600, Voronezh anticline**	Plageoclase-50, quartz-25, sericite, chlorite	$1,4\cdot10^{-11}$	$7,2\cdot10^{-10}$	$7,2\cdot10^{-9}$	$7,0\cdot10^{-8}$	$2,9\cdot10^{-7}$	$4,2\cdot10^{-7}$	$8,3\cdot10^{-7}$	$3,3\cdot10^{-6}$	$4,7\cdot10^{-5}$	up to 320 320—650 650—820 820—1100	0,4 0,84 Anomaly 2,5	—6,0 —2,2 5,5
Quartz diorite 2619, Voronezh antecline **	Plageoclase-40-50, quartz-15, biotite-25, hornblende	$2,5\cdot10^{-10}$	$2,4\cdot10^{-9}$	$1,8\cdot10^{-8}$	$1,0\cdot10^{-7}$	$4,0\cdot10^{-7}$	$6,2\cdot10^{-7}$	$7,7\cdot10^{-7}$	$2,2\cdot10^{-6}$	$1,4\cdot10^{-5}$	up to 650 650—800 800—1050	0,75 Anomaly 2,3	—3,4 4,0
Granodiorite 153, Ural Mts.***	Plageoclase-75, quartz-10, amphibole - 10	$5,9\cdot10^{-10}$	$1,4\cdot10^{-8}$	$1,2\cdot10^{-7}$	$7,7\cdot10^{-7}$	$4,4\cdot10^{-6}$	$5,6\cdot10^{-6}$	$8,3\cdot10^{-6}$	$1,1\cdot10^{-5}$	$5,6\cdot10^{-5}$	up to 900 900—1050	0,61 2,0	—3,3 3,5
Granodiorite 1162, Kazakhstan*	Andecite-45, orthoclase-22, biotite - 18, quartz-20	$1,3\cdot10^{-10}$	$3,8\cdot10^{-9}$	$4,0\cdot10^{-8}$	$3,6\cdot10^{-7}$	$5,4\cdot10^{-7}$	$9,1\cdot10^{-7}$	$1,8\cdot10^{-6}$	$4,4\cdot10^{-6}$	$1,4\cdot10^{-5}$	up to 900 900—1100	0,77 2,34	—2,5 3,0

Appendix 2 is continued on the following page

APPENDIX 2 (continued)

Rock, origin	Mineral composition,%	σ(ohm^{-1}.cm^{-1}) at t,°C				σ(ohm^{-1}.cm^{-1}) at t°C					Temperature range t,°C	E_a,eV	lg σ_0, ohm^{-1}.cm^{-1}
		200	300	400	500	600	700	800	900	1000			
Granodiorite 6-8, Kazakhstan*	Plageoclase-45, potassium-containing feldspar (pellitized) 20-25, quartz-15-20, hornblende-10-12	$5,0\cdot10^{-12}$	$1,5\cdot10^{-10}$	$2,1\cdot10^{-9}$	$1,5\cdot10^{-8}$	$5,9\cdot10^{-8}$	$2,2\cdot10^{-7}$	$5,0\cdot10^{-7}$	$4,0\cdot10^{-6}$	$1,6\cdot10^{-6}$	up to 720 720—1050	0,8 2,0	—3,5 3,0
Diorite 1771, Kazakhstan*	Plageoclase-50, hornblende-22, quartz-18, diorite - 10	$1,9\cdot10^{-10}$	$3,2\cdot10^{-9}$	$3,5\cdot10^{-8}$	$1,4\cdot10^{-7}$	$2,7\cdot10^{-7}$	$9,1\cdot10^{-7}$	$1,2\cdot10^{-6}$	$3,4\cdot10^{-6}$	$1,9\cdot10^{-5}$	up to 900 900—1050	0,62 2,5	—3,0 4,25
Diorite 166, Ural Mts.***	Plageoclase-60, quartz-8, pyroxene-22, biotite - 3	$4,4\cdot10^{-11}$	$1,0\cdot10^{-9}$	$5,3\cdot10^{-8}$	$4,2\cdot10^{-8}$	$1,6\cdot10^{-7}$	$4,4\cdot10^{-7}$	$7,4\cdot10^{-7}$	$2,6\cdot10^{-6}$	$1,2\cdot10^{-5}$	up to 860 860—1050	0,62 2,16	—4,6 3,0
Monzodiorite 2799, Gor'kiy**	Plageoclase-87, microcline-5, biotite-6, muscovite, magnetite - 2	$9,0\cdot10^{-9}$	$2,0\cdot10^{-7}$	$1,2\cdot10^{-7}$	$7,8\cdot10^{-7}$	$3,3\cdot10^{-6}$	$1,3\cdot10^{-5}$	$2,7\cdot10^{-6}$	$8,1\cdot10^{-7}$	10^{-6}	up to 800 800—1050	0,68 Anomaly	—1,0
Monzodiorite 2866, Gor'kiy**	Plageoclase-87, microcline -5, biotite - 4, amphibole - 3	$4,5\cdot10^{-8}$	$5,0\cdot10^{-7}$	$3,3\cdot10^{-6}$	$1,4\cdot10^{-5}$	10^{-6}	10^{-5}	$1,6\cdot10^{-5}$	$5,0\cdot10^{-5}$	$1,5\cdot10^{-4}$	200—500 500—720 720—1050	0,7 Anomaly 1,52	0,1 3,0

*Samples of A. K. Kurskeyev
**Samples of V. E. Dibrov
***Samples of V. B. Baranov

[Commas in tabulated material are equivalent to decimal points.]

APPENDIX 3. Electrical conductivity σ, activation energy E_0 and preexponential coefficient σ_0 in the andesites at high temperatures.

Rock, origin	Mineral composition %	σ(ohm^{-1}·cm^{-1}) at t, °C				σ(ohm^{-1}·cm^{-1}) at t° C					Temperature range t, °C	E_0, eV	lg σ_0, ohm^{-1}·cm^{-1}
		200	300	400	500	600	700	800	900	1000			
Andesitodacite 1379 Kamchatka	Plageoclase-30(labradorite), hornblende-10, volcanic glass-60	1,9·10^{-9}	2,1·10^{-8}	8,3·10^{-7}	6,3·10^{-6}	3,6·10^{-5}	1,2·10^{-4}	4,5·10^{-4}	9,1·10^{-4}	1,8·10^{-3}	up to 350 350—400 400—1050	0,54 2,0 1,0	—4,9 8,75 —1,05
Andesite 1374 Kamchatka	Plageoclase, hyperstene, hornblende, biotiside and cemented by brownish translucent glass	2,0·10^{-8}	4,0·10^{-7}	2,6·10^{-6}	1,6·10^{-5}	7,7·10^{-5}	1,9·10^{-4}	4,8·10^{-4}	9,1·10^{-4}	2,1·10^{-3}	up to 900 900—1050	0,7 1,24	1,1 3,1
Andesite 1694, Sakhalin	—	2,9·10^{-7}	1,2·10^{-6}	3,6·10^{-6}	9,1·10^{-6}	1,1·10^{-4}	5,9·10^{-4}	1,7·10^{-3}	3,6·10^{-3}	6,3·10^{-3}	up to 480 480—750 750—1050	0,35 1,27 0,66	—3,25 3,4 1,0
Andesite 1011, USSR Far East	—	7,7·10^{-9}	4,2·10^{-8}	7,4·10^{-8}	2,9·10^{-7}	5,6·10^{-6}	1,1·10^{-5}	8,3·10^{-5}	1,6·10^{-4}	3,0·10^{-4}	up to 900 900—1050	0,68 0,8	—2,9 1,0
Andesite-basalt 1373, Kamchatka	—	3,3·10^{-9}	5,0·10^{-7}	5,0·10^{-7}	2,0·10^{-6}	6,2·10^{-6}	2,3·10^{-5}	5,3·10^{-5}	1,3·10^{-4}	3,2·10^{-4}	650 650—1050	0,63 1,2	—2,8 2,25
Andesite 1010, USSR Far East	—	9,1·10^{-9}	3,7·10^{-8}	5,8·10^{-8}	8,3·10^{-7}	4,5·10^{-6}	7,7·10^{-6}	4,0·10^{-5}	2,4·10^{-4}	4,2·10^{-4}	up to 700 700—1050	0,74 1,4	—2,75 3,8

[Commas in tabulated material are equivalent to decimal points.]

APPENDIX 4. Electrical conductivity σ, activation energy E_0 and the preexponential coefficient σ_0 of gabbro at high temperatures.

Rock, origin	Mineral composition %	σ ($ohm^{-1} \cdot cm^{-1}$) at t, °C									Temperature range t, °C	E_0, eV	lg σ_0, $ohm^{-1} \cdot cm^{-1}$
		200	300	400	500	600	700	800	900	1000			
	Mamonov complex					Mamonov complex							
Gabbro-norite 2622	Plageoclase-40, potassium-containing feldspar - 15, pyroxene-30, biotite - 7	$7,7 \cdot 10^{-8}$	$5,5 \cdot 10^{-7}$	$5,0 \cdot 10^{-6}$	$1,1 \cdot 10^{-5}$	$7,1 \cdot 10^{-6}$	$1,1 \cdot 10^{-5}$	$2,0 \cdot 10^{-5}$	$6,3 \cdot 10^{-5}$	$1,3 \cdot 10^{-4}$	up to 600	0,7	−0,6
											600—700	Anomaly	
											700—900	0,6	−3,8
											900—1000	1,76	1,75
Gabbro 2609	Plageoclase-35-55, hyperstene-25, amphibole-15, clinopyroxene-15, magnetite-10	$1,7 \cdot 10^{-9}$	$2,3 \cdot 10^{-9}$	$4,0 \cdot 10^{-8}$	$2,3 \cdot 10^{-7}$	$2,7 \cdot 10^{-6}$	10^{-5}	$6,7 \cdot 10^{-5}$	$1,1 \cdot 10^{-4}$	$3,4 \cdot 10^{-4}$	290—550	0,8	−1,2
											550—1050	1,6	2,25
Gabbro-pyroxene, amphibole 2621	Plageoclase-25, horblende - 40, hyperstene-20, clineenstatite - 10 magnetite-5	$5,0 \cdot 10^{-10}$	$5,6 \cdot 10^{-9}$	$8,3 \cdot 10^{-8}$	$4,1 \cdot 10^{-7}$	$3,8 \cdot 10^{-6}$	$4,4 \cdot 10^{-5}$	$3,1 \cdot 10^{-5}$	$3,8 \cdot 10^{-5}$	—	up to 550	0,8	
											550—720	1,2	
											720—950	Anomaly	
Gabbro-norite 2616	Plageoclase-55-60, hyperstene-25, biotite-5	$1,4 \cdot 10^{-10}$	$1,4 \cdot 10^{-9}$	$1,2 \cdot 10^{-8}$	$3,1 \cdot 10^{-8}$	$9,8 \cdot 10^{-8}$	$6,0 \cdot 10^{-7}$	$2,6 \cdot 10^{-6}$	$1,3 \cdot 10^{-5}$	$5,0 \cdot 10^{-5}$	up to 550	0,63	−4,8
											550—900	1,16	−0,1
											900—1050	1,9	3,0
Gabbro-diabase 2618	Plageoclase-54 amphibole-40 (horblende), biotite -16	$3,0 \cdot 10^{-10}$	$7,0 \cdot 10^{-9}$	$1,2 \cdot 10^{-8}$	$3,6 \cdot 10^{-7}$	$2,0 \cdot 10^{-6}$	$7,0 \cdot 10^{-5}$	$1,5 \cdot 10^{-5}$	$1,2 \cdot 10^{-5}$	$2,5 \cdot 10^{-5}$	up to 650	0,78	−2,1
											650—750	0,9÷1,3	1,8
											750—900	Anomaly	
											900—1050	1,2÷1,38	0,5÷0,8

Appendix 4 is continued on the following page.

APPENDIX 4 (continued)

Rock, origin	Mineral composition %	σ ($ohm^{-1} \cdot cm^{-1}$) at t, °C				σ ($ohm^{-1} \cdot cm^{-1}$) at t, °C					Temperature range t, °C	E_a, eV	lg σ_0 $ohm^{-1} \cdot cm^{-1}$
		200	300	400	500	600	700	800	900	1000			
Gabbro 2608	Plageoclase-45, pyroxene-5-10, actinolite -10-15, amphibole-30 biotite-10	$1,2 \cdot 10^{-10}$	$8,0 \cdot 10^{-10}$	$4,0 \cdot 10^{-9}$	$2,9 \cdot 10^{-8}$	$1,4 \cdot 10^{-7}$	$6,2 \cdot 10^{-7}$	$2,5 \cdot 10^{-6}$	$1,1 \cdot 10^{-6}$	$6,5 \cdot 10^{-5}$	up to 500 500—700 700—900 900—1050	0,74 1,0 Anomaly 1,6÷2,1	—2,5 0,3 3,0
Gabbro 2615	Plageoclase-60, pyroxene - 15, biotite - 12, amphibole-7	$1,2 \cdot 10^{-10}$	$2,8 \cdot 10^{-9}$	$2,9 \cdot 10^{-8}$	$1,5 \cdot 10^{-7}$	$6,8 \cdot 10^{-7}$	$2,0 \cdot 10^{-6}$	$2,1 \cdot 10^{-6}$	$1,3 \cdot 10^{-5}$	$5,1 \cdot 10^{-5}$	up to 550 550—800 800—1050	0,8 Anomaly 2,2	—2,75 4,35
Gabbro-diabase 2617	Plageoclase -35 potassium-containing feldspar 5-7, pyroxene-25, biotite-25, quartz 5-7	$1,3 \cdot 10^{-10}$	$2,6 \cdot 10^{-9}$	$1,3 \cdot 10^{-8}$	$7,7 \cdot 10^{-8}$	$2,5 \cdot 10^{-7}$	$4,0 \cdot 10^{-7}$	$1,3 \cdot 10^{-6}$	$6,0 \cdot 10^{-6}$	$2,0 \cdot 10^{-5}$	up to 800 800—1050	0,63 1,7÷2,2	—3,3 2,5÷4,3
Gabbro 2620	Plageoclase-20-35, actinolite-40, biotite-10 quartz - 7	$1,6 \cdot 10^{-10}$	$5,0 \cdot 10^{-10}$	$4,0 \cdot 10^{-9}$	$4,1 \cdot 10^{-8}$	$5,1 \cdot 10^{-7}$	$3,9 \cdot 10^{-7}$	$2,1 \cdot 10^{-7}$	$1,1 \cdot 10^{-6}$	$7,6 \cdot 10^{-6}$	up to 550 550—800 800—1050	0,7 Anomaly 2,2	—3,2 3,3
Gabbro-diabase 2863	Plageoclase-50, microcline -5, hornblende -20-30, biotite-10-15, titanite-2-3	$8,3 \cdot 10^{-10}$	$3,1 \cdot 10^{-9}$	$2,0 \cdot 10^{-8}$	$6,2 \cdot 10^{-8}$	$1,1 \cdot 10^{-7}$	$5,1 \cdot 10^{-7}$	$8,3 \cdot 10^{-7}$	$3,0 \cdot 10^{-6}$	$6,1 \cdot 10^{-6}$	up to 650 650—1050	0,6 1,2	2,0 —1,35

Appendix 4 is continued on the following page.

APPENDIX 4 (continued)

Rock, origin	Mineral composition %	σ(ohm^{-1}.cm^{-1}) at t, °C									Temperature range t, °C	E_0, eV	lg σ_0 ohm^{-1}.cm^{-1}
		200	300	400	500	600	700	800	900	1000			
South Ural Mountains						South Ural Mountains							
Gabbro 1A	Plageoclase -44, amphibole-35, biotite -10, epidote-chlorite-1	$8,3 \cdot 10^{-9}$	—	—	—	$9,7 \cdot 10^{-8}$	$8,6 \cdot 10^{-7}$	$1,4 \cdot 10^{-6}$	$2,8 \cdot 10^{-6}$	$3,4 \cdot 10^{-5}$	up to 700	0,7	—2,41
											700—880	Anomaly	
											880—1050	3,3	9,0
Gabbro 168	Plageoclase-45, pyroxene-45, sphene, apatite, magnetite-10	$6,1 \cdot 10^{-10}$	$2,4 \cdot 10^{-9}$	$5,9 \cdot 10^{-8}$	$9,1 \cdot 10^{-8}$	$3,3 \cdot 10^{-7}$	$5,0 \cdot 10^{-7}$	$7,1 \cdot 10^{-7}$	$3,5 \cdot 10^{-6}$	$4,8 \cdot 10^{-5}$	up to 920	0,65	—3,0
											920—1050	3,0	7,0
Gabbro 14c	Plageoclase-50, hornblende, pyroxene, uralite	$3,3 \cdot 10^{-10}$	$2,5 \cdot 10^{-9}$	$1,8 \cdot 10^{-8}$	$7,2 \cdot 10^{-8}$	$3,4 \cdot 10^{-7}$	$8,3 \cdot 10^{-7}$	$1,8 \cdot 10^{-6}$	$1,9 \cdot 10^{-6}$	10^{-5}	up to 800	0,72	—3,4
											800—1050	1,0	—1,0
Gabbro-diabase 42b	-	$1,8 \cdot 10^{-10}$	$2,2 \cdot 10^{-9}$	$1,3 \cdot 10^{-8}$	—	—	$1,7 \cdot 10^{-7}$	$4,0 \cdot 10^{-7}$	$1,8 \cdot 10^{-6}$	$2,6 \cdot 10^{-5}$	up to 520	0,57	—3,6
											520—950	0,76	—2,85
											950—1050	3,19	7,9
Gabbro 12E	Plageoclase-60, amphibole, pyroxene	$1,2 \cdot 10^{-10}$	$1,7 \cdot 10^{-9}$	$8,3 \cdot 10^{-9}$	$4,0 \cdot 10^{-8}$	$1,7 \cdot 10^{-7}$	$3,0 \cdot 10^{-7}$	$9,1 \cdot 10^{-7}$	$1,9 \cdot 10^{-6}$	$1,1 \cdot 10^{-5}$	up to 450	0,44	—6,3
											450—900	0,88—0,77	—3,5
											900—1050	2,36	5,0
Gabbro 272	-	$5,9 \cdot 10^{-11}$	$7,7 \cdot 10^{-10}$	$6,2 \cdot 10^{-9}$	$1,8 \cdot 10^{-8}$	$5,9 \cdot 10^{-8}$	$9,1 \cdot 10^{-8}$	$2,1 \cdot 10^{-7}$	$1,1 \cdot 10^{-6}$	$6,2 \cdot 10^{-6}$	up to 800	0,6	—4,0
											800—1050	1,9	3,25

(Appendix 4 is continued on the following page

APPENDIX 4. Electrical conductivity σ, activation energy E_0 and the preexponential coefficient σ_0 of gabbro at high temperatures. (continued)

Rock, origin	Mineral composition %	σ(ohm^{-1}.cm^{-1}) at t, °C									Temperature range t, °C	E_0, eV	lg σ_0, ohm^{-1}.cm^{-1}
		200	300	400	500	600	700	800	900	1000			
		Kola Peninsula				Kola Peninsula							
Gabbro 458, Pechenga	Augite-50, plageoclase, amphibole, epidote, chlorite, quartz	$4,3\cdot10^{-10}$	$4,5\cdot10^{-9}$	$4,5\cdot10^{-8}$	$1,9\cdot10^{-7}$	$6,9\cdot10^{-6}$	$7,0\cdot10^{-6}$	$4,6\cdot10^{-5}$	$7,9\cdot10^{-5}$	$2,1\cdot10^{-4}$	100—650 650—1050	0,68 2,3	—3,7 5,6
Meta-diabase 1661, Pechenga	Augite-40, plageoclase, amphibole, epidote, chlorite, magnatite	$1,4\cdot10^{-10}$	$2,5\cdot10^{-9}$	$1,3\cdot10^{-8}$	$6,5\cdot10^{-8}$	$2,5\cdot10^{-7}$	$9,8\cdot10^{-6}$	$2,6\cdot10^{-5}$	$2,0\cdot10^{-5}$	$2,2\cdot10^{-4}$	100—525 525—550 550—900 900—1150	0,64 2,76 0,88 2,64	—4,8 9,6 —1,2 6,0
Gabbro-norite 466, Monchegorsk	—	$1,9\cdot10^{-10}$	$7,9\cdot10^{-9}$	$3,2\cdot10^{-8}$	$2,3\cdot10^{-7}$	$8,5\cdot10^{-7}$	$2,8\cdot10^{-6}$	$1,1\cdot10^{-5}$	$2,9\cdot10^{-5}$	$9,0\cdot10^{-5}$	100—700 700—1100	0,6 2,0	—4,6 3,5
Meta-gabbro 1450, Monchegorsk	—	$1,9\cdot10^{-11}$	$1,3\cdot10^{-10}$	$7,6\cdot10^{-10}$	$3,2\cdot10^{-9}$	$2,2\cdot10^{-8}$	$8,7\cdot10^{-8}$	$5,5\cdot10^{-7}$	$2,2\cdot10^{-6}$	$2,5\cdot10^{-5}$	100—550 550—900 900—1200	0,54 1,1 3,1	—5,2 —2,8 7,0

(Appendix 4 is continued on the following page.)

APPENDIX 4. (continued)

Rock, origin	Mineral composition %	σ(ohm^{-1}·cm^{-1}) at t,°C									Temperature range t,°C	E_0, eV	lg σ_0, ohm^{-1}·cm^{-1}
		200	300	400	500	600	700	800	900	1000			
		Gor'kiy Complex				Gor'kiy Complex							
Cataclastic gabbroid 2795	Plageoclase-86, biotite-11, epidote, pyroxene, sphene-3	$3,4\cdot10^{-8}$	$7,0\cdot10^{-8}$	$8,0\cdot10^{-8}$	$5,5\cdot10^{-5}$	$6,4\cdot10^{-5}$	$1,4\cdot10^{-4}$	$2,7\cdot10^{-4}$	$1,1\cdot10^{-4}$	$1,8\cdot10^{-4}$	up to 300 800—1050	Anomaly 1,22	0,1
Biotized gabbroid 2861	Plageoclase-62, biotite-23, dark-colored mineral is replaced by magnetite-12	$4,8\cdot10^{-8}$	$1,6\cdot10^{-7}$	$7,7\cdot10^{-6}$	$8,8\cdot10^{-5}$	10^{-5}	$1,3\cdot10^{-5}$	$2,7\cdot10^{-5}$	$1,1\cdot10^{-4}$	$1,8\cdot10^{-4}$	up to 750 750—1050	0,58 1,11	—2,0 0,55
Cataclastic gabbro 2794	Biotized plageoclase -56, pyroxene -41, sphene, apatite, hematite - 3	$1,7\cdot10^{-9}$	$4,0\cdot10^{-8}$	$3,0\cdot10^{-7}$	$4,1\cdot10^{-7}$	$1,1\cdot10^{-6}$	$3,8\cdot10^{-6}$	$1,6\cdot10^{-5}$	$5,0\cdot10^{-5}$	$1,3\cdot10^{-4}$	up to 620 620—1050	0,56 1,36	—3,0 1,0
Metasomatic gabbro 2791	Plageoclase -88, microcline, biotite, muscovite -3, ore mineral -1	$1,1\cdot10^{-8}$	$8,3\cdot10^{-8}$	$5,0\cdot10^{-7}$	$1,1\cdot10^{-6}$	$2,0\cdot10^{-6}$	$4,1\cdot10^{-6}$	$9,1\cdot10^{-6}$	$2,8\cdot10^{-5}$	$9,8\cdot10^{-5}$	up to 850 850—1050	0,5—0,58 1,66	—3,5÷3,4 2,2÷3,0
Cataclastic gabbro 2790	Plageoclase -74, albitized pyroxene is replaced by magnetite-11, biotite-13	$1,2\cdot10^{-9}$	$1,5\cdot10^{-8}$	10^{-7}	$3,3\cdot10^{-7}$	$9,9\cdot10^{-7}$	$2,2\cdot10^{-6}$	$5,0\cdot10^{-6}$	$1,3\cdot10^{-5}$	$2,8\cdot10^{-5}$	up to 300 300—900 900—1050	0,26 0,66 1,2	—6,2 —2,0 0,5
Albitized gabbro 2865	Cataclastic plageoclase -72, amphibole -27, sphene, apatite-1	$1,1\cdot10^{-9}$	$6,6\cdot10^{-9}$	$6,6\cdot10^{-8}$	$1,0\cdot10^{-7}$	$2,9\cdot10^{-7}$	$9,8\cdot10^{-7}$	$3,8\cdot10^{-6}$	$1,4\cdot10^{-5}$	$4,0\cdot10^{-5}$	up to 600 600—1050	0,52 1,4	—4÷4,5 0,4

(Appendix 4 is continued on the following page)

APPENDIX 4. (continued)

Rock, origin	Mineral Composition %	σ(ohm^{-1}·cm^{-1}) at t, °C				σ(ohm^{-1}·cm^{-1}) at t, °C					Temperature range t, °C	E_0, eV	lg σ_0 ohm^{-1}·cm^{-1}
		200	300	400	500	600	700	800	900	1000			
Diabase 4a	Plageoclase -60, actinolite-30, titanomagnetite-5, chlorite	$1,4\cdot10^{-9}$	$1,0\cdot10^{-8}$	$6,7\cdot10^{-8}$	$3,2\cdot10^{-7}$	$1,7\cdot10^{-6}$	$8,3\cdot10^{-6}$	$2,3\cdot10^{-5}$	$3,0\cdot10^{-5}$	$9,1\cdot10^{-5}$	up to 450	0,68	−3,4
											450—850	0,9	−1,8
											850—1050	1,4÷1,7	1,5—3,0
Diabase 21a	Plageoclase -50, uralitized pyroxene - 40, chlorite - 5, magnetite - 5	$1,0\cdot10^{-9}$	$3,1\cdot10^{-8}$	$1,9\cdot10^{-7}$	$9,8\cdot10^{-7}$	$3,7\cdot10^{-6}$	$9,1\cdot10^{-6}$	$1,5\cdot10^{-5}$	$2,5\cdot10^{-5}$	$8,3\cdot10^{-5}$	up to 400	0,66	−2,9
											400—700	1,1	1,75
											700—900	Anomaly	
											>900	1,7	2,2
Diabase 5a	—	$5,3\cdot10^{-10}$	$7,1\cdot10^{-9}$	$8,3\cdot10^{-8}$	$2,1\cdot10^{-7}$	$1,2\cdot10^{-6}$	$2,4\cdot10^{-6}$	$3,4\cdot10^{-6}$	$2,0\cdot10^{-5}$	$2,4\cdot10^{-5}$	200—800	0,64	−3,8
											>800	Anomaly	

Remarks. The rocks from the Mamonov and Gor'kiy complexes were made available by V. E. Dibrov and those from the South Ural Mountains - by V. B. Baranov.

[Commas in tabulated material are equivalent to decimal points.]

APPENDIX 5. Electrical conductivity σ, activation energy E_0 and preexponential coefficient σ_0 in dolerite and basalts at high temperatures.

Rock, origin	Mineral composition %	σ(ohm^{-1}. cm^{-1}) at t, °C				σ(ohm^{-1}.cm^{-1}) at t, °C					Temperature range t, °C	E_0, eV	lg σ_0 ohm^{-1}.cm^{-1}
		200	300	400	500	600	700	800	900	1000			
Intermediate grain dolerite 60, Udzha river	Volcanic glass-4-5, titano-magnetite-2-5, evolution of calcite	$1,2\cdot10^{-9}$	$3\cdot10^{-8}$	$1,6\cdot10^{-7}$	$3,6\cdot10^{-7}$	$3,7\cdot10^{-4}$	$2,3\cdot10^{-4}$	$1,4\cdot10^{-4}$	$6,4\cdot10^{-4}$	$3,9\cdot10^{-3}$	100—500 500—650 650—800 800—1200	0,6 3,5 — 1,1	—2,7 15,0 — 1,2
Small grain dolorite 61b, Udzha river	Plageoclase, volcanic glass-15-20, titano-magnetite -2-5 (spongy structure)	$3,2\cdot10^{-9}$	$2,8\cdot10^{-8}$	$1,3\cdot10^{-7}$	$4,1\cdot10^{-7}$	$1,3\cdot10^{-5}$	$2,8\cdot10^{-5}$	$6,4\cdot10^{-5}$	$9\cdot10^{-5}$	$4\cdot10^{-4}$	150—500 500—650 650—700 700—900 900—1100	0,64 1,63 0,64 3,54	—2,0 —4,0 —1,8 5,5
Intermeidate grain dolerite 60-r, Udzha r.	Plageoclase, monocline pyroxene, ore minerals, carbonates	$2,1\cdot10^{-9}$	$2,6\cdot10^{-8}$	$2,2\cdot10^{-7}$	$6,1\cdot10^{-7}$	$9,9\cdot10^{-5}$	$2,9\cdot10^{-5}$	$8\cdot10^{-5}$	$3,4\cdot10^{-4}$	$8\cdot10^{-4}$	100—550 550—600 600—650 650—900 900—1100	0,74 1,9 — 0,74 3,4	—2,0 5,1 — —2,7 10,0
Intermediate graindolerite 83	Plageoclase-41-42, monocline pyroxene-40, olivine-10, ore minerals -4-5	10^{-9}	$5\cdot10^{-9}$	$1,6\cdot10^{-7}$	$6,0\cdot10^{-7}$	$5,8\cdot10^{-6}$	$1,4\cdot10^{-5}$	$5\cdot10^{-5}$	$1,8\cdot10^{-4}$	$4,5\cdot10^{-4}$	100—300 300—900 900—1200	0,54 0,96 1,58	—4,4 0,1 5,6
Intermediate grain dolerite 108, Udzha r.	Plageoclase-40, monocline pyroxene-40, olivine-5, ore minerals-2-3, mesostasis - 10-12	$2,3\cdot10^{-10}$	$5\cdot10^{-9}$	$5\cdot10^{-8}$	$2,1\cdot10^{-7}$	$3,2\cdot10^{-6}$	$8\cdot10^{-6}$	$3,1\cdot10^{-5}$	$8,2\cdot10^{-5}$	$7\cdot10^{-5}$	150—900 900—1200	0,74 3,2	—2,8 8,4

(Appendix 5 is continued on the following page.)

APPENDIX 5. (continued)

Rock, origin	Mineral composition %	σ(ohm^{-1}.cm^{-1}) at t,°C 200	300	400	500	600	700	800	900	1000	Temperature range t,°C	E_0,eV	lg σ_0 ohm^{-1}·cm^{-1}
Large grain dolerite 29, Velroy basin	Plageoclase, monocline pyroxene, olivine, ore minerals, chlorite, apatite	$5\cdot10^{-10}$	$1{,}8\cdot10^{-8}$	$8\cdot10^{-8}$	$2\cdot10^{-7}$	$9{,}9\cdot10^{-7}$	$2{,}4\cdot10^{-6}$	$9{,}9\cdot10^{-6}$	$4{,}3\cdot10^{-5}$	$2{,}3\cdot10^{-4}$	100—650 650—950 950—1200	0,56 1,3 1,66	—3,0 0,75 4,6
Caucasus Mt. dolerites (limits of elec. conductivity)	-	$1{,}04\cdot10^{-9}$	$1{,}6\cdot10^{-8}$	$1{,}3\cdot10^{-7}$	$2{,}1\cdot10^{-6}$	$1{,}2\cdot10^{-5}$	$3{,}4\cdot10^{-5}$	$5{,}5\cdot10^{-5}$	$1{,}2\cdot10^{-4}$	$4{,}1\cdot10^{-4}$	up to 750÷875	0,66÷1,16	—2,0÷2,5
		$6{,}0\cdot10^{-10}$	$5{,}9\cdot10^{-9}$	$9{,}2\cdot10^{-8}$	$5{,}7\cdot10^{-7}$	$8{,}9\cdot10^{-7}$	$1{,}0\cdot10^{-7}$	$4{,}9\cdot10^{-6}$	$2{,}8\cdot10^{-5}$	$4{,}9\cdot10^{-5}$	750—1100	2,2÷4,7	3,0÷14,0
Dolerite 1052, toleite series, Sikhote-Alinsk	Moncline pyroxene, olivine, ilmenite, volcanic glass	$1{,}6\cdot10^{-9}$	$5{,}1\cdot10^{-8}$	$3{,}2\cdot10^{-7}$	$2{,}1\cdot10^{-6}$	$3{,}2\cdot10^{-6}$	10^{-5}	$3{,}2\cdot10^{-5}$	10^{-4}	$3{,}9\cdot10^{-4}$	150—650 650—950 950—1100	0,74 1,16 2,2	—2,9 0,8 5,0
		Basalts from Caucasus Mts.					Basalts from Caucasus Mts.						
Dolerite basalt 1295, Bezumskiy ridge	Plageoclase-66,92; pyroxene-17,65; uralite hornblende-8,99; carbonates -0.96, ore mineral-3.47	$4{,}9\cdot10^{-9}$	$2{,}0\cdot10^{-8}$	$1{,}6\cdot10^{-7}$	$9{,}3\cdot10^{-7}$	$2{,}5\cdot10^{-6}$	$3{,}7\cdot10^{-6}$	$4{,}9\cdot10^{-6}$	$1{,}1\cdot10^{-5}$	$4{,}5\cdot10^{-4}$	150—600 600—800 800—875 875—950 950—1200	0,55 0,32 2,60 0,32 3,0	0,3 —4,0 —5,3 —4,5 7,3
Dolerite basalt 1319, Bezumskiy ridge	Plageoclase-18.38 pyroxene-18.90, olivine-0.63, uralite horblende -7-61, ore mineral - 4.47	$1{,}9\cdot10^{-9}$	$3{,}9\cdot10^{-8}$	$1{,}8\cdot10^{-7}$	$3{,}6\cdot10^{-6}$	$5{,}1\cdot10^{-7}$	$1{,}5\cdot10^{-6}$	$2{,}8\cdot10^{-6}$	$9{,}8\cdot10^{-5}$	$3{,}8\cdot10^{-4}$	150—350 350—650 650—800 800—1050	0,70 0,30 0,74 2,74	—2,3 —5,3 —2,0 7,0

(Appendix 5 is continued on the following page.)

APPENDIX 4. (Continued)

Rock, origin	Mineral Composition %	($ohm^{-1} \cdot cm^{-1}$) at t, °C									Temperature range t, °C	E_0, eV	lg σ_0, $ohm^{-1} \cdot cm^{-1}$
		200	300	400	500	600	700	800	900	1000			
Dolerite basalt 1312, Bezumsky ridge	Plageoclase-69.06; pyroxene-15.97; uralite hornblende -9.82; carbonates -0.35; ore mineral-4.79	$6,4 \cdot 10^{-10}$	$3,9 \cdot 10^{-9}$	$4,6 \cdot 10^{-8}$	$2,9 \cdot 10^{-7}$	$7,6 \cdot 10^{-7}$	$1,6 \cdot 10^{-6}$	$3,5 \cdot 10^{-6}$	$1,1 \cdot 10^{-5}$	$2,5 \cdot 10^{-5}$	200—750 750—800 800—950 950—1100	0,76 0,33 1,04 3,2	—2,3 —4,2 —1,8 8,8
Basalt 1131, Gegam plateau	-	$7,1 \cdot 10^{-10}$	$1,3 \cdot 10^{-8}$	$6,8 \cdot 10^{-8}$	$1,7 \cdot 10^{-7}$	$7,6 \cdot 10^{-7}$	$2,5 \cdot 10^{-6}$	$6,0 \cdot 10^{-6}$	$1,8 \cdot 10^{-5}$	$1,4 \cdot 10^{-4}$	150—450 450—500 500—900 900—1150	0,60 0,86 4,0	—3,4 —2,7 1,4
Basalt 1109, Gegam plateau	Plageoclase-90.92; pyroxene -5.08; olivine-2.64; ore mineral-1.34	$5,6 \cdot 10^{-11}$	$1,4 \cdot 10^{-9}$	$1,8 \cdot 10^{-8}$	10^{-7}	$3,3 \cdot 10^{-7}$	$1,2 \cdot 10^{-6}$	$5,7 \cdot 10^{-6}$	$1,5 \cdot 10^{-5}$	$4,6 \cdot 10^{-5}$	100—650 650—1000	0,82 1,25	2,0 0,6
Small pore tashenite	Plageoclase - 45-50; augite-30-35, ore mineral -8-10, chloritized glass	$1,2 \cdot 10^{-9}$	$2,2 \cdot 10^{-8}$	$1,8 \cdot 10^{-7}$	$1,2 \cdot 10^{-6}$	$4 \cdot 10^{-6}$	$1,2 \cdot 10^{-5}$	$2,8 \cdot 10^{-5}$	$8,1 \cdot 10^{-5}$	$1,4 \cdot 10^{-4}$	150—800 800—1200	0,7 1,6	—2,7 2,7
Olivine basalt 1483, Seychelles Islands	Olivine-40-50, hidden crystalline glass, plageoclase, no secondary changes	$1,4 \cdot 10^{-10}$	$3,9 \cdot 10^{-9}$	$2,0 \cdot 10^{-8}$	$8,9 \cdot 10^{-8}$	$3,0 \cdot 10^{-7}$	$1,6 \cdot 10^{-5}$	$1,5 \cdot 10^{-5}$	$2,9 \cdot 10^{-5}$	$4,0 \cdot 10^{-5}$	150—600 600—1100 1100—1200	0,7 1,6 4,8	—3,2 2,2 15,7

(Appendix 4 is continued on the following page.)

APPENDIX 5. (Continued)

Rock, origin	Mineral composiiton %	σ(ohm^{-1}.cm^{-1}) at t, °C									Temperature range t, °C	E_0, eV	lg σ_0, ohm^{-1}.cm^{-1}
		200	300	400	500	600	700	800	900	1000			
		Sichote-Alinsk Basalts											
Pyroxene basalt 651E, toleite series	Olivine, plageoclase, pyroxene, volcanic glass (mesostasis), magnetite, weak secondary changes	$2,9\cdot10^{-10}$	$8,0\cdot10^{-9}$	$8,0\cdot10^{-8}$	$5,2\cdot10^{-7}$	$1,6\cdot10^{-6}$	$5,1\cdot10^{-6}$	$2,0\cdot10^{-5}$	$6,4\cdot10^{-5}$	$2,0\cdot10^{-4}$	150—750 750—1050	0,78 1,4	—2,9 1,9
Gabbro-basalt 5/166, toleite series	-	$2,8\cdot10^{-10}$	$9,0\cdot10^{-8}$	$9,8\cdot10^{-7}$	$2,2\cdot10^{-6}$	10^{-5}	$2,9\cdot10^{-5}$	$2,6\cdot10^{-4}$	$1,4\cdot10^{-3}$	$4,0\cdot10^{-3}$	150—750 750—850 850—1100	0,75 2,54 1,64	—1,2 8,4 2,4
Diabase porphyrite 650, toleite series	Augite, plageoclase, no secondary changes	$6,6\cdot10^{-10}$	$2,2\cdot10^{-8}$	10^{-7}	$5,1\cdot10^{-7}$	$2,0\cdot10^{-6}$	$4,6\cdot10^{-6}$	$9,6\cdot10^{-6}$	$2,6\cdot10^{-5}$	$1,6\cdot10^{-4}$	150—600 600—850 850—1050	0,74 0,5 2,46	—2,2 —3,5 5,9
		Highly Aluminous Series											
Olivine basalt 14	Plageoclase, augite, olivine, volcanic glass	$5,1\cdot10^{-9}$	$9,6\cdot10^{-8}$	$5,7\cdot10^{-7}$	$2,6\cdot10^{-6}$	$1,1\cdot10^{-5}$	$2,1\cdot10^{-4}$	$4,0\cdot10^{-4}$	$1,2\cdot10^{-3}$	$4,0\cdot10^{-3}$	150—600 600—750 750—1050	0,72 1,68 1,2	—1,2 4,9 2,2
Olivine-plageoclase, large porphyr basalts 271	Plageoclase, pyroxene, magnetite, traces of secondary changes	$2,2\cdot10^{-9}$	$2,6\cdot10^{-8}$	$2,6\cdot10^{-7}$	$6,4\cdot10^{-7}$	$2,0\cdot10^{-6}$	$6,4\cdot10^{-6}$	$9,6\cdot10^{-6}$	$2,0\cdot10^{-5}$	$6,4\cdot10^{-5}$	200—950 950—1050	0,66 2,56	—3,8 6,0
Anamecite 237-21	Plageoclase, hornblende, quartz, volcanic glass	$6,4\cdot10^{-9}$	$1,1\cdot10^{-8}$	$5,1\cdot10^{-8}$	$1,6\cdot10^{-7}$	$1,1\cdot10^{-6}$	$3,2\cdot10^{-6}$	$5,1\cdot10^{-6}$	$2,1\cdot10^{-5}$	$6,6\cdot10^{-5}$	200—500 500—600 600—900 900—1050	0,54 1,05 0,72 3,6	—4,6 0,3 —2,0 8,5
		Alkaline (basic) Basalts											
Basalt 602 2 samples	Plageoclase-48, pyroxene, olivine, magnetite as fine dust, large quantity of glass	10^{-8}	$7\cdot10^{-8}$	$3,2\cdot10^{-6}$	$4,6\cdot10^{-6}$	10^{-5}	$5,7\cdot10^{-5}$	$1,4\cdot10^{-4}$	$5,1\cdot10^{-4}$	$8,9\cdot10^{-4}$	100—500 500—900 900—1100	0,58 0,98 2,52	—3,6 —1,2 7,3

(Appendix 5 is continued on the following page.)

APPENDIX 5. (Continued)

Rock, origin	Mineral composition %	σ ($ohm^{-1} \cdot cm^{-1}$) at t, °C					σ ($ohm^{-1} \cdot cm^{-1}$) at t, °C				Temperature range t, °C	E_0, eV	lg σ_0, $ohm^{-1} \cdot cm^{-1}$
		200	300	400	500	600	700	800	900	1000			
Highly porous basalt 5/22, 2 samples	Plageoclase, augite, pyroxene, olivine, ore mineral, small quantities of volcanic glass	$4 \cdot 10^{-9}$	$7 \cdot 10^{-8}$	$1,6 \cdot 10^{-7}$	$8,2 \cdot 10^{-7}$	$4,0 \cdot 10^{-6}$	$9 \cdot 10^{-6}$	$2,8 \cdot 10^{-5}$	$8,4 \cdot 10^{-5}$	$2 \cdot 10^{-4}$	100—850 850—1100	0,7 1,7	—2,7 2,7
Tracheobasalt 1103	Augite, titanium augite, olivine, analcime, apatite, ilmenite	$2,0 \cdot 10^{-8}$	$9,8 \cdot 10^{-7}$	$4,0 \cdot 10^{-7}$	$9,4 \cdot 10^{-7}$	$4,0 \cdot 10^{-6}$	$1,2 \cdot 10^{-5}$	$5,1 \cdot 10^{-5}$	$2,0 \cdot 10^{-3}$	$1,2 \cdot 10^{-3}$	200—475 475—850 850—1050	0,44 0,82 2,14	—4,7 —1,5 5,5
Tracheo-dolerite 9	Plageoclase, augite, magnetite; glass, (35%); no secondary changes	$6,4 \cdot 10^{-9}$	$6,6 \cdot 10^{-8}$	$1,2 \cdot 10^{-6}$	$4,1 \cdot 10^{-6}$	$2,0 \cdot 10^{-5}$	$5,1 \cdot 10^{-5}$	10^{-4}	$2,1 \cdot 10^{-4}$	$8,2 \cdot 10^{-4}$	150—650 650—850 850—1050	0,78 1,6 4,4	—1,6 2,9 11,4
Nepheline basalt 7	-	$2,0 \cdot 10^{-9}$	$3,2 \cdot 10^{-8}$	$5,1 \cdot 10^{-7}$	$3,2 \cdot 10^{-6}$	$1,2 \cdot 10^{-5}$	$3,4 \cdot 10^{-5}$	$1,2 \cdot 10^{-4}$	$3,2 \cdot 10^{-4}$	$6,6 \cdot 10^{-4}$	150—650 650—1050	0,8 1,1	—1,7 0,9
Olivine basalt 1104, Borisov volcano	Olivine, monoclinic pyroxene, plageoclase, ilmenite; no secondary changes	$1,6 \cdot 10^{-9}$	$2,3 \cdot 10^{-8}$	$2,3 \cdot 10^{-7}$	$6,4 \cdot 10^{-7}$	$1,1 \cdot 10^{-6}$	$5,1 \cdot 10^{-6}$	$6,4 \cdot 10^{-5}$	$1,4 \cdot 10^{-4}$	$2,8 \cdot 10^{-4}$	150—650 650—1050	0,78 1,12	—2,9 1,9
Alkaline (basic) diabase 1102	Hyperstene, alkaline glass	$9,9 \cdot 10^{-10}$	$1,1 \cdot 10^{-8}$	$9,9 \cdot 10^{-8}$	$6,4 \cdot 10^{-7}$	$1,2 \cdot 10^{-6}$	$4,0 \cdot 10^{-6}$	$1,1 \cdot 10^{-5}$	$2,0 \cdot 10^{-5}$	$6,4 \cdot 10^{-5}$	200—950 950—1050	0,78 3,6	—2,4 10,5
Nepheline-leucite basalt 969	-	10^{-9}	$2,0 \cdot 10^{-8}$	$2,0 \cdot 10^{-7}$	$5,1 \cdot 10^{-7}$	$1,1 \cdot 10^{-6}$	$3,2 \cdot 10^{-6}$	10^{-5}	$4,0 \cdot 10^{-5}$	$2,0 \cdot 10^{-4}$	100—800 800—1050	0,67 2,08	—3,9 4,4

(Appendix 5 is continued on the following page.)

APPENDIX 5. (Continued)

Rock, origin	Mineral composition %	σ ($ohm^{-1} \cdot cm^{-1}$) at t, °C									Temperature range t, °C	E_0, eV	lg σ_0, $ohm^{-1} \cdot cm^{-1}$
		200	300	400	500	600	700	800	900	1000			
		Basalts from Baikal Regior				Basalts from Baikal Region							
5g	Augite, labradorite, interspace ore materials	$2,3 \cdot 10^{-7}$	$1,2 \cdot 10^{-6}$	$7,1 \cdot 10^{-6}$	$2,0 \cdot 10^{-5}$	$4,5 \cdot 10^{-5}$	$1,1 \cdot 10^{-4}$	$2,0 \cdot 10^{-4}$	$5,9 \cdot 10^{-4}$	$3,1 \cdot 10^{-3}$	up to 300	0,28	−3,45
											300—850	0,5÷0,6	−1,45÷0,6
											>850	1,54÷1,61	−3,85
517	Augite, labradorite, large inclusions of ore mineral	$2,1 \cdot 10^{-7}$	$2,1 \cdot 10^{-6}$	$7,1 \cdot 10^{-6}$	$1,7 \cdot 10^{-5}$	$9,0 \cdot 10^{-5}$	$1,6 \cdot 10^{-4}$	$2,6 \cdot 10^{-4}$	$8,3 \cdot 10^{-4}$	$2,8 \cdot 10^{-3}$	up to 600	0,5	−2,3
											600—850	0,7	−1,0
											850—1000	1,76	4,4
5d	Augite, olivine, labradorite, glass (there is less of ore mineral than in 5g, 517)	$2,1 \cdot 10^{-8}$	$3,1 \cdot 10^{-7}$	$1,7 \cdot 10^{-6}$	$3,1 \cdot 10^{-6}$	$1,2 \cdot 10^{-5}$	$3,2 \cdot 10^{-5}$	$9,0 \cdot 10^{-5}$	$3,1 \cdot 10^{-4}$	$3,1 \cdot 10^{-3}$	up to 850	0,6	−2,6
											>850	2,0	5,6
518	Small grain glass < 10%, large quantity of ore mineral	$1,6 \cdot 10^{-8}$	$2,8 \cdot 10^{-7}$	$2,8 \cdot 10^{-6}$	$7,7 \cdot 10^{-6}$	$1,9 \cdot 10^{-5}$	$0,9 \cdot 10^{-5}$	$2,6 \cdot 10^{-4}$	$5,5 \cdot 10^{-4}$	$1,7 \cdot 10^{-3}$	up to 600	0,62	−1,15
											600—900	1,0	0,75
											900—1000	1,66	3,5
5e	Well decrystallized	$1,6 \cdot 10^{-8}$	$1,9 \cdot 10^{-7}$	$1,0 \cdot 10^{-6}$	$2,5 \cdot 10^{-6}$	$6,6 \cdot 10^{-6}$	$3,0 \cdot 10^{-5}$	$5,8 \cdot 10^{-5}$	$1,7 \cdot 10^{-4}$	$1,6 \cdot 10^{-3}$	up to 550	0,51	−3,2
											550—850	0,76	−1,8
											>850	2,26	6,0

(Appendix 5 is continued on the folloiwng page.)

APPENDIX 5. (Continued)

Rock, origin	Mineral composition %	σ ($ohm^{-1} \cdot cm^{-1}$) at t, °C					σ ($ohm^{-1} \cdot cm^{-1}$), at t, °C				Temperature range t, °C	E_0, eV	lg σ_0, $ohm^{-1} \cdot cm^{-1}$
		200	300	400	500	600	700	800	900	1000			
506	Analogous to 518	$1,1 \cdot 10^{-9}$	$7,7 \cdot 10^{-8}$	$9,9 \cdot 10^{-7}$	$1,5 \cdot 10^{-6}$	$3,2 \cdot 10^{-6}$	$1,3 \cdot 10^{-5}$	$3,5 \cdot 10^{-5}$	10^{-4}	$7,1 \cdot 10^{-4}$	up to 650 650—850 >850	0,6 1,0 1,8—1,66	—3,3 1,4 4,7
528a	Analogous to 517, but less of ore mineral, glass-40	$3,5 \cdot 10^{-9}$	$5,0 \cdot 10^{-8}$	$2,5 \cdot 10^{-7}$	$1,5 \cdot 10^{-6}$	$2,2 \cdot 10^{-6}$	$1,3 \cdot 10^{-5}$	$4,3 \cdot 10^{-5}$	$1,3 \cdot 10^{-4}$	$1,2 \cdot 10^{-3}$	up to 500 500—850 >850	0,6 1,0 1,7	—2,0 0,5 4,0
525	-	$1,5 \cdot 10^{-8}$	$2,5 \cdot 10^{-7}$	$1,5 \cdot 10^{-6}$	$6,7 \cdot 10^{-6}$	$2,0 \cdot 10^{-5}$	$5,0 \cdot 10^{-5}$	10^{-4}	$2,2 \cdot 10^{-4}$	$3,1 \cdot 10^{-4}$	up to 850 >850	0,64 Melting	—3,9
531	Plageoclase-55, olivine-20, pyroxene-15, glass-5-7, ore minerals-5-7	$5,0 \cdot 10^{-9}$	$5,1 \cdot 10^{-8}$	$2,2 \cdot 10^{-7}$	10^{-6}	$3,6 \cdot 10^{-6}$	$1,4 \cdot 10^{-5}$	$4,3 \cdot 10^{-5}$	$1,3 \cdot 10^{-4}$	$1,2 \cdot 10^{-3}$	100—600 600—900 >900	0,6 1,2 2,8	—3,6 1,3 7,0
520	small grain with large quantities of plageoclase	$5,5 \cdot 10^{-10}$	$9,1 \cdot 10^{-9}$	$5,5 \cdot 10^{-8}$	$1,8 \cdot 10^{-7}$	$6,6 \cdot 10^{-7}$	$1,4 \cdot 10^{-6}$	$4,0 \cdot 10^{-6}$	$1,3 \cdot 10^{-5}$	$1,1 \cdot 10^{-4}$	up to 840 >840	0,6 2,18	—2,16 4,5
523	Plageoclase-60, olivine-20, glass 15, pyroxene-15	$5,2 \cdot 10^{-10}$	$1,3 \cdot 10^{-9}$	$1,3 \cdot 10^{-7}$	$1,9 \cdot 10^{-6}$	$1,1 \cdot 10^{-5}$	$4,5 \cdot 10^{-5}$	$1,2 \cdot 10^{-4}$	$4,3 \cdot 10^{-4}$	$1,1 \cdot 10^{-3}$	up to 800 800—1050	0,82 1,54	0,62 2,75
522	Large grain, glass-10	$1,7 \cdot 10^{-10}$	$1,9 \cdot 10^{-9}$	$1,4 \cdot 10^{-8}$	$1,4 \cdot 10^{-7}$	$1,4 \cdot 10^{-6}$	$1,1 \cdot 10^{-5}$	$2,4 \cdot 10^{-5}$	$1,6 \cdot 10^{-4}$	$5,5 \cdot 10^{-4}$	up to 780 780—1050	0,8 2,1	—1,6 4,0

(Appendix 5 is continued on following page.)

APPENDIX 5. (Continued)

Rock, origin	Mineral composition %	($ohm^{-1}.cm^{-1}$) at t, °C					($ohm^{-1}.cm^{-1}$) at t, °C				Temperature range t, °C	E_0, eV	lg 0_0, $ohm^{-1}.cm^{-1}$
		200	300	400	500	600	700	800	900	1000			
		Basalts from Islands in Indian Ocean					Basalts from Islands in Indian Ocean						
3-3	Decrystallized structure, intermediate grain	$4,5\cdot10^{-8}$	—	$2,9\cdot10^{-6}$	$7,1\cdot10^{-6}$	$3,4\cdot10^{-5}$	—	$2,6\cdot10^{-4}$	$8,3\cdot10^{-4}$	$2,9\cdot10^{-3}$	50—900 900—1000	0,7 1,87	—4,5 4,0
Olivine basalt 3-11		$6,2\cdot10^{-8}$	—	$1,9\cdot10^{-6}$	$6,6\cdot10^{-6}$	$2,4\cdot10^{-5}$	—	$1,6\cdot10^{-4}$	$4,7\cdot10^{-4}$	$2,0\cdot10^{-3}$	50—900 900—1100	0,6 1,87	—1,6 4,0
19-3	Decrystallized structure, intermediate grain, ore mineral	$2,2\cdot10^{-8}$	$3,3\cdot10^{-7}$	$2,3\cdot10^{-6}$	$1,1\cdot10^{-5}$	$3,1\cdot10^{-5}$	$9,0\cdot10^{-5}$	$1,7\cdot10^{-4}$	$4,8\cdot10^{-4}$	$1,7\cdot10^{-3}$	50—900 900—1100	0,45 2,5	—2,9 6,6
19-5	Large grains of titanium magnetite	$2,7\cdot10^{-8}$	$1,4\cdot10^{-7}$	$5,2\cdot10^{-7}$	$2,1\cdot10^{-6}$	$5,2\cdot10^{-6}$	$2,5\cdot10^{-5}$	$6,6\cdot10^{-5}$	$7,6\cdot10^{-4}$	$1,2\cdot10^{-3}$	50—600 600—950 950—1050	0,45 1,1 2,44	—3,3 0,7 8,3
Olivine basalt 7-1	Plageoclase - 55	$6,6\cdot10^{-8}$	$6,2\cdot10^{-7}$	$1,9\cdot10^{-6}$	$3,7\cdot10^{-6}$	$1,1\cdot10^{-5}$	$1,6\cdot10^{-5}$	$5,0\cdot10^{-5}$	10^{-4}	$1,9\cdot10^{-4}$	200—750 750—1050	0,44 0,80	—2,5 —0,5
Gabbro-diabase 173-11, Island Gonwana	Plageoclase (labradorite)-40, clinopyroxene - 53	$2,2\cdot10^{-8}$	$3,3\cdot10^{-6}$	$2,5\cdot10^{-6}$	$1,6\cdot10^{-5}$	$5,8\cdot10^{-5}$	$2,5\cdot10^{-4}$	$5,2\cdot10^{-4}$	$5,8\cdot10^{-4}$	$5,8\cdot10^{-4}$	up to 440 440—800 800—1000	0,65 0,9 Anomaly	—1,4 1,0
175-5	Ore mineral-2, secondary minerals - 5	$1,3\cdot10^{-9}$	$1,5\cdot10^{-8}$	$1,3\cdot10^{-7}$	$1,5\cdot10^{-6}$	$5,8\cdot10^{-6}$	$2,0\cdot10^{-5}$	$5,5\cdot10^{-5}$	$7,1\cdot10^{-5}$	$1,2\cdot10^{-4}$	up to 500 500—850 >850	0,66 0,92 2,08÷2,2	—3,1 —1,75 3,5

(Appendix 5 is continued on the following page.)

APPENDIX 5. (Continued)

Rock, origin	Mineral composition %	σ(ohm^{-1}.cm^{-1}) at t,°C									Temperature range t,°C	E_0,eV	lg σ_0, ohm^{-1}.cm^{-1}
		200	300	400	500	600	700	800	900	1000			
	Basalt from the Indian Ocean rift zone												
54	Weakly decrystallized, ore mineral (1.7 microns)	5,8·10^{-8}	2,8·10^{-7}	1,3·10^{-6}	2,9·10^{-6}	7,6·10^{-6}	2,3·10^{-5}	6,6·10^{-5}	1,6·10^{-4}	3,3·10^{-4}	150—500	0,42	—3,2
											500—600	Anomaly	
											600—1000	0,7	0,25
		5,0·10^{-8}	10^{-6}	2,5·10^{-6}	1,1·10^{-5}	3,3·10^{-5}	7,1·10^{-5}	1,7·10^{-4}	3,0·10^{-4}	6,2·10^{-4}	200—400	0,4	—3,70
											400—1100	0,62	—1,5
54a	Titanomagnetite	1,4·10^{-7}	6,2·10^{-7}	1,2·10^{-6}	2,0·10^{-6}	5,0·10^{-6}	3,7·10^{-5}	1,4·10^{-4}	4,8·10^{-4}	1,2·10^{-3}	200—450	0,2	—4,25
											450—600	0,36	—4,6
161	Fully crystalline ore minerals, strongly altered, oxidized (150 microns)										600—650	Anomaly	
											650—1050	1,14	2,25
		3,1·10^{-7}	2,0·10^{-6}	5,5·10^{-6}	1,1·10^{-5}	1,6·10^{-5}	2,1·10^{-5}	5,0·10^{-5}	1,1·10^{-4}	5,9·10^{-4}	200—525	0,6	—3,0
											525—650	Anomaly	
313	Fine grain ore mineral - 6-8										650—1000	0,68	—1,3
		2,1·10^{-9}	4,3·10^{-8}	2,0·10^{-7}	5,9·10^{-7}	1,2·10^{-6}	4,0·10^{-6}	2,0·10^{-5}	5,1·10^{-5}	2,0·10^{-4}	150—700	0,6	—3,7
											700—1050	1,2	1,4
3/2	-	2,8·10^{-9}	2,2·10^{-8}	1,1·10^{-7}	7,3·10^{-7}	2,1·10^{-6}	8,8·10^{-6}	2,0·10^{-5}	4,4·10^{-5}	1,3·10^{-4}	100—400	0,4	—4,6
											400—850	0,7	—2,85
2/1	-										850—1050	1,6	3,0
		2,6·10^{-9}	1,4·10^{-8}	1,0·10^{-7}	4,0·10^{-7}	1, 6·10^{-6}	7,3·10^{-6}	1,4·10^{-5}	2,6·10^{-5}	6,3·10^{-5}	150—300	0,3	—6,9
											300—900	0,8	—2,6
4/1	-										900—1050	1,8	2,85

Remarks. Basalt samples from the Baikal region were made available by A. Ya. Saltykovskiy, from the Caucasus mountains - by G. T. Prodayvoda and from Sichote-Alinsk - by E. I. Blumshteyn

[Commas in tabulated material are equivalent to decimal points.]

APPENDIX 6. Electrical conductivity σ, activation energy E_0 and preexponential coefficient σ_0 in the xenoliths at high temperatures.

Rock, origin	σ (ohm^{-1}.cm^{-1}) at t, °C											Temperature range t, °C	E_a, eV	lg σ_0, ohm^{-1}.cm^{-1}
	200	300	400	500	600	700	800	900	1000	1100	1200			
Olivinite 1482, xenolith, Avachinsk volcano	$3,2\cdot10^{-11}$	$2,6\cdot10^{-10}$	$4,1\cdot10^{-9}$	$3,2\cdot10^{-8}$	$1,8\cdot10^{-7}$	$8,1\cdot10^{-7}$	$2,0\cdot10^{-6}$	$2,8\cdot10^{-5}$	$1,8\cdot10^{-4}$	$3,6\cdot10^{-3}$	$9,6\cdot10^{-3}$	200—850 850—1200	1,0 3,7	—2,9 11,0
Olivinite 625/4 xenolith in basalt, Lake Baikal	$4,5\cdot10^{-11}$	$1,8\cdot10^{-9}$	$2,2\cdot10^{-8}$	$9,1\cdot10^{-8}$	$3,6\cdot10^{-7}$	$1,6\cdot10^{-6}$	$8,1\cdot10^{-6}$	$1,1\cdot10^{-4}$	$2,8\cdot10^{-4}$	$3,5\cdot10^{-3}$	$3,2\cdot10^{-2}$	150—650 650—900 900—1200	0,78 1,48 3,1	—2,3 —1,8 8,8
Olivinite xenolith in oceanite 1484, Reunion Is.	$1,3\cdot10^{-10}$	$3,5\cdot10^{-9}$	$3,2\cdot10^{-8}$	$1,2\cdot10^{-7}$	10^{-6}	$5,1\cdot10^{-6}$	$2,3\cdot10^{-5}$	$8,3\cdot10^{-5}$	$4,5\cdot10^{-4}$	$3,2\cdot10^{-3}$	$1,6\cdot10^{-2}$	250—550 550—750 750—900 900—1200	0,74 1,13 1,56 2,6	—4,0 0,2 2,7 6,7
Olivine nodule in basalts 780/1B, Lake Baikal	$2,6\cdot10^{-10}$	$5,6\cdot10^{-10}$	$2,3\cdot10^{-9}$	10^{-8}	$3,6\cdot10^{-7}$	$6,4\cdot10^{-7}$	10^{-6}	$2,5\cdot10^{-6}$	$1,1\cdot10^{-5}$	$2,5\cdot10^{-5}$	$5,6\cdot10^{-5}$	150—900 900—1200	0,65 1,6	—3,3 1,3
Pyrope-spinel dunite 1497, tunneled formation "Obnazhennaya"	$2,8\cdot10^{-11}$	$8,0\cdot10^{-10}$	$6,3\cdot10^{-9}$	$4,0\cdot10^{-8}$	$2,8\cdot10^{-7}$	$5,6\cdot10^{-7}$	$1,3\cdot10^{-6}$	$4,5\cdot10^{-6}$	$4,0\cdot10^{-5}$	$6,3\cdot10^{-5}$	$5,0\cdot10^{-4}$	200—850 850—1200	0,82 1,72	—2,0 1,9
Pyrope-spinel dunite 1498, tunneled formation "Obnazhennaya"	$4,0\cdot10^{-11}$	$4,0\cdot10^{-10}$	$4,5\cdot10^{-9}$	$2,8\cdot10^{-8}$	$1,4\cdot10^{-7}$	$4,0\cdot10^{-7}$	$2,5\cdot10^{-6}$	$3,6\cdot10^{-6}$	$8,0\cdot10^{-6}$	$2,8\cdot10^{-5}$	$4,0\cdot10^{-4}$	200—950 950—1000	0,83 1,7	—2,1 1,8
Pyrope peridotite A-66-016, tunneled formation "Obnazhennaya"	10^{-11}	$2,3\cdot10^{-10}$	$4,0\cdot10^{-9}$	$2,8\cdot10^{-8}$	$1,1\cdot10^{-7}$	$5,1\cdot10^{-7}$	10^{-6}	$2,0\cdot10^{-6}$	$8\cdot10^{-6}$	$5,1\cdot10^{-5}$	$1,6\cdot10^{-4}$	150—900 900—1200	0,86 2,24	—2,0 4,75
Spinel-dunite 2162 tunneled formation "Obnazhennaya"	$8,1\cdot10^{-11}$	$1,1\cdot10^{-9}$	$3,6\cdot10^{-9}$	$1,6\cdot10^{-8}$	$9,8\cdot10^{-7}$	10^{-6}	$5,1\cdot10^{-5}$	$3,2\cdot10^{-5}$	10^{-4}	$2,2\cdot10^{-4}$	$1,6\cdot10^{-3}$	150—550 550—1200	0,6 1,92	—4,0 2.4

(Appendix 6 is continued on the following page.)

APPENDIX 6. (Continued)

Rock, origin	σ ($ohm^{-1} \cdot cm^{-1}$) at t, °C						σ ($ohm^{-1} \cdot cm^{-1}$) at t, °C					Temperature range t, °C	E_0, eV	lg σ_0, $ohm^{-1} \cdot cm^{-1}$
	200	300	400	500	600	700	800	900	1000	1100	1200			
Olivine from rock 2162	$6,4 \cdot 10^{-12}$	$2,2 \cdot 10^{-11}$	$9,1 \cdot 10^{-10}$	$9,2 \cdot 10^{-9}$	$1,6 \cdot 10^{-8}$	$8,1 \cdot 10^{-8}$	$5,1 \cdot 10^{-7}$	$1,6 \cdot 10^{-6}$	$1,6 \cdot 10^{-5}$	$1,4 \cdot 10^{-4}$	$9,2 \cdot 10^{-4}$	200—700 700—1050 1050—1200	1,0 1,76 3,8	—3,9 1,7 10,0
Compressed olivine powder 2162	$2,2 \cdot 10^{-12}$	$9,6 \cdot 10^{-12}$	$3,3 \cdot 10^{-10}$	$2,6 \cdot 10^{-9}$	10^{-8}	$5,2 \cdot 10^{-8}$	$1,8 \cdot 10^{-7}$	$7,2 \cdot 10^{-7}$	$2,3 \cdot 10^{-6}$	$7,1 \cdot 10^{-6}$	$2,9 \cdot 10^{-5}$	200—700 700—1050 1050—1200	1,4 1,46 2,3	—3,0 4,0 11,0
Pyrope peridotite with enstatite 2161, tunneled formation "Obnazhennaya"	$8,0 \cdot 10^{-12}$	$3,2 \cdot 10^{-10}$	$7,2 \cdot 10^{-9}$	$1,2 \cdot 10^{-8}$	$5,1 \cdot 10^{-8}$	$2,6 \cdot 10^{-7}$	$1,2 \cdot 10^{-6}$	$9,1 \cdot 10^{-6}$	$4,0 \cdot 10^{-5}$	10^{-3}	$3,3 \cdot 10^{-3}$	200—700 700—1000 1000—1200	0,82 2,12 3,6	—3,4 4,0 11,0
Pyrope peridotite 2163, tunneled formation "Obnazhennaya"	10^{-11}	$3,3 \cdot 10^{-10}$	$2,5 \cdot 10^{-9}$	$1,6 \cdot 10^{-8}$	$4,0 \cdot 10^{-8}$	$1,6 \cdot 10^{-7}$	$5,7 \cdot 10^{-7}$	$2,0 \cdot 10^{-6}$	$6,4 \cdot 10^{-5}$	10^{-4}	$1,6 \cdot 10^{-3}$	150—875 875—950	0,78 1,74	—3,2 1,5
Euclogite-like rock 2177, tunneled formation "Agaztan"	$9,5 \cdot 10^{-10}$	$8,2 \cdot 10^{-9}$	$5,7 \cdot 10^{-8}$	$2,6 \cdot 10^{-7}$	$5,7 \cdot 10^{-7}$	$2,1 \cdot 10^{-6}$	$5,1 \cdot 10^{-6}$	$1,6 \cdot 10^{-5}$	$3,2 \cdot 10^{-5}$	$1,1 \cdot 10^{-3}$	$5,6 \cdot 10^{-3}$	200—750 750—1000 more than 1000	0,72 1,5 5,4	—3,4 1,3 15,0
Dunite AO-151, tunneled formation "Obnazhennaya"	$3,2 \cdot 10^{-12}$	10^{-10}	$1,6 \cdot 10^{-9}$	10^{-8}	$4,1 \cdot 10^{-8}$	$1,6 \cdot 10^{-7}$	$4,0 \cdot 10^{-7}$	$9,2 \cdot 10^{-7}$	10^{-5}	$2,6 \cdot 10^{-4}$	$9,2 \cdot 10^{-4}$	200—900 900—1050 1050—1250	0,86 3,7 3,2	—2,0 9,7 7,3
Olivinite 5831, Kola peninsula	$5,0 \cdot 10^{-12}$	10^{-10}	$5,0 \cdot 10^{-10}$	10^{-8}	$1,2 \cdot 10^{-7}$	$5,0 \cdot 10^{-7}$	$1,4 \cdot 10^{-6}$	$4,0 \cdot 10^{-6}$	$3,2 \cdot 10^{-5}$	$1,4 \cdot 10^{-4}$	$3,6 \cdot 10^{-4}$	150—400 400—875 875—1200	0,68 1,2 2,6	—5,9 1,7 6,7
Olivinite 1423, Kola peninsula	$2,0 \cdot 10^{-12}$	$6,3 \cdot 10^{-10}$	$5,0 \cdot 10^{-9}$	$7,0 \cdot 10^{-8}$	$8,0 \cdot 10^{-7}$	$4,0 \cdot 10^{-6}$	$1,1 \cdot 10^{-5}$	$6,4 \cdot 10^{-5}$	$5,0 \cdot 10^{-4}$	$1,4 \cdot 10^{-3}$	$2,2 \cdot 10^{-3}$	200—500 500—700 700—1200	0,9 1,47 2,0	—2,0 1,8 3,8
Olivinite 1430, Kurginsk formation, Kola peninsula	$4,0 \cdot 10^{-11}$	$5,0 \cdot 10^{-10}$	$2,8 \cdot 10^{-9}$	$2,2 \cdot 10^{-8}$	$2,5 \cdot 10^{-7}$	$1,8 \cdot 10^{-6}$	$7,1 \cdot 10^{-6}$	$3,2 \cdot 10^{-5}$	$4,0 \cdot 10^{-4}$	$8,9 \cdot 10^{-3}$	$2,5 \cdot 10^{-2}$	100—450 450—950 950—1200	0,61 1,44 3,36	—5,8 1,6 11,7

(Appendix 6 is continued on the following page)

APPENDIX 6. (Continued)

Rock, origin	σ (ohm^{-1}.cm^{-1}) at t, °C						σ (ohm^{-1}.cm^{-1}) at t, °C					Temperature range t, °C	E_a, eV	lg σ_0, ohm^{-1}.cm^{-1}
	200	300	400	500	600	700	800	900	1000	1100	1200			
Large crystal olivinite 1473, Lovozero formation, Kola peninsula	$4{,}0\cdot10^{-12}$	$1{,}8\cdot10^{-10}$	10^{-9}	$8{,}1\cdot10^{-9}$	$4{,}0\cdot10^{-7}$	$1{,}6\cdot10^{-6}$	$8{,}9\cdot10^{-6}$	$5{,}0\cdot10^{-5}$	$3{,}2\cdot10^{-4}$	$1{,}1\cdot10^{-3}$	$4{,}0\cdot10^{-3}$	150—550 550—700 700—1200	0,94 — 1,85	—3,4 — 3,8

[Commas in tabulated material are equivalent to decimal points.]

APPENDIX 7. Electrical conductivity σ, activation energy E_0 and preexponential coefficient σ_0 in pyroxenites at high temperatures.

Rock, origin	Mineral composition %	σ ($ohm^{-1}.cm^{-1}$) at t, °C										Temperature range t, °C	E_0, eV	$\lg \sigma_0$, $ohm^{-1}.cm^{-1}$
		200	300	400	500	600	700	800	900	1000	1100			
Monocline pyroxenite 2492 Russian platform	Diopside-70 chlorite-30	$2,0 \cdot 10^{-11}$	$7,1 \cdot 10^{-10}$	$4,0 \cdot 10^{-9}$	$2,0 \cdot 10^{-8}$	$5,3 \cdot 10^{-8}$	$2,5 \cdot 10^{-7}$	10^{-6}	$1,7 \cdot 10^{-6}$	$5,0 \cdot 10^{-6}$	—	up to 600 600—950 >950	0,6 1,0 2,66	—4,2 —2,6 5,75
Pyroxenite 2497, Russian platform	Diopside-80, uralite-10, chlorite-10	$1,1 \cdot 10^{-11}$	$2,1 \cdot 10^{-10}$	$1,1 \cdot 10^{-9}$	$6,2 \cdot 10^{-9}$	$2,6 \cdot 10^{-8}$	$1,3 \cdot 10^{-7}$	$1,4 \cdot 10^{-7}$	$1,1 \cdot 10^{-6}$	$7,7 \cdot 10^{-6}$	—	up to 800 800—1100	0,8 2,0	—4,25 2,3
Pyroxenite-amphibole 2482, Russian platform	Amphibole (uralite)-50, zoisite-50	$2,3 \cdot 10^{-11}$	$3,6 \cdot 10^{-10}$	$2,6 \cdot 10^{-9}$	$1,0$— $1,3 \cdot 10^{-8}$	$4,2$— $5,9 \cdot 10^{-8}$	$1,7 \cdot 10^{-7}$	$8,3 \cdot 10^{-7}$	$3,7 \cdot 10^{-6}$	$9,9 \cdot 10^{-6}$	—	200—580 580—820 820—970 >970	0,6—0,75 1,2—1,30 Anomaly 2,6—2,8	—4,2—4,8 —1,3 3,0
Aplopyroxenite, amphibolized rock 2500, Russian platform	Amphibole (uralite)-30, zoisite-50	$4,8 \cdot 10^{-11}$	$9,1 \cdot 10^{-10}$	$3,0 \cdot 10^{-9}$	$9,1 \cdot 10^{-9}$	$3,0 \cdot 10^{-8}$	$6,3 \cdot 10^{-8}$	$2,1 \cdot 10^{-7}$	$5,0 \cdot 10^{-7}$	$2,3 \cdot 10^{-6}$	—	200—420 420—800 800—900 >900	0,56 0,70 Anomaly 2,5	—5,6 —4,6 2,0
Pyroxenite 1646, Kola peninsula	—	$3,6 \cdot 10^{-10}$	$2,1 \cdot 10^{-9}$	$4,2 \cdot 10^{-9}$	$5,3 \cdot 10^{-8}$	$1,9 \cdot 10^{-7}$	$7,7 \cdot 10^{-7}$	$2,8 \cdot 10^{-6}$	$7,7 \cdot 10^{-6}$	$2,8 \cdot 10^{-5}$	—	up to 450 450—850 >850	0,46 0,97 1,55	—5,4 —1,0 2,85
Pyroxenite, 340, Kola peninsula	Pyroxene (rhombic)-80, secondary (serpentine chlorite)-10	$3,2 \cdot 10^{-12}$	$3,2 \cdot 10^{-11}$	$1,8 \cdot 10^{-10}$	$6,4 \cdot 10^{-10}$	$1,8 \cdot 10^{-9}$	$5,6 \cdot 10^{-9}$	$5,7 \cdot 10^{-8}$	$7,1 \cdot 10^{-7}$	$2,8 \cdot 10^{-6}$	—	100—670 670—1000	0,6 2,2	—6,6 4,2
Olivine pyroxenite 591 Kola peninsula	Pyroxene (rhombic)-90, olivine-80, ore mineral - 2	$4,0 \cdot 10^{-12}$	$5,0 \cdot 10^{-11}$	$4,0 \cdot 10^{-10}$	$3,1 \cdot 10^{-9}$	$8,9 \cdot 10^{-9}$	$5,0 \cdot 10^{-8}$	$3,1 \cdot 10^{-7}$	$5,6 \cdot 10^{-7}$	$6,3 \cdot 10^{-6}$	—	up to 850 850—1100	1,0 2,2	—3,45 4,0

(Appendix 7 is continued on the following page.)

APPENDIX 7. (Continued)

Rock, origin	Mineral composition %	σ (ohm^{-1}·cm^{-1}) at t, °C					σ (ohm^{-1}·cm^{-1}) at t, °C					Temperature range t, °C	E, eV	ln σ, ohm^{-1}·cm^{-1}
		200	300	400	500	600	700	800	900	1000	1100			
Olivine pyroxenite 469 Kola peninsula	Pyroxene-80, olivine-17, ore minerals -2	—	$6,7\cdot10^{-12}$	$1,6\cdot10^{-10}$	$1,4\cdot10^{-9}$	$8,3\cdot10^{-9}$	$3,8\cdot10^{-8}$	$2,2\cdot10^{-7}$	$1,0\cdot10^{-6}$	$5,9\cdot10^{-6}$	—	up to 300 300—800 >800	0,44 0,96 2,2	—9,7 —2,0 5,6
Pyroxenite 1508, xenolith from the ophite lava of Kamchatka volcano	—	—	$4,5\cdot10^{-9}$	$4,0\cdot10^{-8}$	$2,3\cdot10^{-7}$	$7,9\cdot10^{-7}$	$3,1\cdot10^{-7}$	$1,6\cdot10^{-6}$	10^{-5}	$2,8\cdot10^{-5}$	$2,5\cdot10^{-4}$	300—600 600—700 700—950 950—1200	0,72 Anomaly 1,66 2,55	—2,2 2,0 5,6
Olivine pyroxenite 2712, Ural mountains	Pyroxene (diopside)-80, plageoclase-15, horblende-5	$1,2\cdot10^{-10}$	$4,1\cdot10^{-9}$	$5,1\cdot10^{-8}$	$3,2\cdot10^{-7}$	$1,6\cdot10^{-6}$	$5,1\cdot10^{-6}$	$2,6\cdot10^{-5}$	$2,6\cdot10^{-5}$	$1,2\cdot10^{-4}$	10^{-3}	150—550 550—800 800—900 900—1100	0,82 1,1 Anomaly 2,66	—1,9 0,5 7,0
Pyroxene hornblende 1585, Anabar bed	Pyroxene (rhombic)-67, monocline pyroxene-12, hornblende-20-21	$3,1\cdot10^{-10}$	10^{-9}	10^{-8}	$5,6\cdot10^{-8}$	$1,5\cdot10^{-7}$	$8,0\cdot10^{-7}$	$1,6\cdot10^{-6}$	$4,0\cdot10^{-6}$	$1,3\cdot10^{-5}$	$2,8\cdot10^{-4}$	150—950 950—1100	0,81 3,5	2,0 9,4
Pyroxenite 1004, Koksharov formation	—	$4,5\cdot10^{-2}$	$7,7\cdot10^{-2}$	$1,2\cdot10^{-1}$	$2,1\cdot10^{-1}$	$3,2\cdot10^{-1}$	$4,1\cdot10^{-1}$	$4,5\cdot10^{-1}$	$4,7\cdot10^{-1}$	$3,7\cdot10^{-1}$	—	—	—	—
Pyroxenite 1001, Koksharov formation	Titanium-containing augite-70, titanomagnetite-20-25	$5,9\cdot10^{-4}$	$9,1\cdot10^{-4}$	$1,2\cdot10^{-3}$	$3,3\cdot10^{-3}$	$2,0\cdot10^{-2}$	$7,1\cdot10^{-2}$	$1,2\cdot10^{-1}$	$2,0\cdot10^{-1}$	$2,2\cdot10^{-1}$	—	up to 340 340—640 >640	0,08 0,8 0,4	—2,3 3,5
Pyroxenite 1006, Koksharov formation	—	$1,1\cdot10^{-6}$	$1,0\cdot10^{-5}$	$4,0\cdot10^{-5}$	$1,1\cdot10^{-4}$	$3,7\cdot10^{-4}$	$1,0\cdot10^{-3}$	$1,7\cdot10^{-3}$	$2,9\cdot10^{-3}$	$5,3\cdot10^{-3}$	—	up to 450 450—700 >700	0,52 0,65 0,47	—4,3 0,4 —0,5
Pyroxenite 1002,	Eugarine-augite-50, eugarine, alkaline (basic) hornblend, mica-20	$4,5\cdot10^{-7}$	$2,3\cdot10^{-6}$	$3,7\cdot10^{-5}$	$1,0\cdot10^{-4}$	$7,7\cdot10^{-4}$	$1,6\cdot10^{-3}$	$3,6\cdot10^{-3}$	$4,4\cdot10^{-3}$	$5,6\cdot10^{-3}$	—	up to 620 620—1000	0,76 0,36÷0,5	1,1 1—0,75 —0,5
Pyroxenite 1003, Koksharov formation	—	$5,0\cdot10^{-11}$	$1,6\cdot10^{-9}$	$2,0\cdot10^{-9}$	$6,3\cdot10^{-8}$	$2,8\cdot10^{-7}$	$1,5\cdot10^{-6}$	$2,8\cdot10^{-6}$	$2,6\cdot10^{-6}$	$2,0\cdot10^{-5}$	$5,6\cdot10^{-5}$	200—900 900—1050	0,8 2,2	—48 3,87

[Commas in tabulated material are equivalent to decimal points.]

APPENDIX 8. Electrical conductivity σ, activation energy E_0 and preexponential coefficient σ_0, in olivinites at high temperatures.

Rock	Mineral composition %	σ (ohm^{-1}·cm^{-1}) at t, °C									Temperature range t, °C	E_0, eV	$\lg \sigma_0$, ohm^{-1}·cm^{-1}
		200	300	400	500	600	700	800	900	1000			
Olivinite 583	Olivine-69, pyroxene-18, serpentine-8, ore mineral-5	$9,1\cdot10^{-12}$	$3,0\cdot10^{-10}$	$5,0\cdot10^{-9}$	$3,5\cdot10^{-8}$	$1,8\cdot10^{-7}$	$1,0\cdot10^{-6}$	$5,3\cdot10^{-6}$	$2,7\cdot10^{-5}$	$8,3\cdot10^{-5}$	up to 650 650—850 850—1050	0,7 1,3 2,5	—4,4 —0,5 5,4
6014	Olivine-95, serpentine-5	$1,3\cdot10^{-12}$	$1,3\cdot10^{-11}$	$2,1\cdot10^{-10}$	$1,7\cdot10^{-9}$	$2,0\cdot10^{-8}$	$1,7\cdot10^{-7}$	$8,3\cdot10^{-7}$	$2,6\cdot10^{-5}$	$3,2\cdot10^{-5}$	up to 480 480—820 >820	0,82 1,76 2,6	—4,8 0,75 6,8
1381	—	$3,7\cdot10^{-11}$	$7,7\cdot10^{-10}$	$5,6\cdot10^{-9}$	$4,3\cdot10^{-8}$	$2,4\cdot10^{-6}$	$1,7\cdot10^{-6}$	$6,7\cdot10^{-6}$	$2,3\cdot10^{-5}$	$1,1\cdot10^{-4}$	up to 500 500—850 >850	0,75 1,2 2,1	—3,4 0,25 4,0
5683	Olivine-98, serpentine-2	$3,1\cdot10^{-11}$	$3,6\cdot10^{-10}$	$5,6\cdot10^{-9}$	$1,5\cdot10^{-8}$	$5,6\cdot10^{-7}$	$2,4\cdot10^{-7}$	$1,7\cdot10^{-6}$	$8,3\cdot10^{-6}$	$4,2\cdot10^{-5}$	200—550 550—820 >820	0,6 1,15 2,4	—4,25 0,75 6,0
6013	Olivine-100	$3,1\cdot10^{-11}$	$3,0\cdot10^{-9}$	$2,6\cdot10^{-8}$	$2,4\cdot10^{-7}$	$7,2\cdot10^{-7}$	$5,0\cdot10^{-6}$	$3,6\cdot10^{-5}$	$1,1\cdot10^{-4}$	$5,9\cdot10^{-4}$	up to 580 580—900 >900	0,75 1,46 2,2	—2,0 2,0 5,75
Olivinite, direction 1	—	$1,0\cdot10^{-11}$	$2,6\cdot10^{-10}$	$3,4\cdot10^{-9}$	$4,7\cdot10^{-8}$	$3,4\cdot10^{-7}$	$1,1\cdot10^{-6}$	$5,5\cdot10^{-6}$	$1,9\cdot10^{-5}$	$7,7\cdot10^{-5}$	up to 500 500—900 900—1050	0,9 1,0 2,2	—2,5 0,8 5,2
Olivinite, direction 2	—	$1,3\cdot10^{-11}$	$2,9\cdot10^{-10}$	$2,5\cdot10^{-9}$	$1,1\cdot10^{-7}$	$3,8\cdot10^{-7}$	$1,9\cdot10^{-6}$	$1,9\cdot10^{-5}$	$5,1\cdot10^{-5}$	$1,3\cdot10^{-4}$	up to 550 550—1050	0,72 2,0	—3,4 1,0
Olivinite direction 3	—	$1,3\cdot10^{-11}$	$4,8\cdot10^{-10}$	$1,1\cdot10^{-8}$	$4,2\cdot10^{-8}$	$7,7\cdot10^{-7}$	$4,7\cdot10^{-6}$	$1,5\cdot10^{-5}$	$1,3\cdot10^{-4}$	$3,8\cdot10^{-3}$	up to 500 500—800 >800	0,75 1,2 2,2	—3,75 1,5 5,0

[Commas in tabulated material are equivalent to decimal points.]

APPENDIX 9. Electrical conductivity σ, activation energy E_0 and preexponential coefficient σ_0, in dunites at high temperatures.

Rock, origin	Mineral composition %	σ (ohm^{-1}·cm^{-1}) at t, °C										Temperature range t, °C	E_0, eV	lg σ_0, ohm^{-1}·cm^{-1}
		200	300	400	500	600	700	800	900	1000	1050			
Dunite 5556 Ural Mts.	Olivine-50, serpentine-49, chromite-1	$2,5\cdot10^{-6}$	$2,6\cdot10^{-6}$	$5,9\cdot10^{-6}$	$5,0\cdot10^{-6}$	$3,6\cdot10^{-5}$	$1,5\cdot10^{-5}$	$1,9\cdot10^{-5}$	$4,0\cdot10^{-5}$	$1,2\cdot10^{-4}$	—	<520	0,28	−4,9
												520—780	Anomaly	
												>780	1,42	1,5
Dunite 7199	Olivine-50, serpentine-47, chromite-3	$7,1\cdot10^{-8}$	$3,8\cdot10^{-7}$	$3,1\cdot10^{-7}$	$4,0\cdot10^{-6}$	$1,0\cdot10^{-5}$	$2,2\cdot10^{-6}$	$3,6\cdot10^{-6}$	$1,5\cdot10^{-5}$	$3,1\cdot10^{-5}$	—	<700	~0,1	~−4,0
												700—850	Anomaly	
												850—1050	1,7	1,5
Dunite from Armenia	Olivine-55, serpentine-45	$7,2\cdot10^{-8}$	$2,4\cdot10^{-7}$	$3,1\cdot10^{-7}$	$2,8\cdot10^{-6}$	$4,0\cdot10^{-6}$	$1,0\cdot10^{-5}$	$2,2\cdot10^{-6}$	$3,6\cdot10^{-6}$	$1,5\cdot10^{-5}$	$3,1\cdot10^{-5}$	<500	~0,1	−5,5÷−6,0
												500—800	Anomaly	
												>800	1,66	1,6
Dunite 7198, Armenia	Serpentine-95, olivine-1, chromite-4	$1,1\cdot10^{-9}$	$3,6\cdot10^{-9}$	$2,4\cdot10^{-8}$	$4,2\cdot10^{-8}$	$4,4\cdot10^{-9}$	$2,9\cdot10^{-8}$	$1,7\cdot10^{-7}$	$1,1\cdot10^{-6}$	$6,3\cdot10^{-6}$	—	<500	0,52	−4,00
												500—610	Anomaly	
												>610	1,9	2,25
Dunite 6671, Kimpersay	Olivine-40,0, serpentine-59.5, chromite-0.5	$3,1\cdot10^{-9}$	$1,4\cdot10^{-8}$	$5,3\cdot10^{-8}$	$1,0\cdot10^{-7}$	$6,1\cdot10^{-8}$	$6,3\cdot10^{-8}$	$3,0\cdot10^{-7}$	$1,8\cdot10^{-6}$	$1,0\cdot10^{-5}$	$1,4\cdot10^{-5}$	up to 500	0,35	−5,25
												500—680	Anomaly	
												>680	1,90	2,0
Dunite 6672, Kimpersay	Olivine-40.0, serpentine-60, chromite-0.5	$7,7\cdot10^{-9}$	$4,6\cdot10^{-8}$	$1,2\cdot10^{-7}$	$7,2\cdot10^{-8}$	$2,0\cdot10^{-8}$	$1,2\cdot10^{-7}$	$3,8\cdot10^{-7}$	$3,1\cdot10^{-6}$	$1,3\cdot10^{-5}$	$2,1\cdot10^{-5}$	up to 420	0,34	−6,9
												420—620	Anomaly	
												620—800	0,9	−2,0
												>800	1,8	2,0
Dunite 6669, Kimpersay	Olivine-19.8, serpentine-80, chromite-0.2	$1,6\cdot10^{-10}$	$5,1\cdot10^{-9}$	$3,7\cdot10^{-8}$	$3,0\cdot10^{-8}$	$7,3\cdot10^{-8}$	$1,7\cdot10^{-7}$	$6,8\cdot10^{-7}$	$2,3\cdot10^{-6}$	$2,0\cdot10^{-5}$	$3,5\cdot10^{-5}$	<400	0,68	−3,2
												400—600	Anomaly	
												600—850	0,86	−2,3
												>850	2,0	3,5
Dunite 5577, Aldan	Olivine-67.5, serpentine-30, chromite-0.5	$1,5\cdot10^{-11}$	$1,3\cdot10^{-10}$	$9,1\cdot10^{-10}$	$5,6\cdot10^{-9}$	$1,4\cdot10^{-8}$	$2,4\cdot10^{-8}$	$1,7\cdot10^{-7}$	$7,2\cdot10^{-7}$	$9,1\cdot10^{-6}$	$1,6\cdot10^{-5}$	<750	0,64	−5,5
												>750	2,14	3,5

REMARKS. The rocks were made available by B.P. Belikov.

[Commas in tabulated material are equivalent to decimal points.]

/252
/254

APPENDIX 10. Electrical conductivity σ, activation energy E_0 and preexponential coefficient σ_0, in rocks from the Mamonov complex at high temperatures.

Rock, origin	Mineral composition %	σ (ohm^{-1}.cm^{-1}) at t, °C				σ (ohm^{-1}.cm^{-1}) at t, °C					Temperature range t, °C	E_0, eV	lg σ_0, ohm^{-1}.cm^{-1}
		200	300	400	500	600	700	800	900	1000			
Apodunite 2614	Serpentine-55, carbonite-25, magnetite-10	$2,1\cdot10^{-9}$	$3,5\cdot10^{-8}$	$1,1\cdot10^{-7}$	$3,4\cdot10^{-6}$	$4,0\cdot10^{-6}$	$2,1\cdot10^{-5}$	$1,5\cdot10^{-5}$	$9,8\cdot10^{-6}$	$9,6\cdot10^{-6}$	up to 500	0,8	−0,1
											500—800	Anomaly	
											800—1050	1,6	1,5
Serpentinized peridotite 2610	Olivine-85, ore mineral-5, pyroxene-5; secondary one: serpentine-50, carbonite-15, ore mineral - 15	$5,0\cdot10^{-7}$	10^{-6}	$1,5\cdot10^{-6}$	$1,4\cdot10^{-6}$	$2,1\cdot10^{-7}$	$3,2\cdot10^{-7}$	$7,0\cdot10^{-7}$	$2,6\cdot10^{-6}$	$5,8\cdot10^{-6}$	up to 450	0,14	−5,0
											450—650	Anomaly	
											650—1000	1,06	−1,25
Apoperidotite 2611	Serpentine-70, chlorite-12, carbonite-7, magnetite-10	$3,0\cdot10^{-6}$	$4,0\cdot10^{-6}$	10^{-5}	$2,9\cdot10^{-5}$	$1,4\cdot10^{-6}$	$1,4\cdot10^{-7}$	$4,1\cdot10^{-7}$	$1,3\cdot10^{-6}$	$6,6\cdot10^{-6}$	up to 720	Anomaly	
											720—1050	1,4	—
Apodunite 2606	Serpentine-55, amphibole-10, chlorite-5, magnetite -20	$3,5\cdot10^{-6}$	$8,3\cdot10^{-6}$	$1,8\cdot10^{-5}$	$2,4\cdot10^{-6}$	$3,5\cdot10^{-6}$	$6,3\cdot10^{-6}$	$7,1\cdot10^{-6}$	$7,7\cdot10^{-6}$	$2,1\cdot10^{-5}$	up to 400	0,16	−4,1
											400—800	Anomaly	
											800—1050	1,24	−0,5
Apoperidotite 2604	—	$1,4\cdot10^{-5}$	$2,2\cdot10^{-5}$	$4,1\cdot10^{-5}$	$4,5\cdot10^{-5}$	$1,9\cdot10^{-4}$	$4,5\cdot10^{-5}$	$2,1\cdot10^{-5}$	$4,0\cdot10^{-4}$	$4,0\cdot10^{-3}$	Irregular change		

Remarks. The rocks were made available by V. E. Dibrov.

[Commas in tabulated material are equivalent to decimal points.]

APPENDIX 11. Electrical conductivity σ, activation energy E_0 and preexponential coefficient σ_0 in serpentinites at high temperatures.

Rock	Mineral composition,%	σ (ohm^{-1}·cm^{-1}) at t, °C										Temperature range t, °C	E_0, eV	$\lg\sigma_0$ ohm^{-1}·cm^{-1}
		200	300	400	500	600	700	800	900	1000	1050			
Serpentinite 2494	Fully serpentinized olivine, magnatite-5	1,6·10^{-3}	3,5·10^{-3}	3,6·10^{-3}	2,9·10^{-3}	3,3·10^{-3}	7,7·10^{-3}	2,3·10^{-3}	1,1·10^{-3}	5,4·10^{-4}	6,7·10^{-4}	Anomalous change		
Serpentinite 2512	Serpentine-75 (apoolivinite type) pyroxene-5, magnatite and sulfite-20	1,0·10^{-5}	2,0·10^{-5}	3,3·10^{-5}	2,9·10^{-5}	4,4·10^{-5}	1,5·10^{-5}	—	7,7·10^{-6}	2,3·10^{-5}	—	up to 900	Anomaly	
												>900	2,2	4,7
Serpentinite 2514	Pyroxene-15 (altered), serpentine-75, sulfites and magnatites -10	2,0·10^{-6}	2,5·10^{-6}	1,3·10^{-7}	—	3,7·10^{-7}	6,3·10^{-7}	9,1·10^{-7}	2,6·10^{-6}	9,1·10^{-6}	1,8·10^{-5}	up to 800	Anomaly	
												800—1050	1,4	3,3
		2,2·10^{-5}	3,0·10^{-5}	3,0·10^{-5}	—	3,0·10^{-5}	2,0·10^{-5}	2,9·10^{-5}	6,5·10^{-5}	1,6·10^{-4}	2,5·10^{-4}	800—1050	1,4	4,6
Apoperidotite serpentinite 2488	Pyroxene-40 (altered), serpentine-40, magnetite-20	4,8·10^{-6}	7,2·10^{-6}	9,1·10^{-6}	9,1·10^{-6}	1,1·10^{-5}	2,4·10^{-5}	2,6·10^{-5}	5,3·10^{-5}	9,1·10^{-5}	1,1·10^{-4}	up to 650	0,1—5,5	
												650—820	Anomaly	
												>820	1,0—1,5	
Serpentinite 2185	Serpentine-75, pyroxene-10, brucite-3, magnetite-10	7,7·10^{-6}	1,1·10^{-5}	1,4·10^{-5}	1,8·10^{-5}	1,2·10^{-5}	3,2·10^{-5}	4,8·10^{-4}	6,7·10^{-6}	8,3·10^{-6}	—	—	—	—
Serpentinite 2183	Serpentine-75, talcum-2, pyroxene-10, magnetite-10	4,4·10^{-7}	4,8·10^{-7}	2,4·10^{-6}	2,9·10^{-6}	2,9·10^{-6}	6,3·10^{-6}	1,0·10^{-5}	4,7·10^{-6}	1,3·10^{-5}	—	—	—	—
Serpentinite	—	1,1·10^{-8}	3,7·10^{-8}	2,9·10^{-5}	5,6·10^{-5}	9,1·10^{-5}	9,1·10^{-5}	2,4·10^{-5}	2,1·10^{-6}	5,9·10^{-6}	1,1·10^{-5}	up to 820	Anomaly	
												820—1050	2,0	3,0
Serpentinite (Kazakhstan) AV-45	—	2,5·10^{-10}	1,4·10^{-8}	2,8·10^{-8}	1,4·10^{-7}	4,0·10^{-7}	5,9·10^{-7}	7,7·10^{-6}	1,0·10^{-5}	2,1·10^{-4}	—	up to 750	—	—
												750—1050	0,94	1,0
Apoperidotite Serpentinite 2519	Pyroxene-20, serpentine-80, (chrysotile)	1,6·10^{-10}	1,1·10^{-9}	7,2·10^{-9}	3,0·10^{-8}	1,9·10^{-7}	9,1·10^{-7}	5,0·10^{-7}	1,0·10^{-6}	5,3·10^{-6}	8,9·10^{-6}	up to 400	0,56	—4,0
												400—700	1,14	0,1
												700—820	Anomaly	
												>820	1,66	1,5
Serpentinite 2518	Pyroxene-20, serpentine-80, (chrysotile)	3,4·10^{-11}	1,1·10^{-9}	1,7·10^{-9}	4,3·10^{-9}	1,3·10^{-8}	3,0·10^{-8}	1,5·10^{-7}	6,4·10^{-7}	2,6·10^{-6}	5,1·10^{-6}	up to 620	0,54	—5,2
												620—1050	1,75	1,5

[Commas in tabulated material are equivalent to decimal points.]

Remarks. Rocks were made available by V. Ya. Elevich.

APPENDIX 12. Electrical conductivity σ, activation energy E_0 and preexponential coefficient σ_0 in eclogites at high temperatures.

Rock	Mineral composition %	σ (ohm^{-1}·cm^{-1}) at t, °C									Temperature range t, °C	E_0, eV	lg σ_0, ohm^{-1}·cm^{-1}
		200	300	400	500	600	700	800	900	1000			
	Ural Mountains												
	1st Group												
1592	Garnet-64, pyroxene-30, muscovite, quartz, rutile-6,	$5,7\cdot10^{-10}$	$1,7\cdot10^{-9}$	$2,7\cdot10^{-8}$	$1,1\cdot10^{-7}$	—	$2,0\cdot10^{-6}$	$1,5\cdot10^{-5}$	$3,0\cdot10^{-5}$	$7,5\cdot10^{-5}$	200—700 700—1000 >1000	0,86 1,0 3,2	−2,5 0,2 9,5
1593	—	$6,3\cdot10^{-11}$	$4,2\cdot10^{-10}$	$3,6\cdot10^{-9}$	$2,0\cdot10^{-8}$	10^{-7}	$3,6\cdot10^{-7}$	$1,3\cdot10^{-6}$	$3,6\cdot10^{-6}$	$7,7\cdot10^{-6}$	200—600 600—1000 >1000	0,8 1,1 Melting	−3,4 1,1
1594	Garnet-50, pyroxene-45, muscovite, quartz-2, sphene-3	$2,9\cdot10^{-10}$	$5,7\cdot10^{-10}$	$2,9\cdot10^{-9}$	$1,8\cdot10^{-8}$	$8,9\cdot10^{-8}$	$4,1\cdot10^{-7}$	$7,9\cdot10^{-7}$	$4,0\cdot10^{-6}$	$9,3\cdot10^{-6}$	100—350 350—600 >700	0,11 0,89 1,67	−9,3 −2,5 1,65
	2nd Group												
1600	Garnet-65, muscovite-4, epidote-3, amphibole-27	$6,1\cdot10^{-10}$	$5,2\cdot10^{-9}$	$4,5\cdot10^{-8}$	$3,0\cdot10^{-7}$	$7,3\cdot10^{-7}$	$3,0\cdot10^{-6}$	$7,3\cdot10^{-6}$	$2,4\cdot10^{-5}$	$1,2\cdot10^{-4}$	200—800 800—900 >900	0,77 Anomaly 4,0	−2,4 15,3
1601	Garnet-55-60, muscovite-15-20, amphibole-20, sphene-2-3	$3,4\cdot10^{-11}$	$1,4\cdot10^{-10}$	$1,2\cdot10^{-9}$	$6,3\cdot10^{-8}$	$6,3\cdot10^{-7}$	$1,5\cdot10^{-6}$	$3,8\cdot10^{-6}$	$9,5\cdot10^{-5}$	$4,9\cdot10^{-4}$	200—900 >900	0,8 4,0	−2,5 18,0
1603	Garnet-15, pyroxene-20, amphibole-60-65	$7,9\cdot10^{-11}$	$2,2\cdot10^{-10}$	$1,2\cdot10^{-9}$	$8,6\cdot10^{-8}$	$2,8\cdot10^{-7}$	$1,1\cdot10^{-7}$	$3,0\cdot10^{-7}$	$2,0\cdot10^{-6}$	$8,6\cdot10^{-5}$	200—800 800—900 >900	0,83 Anomaly 4,0	−2,7 11,5
1597	Garnet- 55-60, pyroxene-30, muscovite - 3	$9,9\cdot10^{-22}$	$1,8\cdot10^{-10}$	$4,4\cdot10^{-9}$	$5,4\cdot10^{-8}$	$2,2\cdot10^{-7}$	$7,4\cdot10^{-6}$	$5,2\cdot10^{-6}$	$4,9\cdot10^{-6}$	$2,0\cdot10^{-5}$	100—300 300—900 900—1050	0,15 1,06 1,2	−10,5 −1,9 0,5

(Appendix 12 is continued on the following page.)

APPENDIX 12. Electrical conductivity σ, activation energy E_0 and preexponential coefficient σ_0 in eclogites at high temperatures. (Continued)

Rock	Mineral composition %	σ (ohm^{-1}·cm^{-1}) at t, °C									Temperature range t, °C	E_0, eV	$\lg \sigma_0$, ohm^{-1}·cm^{-1}
		200	300	400	500	600	700	800	900	1000			
	3rd Group												
1591	Garnet-50, chlorite-45, muscovite, quartz - 5	$7,6\cdot10^{-10}$	$1,1\cdot10^{-8}$	$7,8\cdot10^{-8}$	$2,7\cdot10^{-7}$	$8,7\cdot10^{-7}$	$1,9\cdot10^{-6}$	$1,5\cdot10^{-5}$	$1,9\cdot10^{-5}$	$6,7\cdot10^{-5}$	200—700 700—900 >950	0,87 0,5 2,0	—3,5 —4,9 8,4
5588	Garnet-24 (almandine), horblende-46, epidote-12, sphene-4, quartz-12, muscovite -0.7	$3,1\cdot10^{-10}$	$4,5\cdot10^{-9}$	$4,4\cdot10^{-8}$	$3,3\cdot10^{-7}$	$9,1\cdot10^{-7}$	$2,9\cdot10^{-6}$	$1,1\cdot10^{-5}$	$1,6\cdot10^{-5}$	$1,7\cdot10^{-4}$	150—550 550—900 900—1000 >1000	0,71 0,9 1,0 Melting	—3,8 1,1 1,0
	Kazakhstan												
KKK-674	Pyrope-60, titanium-olivine-25, serpentine-10, spinel-2-3, ore mineral-1-2	$9,8\cdot10^{-11}$	$2,0\cdot10^{-9}$	$5,7\cdot10^{-8}$	10^{-7}	$4,1\cdot10^{-7}$	$1,2\cdot10^{-6}$	$5,7\cdot10^{-6}$	$1,1\cdot10^{-5}$	$5,5\cdot10^{-5}$	200—825 825—1100	0,75 1,71	—2,0 2,2
KTC-672	Garnet-34, pyroxene-30, fluorite, muscovite -25, zoisite	10^{-9}	$1,2\cdot10^{-8}$	10^{-7}	$5,6\cdot10^{-7}$	$2,1\cdot10^{-6}$	10^{-5}	$2,4\cdot10^{-5}$	$2,5\cdot10^{-5}$	$1,2\cdot10^{-5}$	150—500 500—950 950—1000	0,62 Anomaly 4,2	—1,2 15,0
671	Garnet-15, plageoclase -50, glaucophane-30, quartz-5	10^{-10}	$3,6\cdot10^{-9}$	$2,1\cdot10^{-8}$	$2,1\cdot10^{-7}$	$1,2\cdot10^{-6}$	$6,4\cdot10^{-7}$	$6,4\cdot10^{-7}$	10^{-5}	10^{-4}	150—700 700—900 900—1150	0,7 Anomaly 3,6	0,2 14,0
9152	Garnet-15, omphacite-30, hornblende-15, quartz-5	$1,7\cdot10^{-8}$	$7,1\cdot10^{-8}$	$5,3\cdot10^{-7}$	$1,4\cdot10^{-6}$	$2,8\cdot10^{-6}$	$7,7\cdot10^{-6}$	$2,8\cdot10^{-5}$	$2,9\cdot10^{-5}$	$2,1\cdot10^{-4}$	150—700 700—1000	0,52 1,3	—3,5 1,4

Remarks. The rocks of the 1st, 2nd and 3rd group were made available by V.I. Lennykh and the measurements were made by S. M. Kireyenko. The eclogites of Kazakhstan were made available by B.G. Lutz, A. P. Akimov and A. K. Kurskeyev.

[Commas in tabulated material are equivalent to decimal points.]

APPENDIX 13. Electrical conductivity σ, activation energy E_0 and preexponential coefficient σ_0 in alkaline rocks at high temperatures.

Rock, origin	Mineral composition %	σ (ohm^{-1}.cm^{-1}) at t, °C										Temperature range t, °C	E_0, eV	lg σ_0, ohm^{-1}.cm^{-1}
		200	300	400	500	600	700	800	900	1000	1100			
Lovozero Formation														
Urtite 1475	Nepheline-79, potassium & sodium containing feldspar-7, ferrous-41	$3,2\cdot10^{-9}$	$2,0\cdot10^{-8}$	$8,0\cdot10^{-7}$	$1,6\cdot10^{-7}$	$6,4\cdot10^{-7}$	$3,5\cdot10^{-6}$	$1,3\cdot10^{-6}$	$1,8\cdot10^{-5}$	$1,6\cdot10^{-4}$	$2,0\cdot10^{-3}$	20—400	0,56	—3,9
												400—525	Anomaly	
												525—800	0,58	—3,55
												800—1100	1,0	1,7
Trachetoidal loevrite 1438, along trachetoidal fissure	Nepheline-24, potassium & sodium containing feldspar & albite-35, ferrous-41	8 5 10^{-8}	$1,5\cdot10^{-6}$	$1,2\cdot10^{-6}$	$3,2\cdot10^{-6}$	$8,0\cdot10^{-6}$	$1,5\cdot10^{-5}$	$2,0\cdot10^{-5}$	$6,3\cdot10^{-5}$	$1,8\cdot10^{-4}$	—	350—550	0,25	—4,21
												550—850	0,42	—3,45
												850—1100	1,3	1,7
Trachetoidal loevrite 1438, perpendicular to the trachetoidal fissure	-	$1,5\cdot10^{-8}$	$4,6\cdot10^{-7}$	$4,3\cdot10^{-7}$	$1,5\cdot10^{-6}$	$3,2\cdot10^{-6}$	$5,4\cdot10^{-6}$	$1,1\cdot10^{-5}$	$3,8\cdot10^{-5}$	$1,1\cdot10^{-4}$	—	20—450	0,4	—4,9
												450—900	0,42	—3,15
												900—1100	1,3	1,2
Uvite 1464	Nepheline-36, sodium & potassium containing feldspar-51, ferrous-13	$1,3\cdot10^{-7}$	$6,1\cdot10^{-7}$	$1,4\cdot10^{-6}$	$5,8\cdot10^{-6}$	$3,1\cdot10^{-5}$	$1,8\cdot10^{-5}$	$6,7\cdot10^{-5}$	$1,8\cdot10^{-4}$	$8,6\cdot10^{-4}$	—	20—750	0,66	—1,6
												750—900	Anomaly	
												900—1100	2,88	6,5
Foyaite 1441	Nepheline-36, Sodium & potassium-containing feldspar & albite -67 ferrous - 9	$4,3\cdot10^{-9}$	$4,5\cdot10^{-8}$	$1,3\cdot10^{-7}$	$2,4\cdot10^{-7}$	$9,5\cdot10^{-7}$	$3,3\cdot10^{-6}$	$7,3\cdot10^{-6}$	$2,6\cdot10^{-5}$	$1,3\cdot10^{-4}$	$1,3\cdot10^{-3}$	20—600	0,56	—4,6
												600—900	0,74	—2,2
												900—1100	3,46	9,45

(Appendix 13 is continued on the following page.)

APPENDIX 13. (continued)

Rock. origin	Mineral composition %	σ(ohm^{-1}·cm^{-1}) at t, °C										Temperature range t, °C	E_0, eV	lg σ_0 ohm^{-1}·cm^{-1}
		200	300	400	500	600	700	800	900	1000	1100			
Nepheline syenite 1456	Sodium & potassium-containing feldsper, nepheline, albite, amphibole, eudalite, sphene	$5,7\cdot10^{-9}$	$7,3\cdot10^{-8}$	$2,2\cdot10^{-7}$	$6,4\cdot10^{-7}$	$4,1\cdot10^{-6}$	$4,0\cdot10^{-6}$	$1,9\cdot10^{-5}$	$5,1\cdot10^{-5}$	$5,3\cdot10^{-4}$		20—750 750—1100	0,5 1,83	—3,15 3,5
Khibin Alkaline (basic) Formation														
Trachetoidal iolite 610	Nepheline-66, feldspar-8, eugarine-18, lepidomelane-2, sphene-6	$2,8\cdot10^{-9}$	$2,3\cdot10^{-8}$	$1,0\cdot10^{-7}$	$2,5\cdot10^{-7}$	$7,0\cdot10^{-7}$	$6,5\cdot10^{-6}$	$9,8\cdot10^{-6}$	$8,6\cdot10^{-5}$	—	—	20—730 730—900	0,5 1,7	—4,0 0,8
Eugarine-nepheline rock 739	Eugarine-80-90, nepheline-10-20	$1,5\cdot10^{-8}$	$3,7\cdot10^{-8}$	$1,84\cdot10^{-7}$	$4,1\cdot10^{-7}$	$9,5\cdot10^{-7}$	$5,0\cdot10^{-6}$	$1,1\cdot10^{-4}$	$2,3\cdot10^{-3}$	$3,3\cdot10^{-3}$	—	20—500 500—1100	0,4 1,1	—4,0 4,0
Rischorrite 710	Nepheline-45, feldspar-40, eugarene-10, astrophyllite &lamprophyllite - 5	$5,6\cdot10^{-11}$	$5,6\cdot10^{-10}$	$2,4\cdot10^{-9}$	$1,2\cdot10^{-8}$	$3,2\cdot10^{-8}$	10^{-7}	$1,8\cdot10^{-7}$	$4,1\cdot10^{-7}$	$8,8\cdot10^{-6}$	10^{-4}	200—800 800—1100	0,6 2,7	—4,0 4,9
Urtites (intermediate grain)	Nepheline -80, feldspar-10, eugarine-6, sphene-4	10^{-9}	$3,2\cdot10^{-8}$	$1,6\cdot10^{-7}$	$1,2\cdot10^{-6}$	$2,2\cdot10^{-6}$	$8,2\cdot10^{-6}$	$4,2\cdot10^{-5}$	$9,4\cdot10^{-4}$	$3,8\cdot10^{-3}$	—	200—700 700—1000	0,74 1,2	—2,3 1,2
Synnyr Potassium Formation														
Pseudoleucite syenite 8957	Pseudoleucite-80, orthoclase-15, pyroxene-2 biotite-3	10^{-11}	$6,4\cdot10^{-10}$	$6,4\cdot10^{-9}$	10^{-7}	$4,1\cdot10^{-7}$	$1,2\cdot10^{-6}$	$4,1\cdot10^{-6}$	$6,4\cdot10^{-6}$	$3,2\cdot10^{-5}$	10^{-4}	200—850	0,86	—2,3
Biotite-cimalactite syenite 8996	Calcspar-80-90, biotite-3-8, alkaline hornblende -1-3	$2,4\cdot10^{-10}$	$8,1\cdot10^{-9}$	$8,1\cdot10^{-8}$	$3,2\cdot10^{-7}$	$1,2\cdot10^{-6}$	$2,6\cdot10^{-6}$	10^{-5}	10^{-4}	$4,1\cdot10^{-4}$	$6,1\cdot10^{-4}$	200—900 900—1100	0,68 2,8	—3,7 5,6
Pyroxene biotite 8771	Feldspar-65, biotite-1-5, pyroxene-diopside-10-15	$4,1\cdot10^{-11}$	$2,6\cdot10^{-9}$	$3,2\cdot10^{-8}$	$1,2\cdot10^{-7}$	$4,1\cdot10^{-7}$	$1,2\cdot10^{-6}$	$8,1\cdot10^{-6}$	$1,6\cdot10^{-5}$	$4,1\cdot10^{-5}$	$1,4\cdot10^{-4}$	200—800 800—1100	0,84 2,0	—3,3 3,3

Remark. The samples of rocks from Synnyr formation were made available by L. V. Filippov.

[Commas in tabulated material are equivalent to decimal points.]

APPENDIX 14. Electrical conductivity σ, activation energy E_0 and the preexponential coefficient σ_0 in gneiss and amphibolites at high temperatures.

Rock	Mineral composition %	σ(ohm^{-1}·cm^{-1}) at t, °C: 100	300	400	500	600	700	800	900	1000	Temperature range t, °C	E_0, eV	lg σ_0, ohm^{-1}·cm^{-1}
Plageoclase gneiss-biotite 2792	Plageoclase-76, biotite-22, anatite, sphene-2	1,1·10^{-8}	1,5·10^{-7}	3,1·10^{-7}	3,8·10^{-6}	1,0·10^{-5}	5,5·10^{-6}	4,5·10^{-6}	1,2·10^{-5}	7,7·10^{-5}	200—500 500—850 850—1050	0,66 Anomaly 2,2	−2,5 4,8
Plageogneiss 2575	Oligoclase-40-50, microcline-5-10, quartz-20-30, mica-10-15	2,2·10^{-9}	1,0·10^{-8}	2,9·10^{-8}	1,1·10^{-7}	1,2·10^{-7}	7,7·10^{-7}	1,2·10^{-6}	3,2·10^{-6}	3,4·10^{-5}	200—480 480—920 920—1050	0,5 Anomaly 2,9	−5,6 7,5
Garnet gneiss 2578	Plageoclase-25-30, microcline-10-15, almandine-10-12, quartz-40-50	3,4·10^{-10}	1,2·10^{-9}	1,2·10^{-8}	9,4·10^{-8}	2,9·10^{-7}	7,7·10^{-7}	1,1·10^{-6}	3,1·10^{-6}	3,5·10^{-5}	200—320 320—900 900—1050	0,3 0,74 3,0	−6,6 −3,6 7,25
Biotite gneiss 2565	Oligoclase-48, quartz-45, biotite, muscovite-5	6,9·10^{-11}	1,2·10^{-10}	8,0·10^{-10}	6,1·10^{-9}	3,1·10^{-8}	6,6·10^{-8}	2,0·10^{-7}	9,9·10^{-7}	9,9·10^{-6}	200—320 320—850 850—1050	0,2 0,74 2,5	−9,7 −3,4 5,25
Granite gneiss 2581	Potassium-containing feldspar-30-40, quartz-30-35, biotite, muscovite-5-10	6,2·10^{-11}	8,2·10^{-11}	1,1·10^{-9}	9,0·10^{-9}	1,5·10^{-8}	5,9·10^{-8}	8,3·10^{-8}	2,2·10^{-7}	1,9·10^{-6}	200—850 850—1050	0,86 2,46	−4,6 3,5
Granite gneiss 2796	Plageoclase-47, quartz-40, microcline-6, biotite-3	5,8·10^{-12}	8,3·10^{-10}	4,2·10^{-9}	1,6·10^{-8}	3,3·10^{-8}	1,2·10^{-7}	3,4·10^{-7}	9,9·10^{-7}	9,3·10^{-6}	200—600 600—950 950—1050	0,58 1,0 3,2	−8,8 −1,75 7,5
Plageogneiss with chlorite & biotite 865	—	7,0·10^{-12}	2,7·10^{-10}	1,9·10^{-9}	1,6·10^{-8}	9,1·10^{-8}	7,0·10^{-7}	9,1·10^{-7}	2,7·10^{-6}	1,2·10^{-5}	200—700 700—850 850—1000	0,92 Anomaly 1,86	−2,7 1,4
Amphibolite 861	—	1,1·10^{-8}	7,1·10^{-8}	4,7·10^{-7}	2,0·10^{-6}	1,2·10^{-5}	4,0·10^{-5}	1,1·10^{-4}	3,5·10^{-4}	6,2·10^{-4}	200—500 500—1000	0,81 0,97	−1,6 0,65
Chloride-containing amphibolite rock 2490	—	2,2·10^{-8}	—	3,0·10^{-8}	4,3·10^{-8}	4,3·10^{-8}	3,2·10^{-7}	1,4·10^{-6}	2,9·10^{-6}	9,0·10^{-6}	250—450 500—550 550—900 900—1050	0,6 Anomaly 1,25 1,3	−3,2 −1,3 0,9
Amphibolite 2034	—		2,0·10^{-8}	2,0·10^{-7}	1,4·10^{-6}	2,5·10^{-6}	8,3·10^{-6}	1,3·10^{-5}	3,1·10^{-5}	5,0·10^{-5}	300—500 500—550 550—1000	0,8 Anomaly 0,7	−1,25 2,5

[Commas in tabulated material are equivalent to decimal points.]

REFERENCES /266

1. Volarovich, M.P., Issledovaniye fizicheskikh svoystv gornykh porod pri vysokikh davleniyakh i temperaturakh [Study of Physical Properties of Rocks at High Pressures and Temperatures], Geophysical Digest, excerpt 9 (No.11), 3, Kiev, 1964.

2. Volarovich, M.P., "Geophysical aspect of the problem of elastic and electrical properties of rocks at pressures up to tens of kilobars," Geophys. Mongr.,No.12,"The crust and upper mantle of the Pacific area," 1968, p. 517

3. Tikhonov, A.N., "Determination of electrical properties of the deep layers within the Earth's crust," Proceedings of the Academy of Sciences of the USSR, 3, No. 2 (1950).

4. Van'yan, L.L. Osnovy elektromagnitnykh zondirovaniy [Fundamentals of Electromagnetic Probing], Nedra Press, 1965.

5. Berdichevskiy, M.N., Elektricheskaya razvedka metodom magnitno-tellurichеskogo profilirovaniya [Electrical Probing by the Magnetotelluric Method of Investigation], Nedra Press, 1968.

6. Tikhonov, A.N., N.V. Lipskaya, N.A. Deniskin and N.N. Nikiforova, "Future trends in the in-depth magnetotelluric probing. From the digest Electromagnetic Probing and the Magnetotelluric Methods of Probing," Publication of the Leningrad State University, Leningrad, 1963, pp. 132-139.

7. Dmitriyev, V.I., Metod rascheta magnitno-tellurichеskogo polya v neodnorodnom sloye s proizvol'nym izgibom nizhney poverkhnosti [Field Calculation by the Magnetotelluric Method Within the Inhomogeneous Layer with an Arbitrarily-Flexed Bottom Surface], Applied Geophysics, excerpt 41, 1965.

8. Rotanova, N.M., "Interior structure of the Earth on the basis of magnetic data," Publication of the Institute of Terrestrial Magnetism, the Ionosphere and Radiowave Propagation, Academy of Sciences of the USSR, Vol. 4, no. 18, (1966).

9. Enenshteyn, B.S., E.L. Krul', N.V. Lipskaya, O. A. Skugarevskaya and M.A. Ivanov, "Experience of joint studies by the methods of frequency and magnetotelluric probings," from the digest "Magnetotelluric methods in the investigation of the structure of the Earth's crust and of the upper mantle," No. 4, Publication of the Nedra Press, 1969.

10. Sadovskiy, M.A., "Essential problems of geophysicists within the complex of sciences about the Earth," Vestn. AN SSSR, No.1, (1968)

11. Lubimova, E.A., Termika Zemli i Luny [Thermal State of the Earth and of the Moon], Nauka Press, 1968.

12. Magnitskiy, V.A., Vnutrenneye stroeniye i fizika Zemli [Interior Structure and Physics of the Earth], Nedra Press, 1965.

13. Zharkov, V.N. and V.A. Kalinin, Uravneniya sostoyaniya tverdykh tel pri vysokikh davleniyakh i temperaturakh [Equations of the State of Solid Bodies at High Pressures and Temperatures], Nauka Press, 1968.

14. Bogoroditskiy, N.L., Yu. M. Volokobinskiy, A.A. Vorob'ev and B.M. Tareyev, [Teoriya dielektrikov] Theory of Dielectrics, Energy Press, 1965.

15. Poluprovodniki v nauke i tekhnike [Semiconductors in Science and Technology], Part 1, Edited by A.F. Ioffe, Academy of Sciences of the USSR, 1957.

16. Lidyard, A., Ionic Conductivity in Crystals, Foreign Literature Press, 1962.

17. Skanavi, G. I., Fizika dielektrikov (oblast' slabykh poley) [Physics of Dielectrics (Weak Field Region)], State Technical and Theoretical Press (Gostekhteoretizdat), 1949.

18. Panchenko, V.V., "Temperature dependence of dielectric penetrability in ionic crystals," FTT (Solid State Physics), vol. 6, excerpt 2 (1964). /267

19. Parkhomenko, E.I., Elektricheskiye svoystva gornykh porod [Electrical Properties of Rocks], Nauka Press, 1965.

20. Volarovich, M.P., "Study of physical properties of rocks at high pressures and temperatures," Institute of the Physics of the Earth, Academy of Sciences of the USSR, No. 37 (204) (1966).

21. Volarovich, M.P., E.I. Bayuk and K.A. Valeyev, "Simultaneous measurement of the speeds of elastic waves and of the electrical resistivity in the three-phase systems - the sedimentary rocks at pressures of up to 3000 kg/cm^2," Kolloid. Zh. 28, No. 4 (1966).

22. Cherenpanov, A.M. and S.T. Tresvyatskiy, Vysokoogneupornyye materialy i izdeliya iz okislov [High Heat Resistance Materials and Manufactured Products, Made of Oxides], Metallurgiya Press, 1964.

23. Oreshkin, Ya. T. and G. Ya. Rudas, "The questions of thermal aging of oxides," Presentation at the VI Scientific Conference of Novokuznetsk Pedagogic Institute of Physcal and Mathematical Sciences, Novokuznetsk, 1963.

24. Lempicki, A., "The electrical conductivity of MgO single crystals at high temperatures," Proc. Phys. Soc. B, 66, N400B, 4 (1953).

25. Mansfield, R., "The electrical conductivity and thermoelectric of magnesium oxide," Proc. Phys. Soc. B, 66, N403B, 7 (1953).

26. Yamaka, E. and K. Sawamoto, "Electrical conductivity of magnesium oxide of single crystals," Phys. Rev.91/4, 882 (1953).

27. Day, H.R., "Irradiation-induced photoconducivity in magnesium oxide," Phys. Rev. 91/4, 882 (1953).

28. Hauffe, K. and G. Tränckler, "Calcium oxide, the amphoteric semiconductor," Z. Phys. 136, File 2, 166 (1953).

29. Pal'guyev, S.F. and A.D. Neuymin, "On the nature of electrical conductivity in oxides of beryllium, magnesium, calcium and strontium at high temperatures," FTT [Solid State Physics] 4/4 (1962)

30. Sitidze, Yu. and Kh. Sato, Ferrity [Ferrites], Mir Press, 1964.

31. Sirota, N.N. and E.Z. Kantsel'son, "The electrical conductivity in nickel-magnesium-zinc ferrites and the related temperature dependence," from the digest Ferrity [Ferrits], Publication of the Byelorussian Academy of Sciences of the USSR, 1960.

32. Belov, K.P. et al., Redkozemel'nyye ferro i antiferromagnetiki [Rare Earth Ferro and Antiferromagnetic Materials], Nauka Press, 1965.

33. Tyrov, E.A. and Yu.I. Irkhin, "Phenomenological theory of electrical conductivity in ferrites and in antiferromagnetic materials," from the digest Ferrity [Ferrites], Publication of Byelorussian Academy of Sciences of the USSR, 1960.

34. Gardner, E.A., F. Sweett and D.W. Tanner, "The electrical properties of alpha ferric oxide I-II," J.Phys. Chem. Solids 24/10 (1963).

35. Morin, F.J., "Electrical properties of α Fe_2O_3 containing titanium," Phys. Rev. 83, 1005 (1951).

36. Poluprovodniki [Semiconductors], edited by N. B. Khepeney , Foreign Literature Press, 1962.

37. Zheludev, I.S., Fizika kristallicheskikh dielektrikov [Physics of Crystalline Dielectrics], Nauka Press, 1968.

38. Kerkhoff, F., "Transfer numbers in KCl crystal," Z. Phys. 130, File 4 (1951).

39. Vorob'ev, A.A., Fizicheskiye svoystva ionnykh kristallicheskikh dielektrikov [Physical Properties of the Ionic Crystalline Dielectrics], Book 1, Publication of Tomsk University, Tomsk, 1960.

40. Betekhtin, A.G., Kurs mineralogii [Course in Mineralogy], State Geological Technical Press (Gosgeoltekhizdat), 1961.

41. Oreshkin, I.T., Elektroprovodnost' ogneuporov [Electrical Conductivity in the Heat-resistant Materials], Metallurgiya Press, 1965.

42. Bradley, R.S., A.K. Jamil and D.C. Munro, "Electrical conductivity of fajalite and shpinel," Nature 193, 965 (1962). /268

43. Bradley, R.S., A.K. Jamil and D.C. Munro, "The electrical conductivity of olivine at high temperatures and pressures," Geochim. et cosmochim. acta, 28/11, 1669-1678 (1964).

44. Noritomi, K., "The electrical conducivity of rock and the determination of the electrical conductivity of the earth's interior," J. Mining Coll. Akita Univ. Ser. A, 1/1 (1961).

45. Ovchinnikov, L.N., A.S. Shur and N.T. Elkina, "Thermoanalytical study of amphibolites from some scarry zones in the Ural mountains," Proceedings of the First Conference on Thermography, Kazan', 1953.

46. Parkhomenko, E.I., A.A. Berezutskaya and B.M. Urazayev, "Electrical conductivity of the Kazakhstan rock at high temperatures," Proceedings of the Institute of Physics of the Earth, Academy of Sciences of the USSR, No. 37 (204), 1966.

47. Golovin, A.A., "Thermal expansion of nepheline," Geologiya i geofiz., 12 (1965).

48. Dmitriyev, A.P., et al., Fizicheskiye svoystva gornykh porod pri vysokikh temperaturakh [Physical Properties of Rocks at High Temperatures], Nedra Press, 1969.

49. Spravochnik fizicheskikh konstant gornykh porod [Manual of Physical Constants of Rocks], edited by S. Clark, Mir Press, 1969.

50. Sobolev, V.S., Vvedeniye v mineralogiyu silikatov [Introduction to the Mineralogy of Silicates], Publication of the L'vov State University, 1949.

51. Galdin, N.E., "Physical properties of oxides and silicates at high presures and temperatures," Geokhimiya, 2,(1970).

52. Galdin, N.E., "Density and elastic parameters of oxides and silicates at high presures," Geokhimiya, 1,(1969).

53. Belikov, B.P., K.S. Aleksandrov and T.V. Ryzhova, Uprugiye svoystva porodoobrazuyushchikh mineralov i gornykh porod [Elastic Properties of the Rock-Forming Minerals and of the Rocks], Nauka Press, 1969.

54. Volarovich, M.P., A.K. Kurskeyev, I.S. Tomashevskaya and B.M. Urazayev, "Speeds of longitudinal waves in the samples of intrusive rocks of Central Kazakhstan, exposed to the all-around high presures," Institute of Physics of the Earth, Academy of Sciences, USSR, No. 37, (204) 1966.

55. Urazayev, B.M., E.I. Parkhomenko, A.K. Kurskeyev and A.P. Dauylbayev, "Experimental study of electrical properties of the rocks in Kazakhstan at high pressures and temperatures," from the digest Fizicheskiye svoystva gornykh porod pri vysokikh termodinamicheskikh parametrakh [Physical Properties of Rocks in the Presence of High Therodynamic Parameters], Naukova Dumka Press, 1971.

56. Zavaritskiy, A.N., Izverzhennye gornye porody [Igneous Rocks], Publication of the Academy of Sciences of the USSR, 1956.

57. Stewells, D., Elektricheskiye svoystva stekla [Electrical Properties of Glass], Foreign Literature Press, 1961.

58. Bondarenko, A.T and I.S. Fel'dman, "High temperature electrical conductivity in olivines and the geoelectrical model of the upper mantle," from digest Fizicheskiye svoystva gornykh porod pri vysokikh termodinamicheskikh parametrakh [Physical Properties of Rocks in the Presence of High Thermodynamic Parameters], Naukova Dumka Press, 1971.

59. Eitel, V., Fizicheskaya khimiya silikatov [Physical Chemistry of Silicates], Foreign Literature Press, 1962.

60. Zakirova, F.S., "Change of specific conductance in minerals and rocks as a function of age," Dokl. AN SSSR 154/6 (1964).

61. Vorob'yev, A.A., E.K. Zavadovskaya and A. V. Kuz'mina, Zapasnaya energiya v shchelochnogaloidnykh soedineniyakh [Stored Energy in the Alkaline Haloid Compounds], Tomsk University, 1969.

62. Lomidze, M.G. and V.V. Ploshko, "New findings of serpentinites in the Soviet Carpathian Mountains," Sov. geologiya, 7, (1969).

63. Lur'ye, M.L. and V.L. Masaytis, "Fundamentals of geology and petrology in the trap formation of Siberian platform," from the digest Bazal'ty plato [Basalts of the Plateau], Nauka Press, 1964.

64. Lebedev, A.P., "Comparison of trap magnetism in Siberian platform and in some other areas of the world," from the digest Bazal'ty plato [Basalts of the Plateau], Nauka Press, 1964. /269

65. Masaytis, V.L., Magmaticheskiye trappovye intruzii severa Sibirskoy platformy [Magmatic Trap Intrusions in the Northern Siberian Platform], Nauka Press, 1967.

66. Vilenskiy, A.M., Petrologiya intruzivnykh trappov severa Sibirskoy platformy [Petrology of Intrusive Traps in the Northern Siberian Platform], Nauka Press, 1967.

67. Kuznetsov, A.A., et al., "Utilization of thermography in the study of traps, in the North-western Siberian platform," Dokl. AN SSSR 163/2 (1965).

68. Mazurin, O.V., Elektricheskiye svoystva stekol [Electrical Properties of Glasses], Goskhimizdat Press, Leningrad, 1962.

69. Sobolev, N.V., "Xenoliths of eclogites from kimberlite tunneled protrusions as the fragments of the material in the upper mantle. The crust and upper mantle," Presentations of the Soviet Geologists at the 23rd Congress of Geology, Nauka Press, 1968.

70. Sobolev, V.S., "Physical and chemical conditions of mineral formation in the Earth's crust and in the mantle," Geologiya i geofiz., No. 1 (1964).

71. Sobolev, N.V. and N.V. Lodochnikova, "Mineralogy of garnet peridotites," Geologiya i geofiz., No. 6 (1962).

72. Sobolev, V.S. and N.V. Sobolev, "Xenoliths in kimberlites of the northern Yakutiya and the questions of the Earth's mantle structure," Dokl. AN SSSR 158/1 (1964).

73. Sobolev, N.V., "Xenolith of eclogite with ruby, Dokl. An SSSR 157/6 (1966).

74. Sobolev, N.V. and I.K. Kuznetsova, "Some new data on mineralogy of eclogites from kimberlite tunneled protrusions in Yakutiya," Dokl. AN SSSR 163/2 (1965).

75. Sobolev, N.V. and I.K. Kuznetsova, "Mineralogy of diamond-containing eclogites," Dokl. AN SSSR 167/6 (1966).

76. Bobriyevich, A.P., I.P. Ilupin, A.A. Ponkratov and G. I. Smirnov, "Some new data on petrography and mineralogy of kimberlites from Yakutiya," from the digest Bazal'ty plato [Basalts of the Plateau], Nauka Press, 1964.

77. Bobriyevich, A.P., "Learning of the basic composition of the ultrabasic layer in the Earth on the basis of study of inclusions of pyrope-containing ultrabasic rocks in kimberlites," Geologiya i geofiz. No. 3 (1965).

78. Bobriyevich, A.P., M.N. Bondarenko and M.A. Gnevushev, et al., Almaznye mestorozhdeniya Yakutii [Diamond Deposits in Yakutiya], Gosgeoltekhizdat Press, 1959.

79. Bobriyevich, A.P., et al., Petrografiya i mineralogiya kimberlitovykh porod Yakutii [Petrography and Mineralogy of Kimberlite Rocks in Yakutiya], Nedra Press, 1964.

80. Frantsenson, E.F., "Composition and structure of kimberlite tunneled exrusion 'Mir'," Yakut Siberian Branch of the Academy of Sciences of the USSR, excerpt 8, 1962.

81. Frantsenson, E.F., Petrologiya kimberlitov [Petrology of Kimberlites], Nedra Press, 1968.

82. Ilupin, I.P., "The question of the relationship between the chemical and mineral composition of kimberlites," Moscow Institute of Geological Exploration, No. 39, 1963.

83. Koval'skiy, V.V., Kimberlitovye porody Yakutii [Kimberlite Rocks of Yakutiya], Publication of the Academy of Sciences of the USSR, 1963.

84. Leont'ev, L.N. and A.A. Kadenskiy, "The nature of kimberlite tunneled extrusion of Yakutiya," Dokl. AN SSSR 115/2 (1957).

85. Koval'skiy, V.V. and K.N. Nikishov, "Some questions of the genesis of xenoliths in kimberlites," from the digest Ksenolity i gomogennye vkliucheniya [Xenoliths and Homogeneous Inclusions], Nauka Press, 1969.

86. Sobolev, V.S., et al., "Xenoliths of diamond-rich pyrope serpentines from the tunneled extrusion Aykhal in Yakutiya," Dokl. AN SSSR 188/5 (1969).

87. Bondarenko, A.T. and D.I. Savrasov, "Electrical conductivity of eclogites and kimberlites in the tunneled extrusions of Yakutiya at high temperatures, in conjunction with the questions of the upper mantle structure," Geologiya i geofiz. No. 5 (1969). /270

88. Bondarenko, A.T., "Some general data on the electrical properties of magmatic rocks and the relationship between the electrical conductivity and the structure of the Earth," Geofizicheskiy sbornik [Geophysical Digest], No. 37, Naukova Dumka Press, Kiev, 1970.

89. Bondarenko, A.T., "Some general data on electrical conductivity of igneous rocks at high temperatures, in conjunction with the structure of the Earth's crust and of the upper mantle," Dokl, AN SSSR, 178/5 (1968).

90. Bondarenko, A.T., "Electrical conductivity of igneous rocks on the Kola peninsula at high temperatures," Institute of the Physics of the Earth, Academy of Sciences of the USSR, No. 37 (204), 1966.

91. Volarovich, M.P., E.I. Parkhomenko and A.T. Bondarenko, "Study of the electrical resistivity in the basic, ultrabasic and alkaline rocks and minerals at high pressures and temperatures," Institute of Physics of the Earth, Academy of Sciences of the USSR, No. 37 (204), 1966.

92. Moiseyenko, U.I., L.S. Sokolova and V.E. Istomin, Elektricheskie i teplovye svoystva gornykh porod [Electrical and Thermal Properties of Rocks], Nauka Press, 1970.

93. Bondarenko, A.T., A.I. Levykin and G.T. Prodayvoda, "Study of electrical and elastic properties of basalts at high pressures and temperatures in conjunction with the specifics of their structural and tectonic position," from digest Fizicheskiye svoystva gornykh porod pri vysokikh termodinamicheskikh parametrakh [Physical Properties of Rocks in the Presence of High Thermodynamic Parameters], Naukova Dumka Press, 1971.

94. Kutolin, V.A., "The question of composition of the upper mantle in conjunction with the study of the ultrabasic inclusions in basalts," Dokl. AN SSSR 194/2 (1970).

95. Vorob'yev, A.A., Fizicheskie svoystva ionnykh kristallicheskikh dielektrikov [Physical Properties of the Ionic Crystalline Dielectrics], Book 2, Tomsk University, 1961.

96. Deer, W.A., R.A. Haun and G. Süssman, Porodoobrazuyushchie mineraly [Rock-Forming Minerals], Mir Press, 1965.

97. Bowen, N.L. and I.F. Schairer, "The system MgO-FeO-SiO_2," Amer. Sci., ser. 5, 229 (1935).

98. Atlas, L., "The polymorphism of $MgSiO_3$ and solid state equilibria in the system $MgSiO_3$-$CaMgSi_2O_6$," J. Geol. 60, 125 (1952).

99. Belinskiy, V.V. and G.V. Pinus, "Cleavage in olivines and its pertrogenic importance," Geologiya i geofiz. No. 5, (1969).

100. Zharkov, V.N., "Thermodynamics of the Earth's exterior," Publication of the Academy of Sciences of the USSR, Geophysics Series, No. 9, 1959.

101. Coster, H.P., "The electrical conductivity of rocks at high temperatures," Monthly Notices Roy. Astron. Soc. Geophys. Suppl. 5, N 6 (1948).

102. Hughes, H., "The pressure effect on the electrical conductivity of peridotite," J. Geophys. Res. 60/2 (1955).

103. Hamilton, R.M., "Temperature variation at constant pressures of the electrical conductivity of periclase and olivine," J. Geophys. Res. 70/22 (1965).

104. Subbotin, S.I., G.L. Naumchik, I.Sh. Rakhimova, Mantiya Zemli i tektogenez [Mantle of the Earth and the Tectogenesis], Nauka Dumka Press, Kiev, 1968.

105. Rub, M.G. and B.L. Zalishchak, "Alkaline intrusive rocks in the Soviet maritime region," Publication of the Academy of Sciences of the USSR, Geology series, No. 10, 1964.

106. Hess, H.H., Serpentinizatsiya, orogenez i eneyrogenez [Serpentinization, orogenesis and eneurogenesis], from the digest Zemnaya kora [Earth's Crust], Foreign Literature Press, 1957.

107. Lablocki, C.J., "Electrical properties of serpentinite from Mayaquer, Puertorico. A study of serpentinite," National Academy of Sciences, National Research Council, N 1188, 1964. /271

108. Belov, K.I., A.A. Popova and E.V. Talalaeva, "Electrical and galvanic-magnetic properties of the manganous ferrite monocrystals," Kristallografiya 3, excerpt 6 (1958).

109. Belov, K.I., A.S. Pakhomov and E.V. Talalaeva, "Measurement of the galvanic-magnetic effect near the Curie temperature," Solid State Physics 3, excerpt 2 (1961).

110. Parkhomenko, E.I., Z. Dvorak and B. N. Belikov, "Effect of serpentinization on the electrical and elastic properties in rocks at high temperatures and pressures," Presentation at the Conference on the Physics of Rocks and Correlated Processes, Moscow, 1971.

111. Dvorak, Z. and E.I. Parkhomenko, "Temperature and frequency dependence of electric parameters of igneous rocks," Studia Geophys. et Geodaet. Roc. 15, N 1 (1971).

112. Dobretsov, N.L., "Genesis of hyperbasites," Geologiya i geofiz. No. 3 (1964).

113. Efimov, I.A., "Stratigraphy and metamorphic fractionation of Precambrian rocks in the Kokchetava mound," Kazakh SSR Academy of Sciences, Geology series, No. 1, 1968.

114. Rozen, O.M., "Hyperstene granulite in the Precambrian Kokchetava formation," Zap. Vses. mineral. obshchestva 95/5 (1966).

115. Volarovich, M.P., E.I. Parkhomenko and S.M. Kireyenkova, "Effect of the degree of metamorphism on the electrical and elastic parameters in eclogites of the South Ural mountains at high pressures and temperatures," Conference on the Physics of Rocks and Concurrent Processes, Moscow, 1971.

116. Vorob'yeva, O.A., "Problems of alkaline magnetism," from the digest Problemy magmy i genezisa isverzhennykh porod [Problems of Magma and the Genesis of Igneous Rocks], Publication of the Academy of Sciences of the USSR, 1963.

117. Sedetski-Kardosh, E., "Geochemistry of alkaline igneous rocks," from the digest Problemy geokhimii [Problems of Geochemistry], Nauka Press, 1965.

118. Shcherbina, V.V., "Differences in geochemical process, occurring with the participation of potassium and sodium," Geokhimiya, No. 3 (1963).

119. Galakhov, A.V., "Chemical composition of rocks in Khibin alkaline formation," Dokl. AN SSSR 171/5 (1966).

120. Gerasimovskiy, V.I., V.N. Volkov and L.N. Kocharka, et al., Geokhimiya Lovozero shchelochnogo massiva [Geochemistry of Lovozero Alkaline Formation], Nauka Press, 1966.

121. Galakhov, A.V., "Manifestation of the alkaline ultrabasic magmatism in Khibin tundra (Kola Peninsula)," Dokl. AN SSSR 170/3 (1966).

122. Zlobin, B.I., "Paragenesis of the dark colored minerals from alkaline rocks in conjunction with the new expression for the coefficient of agpaitic state," Geokhimiya, No. 5 (1969).

123. Moorehouse, W., Prakticheskaya petrografiya [Practical Petrography], Foreign Literature Press, 1963.

124. Volarovich, M.P. and A.T. Bondarenko, "Investigation of the frequency relationship in the electrical properties of igneous rocks on the Kola Peninsula," Proceedings of the Institute of the Physics of the Earth, Academy of Sciences of the USSR, No. 37 (204), 1966.

125. Galdin, N.E., "Effect of high pressure on the velocity of longitudinal waves in gneiss and crystalline shales of the north-western part of the Kola Peninsula," Proceedings of the Institute of the Physics of the Earth, Academy of Sciences of the USSR, No.37 (204), 1966.

126. Popov, A.A., "Interaction parameters of the feldspar and water in dynamic conditions. Experimental studies in the area of processes, occurring at great depth," Publication of the Academy of Sciences of the USSR, 1962.

127. Itsikson, G.V., Kristallokhimicheskoye fraktsionirovaniye kaliya i natriya v metamorficheskikh protsessakh i ego metallogeneticheskoye znacheniye. Regional'nyy metamorfizm i metamorfogennoye rudoobrazovaniye [Crystallochemical fractionation of potassium and sodium in the course of metamorphic processes and its metallogenic importance. Regional metamorphism and the metamorphic ore formation], Nauka Press, 1970.

128. Belov, I.V., "Expanded formula of beryl," Geokhimiya, No. 8 (1959). /272

129. Bondarenko, A.T., "Electrical properties of alkaline rocks within Khibin and Lovozero formations," Publication of the Academy of Sciences of the USSR, Physics of the Earth series, No. 4, 1972.

130. Parkhomenko, E.I. and Z. Dvorak, "Dependence of electrical parameters in the rocks as a function of temperature and frequency of electric field," Publication of the Academy of Sciences of the USSR, Physics of the Earth Series, No. 5, 1971.

131. Bridgman, P. W., Noveyshiye raboty v oblasti vysokikh davleniy [Newest Studies in the Area of High Pressures], Foreign Literature Press, 1948.

132. Lacam, A. and M. Lallemand, "Effect of pressure on the electrical conductivity of solids," J. Phys. 55/4 (1964).

133. Kurnick, S.W., "The effect of hydrostatic pressure on ionic conductivity of AgBr," J. CHem. Phys. 20, 218, (1952).

134. Zharkov, V.N., "Electrical conductivity and temperature of the Earth's crust and mantle," Publication of the Academy of Sciences of the USSR, Geophysics Series, No. 4, 1958.

135. Bardeen, J., "Pressure change of resistance of tellurium," Phys. Rev. 75/11 (1949).

136. Bardeen, J. and W. Shockley, "Deformation potentials and mobilities in nonpolar crystals," Phys. Rev. 80/1 (1950).

137. Nathan, M., W. Paul and H. Brooks, "Interband scattering in n-type germanium," Phys. Rev. 124/2 (1961).

138. Samara, G.A. and A.A. Giardini, "Compressibility and electrical conductivity of cadmium sulfate at high pressures," Phys. Rev. 140 (1A), 388 (1965).

139. Slutskiy, A.B., "Change of electrical conductivity in the course of polymorphous conversion, syenite-sillimanite (Al_2SiO_5) at high temperature and pressure," Dokl. AN SSSR 179/4 (1968).

140. Bridgman, P.W., "The effect of pressure on the electrical resistance of certain semiconductors," Proceedings of the American Academy of Arts and Sciences 81/169(1951).

141. Bridgman, P.W., "The electrical resistance of 72 elements and compounds up to 10,000 kg/cm^2," Proceedings of the American Academy of Arts and Sciences 81/16 (1952).

142. Bridgman, P.W., "Further measurements of the effect of pressure on the electrical resistance of germanium," Proc. Amer. Acad. Arts and Sci. 82/71 (1952).

C-4

143. Paul, W. and H. Brooks, "Pressure dependence of the resistivity of germanium," Phys. Rev. 94/5, 1128 (1954).

144. Paul, W. and G.L. Pearson, "Pressure for dependence of the resistivity of silicon," Phys. Rev. 98, N 1755 (1955).

145. Vereshchagin, L.F., A.A. Semerchan, S.V. Popova and N.N. Kuzin, "Change of electrical resistivity in semiconductors at the pressures of up to 300 kg/cm^2," Dokl. AN SSSR 145/4 (1962).

146. Ryabinin, Yu.N., L.D. Livshits and L.F. Vereshchagin, "Change of electrical conductivity in silicon at high pressure," Journal of Tech. Phys.23/7 (1958).

147. Vereshchagin, L.F., A.A.Semerchan, S.V. Popova, "Study of electrical conductivity in cerium, lanthanum and niobium at the pressures of up to 250,000 kg/cm^2," Dokl. AN SSSR 138/5 (1965).

148. Semerchan, A.A., N.N. Kuzin and L.F. Vereshchagin, "Temperature dependence of electrical resistivity in the polycrystalline graphite at the pressures of up to 250,000 kg/cm^2," Dokl. AN SSSR 146/4 (1962).

149. Jost, W. and C. Mennonoh, "The pressure dependence of ionic conductivity of silver halides," Z. phys. Chem. 196, 188 (1950).

150. Shapiro, I. and I.M. Koltoff, "Effect of pressure on the electrical conductivity of silver halides," J. Chem. Phys., 17, 1119 (1948).

151. Parkhomenko, E.J., Electrical properties of rocks, Plenum Press, New York, 1967. /273

152. Amimoto, S. and H. Fujisawa, "Demonstration of electrical conductivity jump produced by the olivine-shpinell transition," J. Geophys. Res.70/2 (1965).

153. Dobrynin, V.M., Fizicheskiye svoystva neftegazovykh kollektorov v glubokikh skvazhinakh [Physical Properties of the Oil and Gas Collectors in Deep, Drilled Holes], Nedra Press, 1965.

154. Marmorshteyn, L.M and I.M. Petukhov, "Study of electrical conductivity, porosity and penetrability of the rocks in the conditions similar to the formation environment," from digest Fiziko-mekhanicheskiye svoystva gornykh porod verkhney chasti Zemnoy kory [Physical and Mechanical Properties of the Rocks in the Upper Part of the Earth's Crust], Nauka Press, 1968.

155. Morozovich, L.R., "Change in the collecting properties of rocks as a function of all-around pressure environment," Proceedings of the Scientific and Technical Council on Deep Drilling and Probing, excerpt 4, Nedra Press, 1965.

156. Fett, I., "Effect of the rock and formation pressure on the porosity parameter. Questions of industrial geophysics," Translated from English by the State Topographic Technical Press (Gostoptekhizdat), 1959.

157. Brace, W.F., A.S. Orange and T. R. Madden, "The effect of pressure on the electrical resistivity of water-saturated crystalline rocks," J. Geophys. Res. 70/22 (1965).

158. Volarovich, M.P., E.I. Parkhomenko and E.I. Bauk, "Relationship between the electrical and elastic parameters of the rocks," from the digest Fizicheskiye svoystva gornykh porod pri vysokikh termodinamicheskikh parametrakh [Physical Properties of the Rocks in the Presence of High Thermodynamic Parameters], Naukova Dumka Press, 1971.

159. Wolarawitsch, M.P., E.I. Parchomenko and A.T. Bondarenko, "Electrical conductivity of rocks at high pressures and temperatures," Presentations at the Symposium "Comprehensive Study of the Geoelectrical Constants in the Earth's Crust and in the Upper Mantle," Leningrad, 18, 11, 1970, p. 1.

160. Dobrynin, V.M., Deformatsii i izmeneniya fizicheskikh svoystv kollektorov nefti i gaza [Deformations and change of physical properties in the gas and oil collectors], Nedra Press, 1970.

161. Avchyan, G.M., A.A. Matveyenko and Z.B. Stefankevich, "Effect of pressure and temperature on the physical properties of sedimentary rocks, saturated with liquid," from digest Fiziko-mechanicheskiye svoystva gornykh porod verkhney chasti Zemnoy kory [Physical and Mechanical Properties of the Rocks in the Upper Part of the Earth's Crust], Nauka Press, 1968.

162. Lebedev, E.B. and N.I. Khitarov, "Beginning of granite melting and the electrical conductivity of its melt as a function of high water vapor pressure," Geokhimiya, No. 3 (1964).

163. Bayduk, B.V., Mekhanicheskiye svoystva gornykh porod pri vysokikh davleniyakh i temperaturakh [Mechanical Properties of the Rocks at High Pressures and Temperatures], State Topography Press (Gostoptekhizdat), 1963.

164. Volarovich, M.P., D.B. Balashov, I.S. Tomashevskaya and V.A. Pavlogradskiy, "Study of the effect of uniaxial compression on the velocity of elastic waves in the samples of rocks exposed to high hydrostatic pressure," Publication of the Academy of Sciences of the USSR, Geophysics Series, No. 8, 1963.

165. Sovremennaya tekhnika sverkhvysokikh davleniy [Contemporary Technology of Ultrahigh Pressures], Mir Press, 1964.

166. Equipment for ultrahigh pressure. Digest of National and Foreign Bibliography for the Years 1950-1960, All-Union Scientific Research Institute of Metallurgy - Siberian Branch, 1961.

167. Swenson, K., Fizika vysokikh davleniy [Physics of High Pressures], Foreign Literature Press, 1963.

168. Slutskiy, A.B., "Study of the effects of high temperature and pressures up to 35 kbar and the temperatures up to 1500°C on the electrical conductivity in solid dielectrics," Pribory i tekhnika eksperimenta, No. 6 (1969.

169. Tsiklis, D.S., Tekhnika fiziko-khimicheskikh issledovaniy pri vysokikh davleniyakh [Technology of Physical and Chemical Studies at High Pressures], Goskhimizdat Press, Moscow, 1958.

170. Beresnev, B.I., L.F. Vereshchagin, Yu. N. Ryabinin and L.D. Livshits, Nekotorye voprosy bol'shikh plasticheskikh deformatsiy metallov pri vysokikh davleniyakh [Some Questions of Extensive Plastic Deformations of Metals at High Pressures], Publication of the Academy of Sciences of the USSR, 1960. /274

171. Moiseyenko, U.I., V.E. Istomin and G.D. Ushakov, "Effect of the one-sided pressure on the electrical resistivity in rocks," Dokl. AN SSSR 154/2 (1964).

172. Bridgman, P.W., Fizika vysokikh davleniy [Physics of High Pressures], Joint Scientific and Technical Publishing House, 1935.

173. Volarovich, M.P., B.M. Urazayev, E.I. Parkhomenko and A. A. Berezutskaya, "Electrical conductivity of sedimentary and igneous rocks in Central Kazakhstan, exposed to high pressures and temperatures," Publication of the Kazakh Branch, Academy of Sciences of the USSR, No. 2, 1971.

174. Schult, A. and M. Schober, "Measurement of electrical conductivity of natural olivine at temperatures up to 950°C and pressures up to 42 kbar," München, Z. Geophysik, 35, H.2, 105-112 (1969).

175. Termoanaliticheskie issledovaniya v sovremennoy mineralogii [Thermoanalytical Studies in Contemporary Mineralogy], Nauka Press, 1970.

176. Khitarov, N.I. and A.B. Slutskiy, "Effect of the pressure on the melting temperature of albite and basalt (on the basis of measured electrical conductivities)," Geokhimiya, No. 12 (1965).

177. Parkhomenko. E.I. and A.T. Bondarenko, "Electrical conductivity of rocks at high pressures, exposed to one-sided pressure," Proceedings of the Institute of Earth Physics, Academy of Sciences of the USSR, No. 23 (190), 1962.

178. Parkhomenko, E.I. and A.T. Bondarenko, "Study of electrical resistivity in rocks at the pressures of up to 40,000 $kg.cm^2$ and temperatures up to 400°C," Publication of the Academy of Sciences of the USSR, Geophysics Series, No. 12, 1963.

179. Dvorak, Z. and E.I. Parkhomenko, "Pressure and temperature dependence of electric conductivity of some basic and ultrabasic rocks," Geophys. Sborn., N 263-287 (1967).

180. Vagshal', D.S., "Electrical conductivity of serpentinites," Dokl. AN SSSR 190/3 (1970).

181. Moskaleva, S.V., "Problems of upper mantle and genesis of hyperbasites," Dokl. AN SSSR 156/5 (1964).

182. Dortman, N.B., V.I. Vasil'yeva and A.K. Veynberg, et al., Fizicheskie svoystva gornykh porod i poleznykh iskopaemykh SSSR [Physical Properties of the Rocks and Useful Minerals in the USSR], Nedra Press, 1964.

183. Avchyan, G.M., Fizicheskie svoystva osadochnykh gornykh porod pri vysokikh davleniyakh i temperaturakh [Physical Properties of Sedimentary Rocks at High Pressures and Temperatures], Nedra Press, 1972.

184. Parkhomenko, E.I. and A.T. Bondarenko, "Effect of uniaxial pressure on the electrical resistivity in rocks," Publication of the Academy of Sciences of the USSR, Geophysics Series, No. 2, 1960.

185. Parkhomenko, E.I., "Factors which determine electrical parameters of the minerals and rocks at high temperatures and pressures," from the digest Fizicheskiye svoystva gornykh porod pri vysokikh termodinamicheskikh parametrakh [Physical Properties of the Rocks in the Presence of High Thermodynamic Parameters], Naukova Dumka Press, 1971.

186. Chernyak, G. Ya., "Electrical aqueous-physical properties of porous rocks," Series 12, Gidrogeologiya i inzhenernaya geologiya [Hydrogeology and Engineering Geology], 1969.

187. Fel'dman, I.S., "Utilization of results in deep magnetotelluric sounding in the study of structure of the Earth's crust and of the upper mantle," Ph.D. Thesis of the author, from the Moscow State University, 1969.

188. Rikitaki, T., Elektromagnetizm i vnutrenneye stroenie Zemli [Electromagnetism and Structure of the Earth's Interior], Nedra Press, 1968.

189. Bulmasov, A.P. and V.P. Gornostaev et al., "Deep magnetotelluric sounding in the Baikal region," from the digest Baykal'skiy rift [Baikal Rift], Nauka Press, 1968.

190. Berdichevskiy, M.N. et al., "Anomaly in electrical conductivity of the Earth's crust in Yakutiya," Publication of the Academy of Sciences of the USSR, Physics of the Earth Series, No. 10, 1969. /275

191. Kovtun, A.A., O.M. Raspopov and V.A. Troitskaya, et al., "Magnetotelluric sounding in the region of Port of France (Kergelen), Publication of the Academy of Sciences of the USSR, Physics of the Earth Series, No. 7, 1968.

192. Gokhberg, M.B., V.G. Dubrovskiy and K. Nepesov, "Utilization of magnetic storm data for deep sounding in Turkmeniya," Publication of the Academy of Sciences of the USSR, Physics of the Earth Series, No. 12, 1968.

193. Lybimova, E.A., "Thermal anomaly in the area of Baikal rift," from the digest Baykal'skiy rift [Baikal Rift], Nauka Press, 1968.

194. Lysak, S.V., "Some data on thermal waters and geothermal conditions in Baikal region," Baykal'skiy rift [Baikal rift], Nauka Press, 1968.

195. Berdichevskiy, M.N., V.G. Dubrovskiy, K.I. Nepesov, V.V. Solokhov and E. B. Faynberg, "Geoelectrical characteristic of the Earth's crust and of the upper mantle in Turkmeniya," Publication of the Academy of Sciences of the USSR, Physics of the Earth Series, No. 11, 1970.

196. Belousov, V.V., Zemnaya kora i verkhnyaya mantiya materikov [Earth's Crust and Upper Mantle of the Continents], Nauka Press, 1966.

197. Lubimova, E.A., "Investigation of thermal flows from the Earth's interior," Publication of the Academy of Sciences of the USSR, No. 1, 1968.

198. Lubimova, E.A., "Estimation of the interior thermal flow distribution for the southwestern part of the USSR," from the digest Problemy glubinnogo teplovogo potoka [Problems of the Deep Interior Thermal Flow], Nauka Press, 1967.

199. Smirnov, Ya.B., "Thermal energy of the Earth and its geologic origin," Dokl. AN SSSR 177/2 (1967).

200. Bolotovskaya, N.A., "New data on the governing laws in the position of the hercynian alkaline rocks in the eastern part of the Baltic plate," Dokl. AN SSSR 173/3 (1967).

201. Keller, G.V., L.A. Anderson and G.V. Pritchart, "Geophysical survey investigations on the electrical properties of the crust and upper mantle," Geophysics, No. 6 (1966).

202. Rotanova, N.M., "Mapping of conductivity and of the thickness of nonconducting layer, based on the geomagnetic data," Geomagnetizm i aeronomiya VI/1 (1966).

203. Matveyeva, N.N. and L.S. Chepkunas, "Layer of decreased velocities in the Earth's crust," from the digest Voprosy dinamicheskoy teorii rasprostraneniya seysmicheskikh voln [Dynamic Theory of the Propagation of Seismic Waves],9, 1968.

204. Tokarev, V.A., "Major deep fissures on the Kola Peninsula," from the digest Geologicheskoe stroenie, razvitie i rudonosnost' Kol'skogo poluostrova. Apatity [Geologic structure Development and Ore Deposits on Kola Peninsula. Apatites], 1968.

205. Novitskiy, G.I., "First experimental probing by dipole electromagnetic sounding on the Kola Peninsula," from the digest Geologiya i glubinnoe stroenie vostochnoy chasti Baltiyskogo shchita [Geology and Interior Structure of the Eastern Part of the Baltic Plate], Nauka Press, 1968.

206. Rokityanskiy, I.I., K.I. Zybin, D.A. Rokityanskaya and R.V. Shchepetnov, "Magnetotelluric soundings of the formations at the geophysical stations in Borok, Lovozero, Petropavlovsk-Kamchatskiy," Materials of the All-Union Conference of 1961, Leningrad State University Press, 1963.

207. Egorov, Yu.M. and V.G. Chernozemova, "Results of magneto-telluric sounding in the area of geophysical station Lovozero," Publication of the Academy of Sciences of the USSR, Physics of the Earth Series, No. 2, 1965.

208. Klark, S.P. and A.E. Ringwood, "Density distribution and constitution of the mantle," Res. Geophys., 2 (1964).

209. Vladimirov, N.P. and A.T. Bondarenko, "Results of the deep magnetotelluric sounding in Lovozero," Publication of the Academy of Sciences of the USSR, Physics of the Earth Series, No.11, 1970. /276

210. Fujisawa, H., "Temperature and discontinuities in the transition layer within the Earth's mantle," Techn. Res. ISSP, ser. A, N 272 (1967).

211. Parkhomenko, E.I., "Nature of the layers with high electrical conductivity in the Earth's crust and in the upper part of the mantle, according to the laboratory data," from the digest Fizicheskiye svoystva gornykh porod pri vysokikh termodinamicheskikh parametrakh [Physical Properties of the Rocks in the Presence of High Thermodynamic Parameters], Naukova Dumka Press, 1971.